# RELIABILITY OF SHALLOW FOUNDATIONS DESIGNED USING LRFD CONSIDERING UNCERTAINTY FROM DIFFERENT NUMBERS OF STRENGTH MEASUREMENTS

---

A Dissertation

presented to

the Faculty of the Graduate School

at the University of Missouri-Columbia

---

In Partial Fulfillment

of the Requirements for the Degree

Doctor of Philosophy

---

by

DAN DING

Dr. J. Erik Loehr, Dissertation Supervisor

December 2014

RELIABILITY OF SHALLOW FOUNDATIONS DESIGNED USING LRFD CONSIDERING UNCERTAINTY FROM DIFFERENT NUMBERS OF STRENGTH MEASUREMENTS

---

Presented by Dan Ding

A candidate for the degree of

Doctor of Philosophy

And hereby certify that, in their opinion, it is worthy of acceptance.

---

Dr. J. Erik Loehr, P.E., Supervising Professor

---

Dr. Paul L. Speckman, Committee Member

---

Dr. William J. Likos, Committee Member

---

Dr. John J. Bowders, P.E, Committee Member

---

Dr. Brent L. Rosenblad, Committee Member

# DEDICATION

To my parents,

For their love and support

# ACKNOWLEDGEMENTS

I always feel grateful for having the opportunity to study and perform research in Geotechnical Engineering at the University of Missouri. I would like to express my sincere appreciation to my advisor Dr. Erik Loehr. His personality, wisdom and his rigorous attitude toward research and teaching have had a great influence on me. His willingness and patience to share his thoughts, experience and advice have encouraged me to never stop learning.

I would like to thank Dr. William Likos for his generous support in my study and research. I really appreciate his help, patience, advice and the opportunity to work with him. Many thanks to Dr. Paul Speckman for valuable help with all the statistical questions and for serving as a member of my dissertation committee. Dr. John Bowders is the first professor I met with when I came to MU. His enthusiasm and easy-going attitude helped me join in our group quickly. I would like to thank him for his help during all these years and for serving as a member of my dissertation committee. I would like to thank Dr. Brent Rosenblad for the opportunity of working as a teaching assistant for his classes and for serving as a member of my dissertation committee. At last, I would like to thank our Geotechnical group for their precious friendship and support.

# TABLE OF CONTENTS

# TABLE OF FIGURES

# LIST OF TABLES

# Chapter 1 Introduction

## 1.1 Introduction

Engineers and researchers have dealt with uncertainties in geotechnical engineering for decades. Design methods have been developed to account for this uncertainty in ways that range from (1) using engineering experience and judgment, to (2) applying factors of safety, to (3) adopting load and resistance factor design (LRFD) or partial factor design methods, to (4) most recently, incorporating probabilistic theory into LRFD or partial factor design to conduct reliability based designs.

No matter what design method is used, the most important thing is to understand the true soil properties and acquire a sound knowledge of the ground conditions at a site. Generally, uncertainty in geotechnical engineering has been categorized into two broad types— aleatory and epistemic uncertainty— where aleatory uncertainty reflects the natural variability in soil properties, while epistemic uncertainty reflects uncertainties due to lack of knowledge. The sources of uncertainties in geotechnical designs include natural soil variability; uncertainty introduced during boring, sampling, and testing; uncertainty introduced when applying statistical, mathematical or simulation models; and uncertainty introduced when choosing a design model. Natural soil variability cannot be reduced or eliminated by any means; however, epistemic uncertainty can be controlled to some certain level depending upon the quantity and quality of site characterization activities. For example, uncertainty introduced from boring, sampling and testing can be kept at a consistent and controlled level by using state of the art boring, sampling and testing

techniques. Uncertainty introduced due to variability in particular design methods can be improved by selecting more reliable design methods when several methods are available.

In contrast, uncertainty attributed to knowledge of geotechnical design parameters may vary substantially from one site or project to the next depending on the variability of a specific site and the quantity and quality of site characterization activities performed for a specific project. With small numbers of measurements or inadequate site information, uncertainty in geotechnical design parameters may be great, thus leading to designs that are either more costly than is truly required or to performance problems if designs do not achieve appropriate levels of reliability. Obtaining more information generally provides a better understanding of soil properties at the site so that soil parameters can be more accurately characterized to reflect true soil properties. However, it is sometimes difficult to conduct comprehensive site characterization due to constraints of site conditions, time and budget. In cases where sufficient measurements are not available, interpreted design parameters may not reflect the true soil properties and resulting designs could be subject to unnecessary risks or unnecessary costs.

When adequate numbers of measurements or other sources of information are not available to interpret the true soil properties, design has to be conducted based on a small number of measurements or inadequate site information. In such cases, conservative designs are usually developed to compensate for uncertainties and unknowns and to ensure design safety. However, applying overly conservative assumptions will lead to over conservative designs, which may cause less than satisfactory designs to be realized. Thus, applying a rational method to design conservatively at a certain level of reliability is necessary which might avoid excessively over conservative designs.

## 1.2 Objectives and Scope

Common questions posed when evaluating site characterization activities include: Do we have enough information to obtain accurate soil properties? How many measurements are necessary to obtain design parameters with reasonable accuracy? What consequences may be realized if there are a small number of measurements? How reliable will the designs be if potentially small numbers of measurements are used for design? The research described in this thesis was performed to provide information and techniques to help answer these questions. The research centered around performing quantitative analyses to evaluate the reliability of shallow foundations designed using load and resistance factor design considering different numbers of soil strength measurements. The principle product of this research is a proposed method to practically account for uncertainty that is introduced when the number of measurements for relevant design parameters is small.

The scope of this research included the following activities:

- Comprehensive site characterizations were completed at four different soil sites; from these measurements, relevant soil design parameters were evaluated using two regression models that were deemed to represent the true soil properties at each site.
- Analyses were performed to quantitatively evaluate the effect of the number of measurements on the estimated value and uncertainty of relevant design parameters.
- Probabilistic analyses were performed using random subsampling from the population of measurements obtained at each site to study the effect of the number

of measurements on the reliability of spread footings designed using load and resistance factor design (LRFD).

- Several alternative methods, including a new proposed method, to practically account for the uncertainty in soil design parameters were evaluated considering different numbers of measurements.
- Conclusions and recommendations regarding the benefits and limitations for these alternative methods were then developed based on the results of the evaluations conducted.

## 1.3 Overview of Thesis

The research in this thesis is presented in eleven chapters. Chapter 1 is the current chapter, which provides an introduction to the research effort.

In Chapter 2, a literature review is provided to summarize previous studies on characterizing uncertainty in soil properties, followed by a summary of alternative design methods focusing on how they deal with uncertainty. Problems and research associated with small numbers of measurements and inadequate site investigation are also summarized. Finally, existing methods to account for uncertainties when the number of measurements is small or the site information is inadequate are categorized into three general methods.

Chapter 3 provides an overview of site characterization activities performed as part of this research. General descriptions of each site are provided and results of laboratory measurements are presented.

Chapter 4 describes the regression models developed to represent the “true” soil parameters at each site. Sources of uncertainties presented for undrained shear strength are

briefly summarized and probabilistic measures of variability and uncertainty of undrained shear strength are presented for each site.

In Chapter 5, a load and resistance factor design (LRFD) method is presented for design of spread footings at the Strength I limit state. Given reasonable assumptions regarding the uncertainty present for the design model and design parameters, calibrated resistance factors are provided as a function of the uncertainty present for undrained shear strength for different target probabilities of failure.

To better understand how the reliability of designs is affected by different numbers of measurements, the value and uncertainty of soil design parameters are presented in Chapter 6. Best fit models for undrained shear strength are plotted along with values for the total and "model" uncertainty as a function of the number of measurements to illustrate the effect of number of measurements on interpreted design parameters.

Chapter 7 presents results of analyses conducted to evaluate how the reliability of spread footings design using load and resistance factor design are affected by different numbers of measurements. A random subsampling protocol is introduced and three categories of cases are adopted for evaluation. The effect of considering different target probabilities of failure, different design depths, spatial averaging, total population size, different regression models and site variability are also discussed.

Chapter 8 describes results of analyses performed to evaluate an existing method to account for the uncertainty in undrained shear strength when the number of measurements is small. A new method to account for uncertainty in relevant design parameters using statistical inference is introduced in Chapter 9. Results of analyses to evaluate the proposed

methods similar to those described in Chapter 8 are presented to demonstrate the effectiveness of the proposed method.

Chapter 10 describes comparisons of results for the evaluations presented in Chapter 7, Chapter 8 and Chapter 9 considering different numbers of measurements. The relative advantages and disadvantages of the three alternative methods are presented along with practical implications that are associated with use of the respective methods.

Finally, conclusions drawn from the analyses and evaluations presented in previous chapters are presented in Chapter 11. Recommendations are provided for practical implementation and future studies, and the limitations and difficulties associated with both research and application of the alternative techniques are described.

# Chapter 2 Literature Review

## 2.1 Introduction

Reliability-based design (RBD) methodologies have been developed worldwide during the past 30 years, and researchers have long been aware of the importance of evaluating variability and uncertainty in geotechnical engineering design. Terzaghi always emphasized the uncertainty associated with design in practice (Terzaghi et al., 1960). In the 2nd Terzaghi Lecture in 1964, Casagrande first talked about "calculated risk" in earthwork and foundation designs (Casagrande, 1965). Since that time, systematic research has been conducted in this area. Whitman gave the 17th Terzaghi Lecture on evaluating "calculated risk" in 1981 (Whitman, 1984), and Christian posed the question "How well do we know what we are doing?" when evaluating geotechnical engineering reliability in 2003 (Christian, 2004). Significant work has been conducted by G.B. Baecher, J.T. Christian, G.A. Fenton, R.B. Gilbert, D.V. Griffith, F.L. Kulhawy, S. Lacasse, K.K. Phoon, W.H. Tang, E.H. Vanmarcke, T.H. Wu and many other researchers to contribute to the body of knowledge evaluating variability and uncertainty in geotechnical engineering and the application of reliability-based design methods.

In this chapter, previous work on variability and uncertainty analyses in geotechnical engineering is summarized. Alternative design methods to consider such variability and uncertainty are then described along with methods for using reliability analysis to calibrate load and resistance factor design. Problems associated with use of small numbers of measurements and inadequate site information for geotechnical design are then discussed and existing approaches to consider the effect of numbers of measurements are presented.

## 2.2 Variability and Uncertainty in Geotechnical Engineering

Based on the importance of properly characterizing and evaluating soil and rock properties, the work of several researchers that have conducted significant work on characterizing variability and uncertainty in soil properties is described along with the systematic methods they developed to accompany their studies.

### 2.2.1 Baecher and Christian

In 1982, while conducting site characterization on rock masses, Baecher first summarized two primary sources of variability in rock mass properties determined from site investigations as inherent spatial variation and errors introduced by sampling and testing (Baecher, 1982). Baecher outlined an approach for dealing with the great uncertainty in joints of rock masses based on statistical reasoning and formal inference (Baecher, 1982; Einstein and Baecher, 1983). Using probabilistic approaches in site exploration (Baecher, 1972), Baecher further concluded that the sources of uncertainties are geological uncertainty from the site formations, geometry and history; model uncertainty from selections of physical models; parametric uncertainty resulting from spatial variability, measurement error and estimation bias; and finally, uncertainty caused by omissions or overlooking geological details (Baecher, 1983; Baecher, 1984; Baecher, 1987).

Christian, Ladd and Baecher (1994) represented uncertainties in soil/rock properties by placing them into two main categories: (1) data scatter, which includes real spatial variation and random testing errors, and (2) systematic error, caused by statistical error and measurement bias as shown in Figure 2.1. Measurement bias is primarily due to the effects of sample disturbance, while statistical error is mainly caused by using limited numbers of

measurements. The statistical error exists in estimating both the mean and uncertainty of soil properties, however, the most significant error is in the mean soil property which is approximately calculated by (Baecher, 1987):

$$V_{m_x} = V_z/n \qquad \text{(Eq. 2.1)}$$

where $V_{m_x}$ is the statistical error in mean soil properties, $V_z$ is the variance in measurements and *n* is the number of measurements.

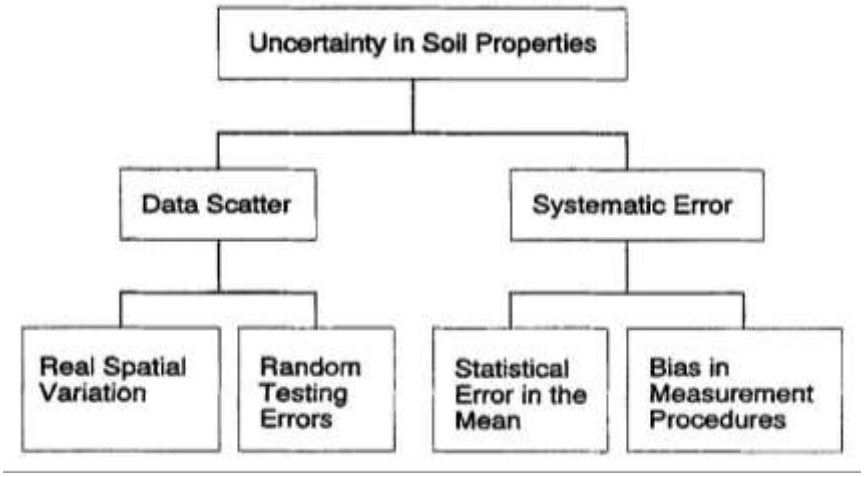


Figure 2.1 Uncertainty in soil properties (Christian, Ladd, and Baecher, 1994).

In the book, *Reliability and Statistics in Geotechnical Engineering*, Baecher and Christian (2003) adopted Hacking's definition (Hacking, 1975) for two main categories of uncertainty— aleatory and epistemic uncertainty— which reflect natural variability and lack of knowledge, respectively. Further, Baecher and Christian summarized the uncertainty in geotechnical engineering design into three major categories as shown in Figure 2.2.

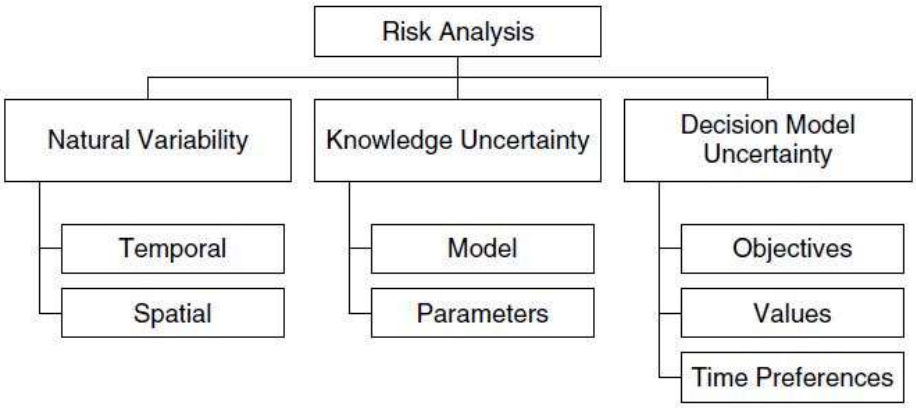


Figure 2.2 Categories of uncertainty in risk analysis (Baecher and Christian, 2003).

Baecher and Christian's *natural variability* is the inherent variability of soil properties, which considers the variability over time and space expressed as the variability at a single location with changes of time (temporal) and variability over space at a single time (spatial). The natural variability is also known as the aleatory uncertainty.

Baecher and Christian's *knowledge uncertainty* is also called subjective uncertainty because it has been brought into design due to lack of information, lack of data and lack of understanding. Knowledge uncertainty is an alternative term for epistemic uncertainty. Figure 2.2 shows how knowledge uncertainty can be further divided into model and parameter uncertainty. Baecher and Christian further refined these subcategories in their book by discussing site characterization uncertainty, model uncertainty, and parameter uncertainty in geotechnical applications. Site characterization uncertainty is the uncertainty introduced during boring, sampling and testing. Model uncertainty relates to the mathematical model(s) chosen for simulating real situations, and parameter uncertainty is the uncertainty in parameters estimated from, or for, the model(s).

Baecher and Christian's *decision model uncertainty* in geotechnical design involves implementation of the designs that incorporates both aleatory and epistemic uncertainties.

However, Baecher and Christian (2003) mentioned that separation between aleatory and epistemic uncertainties is "not an immutable property of nature, but an artifact of how we model things". By assuming natural variations are random, which is not strictly true, some uncertainty about natural variations has been transferred from epistemic uncertainty to aleatory uncertainty, although the total uncertainty is still the same (Baecher and Christian, 2003). Baecher and Christian further concluded that "all the uncertainties dealt with in risk analysis are caused by limited knowledge: there is no such thing as randomness." (Baecher and Christian, 2000).

In the 39th Terzaghi Lecture, Christian summarized developments for characterizing uncertainty in geotechnical engineering and talked about existing problems in geotechnical engineering reliability (Christian, 2004). Christian notes that the central problem in geotechnical engineering is to establish the properties of soil that will be used in design. When establishing soil properties for a site, statistical methods are commonly applied; the most common method is fitting a regression model with depth. Variability in the measured soil properties will be observed as data scatter about the established trend. Some people incorrectly believe that variability will be reduced by fitting a more complicated model. With a more sophisticated statistical model, although the data scatter about the trend will be reduced, the uncertainty in how well the model represents the actual conditions will simultaneously increase. Model selection is not an artifact of nature but instead represents a modeling decision (Christian, 2004).

To analyze the variability and uncertainty in soil and rock parameters, statistical methods have been adopted. Baecher applied the first order second moment method to analyze data scatter and uncertainty in rock masses (Baecher, 1983). Christian and Baecher

(2006) used Bayesian logic to obtain the probability of acquiring a model which can reflect true soil properties by updating observed data. After conducted massive research work on reliability based design, Baecher and Christian concluded that it is very difficult to acquire the actual variability and uncertainty of soil and rock properties, and that it may not even be possible, due to the multiple sources of uncertainties brought in during obtaining, modeling and evaluating the soil and rock properties (Christian and Baecher, 2011).

### 2.2.2 Ang and Tang

Ang and Tang (2007) also adopted the two broad categories of uncertainty, aleatory and epistemic uncertainty. They considered aleatory uncertainty to be data based and associated with natural randomness, while epistemic uncertainty is knowledge based and associated with inaccuracies in prediction and estimation of reality. Tang (1984) summarized that the sources of uncertainties in characterizing soil properties in homogenous layers include inherent spatial variability, random test errors, systematic test bias, calibration errors and estimation error.

Ang and Tang (2007) recommended that aleatory and epistemic uncertainties and their effects be treated separately because of the different sources and effects of these two types of uncertainties. Aleatory uncertainty is associated with inherent variability that cannot be reduced. Furthermore, the effect of aleatory uncertainty in engineering applications provides a calculated probability. Ang and Tang (1975) regarded soil properties to be random and used histograms to represent the variability in natural soil properties. By using probability theory, variability in experimental data is calculated to reflect natural randomness as an aleatory type of uncertainty and the sample variance is estimated by:

$$var(x) = \frac{1}{n-1}\sum_{i=1}^{n}(x_i - \bar{x})^2 \quad \text{(Eq. 2.2)}$$

where $n$ is the number of measurements; $x_i$ is the $i^{th}$ measurement and $\bar{x}$ is the arithmetic average value for all measurements.

The variance calculated by Eq.2.2 reflects the variability in experiment data which is called data uncertainty in this thesis. When a great number of measurements are available, the variability will approach the "true" variability which is the natural randomness.

Epistemic uncertainty is considered to be knowledge based because uncertainty has been introduced into design when mathematical models (or similar simulation, physical or experimental models) are applied to represent real world analysis and predictions. Epistemic uncertainty is expressed as the uncertainty in the calculated probability or risk and it may be reduced by acquiring more knowledge of the real world.

For $n$ measurements of soil parameters, there is epistemic uncertainty underlying the estimated average, called the sampling error, which can be represented by:

$$var(\bar{x}) = \frac{1}{n} \cdot var(x) \quad \text{(Eq. 2.3)}$$

where $var(\bar{x})$ is the variance in estimated true soil parameters, which is called model uncertainty in this thesis. The model uncertainty reflects the epistemic uncertainty in estimating true soil properties when using calculations and statistical models. The model uncertainty tells how well the statistical models can reflect the true soil properties.

In engineering applications, Ang and Tang stated that the epistemic uncertainty is as important as the aleatory uncertainty. Furthermore, they emphasized that "Quite often, the epistemic uncertainty may be more significant than the aleatory uncertainty." (Ang and Tang, 2007) When observational data is limited, estimations based on that information

will have great error. When applying mathematical models (or simulations or laboratory models), no matter how sophisticated models are used, since these models are based on idealized conditions or assumptions, the models may not reflect true soil properties. Under such circumstances, Ang and Tang (1975) made it clear that "the uncertainties associated with prediction and model error may be much more significant than those associated with the inherent variability." The research of this thesis emphases on the epistemic uncertainty brought into design when applying statistical models to reflect true soil properties. The uncertainty is called model uncertainty in this thesis and the model uncertainty is regarded to be the most significant uncertainty that will affect the reliability of designs.

To analyze the aleatory and epistemic uncertainty, Ang and Tang (2007) provided the basics of probability and statistical methods with emphasis from probability models and statistical inference to regression models and Bayesian updates. Their work has helped reduce the uncertainty of predictions from correlation models (Zhang et al., 2004) and has been used to calibrate the different model uncertainties when using geotechnical design models for prediction (Zhang et al., 2009). Furthermore, the probabilistic methods have also been applied in decision, risk and reliability analysis (Ang and Tang, 1984).

### 2.2.3 Lacasse and Nadim

Lacasse and Nadim (1996) also emphasized the importance of recognizing the type of uncertainties when evaluating data and categorized the uncertainties associated with a geotechnical engineering problem into aleatory and epistemic categories. These types of uncertainties are summarized in Figure 2.3. Lacasse and Nadim's *aleatory uncertainty* is similar to Ang and Tang's *aleatory uncertainty* which is the spatial variability of soil properties. Lacasse and Nadim categorized statistical uncertainty, measurement

uncertainty and model uncertainty into epistemic uncertainty. However, Lacasse and Nadim's model uncertainty is different from Baecher and Christian's model uncertainty in Figure 2.2. Lacasse and Nadim's model uncertainty refers to design model uncertainty which is the uncertainty from selecting a physical design model (i.e., a foundation type) and it is equivalent to Baecher and Christian's decision model uncertainty in Figure 2.2. Different from Baecher and Christain and Ang and Tang, Lacasse and Nadim took human error into account and regarded it as the third source of uncertainty. Usually, this type of uncertainty can be controlled and avoided if engineers have acquired necessary knowledge and skills and be aware of what they are doing and understand how to conduct designs and construction in the right way. However, ignoring this type of uncertainty probably will cause serious problems in designs (Bea, 2006).

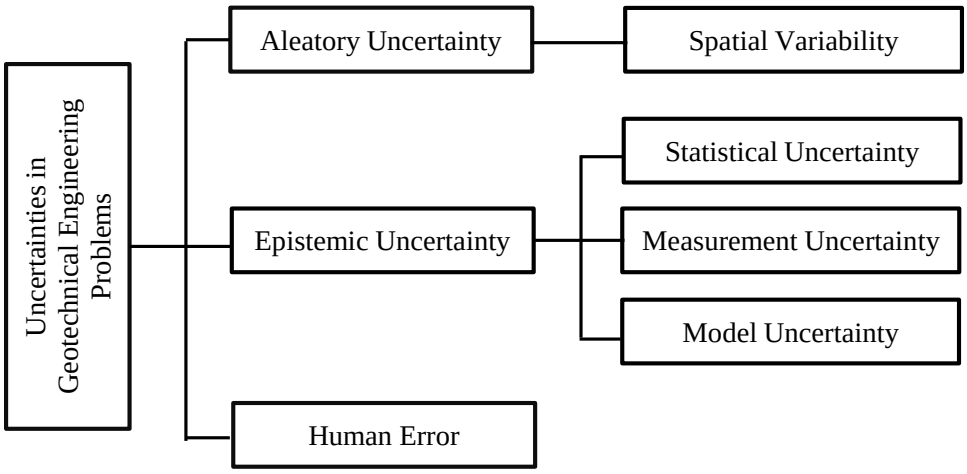


5Figure 2.3 Types of uncertainties in geotechnical engineering problems (Summarized from Lacasse and Nadim 1996).

Lacasse and Nadim applied probabilistic analysis on offshore structures and suggested engineers should combine data, knowledge about the data, and knowledge of site geology and consider both the quality of data and geological evidence with engineering judgment when characterizing uncertainties in soil properties. Lacasse and Nadim (1994)

and Nadim et al. (1994) showed that the reliability of geotechnical analysis is affected differently by uncertainties in different soil properties. When evaluating uncertain soil properties, a mean and standard deviation or coefficient of variation and a probability distribution function are recommended. Lacasse and Nadim also recommended that consistent data populations should be used to estimate soil properties whereby most probable or "characteristic" values of soil properties can be selected for designs. Lacasse emphasized that design model uncertainty resulting from application of design calculation models is significant and should be characterized by its mean, coefficient of variation and probability distribution and then be further considered in design (Lacasse and Nadim, 1996).

Lacasse and Nadim (1998) further evaluated geotechnical variability and uncertainty for use in reliability analyses and risk assessments. This work provides a framework for systematic use of engineering judgment in decision making. In risk assessment procedures, the first step is always to quantify the geology and engineering parameters (Lacasse et al., 2007) and consider the epistemic uncertainty of parameter uncertainty, model uncertainty, and behavior uncertainty and the human error to estimate the likelihood of failure (Lacasse et al., 2004).

### 2.2.4 Kulhawy and Phoon

Phoon and Kulhawy (1996, 1999a, 1999b) considered three primary sources of uncertainty in characterizing geotechnical variability: (1) inherent variability, (2) model uncertainty and (3) measurement error. Figure 2.4 illustrates the general representation of uncertainty for soil properties considered by Kulhawy and his co-authors. Inherent variability is modeled using a coefficient of variation and scale of fluctuation for a

homogenous random field model (Phoon and Kulhawy, 1996). Unlike the model uncertainty considered in research described previously, the model uncertainty considered by Kulhawy and Phoon represents transformation model uncertainty, which reflects uncertainty resulting from application of empirical models or correlation models to convert indirect measurements to required design parameters (Phoon and Kulhawy, 1999a). Measurement error is introduced during the measurement process by equipment, procedural/operator and random testing effects (Phoon and Kulhawy, 1999b).

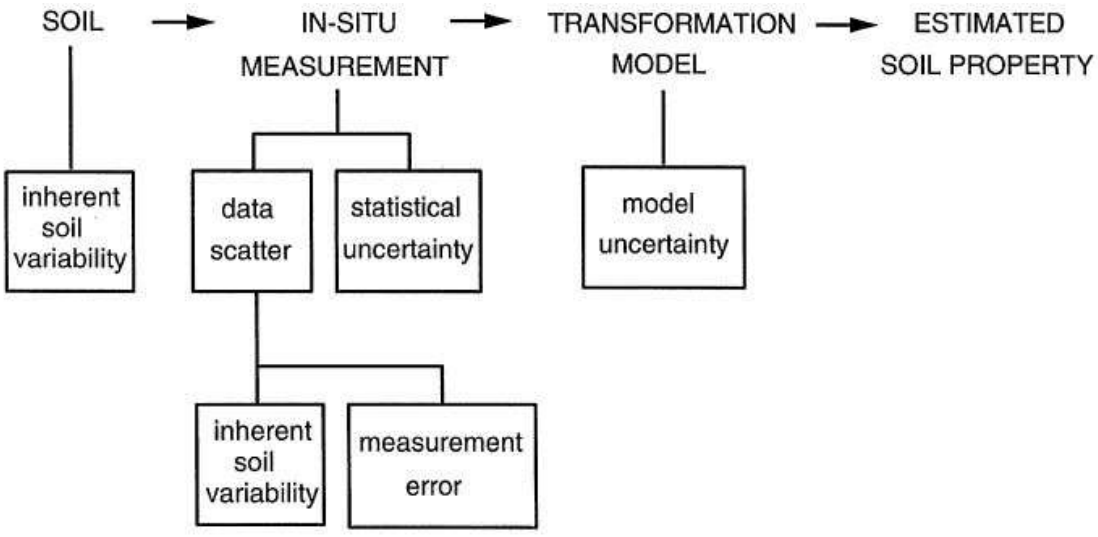


Figure 2.4 Uncertainty in soil property estimates (Kulhawy, 1993; Phoon et al., 1995).

Similar to the data scatter refined by Christian, Ladd and Baecher (1994) as shown in Figure 2.1, Kulhawy and Phoon considered the combined effects from inherent soil variability and measurement error are shown as data scatters (Figure 2.4). The measurement error are caused by equipment, procedural/operator and random testing effects, where the equipment effects are caused by the variations in equipment testing system, the measurement error from procedural-operator effects are caused by limitations in testing standards and testing procedures, and the measurement error from random testing

effects refers to remaining scatters in the results that is not caused by soil inherent variability. In Figure 2.4, the statistical uncertainty has been summarized into a separate subcategory of in-situ measurements from data scatter, however, measurement errors which cause data scatter are also affected by statistical uncertainty from a limited number of measurements or limited site information. Thus the statistical uncertainty is sometimes analyzed with measurement error and statistical uncertainty can be minimized by taking more measurements.

To evaluate geotechnical variability, the inherent variability, measurement error and transformation model uncertainty are regarded as independent variables and assessed separately (Phoon and Kulhawy, 1999a; 1999b). A first order second moment probabilistic approach is then applied to combine the different sources of uncertainties for soil geotechnical variability evaluation.

For "direct" measurements, i.e., undrained shear strength measured from unconsolidated undrained triaxial compression tests, the total variability of a soil design parameter soil property is described as:

$$\xi_m(z) = t(z) + w(z) + e(z) \qquad \text{(Eq.2.4)}$$

where $\xi_m$ is the measured soil design parameter, *t* is the deterministic trend with depth, *w* is the inherent variability and *e* is the measurement error. Thus, the mean (*m*) and variance ($SD^2$) of the soil property can be calculated by:

$$m_\xi = t \qquad \text{(Eq. 2.5)}$$

$$SD_\xi^2 = SD_w^2 + SD_e^2 \qquad \text{(Eq. 2.6)}$$

For indirect measurements, where measurements are required to be transformed into required design parameters, i.e., cone penetration tests, an empirical model or a correlation

model is applied to convert test measurements to design parameters. A transformation function *T* is incorporated as:

$$\xi_d = T(\xi_m, \varepsilon) \quad \text{(Eq. 2.7)}$$

where $\xi_d$ is the design parameter and $\varepsilon$ is the transformation uncertainty. The total variability of the design property is then represented as:

$$\xi_d = T(t + w + e, \varepsilon) \quad \text{(Eq. 2.8)}$$

The mean and variance of design property can be calculated by:

$$m_{\xi_d} \cong T(t, 0) \quad \text{(Eq.2.9)}$$

$$SD_{\xi_d}^2 \cong \left(\frac{\partial T}{\partial w}\right)^2 \cdot SD_w^2 + \left(\frac{\partial T}{\partial e}\right)^2 \cdot SD_e^2 + \left(\frac{\partial T}{\partial \varepsilon}\right)^2 \cdot SD_\varepsilon^2 \quad \text{(Eq. 2.10)}$$

Using first order second moment method, Kulhawy and Phoon summarized the coefficient of variation, mean and approximate range of soil inherent variability, measurement error and transformation model as well as the scale of fluctuation for various soil parameters based on extensive literature review. For undrained shear strength of clay measured by undrained triaxial compression tests, they summarized that the typical range for *COV* of inherent variability is 10-30% which is the smallest range among all.

Kulhawy and Phoon also conducted research on statistical analysis of soil properties using statistical based methods and computations. Phoon et al. (2003) applied modified Bartlett statistics as inferential statistics to identity the statistically homogenous soil layer before conducing statistical analysis on a given soil profile. Stochastic data is modeled and simulated as non-Gaussian random vectors to be a basic component in reliability design and geostatistics (Phoon, 2006). Multivariate correlation and basic Bayesian updates were applied to reduce the uncertainty in soil shear strength by combining shear strength results from different sources of direct and indirect measurements (Ching et al., 2010)

### 2.2.5 Whitman

Whitman (1984) categorized sources of uncertainties into spatial variability, measurement noise and systematic errors. He considered spatial variability to be natural random variability and measurement noise to be caused by error from testing effects. Systematic errors include statistical error in soil design parameters when estimate the design parameters from a finite number of measurements. Systematic errors also include measurement bias from sampling disturbance and testing errors. According to Whitman (1984), the uncertainty from statistical error and measurement bias "propagates unchanged through the analysis," while spatial variability and measurement noise "average over the volume of soil."

To avoid overestimating the uncertainty of soil properties, Whitman suggested that the degree of uncertainty that arises from different sources should be determined separately. Whitman also suggested to consider the autocorrelation distance and scale of fluctuation. Nevertheless, when the scale of fluctuation is small, only the system error remains and contributes to observed scatter. Thus, it is more important to acquire the systematic errors— statistical error and measurement bias— when estimate soil design parameters using measurements in vertical depth range, which is the case in the research of this thesis.

When evaluating "quantified risk" in geotechnical engineering, Whitman (1984) argued that probability theory can facilitate achieving balance between the consequences of uncertain knowledge and the costs of reducing that uncertainty. Almost every factor considered in engineering design is a random variable with different uncertainties. The mean, coefficient of variation and probability distribution are effective ways to describe uncertainty for these random variables. Whitman (1984) further conducted case studies

and concluded that the frequency of actual structure failures usually exceeded predictions because failure modes and human errors were not taken into account.

Whitman's sources of uncertainty in geotechnical designs can be expanded into: (1) soil spatial variability, (2) measurement noise, (3) statistical errors, (4) measurement bias, and (5) failure models and human errors. Both spatial variability and measurement noise are shown as data scatters, however, the measurement noise caused by error from testing effect should not be allowed to affect parameter selection and should be identified and eliminated for future analysis (Whitman, 2000).

### 2.2.6 Wu

Wu (2013) categorized the principal uncertainties in geotechnical design into material model uncertainties and analytical model uncertainties. The uncertainties of a material model include material variability, and testing and modeling errors caused by applying mathematical models designed to transform site exploration data into models used for obtaining soil design parameters. The analytical model is the model used in the design stage to calculate the foundation performance using characterized soil design parameters. Thus, the uncertainty in geotechnical design is a combination of uncertainties from both the material model and analytical model.

In foundation designs, the evaluated soil strength has a great effect on foundation safety, and measurements from laboratory and field testing vary from point to point due to random variation in soil (Wu and Kraft, 1967). Uncertainties in soil strength measurements also arise from inaccuracies and shortcomings in strength tests (Wu, 1974). A probabilistic method for constructing probability contour maps from equal probability lines is useful when determining soil strength at unobserved points based on soil classification at

observed points (Wu and Wong, 1981). Although the same soil property measured with different testing methods may have different uncertainties due to the test conditions, and parameters used in the methods for interpretation (Wu et al., 1987), the best method for reducing uncertainty of soil properties is combining soil information from multiple sources and update site information using prior information (Wu et al., 1989). Wu (2011) further adopted Terzaghi and Peck's observational method (Peck, 1969) by incorporating analytical models. The Bayesian theorem is applied to provide a framework for the observational method by taking original assumptions as prior information, the measured properties as likelihood and the updated properties as the posterior distribution to obtain soil parameters which can reflect the true soil properties.

### 2.2.7 Griffiths and Fenton

Unlike most previous researchers, Griffiths and Fenton focused on the aleatory uncertainty—the natural variability of soils. Their research focuses on the spatial variability of soil properties and reliability-based design using random field finite element models. Griffiths and Fenton adopted Vanmarcke's random field theory, which uses the correlation structure of one dimensional random processes in terms of a variance function and a scale of fluctuation (Vanmarcke, 2010). The random field theory facilitates development of models for analyzing soil spatial variability and is the fundamental theory incorporated in reliability analysis by Griffiths and Fenton. Griffiths and Fenton use the positive correlation observed between soil properties measured at close locations to reflect the soil information at the site.

Since soil properties are usually measured over finite domains which show scale effects, Fenton and Vanmarcke (1990) proposed the local average subdivision (LAS)

algorithm, combining it with the finite element (FE) method, to produce realizations of a local average random process to simulate the soil property at each location in a soil mass as a random variable. Fenton and Griffith further have combined random field theory and the finite element method with Monte Carlo simulation methods to develop the random finite element method (RFEM) in reliability-based design (Griffiths et al., 2006).

Fenton conducted research on quantifying soil properties to derive spatial correlation structures to make inferential characterization of other sites with similar soil engineering properties (Fenton, 1999a; Fenton, 1999b). Two stochastic soil models for spatial correlation structure are usually considered in their work: fractal and finite scale models. The fractal model, or "long-memory" model, considers the horizontal correlation distance for transported soils, erosion and weathering process during soil formation. The finite scale, or "short-memory" model is an exponentially decaying correlation function, which assumes that spatial correlation decreases with the distance between two measuring points. Fenton analyzed cone penetration tests (CPT) tip resistance measurements using the fractal model; and developed a global correlation model for characterizing spatial variability of tip resistance (Fenton and Vanmarcke, 1990).

### 2.2.8 Others

Many other researchers have also worked on summarizing and quantifying geotechnical uncertainties. Yong (1984) concluded that the major reasons for differences in measured soil properties are due to the material itself, methods of sampling, types and procedures of soil testing and selection of models for data analyses. Bea (2006) developed approaches and strategies to address the third category of uncertainty from Lacasse and Nadim (1996) — human error— to improve quality and reliability in geotechnical

engineering. Gilbert addressed the importance of model uncertainty in design models since model parameters cannot be known with certainty and Gilbert mentioned that ignoring model uncertainty will underestimate the uncertainty in the prediction (Gilbert et al., 2000). Effective ways to reduce uncertainties to a controlled level will include combining understanding and knowledge gained during site exploration, along with sampling and testing using engineering judgment, and correct interpretation and data processing (Becker, 1997). Considering different sources of uncertainty in design, Peck (1977) emphasized that geotechnical engineers should carefully characterize the soil properties, particularly the shear strength and compressibility of soil and rock.

### 2.2.9 Terminology Adopted in the Research Described in Thesis

As described in this section, different researchers have used different interpretations to refine different sources of uncertainty for geotechnical design parameters. In general, almost every researcher categorizes soil inherent variability as the aleatory uncertainty. Baecher and Christian, and Kulhawy and Phoon concluded that data scatters are reflected by inherent variability and measurement error. Griffiths and Fenton's research focuses on the aleatory uncertainty— soil spatial variability.

The subcategories of epistemic uncertainty were summarized differently among researchers, however, all studies agree that the epistemic uncertainty is caused by lack of knowledge. The major sources of epistemic uncertainty are statistical uncertainty, measurement uncertainty, and design uncertainty. In different literatures, the term of model uncertainty actually defined different sources of uncertainty. Kulhawy and Phoon refer model uncertainty to the uncertainty caused by using correlation models to convert indirect measurements to characterize design parameters. Baecher and Christian, Lacasse

and Nadim and Gilbert use the term of model uncertainty for uncertainty from design physical models, which is alignment with Wu's analytical model uncertainty. In the book, *Reliability and Statistics in Geotechnical Engineering*, Baecher and Christian (2003) related model uncertainty to the uncertainty caused by adopting mathematical and they have decision model uncertainty for uncertainty from physical design model in risk analysis. In statistical analysis, model uncertainty refers to uncertainty in estimated mean value from the statistical models.

In the research described in this thesis, total uncertainty, model uncertainty and data uncertainty are used to describe uncertainties in soil design parameters. Model uncertainty is used to represent the uncertainty that occurs when applying statistical models to estimate soil design parameters following Baecher and Christian's model uncertainty. Model uncertainty reflects the uncertainty in the estimated true soil parameters and is dependent on the quantity of measurements available to establish the model. Data uncertainty is used to represent the variability of measurements and it is regarded to be the aleatory type of uncertainty as mentioned by Ang and Tang. Total uncertainty is the sum of model and data uncertainty and reflect the total uncertainty in design parameters which is the uncertainty in predicted design parameters. The research described in this thesis focuses on one category of the epistemic uncertainties—the uncertainty due to lack of data. Thus, the predominant focus of this research is on model uncertainty.

## 2.3 Alternative Methods for Design

Several different methods have been adopted to account for variability and uncertainty in design— the allowable stress design, load and resistance factor design, partial factor design and reliability based design. The allowable stress design (ASD)

approach has been, and continues to be, commonly applied in geotechnical engineering practice worldwide since 60s. Load and Resistance Factor Design (LRFD) methods have more recently been adopted in United States, particularly for design of transportation infrastructure. A similar approach, called the Partial Factors approach, has also recently been adopted in Europe and Canada. Finally, reliability-based design (RBD) directly incorporates more rigorous reliability analyses to evaluate and account for variability and uncertainty in design using probability theory. In the United States, load and resistance factor design (LRFD) is often implemented using probabilistically calibrated load and resistance factors; in such cases LRFD and RBD are clearly related.

### 2.3.1 Allowable Stress Design (ASD)

Allowable stress design is a traditional design method that has been widely applied in geotechnical engineering practice. The ASD approach usually adopts an empirical factor, termed the factor of safety (*FS*), to collectively account for all sources of variability and uncertainty in design (e.g., from design parameters, from design methods, etc.). For strength limit states, design is performed by requiring the estimated load(s) to be less than the value of ultimate resistance(s) divided by a factor of safety. The selected or required factors of safety vary depending on the specific design problem. A factor of safety of approximately 3.0 is usually considered to be adequate for foundation bearing capacity problems (Terzaghi et al., 1996), although values may range from 2 to 4 in cases where variability and uncertainty is particularly small or great. A factor of safety of 1.3 to 1.5 is commonly selected for slope stability problems and a factor of safety of approximately 2.0 is commonly required for design of earth retaining structures.

In practice, selection of a factor of safety in ASD is somewhat subjective and largely based on experience. The ASD approach does not always accurately and adequately account for the variability and uncertainty of load(s) and resistance(s); use of similar values for *FS* does not necessary produce the same reliability. For example, Meyerhof (1976) demonstrated that different probabilities of failure are obtained when designs are performed with different variability and uncertainty, even when using the same factor of safety (Figure 2.5). Christian and Urzua (2009) further complemented Meyerhof's figure by showing probabilities of failure calculated at different standard deviation values. The results illustrated that when the standard deviation is greater than approximately 0.3, the probability of failure is significantly reduced by decreasing the standard deviation, while increasing the factor of safety has minimal effects on the probability of failure (Figure 2.6).

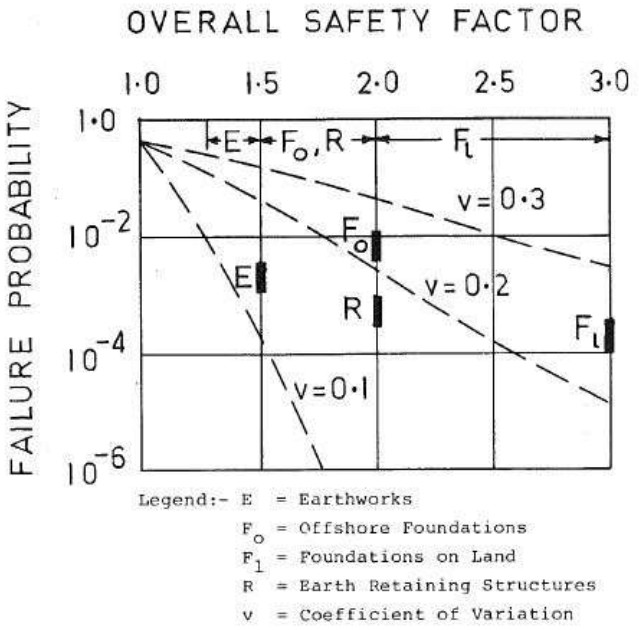


Figure 2.5 Calculated probabilities of failure for designs using different factors of safety with different soil variability (Meyerhof, 1976).

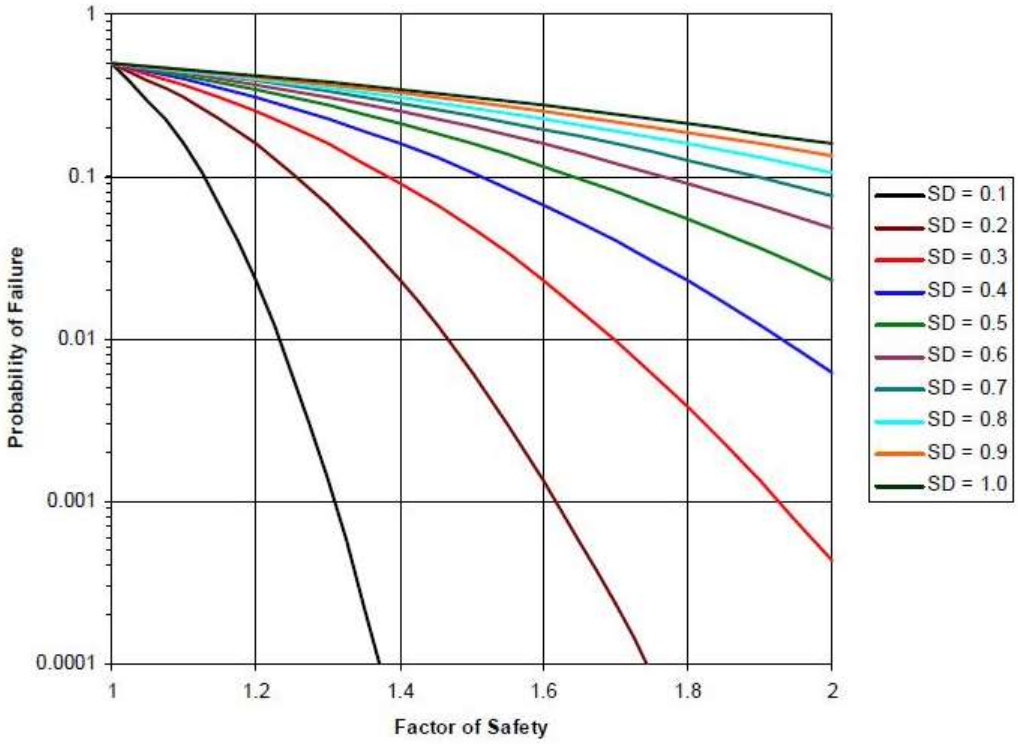


Figure 2.6 Probability of failure versus normal distributed factor of safety (Christian and Urzua, 2009).

### 2.3.2 Load and Resistance Factor Design (LRFD)

Load and resistance factor design (LRFD) is commonly considered to be a more rational and precise approach for design because it separately accounts for variability and uncertainty in load(s) and resistance(s), or components of loads and resistances by applying different load and resistance factors. The LRFD design criteria adopted by the American Association of State Highway and Transportation Officials (AASHTO, 2010) is commonly expressed as:

$$\phi \cdot R_n \geq \sum \eta_i \cdot \gamma_i \cdot Q_i \qquad \text{(Eq. 2.11)}$$

where $\phi$ is the resistance factor, $R_n$ is the nominal resistance, $\eta_i$ is load modifier to account for effects of ductility, redundancy and operational importance, $\gamma_i$ is a load factor and $Q_i$ is a specific load effect.

In LRFD, different load and resistance factors are commonly applied for different limit states to reflect differences in variability and uncertainty for different limit states, and to reflect different target reliabilities for different limit states. Limit states are conditions when a structure, or component ceases to fulfill the function for which it was designed. Five different classes of limit states are addressed in the AASHTO design specifications (AASHTO, 2010): strength limit states, service limit states, extreme event limit states, fatigue limit states and construction limit states. Strength limit states are further subdivided into the Strength I, Strength II, Strength III, Strength IV and Strength V limit states based on different applicable load combinations. Similarly, the service limit state is subdivided into the Service I, Service II and Service III limit states and the extreme event limit state is subdivided into the Extreme Event I and Extreme Event II limit states.

For design of spread footing foundations, performance is generally evaluated for appropriate strength limit states and the Service I limit state. Evaluations for the strength limit states include bearing resistance, sliding resistance, overturning resistance and structural capacity. Evaluations for the Service I limit state include settlement and overall stability.

### 2.3.3 Partial Factor Design

The partial factors design approach (CEN, 2004) is used for design in Europe and Canada. Partial Factors design applies different "partial" factors of safety to design parameters that contribute to load and/or resistance, rather than to the aggregate load and/or resistance as is done in LRFD. The motivation underlying the partial factor approach is that it is the variability and uncertainty in the design parameters that predominate

variability and uncertainty in design: thus, it makes more sense to apply factors to the parameters that contribute more significantly.

Considering ultimate limit state (similar to the strength limit states in U.S. practice), the partial factors design approach adopts different partial factors of safety that are applied to load(s) and strength(s) separately. Loads are multiplied by load partial factors to obtain design loads and strength parameters are divided by strength partial factors to obtain design strength parameters to calculate resistance:

$$\text{Factored load} = \text{Load} \times \text{Load partial factor} \qquad \text{(Eq. 2.12)}$$

$$\text{Factored Strength} = \frac{\text{Strength}}{\text{Strength partial factor}} \qquad \text{(Eq. 2.13)}$$

As illustrated in Figure 2.7, the resistance components commonly include the soil design parameters of cohesion intercept and angle of internal friction. Different partial factors are used to factor each parameter separately. The resulting factored parameters are then used to determine the factored resistance for design. Like LRFD, the Partial Factors design criterion is satisfied if the factored load does not exceed the factored resistance.

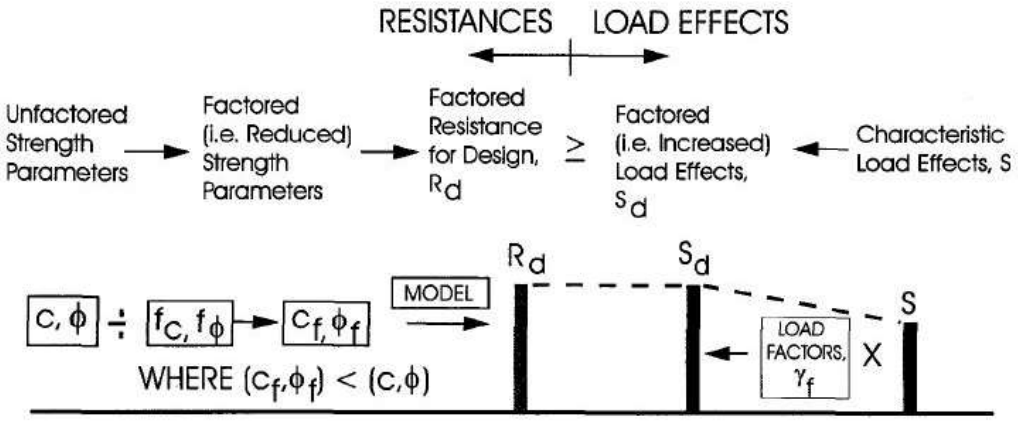


Figure 2.7 The European partial factor design approach (Becker, 1997).

### 2.3.4 Reliability Based Design (RBD)

Any design methods incorporating reliability analysis can be classified as reliability based design (RBD). To evaluate the design reliability, probability theory is applied to quantify design reliability in the form of the probability of failure. In such analyses, important design parameters and load components are modeled as random variables. The probability of failure implies adverse performance. In the United States, load and resistance factor design (LRFD) is often implemented using probabilistically calibrated load and resistance factors; in such cases LRFD and RBD are clearly related. In Europe and Canada, Partial Factor design sometimes adopts design parameters as random variables following specific distributions; in such cases Partial Factor and RBD are related. Phoon and Kulhawy have conducted comprehensive research on transmission line structures using load and resistance factor design. Phoon et al. (2003a; 2003b) have developed single and multiple resistance factors probabilistically at certain levels of reliability. Goh et al. (2003) used a neural network to model the limit state surface for reliability analysis. Griffiths and Fenton have adopted random field finite element to simulate soil properties and then performed reliability based analysis for research of stability of undrained clay slopes (Griffiths and Fenton, 2000), underground pillar stability (Griffiths et al., 2002), shallow foundation settlement (Fenton and Griffiths, 2005), shallow foundation bearing capacity (Griffiths and Fenton, 2001; Fenton and Griffiths, 2007; Fenton et al., 2008; Griffiths et al., 2002; Griffiths et al., 2006; Fenton et al., 2008), ultimate limit design for deep foundations (Fenton and Naghibi, 2011; Naghibi and Fenton, 2011), and retaining wall designs (Fenton et al., 2005). Gilbert have conducted research on reliability of offshore piles considering soil spatial variability (Gilbert et al., 1999).

## 2.4 Probabilistic Calibration of Factors for LRFD

For strength limit states, when considering load and resistance as random variables, the probability of failure can be determined with known mean and standard deviation of load and resistance. Given the probability density functions, the probability of failure can be graphically represented as shown in Figure 2.8.

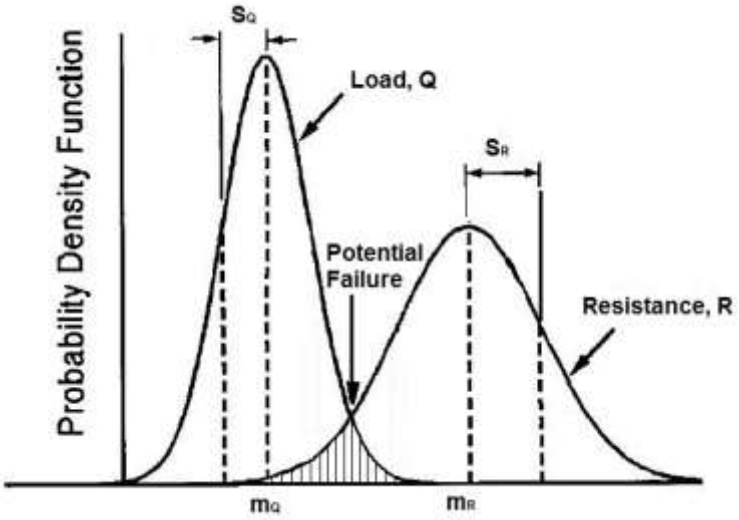


Figure 2.8 Probabilistic density function for normally distributed load and resistance (Modified from Phoon et al., 2003a).

For resistance, $R$ and load, $Q$, the limit state function $g(R,Q)$ and the failure probability, $p_f$ are expressed as:

$$g(R,Q) = R - Q \quad \text{(Eq. 2.14)}$$

$$p_f = p(R - Q < 0) = p(g < 0) \quad \text{(Eq. 2.15)}$$

As shown in Figure 2.9, the safety margin, $M = R - Q$, will be normally distributed with mean, $m_M$, and standard deviation, $s_M$, when the load and resistance are both normally distributed.

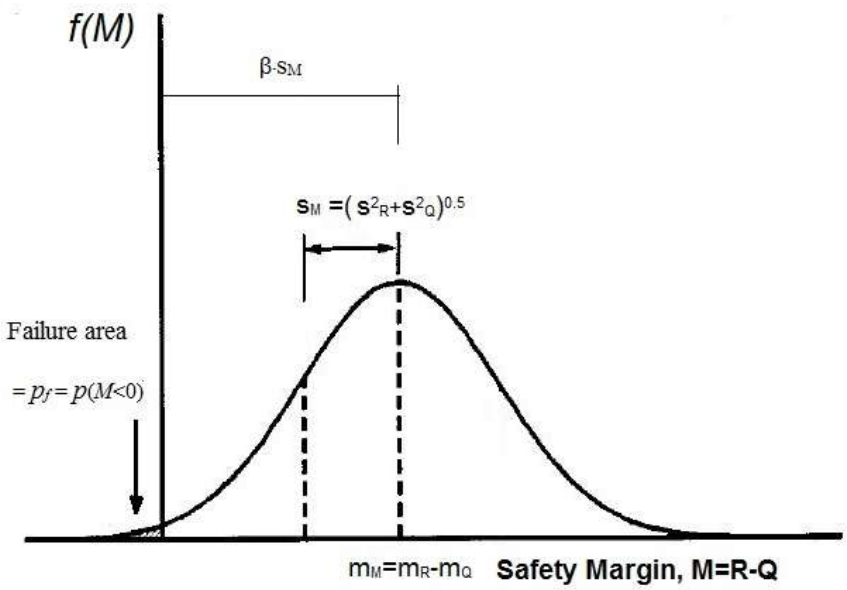


Figure 2.9 Safety margin with normally distributed load and resistance (modified after Phoon, et al., 2003a).

The mean and standard deviation of the safety margin can be calculated as:

$$m_M = m_R - m_Q \quad \text{(Eq. 2.16)}$$

$$s_M^2 = s_R^2 + s_Q^2 \quad \text{(Eq. 2.17)}$$

where $m_M$ and $s_M^2$ are the mean and variance of *M*, respectively, $m_R$ and $s_R^2$ are the mean and variance of *R*, respectively, and $m_Q$ and $s_Q^2$ are the mean and variance of *Q*, respectively. Thus, the probability of failure can be calculated as:

$$p_f = p(R < Q) = p(R - Q < 0) = P(M < 0) = \Phi(-\frac{m_M}{s_M}) \quad \text{(Eq. 2.18)}$$

The reliability index, $\beta$, defined as the number of standard deviations of *M* between the mean of *M* and the origin (Figure 2.9) is often used as an alternative to the probability of failure to represent the degree of reliability. The reliability index is related to the probability of failure as:

$$\beta = -\Phi^{-1}(p_f) = \Phi^{-1}(1 - p_f) = \frac{m_M}{s_M} = \frac{m_R - m_Q}{\sqrt{s_R^2 + s_Q^2}} \quad \text{(Eq. 2.19)}$$

The reliability index increases when $p_f$ decreases. Considering the traditional ASD factor of safety, $FS$, and the reliability index can also be calculated from a reliability assessment as (Figure 2.10):

$$\beta = \frac{m_{FS}-1}{\sqrt{(m_{FS}\cdot COV_R)^2+COV_Q^2}} \qquad \text{(Eq. 2.20)}$$

where $m_{FS} = m_R/m_Q$ is the mean value of the factor of safety, $COV_R = s_R/m_R$ , is the coefficient of variation for resistance, and $COV_Q = s_Q/m_Q$ is the coefficient of variation for load.

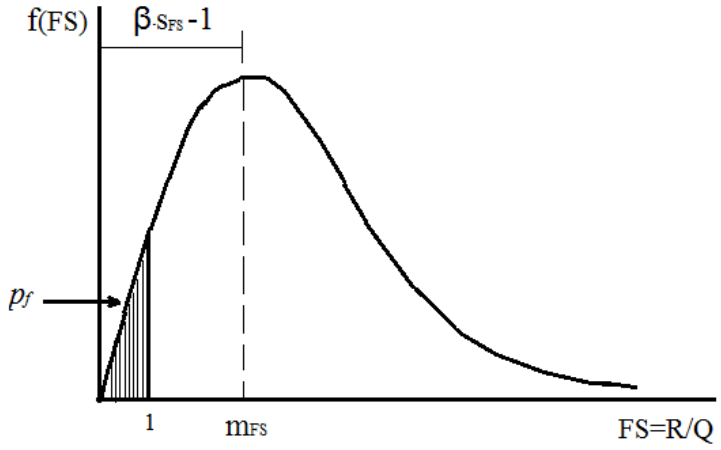


Figure 2.10 Reliability index with factor of safety (modified after AASHTO, 2010).

When resistance and load are lognormally distributed, the reliability index is similarly calculated as:

$$\beta = \frac{ln\left(\frac{m_R}{m_Q}\sqrt{\frac{1+COV_R^2}{1+COV_Q^2}}\right)}{\sqrt{ln\left[(1+COV_R^2)\cdot(1+COV_Q^2)\right]}} = \frac{ln\left(m_{FS}\cdot\sqrt{\frac{1+COV_R^2}{1+COV_Q^2}}\right)}{\sqrt{ln\left[(1+COV_R^2)\cdot(1+COV_Q^2)\right]}} \qquad \text{(Eq. 2.21)}$$

Equations 2.20 and 2.21 are simplified for cases where variability and uncertainty in the loads and resistances are lumped together. However, in many cases foundation resistance is derived from several components that may include foundation weight, side

resistance, tip resistance, etc. and each of these components may have different variability and uncertainty. In such cases, lumping the variability and uncertainty together and using a single factor may not accurately represent the variability and uncertainty in the total resistance. Several methods are available to better approximate the true value of reliability index and probability of failure, where the most widely used ones are the first order second moment (FOSM) method, the Hasofer-Lind (FORM) method and the Monte Carlo (MC) simulation method.

The first order second moment (FOSM) method first defines the variables, *X*, which contribute to variability and uncertainty. The FOSM method then uses the first and second terms of a Taylor series expansion to estimate the mean and variance of a performance function *F* to calculate the probability of failure and reliability index:

$$E(F) \cong F(X_1, X_2, \dots, X_n) \qquad \text{(Eq. 2.22)}$$

$$\sigma_F^2 \cong \sum_{i=1}^{n} \sum_{j=1}^{n} \frac{\partial F}{\partial X_i} \frac{\partial F}{\partial X_j} \rho_{X_i X_j} \sigma_{X_i} \sigma_{X_j} \qquad \text{(Eq. 2.23)}$$

The Hasofer-Lind approach or first order reliability method (FORM) uses random variables that are reformulated into dimensionless variables, $x_i' = (x_i - \mu_{x_i})/\sigma_{x_i}$. Dimensionless variable as axes are then defined using geometrical interpretation and a critical surface or line of the safety margin is determined. Finally, the shortest distance from the critical surface to the origin is calculated to be the reliability index. The Lagrangian multiplier approach and Taylor series are usually used to solve the nonlinear algorithm.

The Monte Carlo (MC) simulation method uses statistical parameters of random variables to randomly generate a great amount of data that simulate possible values of all probabilistic variables and then performs calculations using those generated values to

simulate potential outcomes. This process is a repeated sampling of the stochastic process and the output is then analyzed statistically to determine a probability of failure or related measure of reliability. With sufficient numbers of simulations, the output can reach high accuracy and precision for further study. The Monte Carlo method is very powerful, since it can simulate any probability density distribution and consider different correlation structures inside and between random variables.

## 2.5 Influence of Small Number of Measurements or Inadequate Site Information

No matter what design method is applied, obtaining adequate site information is essential to effective design. Adequate site information plays an important role in engineering design by providing a reasonable understanding of local site conditions and suitable methods for evaluating soil design parameters that accurately reflect the true soil properties. Littlejohn et al. (1994) concluded that inadequate site investigation may put projects at risk. Inadequate site investigation may also cause costly, overdesigned foundations and expensive problems (Temple and Stukhart, 1987).

The true uncertainty is always unknown but it can be reduced by more extensive exploration (Christian and Urzua, 2009). With more measurements, there is more confidence that design parameters will reflect the true soil properties of the site and design parameters will have less uncertainty and more accuracy thus leading to more appropriate designs. More borings, more samples and more tests are generally desirable. However, it is impractical to sample all soils at a site; moreover, due to limitations of site conditions, time and budget, it is seldom feasible to obtain as many measurements as engineers would like. Thus, soil design parameters interpreted from small numbers of measurements may not accurately represent the true soil properties. The worst scenario is that the estimated

soil properties are seriously in error, thus creating a false confidence in the soil design parameters (Tversky and Kahneman, 1971; Baecher, 1982; Baecher, 1983; Littlejohn et al., 1994; Phoon and Kulhawy, 1999b; Christian, 2004; Mitchell, 2009; Baecher et al., 2010).

Christian (2000) determined that, in order to obtain 90% confidence that the observed values represent 99% of the population, at least 388 tests are needed. As shown in Figure 2.11, with 60 independent measurements, there is only 10% confidence that 99% of the population will be observed; however, there is 80% confidence that 95% of the population will be included by observed values and almost 100% confidence that 90% of population will be represented by observed values. With only ten independent measurements, there is a negligible chance that 99% of population can be represented, 10% probability that 95% of population can be represented, 20% chance that 90% of population can be represented and about 40% probability that 80% of population can be represented by the ten independent measurements.

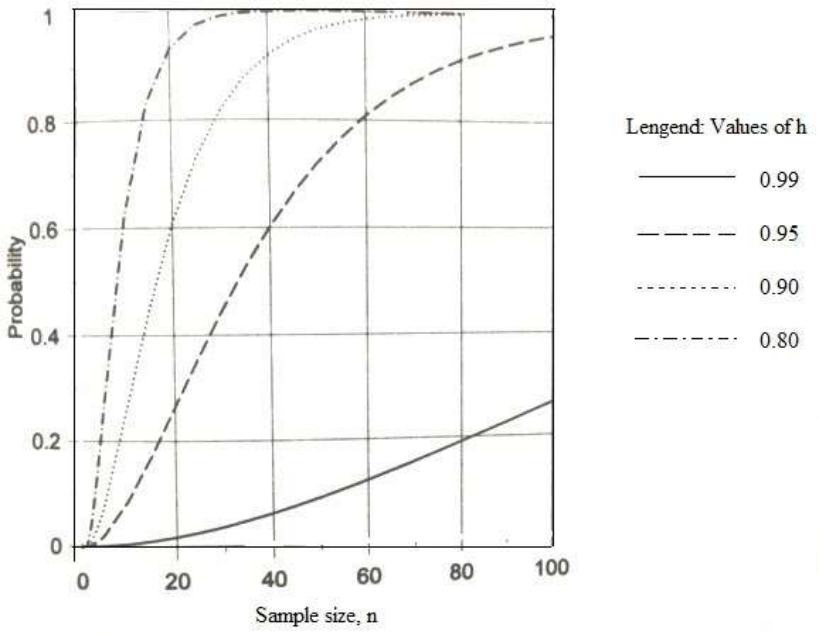


Figure 2.11 Probability of capturing *h* fraction of the distribution in a sample of *n* statistically independent tests (Christian, 2000).

Since small numbers of measurements are unlikely to represent the total population, the uncertainty in soil design parameters interpreted from small numbers of measurements may be either underestimated or overestimated. This leads to the potential for unconservative or over conservative designs that do not accurately account for the variability and uncertainty present for a particular case. When performing foundation designs, if the uncertainty in soil design parameters interpreted from a small number of measurements is less than the true uncertainty, the design is likely to be unconservative and may have performance problems. In contrast, if the uncertainty in soil design parameters interpreted from a small number of measurements is greater than the true uncertainty, the design may be over conservative and cost much more than necessary. These issues are complicated when considering that prudent engineers will rightfully introduce additional conservatism for design when confidence in interpreted design parameter is low. Nevertheless, interpretation of design parameters from small numbers of measurements increases the likelihood of producing unconservative or over conservative designs.

Goldsworthy (2006) conducted comprehensive research in his doctoral thesis to quantify the risk of geotechnical site investigation under the advisement of Jaksa. Goldsworthy's work emphasized the effect of site investigation on the settlement of pad foundations. To fulfill the purpose of research, Goldsworthy simulated a site with dimensions of $30\text{m} \times 30\text{m}$ and a depth of 50m using a 3D random field model. Each finite element was $0.5\text{m} \times 0.5\text{m} \times 0.5\text{m}$ in the model. This site was called a full acknowledge site.

Goldsworthy then used a site investigation plan locating within a $20\text{m} \times 20\text{m}$ area. Each single sampling location in the area reflected a vertical borehole with 60 measurements of elastic moduli, *E*, from cone penetration test (CPT) spaced at 0.5m. The uncertainty was calculated as the total uncertainty which included natural variability, measurement error and transformation error. The foundation was designed using Schmertmann's settlement method (1978).

The design parameter used to calculate foundation area was obtained from site investigation plan. The designed foundation area was further compared with the optimal foundation area sized using full knowledge of the entire 3D random field model. If the foundation area was larger than the optimal foundation area, it was regarded as over design, whereas, if the foundation area was smaller than the optimal foundation area, it was regarded as under design. Goldsworthy avoided using probability of failure in his research, however, the probability of under designs is equivalent to the probability of failure. Goldsworthy and Jaksa (Goldsworthy et al., 2004; 2005; 2006; 2007; Jaksa et al., 1997; 2003; 2005) concluded that increasing the number of sampling locations will result in:

- The probability of under design increases and the probability of over design decreases with more sampling locations. The probabilities of under and over designs are relatively constant when more than 10 sampling locations are considered.
- The probability of optimal design rises as the number of sampling locations increases and the probability increases at the same rate for each soil conditions investigated.

- For soil with $COV$ less than 20%, the probability of under design (probability of failure) is hardly affected by increasing the number of sampling locations.

Goldsworthy explained that the probability of under design (probability of failure) increasing with more sampling locations was due to the fact that standard deviation of design parameter, *E*, had been reduced by increasing sampling locations. Use of the reduced parameter would size a smaller average total foundation area, thus, causing more under designed foundations. However, the underlying reason for this result was that the sampling domain in the random filed model was small, thus the variability of design parameters calculated from sampling was usually smaller than the soil variability of the random field model.

Goldsworthy (2006) also compared results using different testing types —Cone Penetration test (CPT), Dilatometer test (DMT), Standard penetration test (SPT) and Triaxial test (TT). In the vertical direction of each sampling location, CPT measurements were located at every 0.5 m, DMT measurements were located at every 1.5 m, SPT were located at every 1.5 m, and TT measurements were located at every 15 m. The results showed that SPT provided lowest probability of under design and highest probability of over design. DMT and CPT had similar probabilities for both under design and over design. TT was highly affected by increasing sampling locations, while, SPT was least affected by increasing sampling locations. Goldsworthy recommended to select a test type with a low transformation model error (i.e., TT) when the number of sampling locations is large and to pick a test type with a low measurement error (i.e., SPT) when the number of sampling locations is small. Goldsworthy further conducted risk analysis by assigning cost of foundation system and foundation failure and concluded that improving site investigation

to obtain more information will reduce the risk of foundation failures and thus reduce the penalty cost of failure (Goldsworth et al., 2004; 2007).

In practice, it is relatively uncommon for engineers to obtain as much site information to perform design and construction as is desired. Based on engineering experience and local practices, different engineers may have different confidence levels in interpreted results from small numbers of measurements. In some cases, soil parameters interpreted from small numbers of measurements might be regarded as being representative of true site conditions. However, things are not always what they seem, and engineers may not truly know as much as they think (Baker, 2010). Several different approaches may be considered to compensate for having insufficient site information and to improve confidence that designs will perform acceptably despite having small numbers of measurements. Those approaches can be categorized into: (1) use of characteristic design value, (2) use of greater uncertainty, and, (3) use of engineering judgment and conservative design.

- Use of characteristic design value

Becker (1997) mentioned that in the absence of information for statistical purposes, a characteristic value that represents the engineers' best estimate of likely value may be used for design. One possible interpretation is to choose the value at which 75% of total population of measurements is greater than the value. In Eurocode 7, the strength value used for design is the characteristic value that is the 95% lower bound value (CEN, 2004). Gilbert et al. (2000) applied nominal bias factor to nominal design values of resistance and load using maximum value of factored load and minimum value of factored resistance.

Najjar and Gilbert (2009) further applied a mixed probability distribution of capacity and use the lower bound of capacity values instead of using mean capacity values.

- Use of greater uncertainty

When soil data or site specific information is limited, guidelines on the probable range of coefficient of variation is very useful (Phoon and Kulhawy, 1999a). Duncan (2000) used a simplified method to estimate the standard deviation for a soil property called the $6\sigma$ method, which assumes that the standard deviation is equal to the range of values divided by 6. Based on Duncan's $6\sigma$ method, a modified $6\sigma$ method (Foye et al., 2006a) was applied as the $N\sigma$ method when relatively few measurements are available. The standard deviation is taken to be equal to the range of values divided by $N_\sigma$ where $N_\sigma$ depends on the number of measurements. The method was further applied to find the 80% exceedance line below the regression line of mean strength and then uses the reduced value where 80% of data is said to lie above it for conservatism in case of limited data (Foye et al., 2006b).

Most recently, Loehr et al. (2011a) applied a penalty function to have greater uncertainty in design parameters when the number of measurements is small. The penalty function uses an uncertainty modifier, $\zeta$, to multiply standard deviation, $\sigma$, where $\zeta$ is greater than one and depends on the number of measurements. The penalty function will be discussed in details in Chapter 8.

Shirato et al. (2003) adopted an alternative way of using greater uncertainty. Shirato applied a modification factor on the slope parameter ($\beta_1$) of regression model (intercept parameter, $\beta_0$= 0). The regression model was developed based on available test data of vertical load test on pile. The modification factor was developed by using mean value of

$\beta_1$ divided by lower limit value of $\beta_1$. The modification factor is affected by the number of test data and the value is greater than one.

- Use of engineering judgment and conservative design

Christian (2004) summarized three methods when uncertainty is unknown: (1) adopt excessively conservative factor of safety, (2) make assumptions using average experience, and (3) use Peck's observational method (1969) to start based on information secured, gradually collect information and update design during construction.

Griffiths and Fenton (2006) used random field finite element method to analyze bearing capacity of footings. The results indicated that since the correlation length is generally unknown at a site, when there is no more information available, use of the worst-case correlation length will provide conservative estimates of probability of bearing failure. The worst-case correlation length was further selected to predict the bearing capacity of spatially random soils using random field finite element method (Fenton and Griffiths, 2003). Fenton and Naghibi concluded that since correlation length is very hard to estimate and is unknown for most sites, the lowest resistance factor obtained at the worst correlation length should be used (Fenton and Naghibi, 2011; Naghibi and Fenton, 2011).

When the site is not well known, engineers tend to design conservatively to ensure enough safety. However, overconservatism is often most wasteful than is realized and leads to less satisfactory solutions (Peck, 1977).

## 2.6 Summary

In this chapter, existing work in areas of uncertainty of soil properties, alternative methods for designs and design using small numbers of measurements has been summarized. The uncertainty of soil design parameters has been categorized into aleatory

uncertainty and epistemic uncertainty where the aleatory uncertainty is the soil natural variability and epistemic uncertainty is mainly due to lack of knowledge. The definition of model uncertainty— one subcategory of epistemic uncertainty— is not in agreement among different researchers and is sometimes confusing. In this thesis, model uncertainty refers to statistical uncertainty introduced when adopting statistical models to estimate soil parameters, which reflects the uncertainty in estimated mean value of soil parameters.

The awareness of importance of performing effective site characterization has gradually been raised. The uncertainty in soil design parameters interpreted from a small number of measurements may be either under-estimated or over-estimated, causing foundation designs to be either at risk or costly. However, there is few studies on how the reliability of foundations, especially for designs using Load and Resistance Factor Design, is affected by the number of measurements quantitatively.

Furthermore, when conducting designs using small numbers of measurements or insufficient site information, engineers usually choose to design conservatively to ensure enough safety of foundations. However, foundations should not be designed conservatively without control. The research described in this thesis proposes a rational approach based on statistical inference for use of greater uncertainty in design parameters.

# Chapter 3 Laboratory Measurements for Field Test Sites

## 3.1 Introduction

To evaluate the effect of the number of measurements on the reliability of shallow foundations designed using Load and Resistance Factor Design (LRFD), empirical data were acquired from several soil sites. In this research, undrained shear strength measurements were used for design. The measurements were obtained from laboratory unconsolidated-undrained (UU) type triaxial compression tests using soil specimens acquired from a comprehensive site characterization program. The site characterization program is described in this chapter. General site conditions present at each of the sites are presented along with results from laboratory measurements performed on specimens from each site. Only undrained shear strength measurements are used in research, however, measurements from other types of testing are introduced to illustrate the site conditions and the scope of the site characterization projects.

## 3.2 Scope and Objectives for Site Characterization Program

The comprehensive site characterization project was jointly conducted by researchers from the University of Missouri (MU), Missouri University of Science and Technology (Missouri S&T), and the Missouri Department of Transportation (MoDOT). An important objective of the site characterization and testing program was to evaluate variability and uncertainty of soil parameters established from improved site characterization practices, with particular focus on implementation within the context of Load and Resistance Factor Design (LRFD). Four soil sites—the Pemiscot site, the St.

Charles site, the New Florence site and the Warrensburg site—were selected to generally represent soil conditions in Missouri where site characterization methods could potentially be modified to improve design practice. At each site, a relatively large number of high quality soil samples were obtained and tested to measure common geotechnical engineering design parameters. Additional "rock sites" were also characterized similarly, but these efforts are beyond the scope of the present work.

The locations of selected soil testing sites are shown in Figure 3.1. Each site represents one physiographic region in Missouri. The Pemiscot soil site is an alluvial site composed predominantly of soft, fat clays and is located in Pemiscot County in southeastern Missouri near the city of Hayti Missouri, within the Coastal Plain physiographic region. The site is located adjacent to Missouri Highway 412 near an elevated section of the roadway. Three borings were performed at the Pemiscot site.


Figure 3.1 Locations of four testing sites.

The St. Charles site is composed of soft, fat clays overlying alluvial sands and is located near St. Charles Missouri (St. Louis metropolitan area), within the Till Plain

physiographic region. The site contains an existing raised interchange along Missouri Highway 370, and is bound by Elm Street/Newtown Boulevard to the west and the MO370 on/off ramps to the north and south. The St. Charles site is an alluvial site located near the confluence of the Missouri and Mississippi rivers. Three borings were conducted at the St. Charles site.

The New Florence site is located in the Dissected Till Plain physiographic region at the interchange (Exit 175) for Interstate 70 at Missouri Highway 19 near the town of New Florence Missouri. The New Florence site is an "upland" site composed of relatively stiff clay overlying sandstone, limestone and/or shale bedrock. Several borings were performed at the New Florence site.

The Warrensburg site is composed of generally soft, silty soils overlying shale, sandstone, or limestone bedrock. The Warrensburg site is located in the Western Plain physiographic region, along a portion of a new bypass for Missouri Highway 13 around the city of Warrensburg, Missouri. Sampling and testing for the current work was performed prior to construction of a new overpass that crosses waterways and railroads in the vicinity of the boring locations. Borings for the present work were located along the new roadway alignment, just south of U.S. Highway 50. Three borings were conducted at the Warrensburg site.

At each site, both state of the art and state of the practice sampling and testing techniques were adopted to allow for comparison of variability and uncertainty that may be introduced by different sampling and testing methods. The test results used for the current work are those determined following state of the art practices, as described in more detail in the subsequent section.

## 3.3 Boring and Sampling Methods

A common goal for boring and sampling projects is to obtain high quality soil samples that can be used to establish soil engineering parameters that reflect the true site conditions. However, soil property measurements can be significantly affected by disturbance introduced during the process of sampling and testing that may increase uncertainty in laboratory measured soil parameters (Ladd and Lambe, 1963). Moreover, disturbance will often lead to conservative estimates of soil engineering parameters, and thus, conservative designs that may be more costly than necessary. The primary motivation for improving site characterization practices is, therefore, to reduce bias and uncertainty in estimated soil parameters.

Great uncertainty can be introduced during boring, sampling and testing procedures, in order to control these uncertainty at a consistent level, sampling disturbance need to be minimized. State of the art sampling techniques (Santagata and Germaine, 2002; Ladd and DeGroot, 2003; DeGroot et al., 2005; Hight, 2003) were conducted to minimize disturbance which involve:

- Using heavy drilling mud to maintain borehole stability and reduce the magnitude of stress relief during boring and sampling;
- Using large diameter, thin-walled, fixed-piston samplers with sharp cutting edges;
- Careful handling, transportation, and storage;
- Transporting and storing sampling tubes vertically;
- Storing samples in a high humidity environment with controlled temperature;

- Careful extraction of samples from sampling tubes that generally includes cutting of the tubes, breaking bonds at the soil-tube interface, and extruding the sample in the same direction as sampling in the field;
- Trimming of specimens to remove soil that has been distorted; and
- Testing specimens as soon after sampling as possible.

Three different types of borings, designated as "research" borings, "sister" borings, and "historical" borings, were completed for the site characterization program (Ding et al., 2014). All research borings were completed using "state of the art" drilling, sampling, and testing procedures whereas all sister and historical borings were completed using "state of the practice" drilling, sampling, and testing procedures. Only measurements from the research borings are presented and used for research described in this thesis and uncertainty introduced during boring, sampling and testing is assumed to be controlled at a consistent level.

All research borings were advanced using rotary wash boring methods with samples obtained using an Osterberg hydraulic piston sampler. Rotary wash boring methods were selected to reduce disturbance resulting from stress relief and to facilitate removal of cuttings. Drilling slurries consisting of mixtures of water and powdered bentonite were used to produce drilling slurry with suitable viscosity and density. Periodic measurements of Marsh Funnel viscosity and slurry density were taken for quality control of the drilling fluid consistency. A 3-inch diameter Osterberg hydraulic piston sampler with continuous sampling was used to obtain samples with a 2.5 ft push followed by cleanout with a tri-cone bit before attempting a subsequent sample. At the New Florence site, where the soil profile includes stiff clays and silts, use of rotary wash boring methods proved to be

problematic, thus, hollow stem auger boring methods were applied at this particular site. When soil at the New Florence site became too stiff for sampling with the Osterberg sampler, samples were acquired by pushing conventional 3-inch diameter Shelby tubes. In the stiffest soils, a 3-in diameter Pitcher sampler was utilized. Drilling and sampling at each of the four sites were completed within a two-week time interval such that samples could generally be considered time invariant.

Sample tubes acquired from the research borings were carefully handled and double-sealed on both ends with O-ring compression seals and plastic caps to prevent moisture loss during transportation and storage. All sample tubes were stored vertically in padded containers for transport to one of two laboratories for testing. Upon arrival at the laboratories, sample tubes were stored in a refrigerated and humidified environment until specimens were cut from the tubes and trimmed for testing.

## 3.4 Laboratory Testing Methods

Four types of laboratory performance tests were performed on soil samples acquired from each site: unconsolidated-undrained (UU) type triaxial compression tests, constant rate of strain (CRS) type one-dimensional consolidation tests, consolidated-undrained ($\overline{CU}$) type triaxial compression tests with pore water pressure measurements and constant volume direct simple shear (DSS) tests. At least two UU tests, one CRS test and one $\overline{CU}$ test were performed on soil samples selected from each tube. Additional laboratory tests were also performed for each tube to allow for characterization of the respective samples. These tests included Atterberg Limits tests, hydrometer tests, specific gravity tests and X-ray diffraction (XRD) tests.

### 3.4.1. Unconsolidated-Undrained (UU) Type Triaxial Compression Tests

Unconsolidated undrained (UU) type triaxial compression tests were conducted on materials sampled from each of the four sites following American Society for Testing and Materials (ASTM) standard D2850 (Figure 3.2). Specimens were carefully trimmed to create cylindrical specimens with 1.5 inch diameter and 3 inch height. A thin-layer latex membrane was carefully placed around the specimen using a membrane expander and two o-rings were placed on the top and bottom caps, respectively. With all drainage lines closed, the triaxial cell was assembled and slowly filled with water. After applying a cell pressure equal to the estimated in-situ vertical total stress for the depth where the specimen was taken. Specimens were then sheared to failure at a strain rate of 1%/min.

(a) (b) (c) (d)

Figure 3.2 UU type triaxial compression test: (a) specimen trimming, (b) after trimming, (c) setting specimen in the cell, and (d) after shearing.

### 3.4.2. Constant Rate of Strain (CRS) Type 1-D Consolidation Tests

Constant Rate of Strain (CRS) type 1-D consolidation tests were performed on trimmed soil specimens following ASTM D4186. After breaking the soil-tube interface using a wire saw and extruding the sample, specimens for CRS tests were carefully trimmed into a 2.5-in diameter sharp-edge steel consolidation ring. Boiled and cooled

porous stones were set on the top and at the bottom of the specimen along with saturated filter paper. The cell was locked and a seating load was applied to prevent the specimen from swelling after the cell was filled with de-aired water. The cell and base pressures were then gradually increased to 30 psi to saturate the soil specimen. A quick B-check was performed to check for saturation. After saturation, the specimen was consolidated at a constant rate of strain for a loading-unloading-reloading-unloading sequence. The rate of strain was slightly adjusted to keep a base excess pore water pressure ratio ($\Delta u/\sigma_v'$) in the range of 3%-15% and was constant throughout loading.

3.4.3. Consolidated-Undrained ($\overline{\text{CU}}$) Type Triaxial Compression Tests

Consolidated-undrained ($\overline{\text{CU}}$) type triaxial compression tests with pore water pressure measurements were performed in general accordance with ASTM D4767 (Figure 3.3). The trimmed, 1.5-inch diameter cylindrical specimens were carefully wrapped with filter paper strips and placed in the triaxial cell. After placing the porous stones and filter paper, thin latex membranes were placed around the specimen and sealed with O-rings against the top and bottom platens. Drainage lines were connected to both ends of each specimen. The triaxial cell was then gradually filled with water. Cell pressure and back pressure were applied to the sample using de-aired water for saturation. The effective stress during the saturation stage was kept at 5 psi. Specimen $B$-values (Skempton, 1954) were checked daily until the specimen was fully saturated with a $B$-value of 0.97-1.0.

Following saturation, specimens were isotropically consolidated to stresses greater than twice the preconsolidation stress, then unloaded to some target effective stress following SHANSEP procedures to achieve a specified target overconsolidation ratio ($OCR$) and to minimize effects from sample disturbance (Ladd and DeGroot, 2003).

Volume changes during consolidation were measured using a 1 mL pipette on a pressure panel board. Following consolidation, the specimen height was measured and the specimen was sheared under undrained conditions at a shear rate of $\left(\frac{4\%}{10 \cdot t_{50}}\right)$. Target $OCR$s generally ranged from 1.0 (normally consolidated) to 7.5 for specimens from the Warrensburg, St. Charles, and Pemiscot sites. Specimens from the New Florence site were not consolidated following SHANSEP procedures, but were simply consolidated to target effective stresses greater than preconsolidation stress in a single consolidation increment.

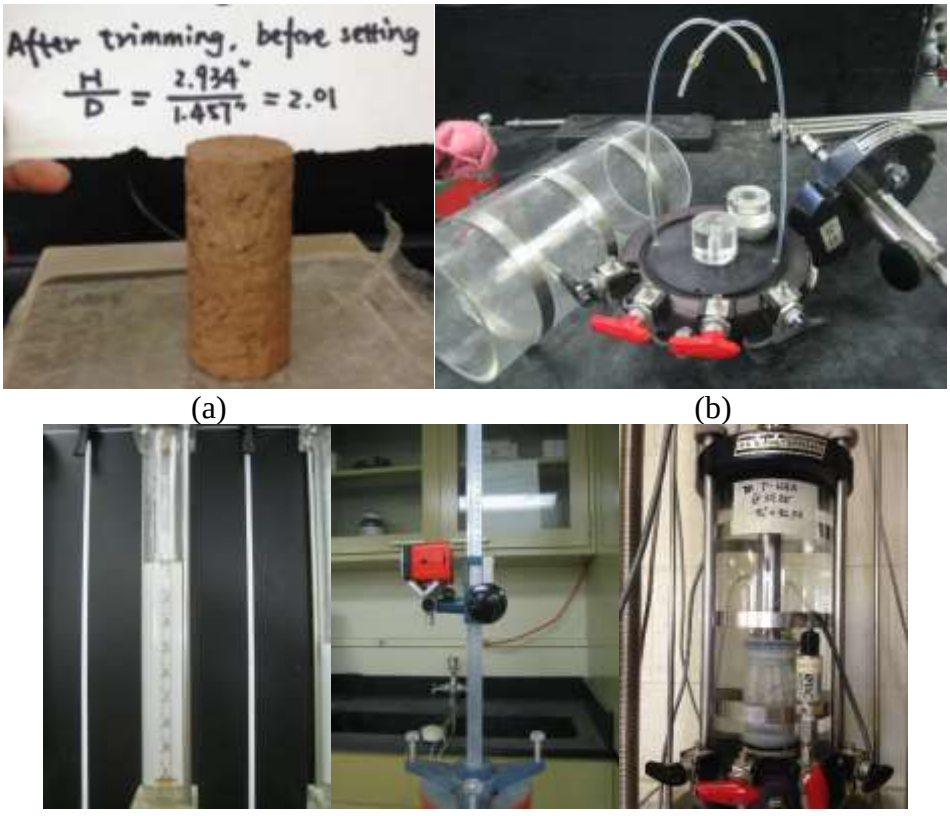


(a) (b)

(c) (d) (e)

Figure 3.3 $\overline{CU}$ type triaxial compression test: (a) specimen after trimming, (b) triaxial cell, (c) pipette used to measure volume change during consolidation, (d) device to measure specimen height after consolidation, and (e) specimen being sheared.

3.4.4. Direct Simple Shear (DSS) Tests

Constant volume direct simple shear tests were performed on samples acquired using state of the art sampling techniques at the St. Charles site following ASTM D6528 (Figure 3.4). Specimens with a height of 0.7 inch and diameter of 2.6 inch were sealed in a latex membrane and confined by a set of steel rings. Test specimens were consolidated to stresses greater than twice the preconsolidation stress, then unloaded to some target effective stress with a specified target $OCR$. Specimens were consolidated to $OCR$'s between 1.0 and 8.0. After consolidation, specimens were sheared at a rate of $\left(\frac{4\%}{10 \cdot t_{50}}\right)$ while maintaining a constant sample height to simulate consolidated-undrained conditions.

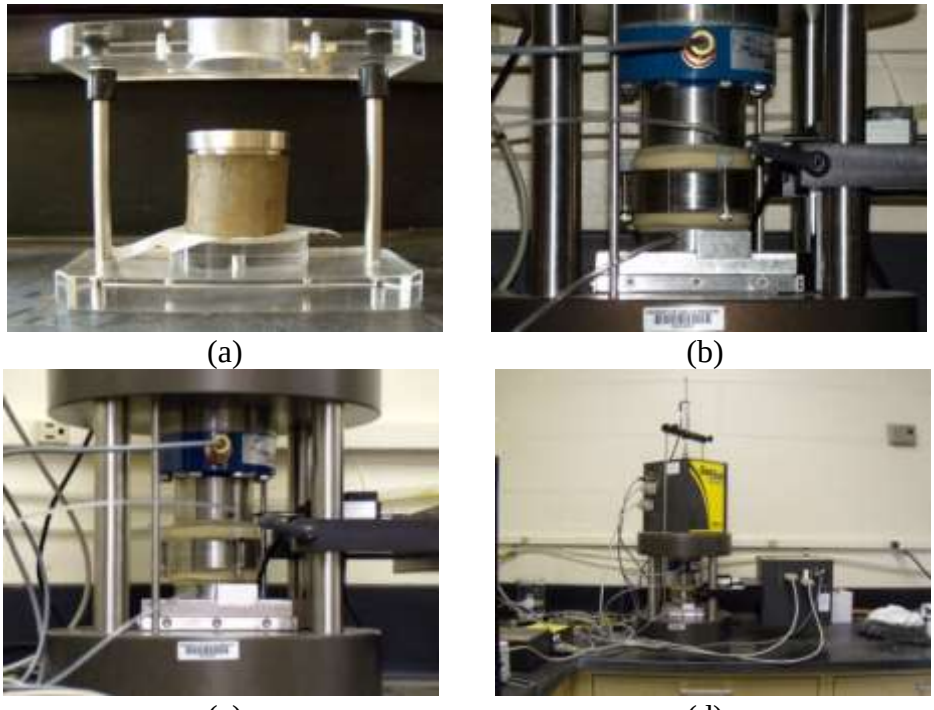

(a) (b) (c) (d)

Figure 3.4 Direct simple shear test: (a) sample prepared for trimming, (b) assembled apparatus, (c) testing, and (d) testing system.

## 3.5 Laboratory Measurements for Pemiscot Site

Three borings designated as P-B2, P-B5 and P-B7, were completed at the Pemiscot site at the locations shown in Figure 3.5. Soil samples obtained from borings P-B2 and P-B7 were transported to the MU laboratory for testing and are presented herein. Testing of samples from P-B5 were conducted at another laboratory; results of these tests are not included in this thesis.

General soil profiles, measured natural water contents ($w_n$) and Atterberg limits ($w_P$ and $w_L$), specific gravity ($G_s$), total unit weight ($\gamma_T$) and undrained shear strength ($s_u$) are plotted in Figure 3.6. The Pemiscot site is an alluvial site composed predominantly of soft, fat clays. This site is composed of 69 feet of soft clay overlying alluvial sands. The ground water table at this site was located near the ground surface at a depth of approximately 3.2 feet. Mean specific gravity was 2.72 and the average total unit weight was 103 lb/ft$^3$.

Figure 3.5 Pemiscot site boring locations.

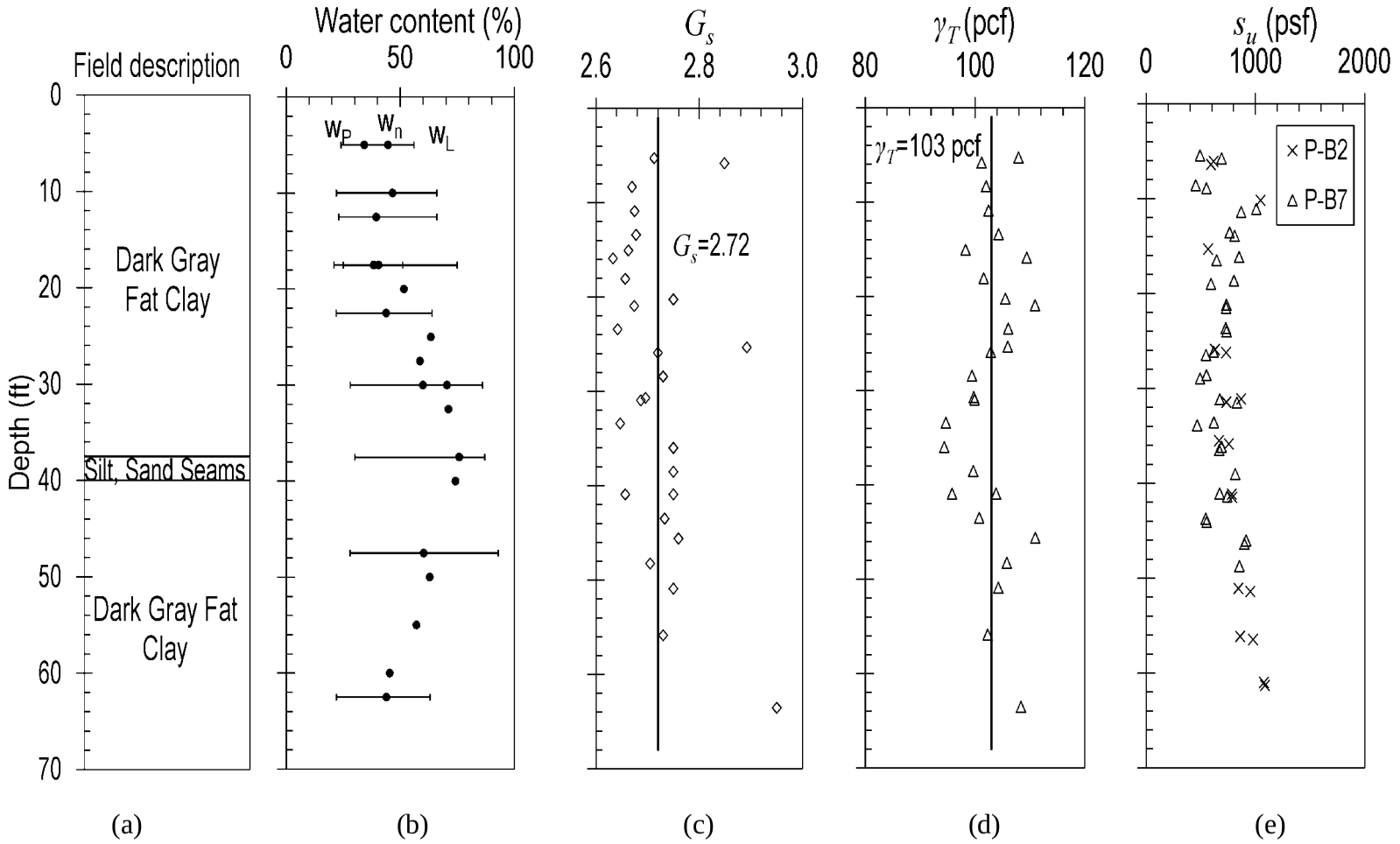


Figure 3.6 Laboratory measurements for the Pemiscot site: (a) field description, (b) water content and Atterberg Limits, (c) specific gravity, (d) total unit weight, and (e) undrained shear strength.

Measurements of preconsolidation stress ( $\sigma_p'$ ), compression index ( $C_c$ ), recompression index ($C_r$) and coefficient of consolidation ($c_v$) are plotted versus depth in Figure 3.7. These measurements show that the soil at the Pemiscot site is over-consolidated to depths of approximately 50 feet, with $OCR$ generally decreasing with increasing depth from values of approximately 8.0 near the ground surface to 1.0 at a depth of approximately 50 feet. The average compression index is 0.45 for soils above 30 feet and 0.808 for soils below 30 feet. The average recompression index is 0.063 over the entire depth range. The mean coefficient of consolidation is 4.9 ft$^2$/day.

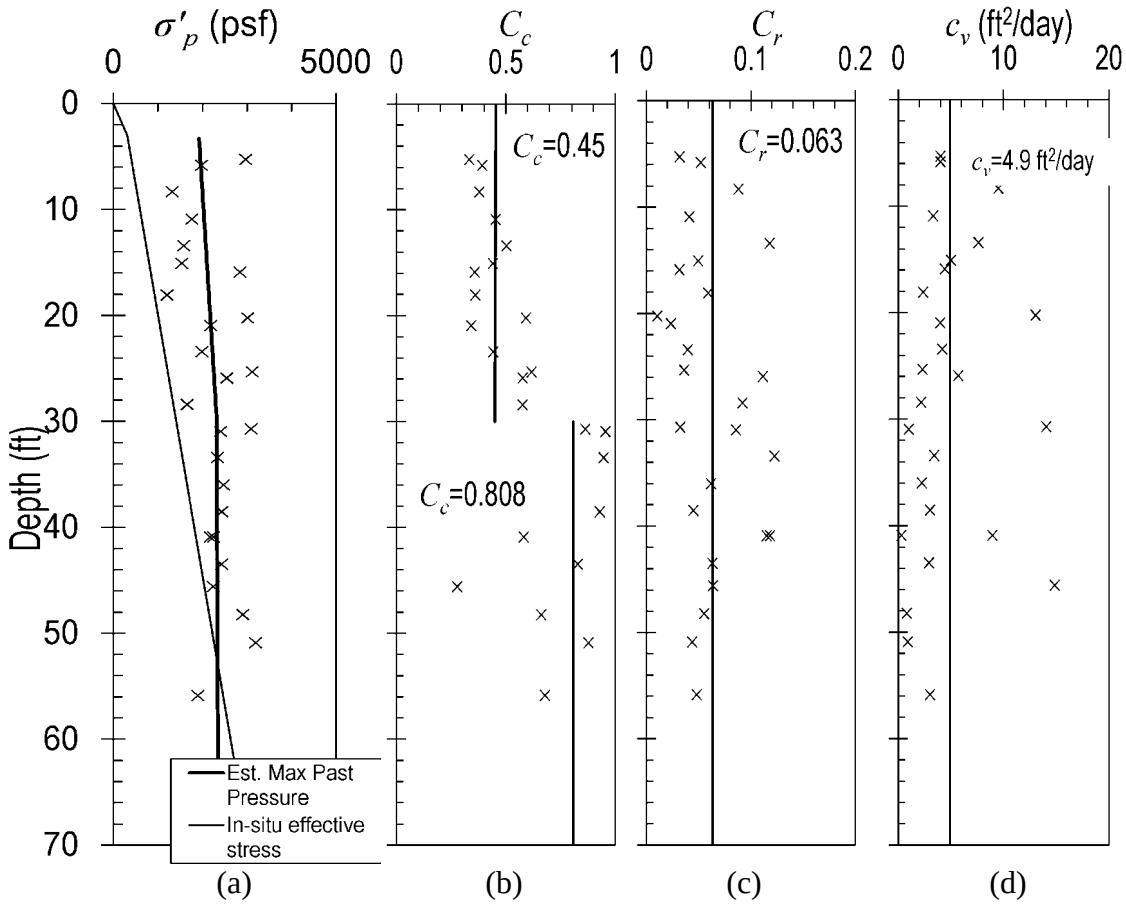


Figure 3.7 Measurements for consolidation parameters from the Pemiscot site: (a) preconsolidation stress, (b) compression index, (c) recompression index, and (d) coefficient of consolidation. (Ding et al., 2014)

Interpretations from the $\overline{CU}$ type triaxial compression tests are shown in Figure 3.8. Figure 3.8a shows the modified Mohr-Coulomb diagram and while Figure 3.8b shows the relationship between normalized undrained shear strength ($s_u/\sigma'_{vc}$) and $OCR$. The effective stress angle of internal friction is observed to be 17 degrees and the effective stress cohesion intercept is 4.3 psi based on these measurements. The normalized undrained shear strength parameters, $S$ and $m$, are $S = 0.25$ and $m = 0.77$.

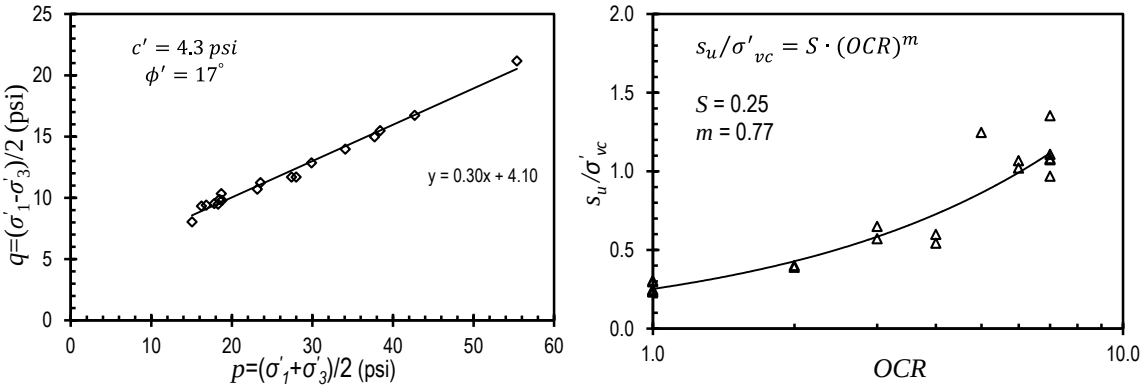


(a) (b)

Figure 3.8 Measurements from $\overline{CU}$ type triaxial compression tests for the Pemiscot site: (a) modified Mohr-Coulomb diagram, and (b) normalized undrained shear strength.

## 3.6 Laboratory Measurements for St. Charles Site

Four borings were conducted at the St. Charles site at the locations shown in Figure 3.9. Soil samples acquired from borings SC-B1, SC-B2 and SC-B3 were tested at MU laboratory and the testing results are described herein. General soil profiles, measured natural water contents ($w_n$) and Atterberg limits ($w_P$ and $w_L$), specific gravity ($G_s$), total unit weight ($\gamma_T$) and undrained shear strength ($s_u$) are plotted in Figure 3.10. The subsurface at the St. Charles site is composed of approximately 36 ft of soft, fat clay overlying alluvial sands. The ground water table was located at a depth of approximately 23 ft. The mean specific gravity from samples taken throughout the 36 ft sampling depth was 2.74 and the total unit weight over the same depths was 110 lb/ft$^3$.

Figure 3.9 St. Charles site boring locations.

Measurements of preconsolidation stress ( $\sigma_p'$ ), compression index ( $C_c$ ), recompression index ($C_r$) and coefficient of consolidation ($c_v$) are shown in Figure 3.11. The interpreted preconsolidation stress shown suggests that the soil is overconsolidated to depths of approximately 20 feet where the soil becomes normally consolidated. At greater depths, the preconsolidation measurements indicate that soil is again lightly overconsolidated. The compression index, recompression index and coefficient of consolidation were practically constant over the depth range of the measurements. The mean values of compression index and recompression index from all measurements are 0.384 and 0.035, respectively. The average coefficient of consolidation was 14.7 $ft^2$/day.

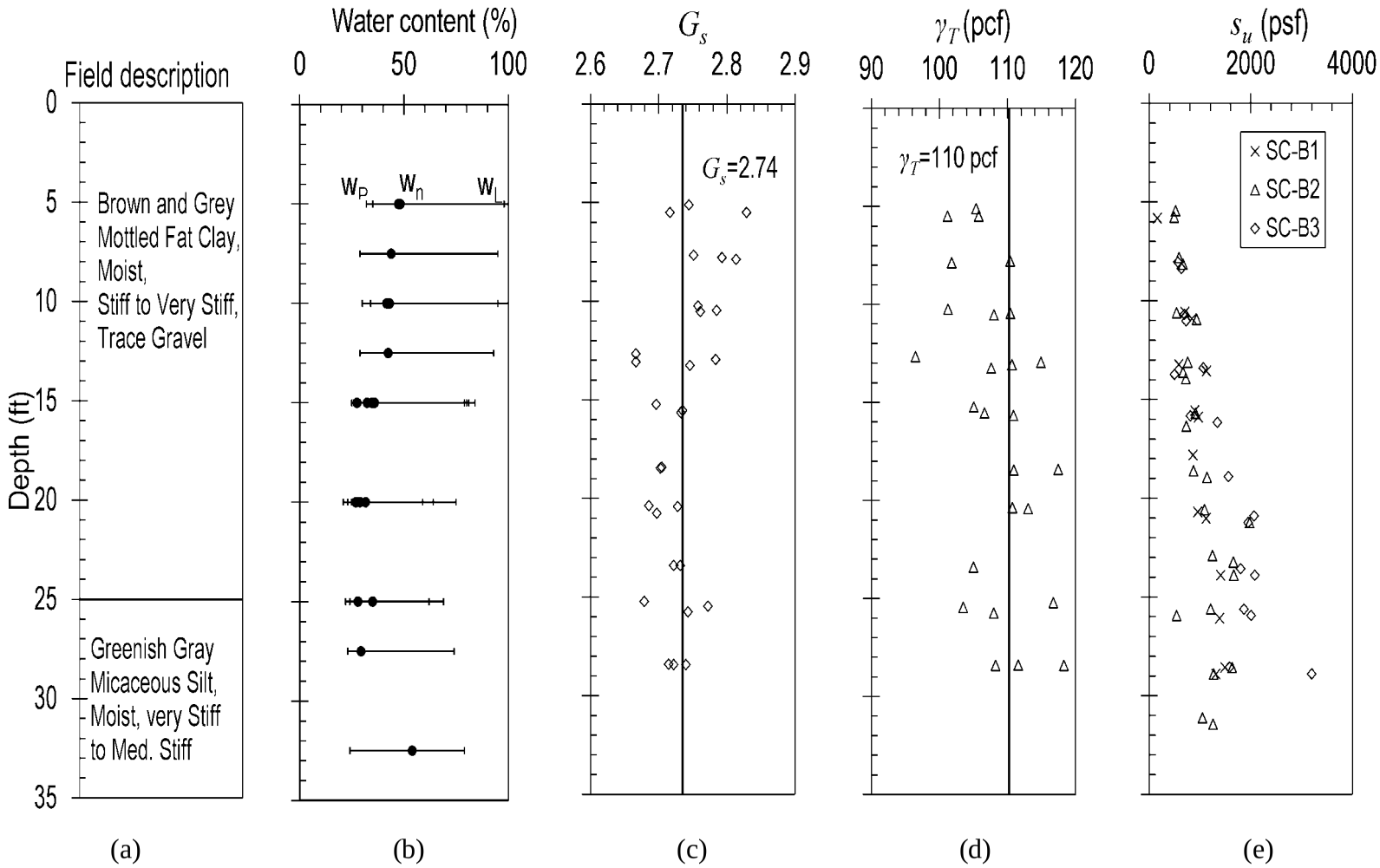


Figure 3.10 Laboratory measurements for the St. Charles site: (a) field description, (b) water content and Atterberg Limits, (c) specific gravity, (d) total unit weight, and (e) undrained shear strength.

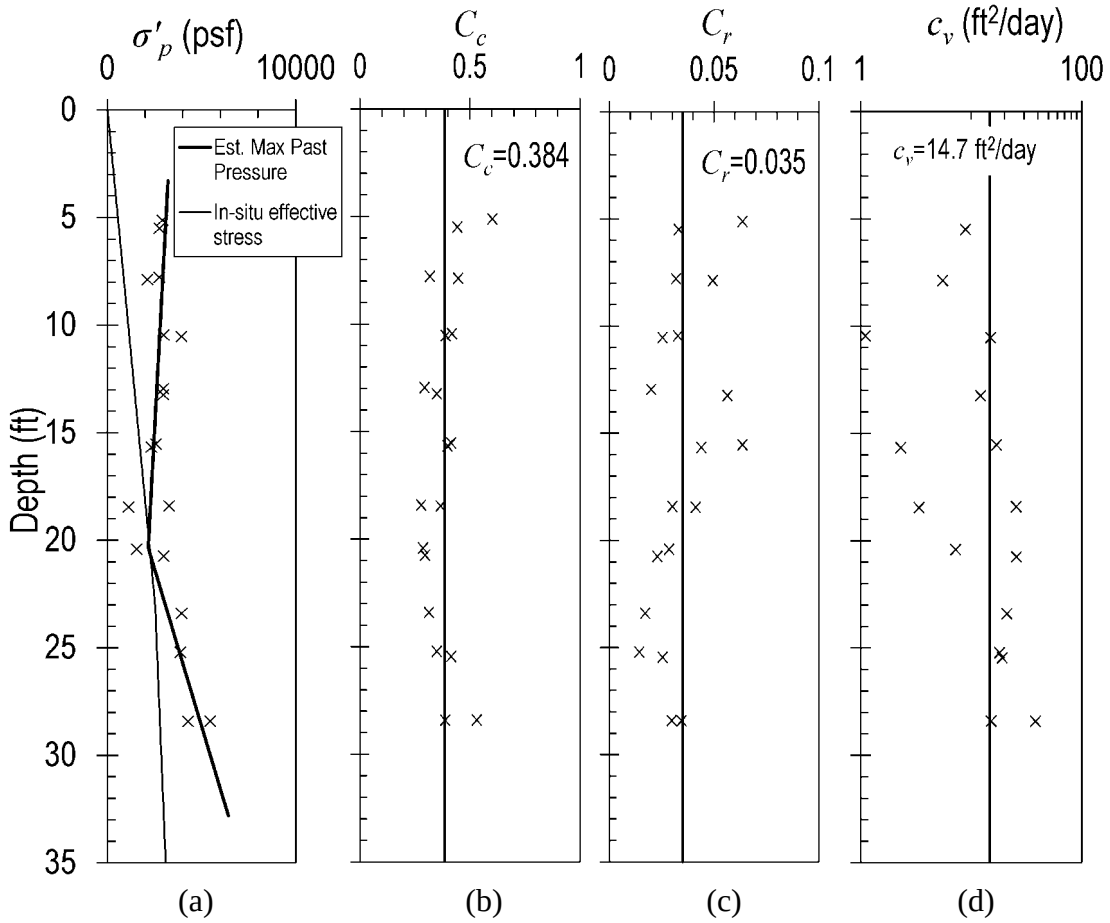


Figure 3.11 Measurements for consolidation parameters from the St. Charles site: (a) preconsolidation stress, (b) compression index, (c) recompression index, and (d) coefficient of consolidation. (Ding et al., 2014)

Interpretations from $\overline{CU}$ type triaxial compression and DSS testing results are shown in Figures 3.12 and 3.13, respectively. Figures 3.12 shows the modified Mohr Coulomb diagram and normalized undrained shear strength determined from the triaxial tests that were conducted according to SHANSEP procedures. The angle of internal friction and cohesion intercept in terms of effective stresses are 23 degrees and 1.9 psi, respectively. The normalized undrained shear strength parameters, $S$ and $m$, are $S$=0.34 and $m$=0.75. Similar parameters determined from results of the DSS tests are $S$=0.27 and $m$=0.69 as shown in Figure 3.13.

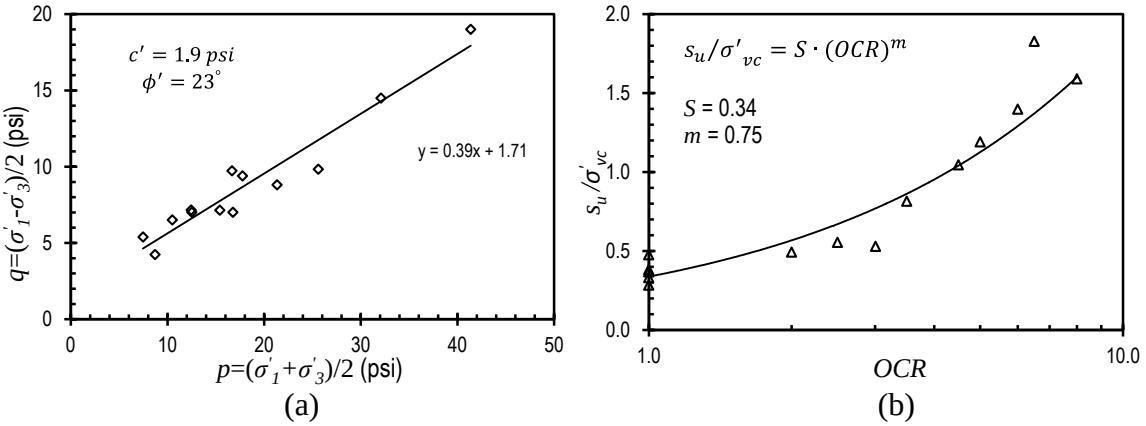


(a) (b)

Figure 3.12 Measurements from $\overline{CU}$ type triaxial compression tests for the St. Charles site: (a) modified Mohr-Coulomb diagram, and (b) normalized undrained shear strength.

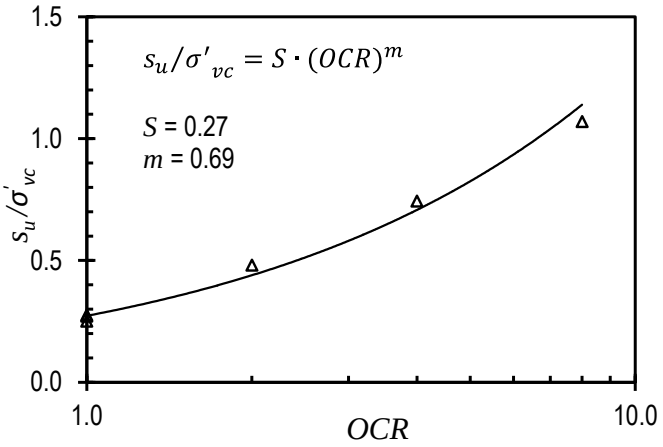


Figure 3.13 Normalized undrained shear strength measurements from DSS tests for the St. Charles site.

## 3.7 Laboratory Measurements for New Florence Site

Due to difficulties encountered in retaining adequate samples, numerous borings were performed at the New Florence site. Locations of borings where samples used for obtaining the test results presented in this section are shown in Figure 3.14. Figure 3.15 shows the results of measurements of water content, Atterberg Limits, specific gravity, total unit weight, and undrained shear strength. These measurements indicate that the soil profile at the New Florence site is predominantly composed of stiff, fat clay to depths exceeding 45 feet, with some sandstone and glacial gravel. The ground water table was

located below 46 ft at the time of sampling, beyond the depths of sampling and testing conducted for the present study. The mean specific gravity over the sampling interval was 2.63. The mean total unit weight was 122 lb/ft$^3$.


Figure 3.14 New Florence site boring locations.

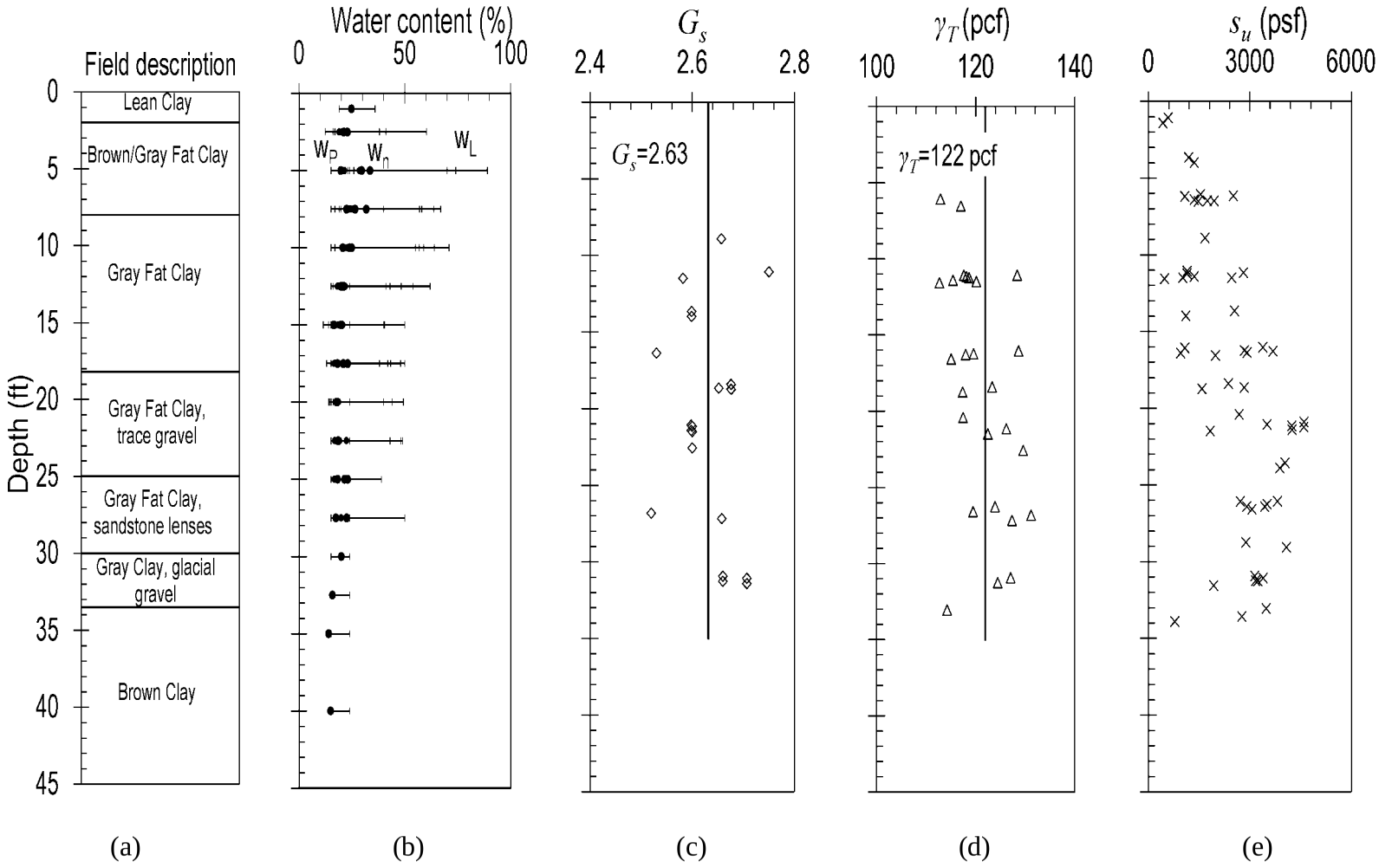


Figure 3.15 Laboratory measurements for the New Florence site: (a) field description, (b) water content and Atterberg Limits, (c) specific gravity, (d) total unit weight, and (e) undrained shear strength.

Measurements of preconsolidation stress ( $\sigma_p'$ ), compression index ( $C_c$ ), recompression index ($C_r$) and coefficient of consolidation ($c_v$) are shown in Figure 3.16. Only five constant rate of strain consolidation tests were conducted on samples from the New Florence site. The measurements indicate great preconsolidation stress at this site. However, it should be noted that measurements from 1-D incremental load consolidation tests suggest substantially lower preconsolidation stress than is shown in Figure 3.16. The mean values of compression index and recompression index from the measurements shown are 0.30 and 0.018, respectively. The average value of coefficient of consolidation is 11.5 $ft^2$/day.

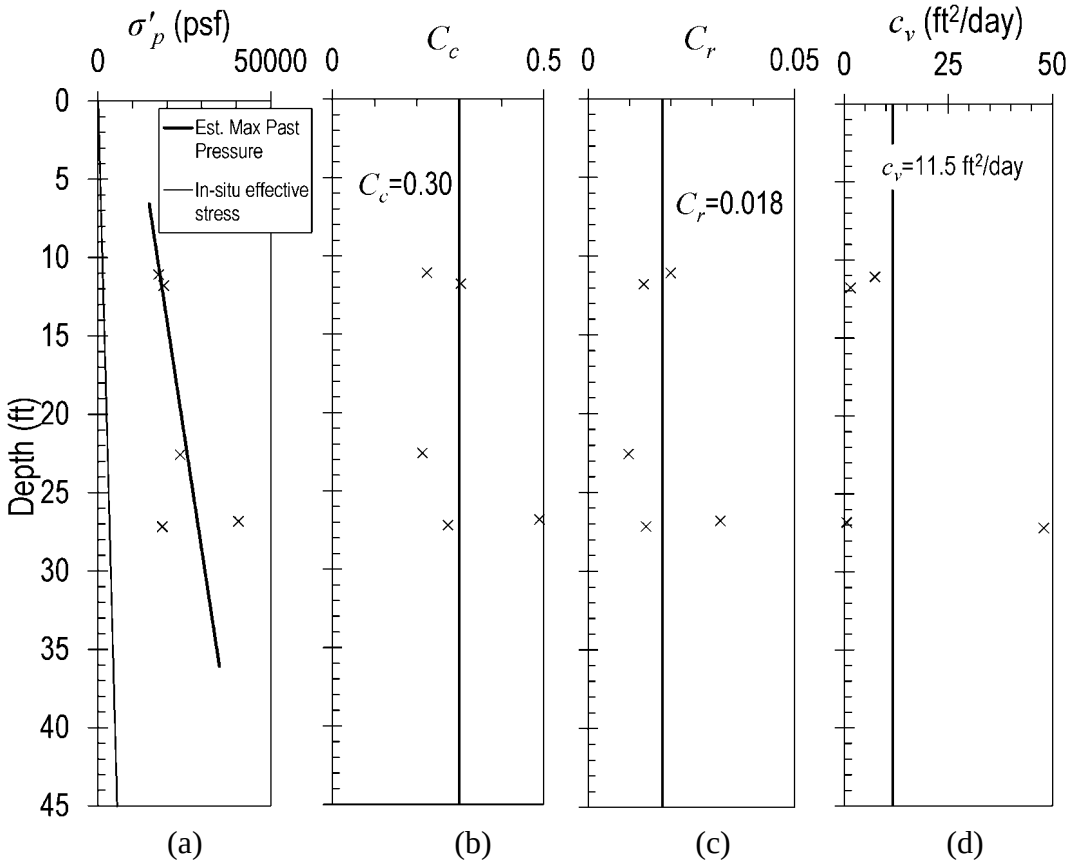


Figure 3.16 Measurements for consolidation parameters from the New Florence site: (a) preconsolidation stress, (b) compression index, (c) recompression index, and (d) coefficient of consolidation. (Ding et al., 2014)

Interpretations from $\overline{CU}$ type triaxial compression test measurements are shown in Figure 3.17. Since 1-D CRS consolidation testing results show substantially greater preconsolidation stresses than expected, all soil specimens were consolidated to effective stresses greater than preconsolidation stresses measured from 1-D incremental load consolidation tests and then sheared under undrained conditions. Figure 3.17 shows the modified Mohr Coulomb diagram with estimated effective stress shear strength parameters. The angle of internal friction and cohesion intercept in terms of effective stresses are 26 degrees and 1.8 psi, respectively.

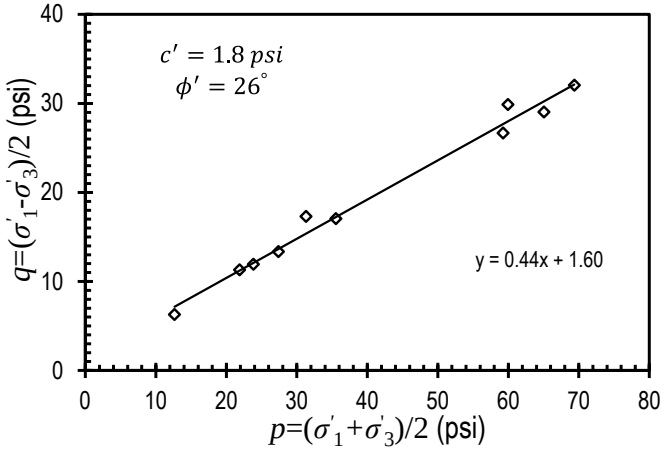


Figure 3.17 Modified Mohr Coulomb diagram showing measurements from $\overline{CU}$ type triaxial compression tests for samples from the New Florence site.

## 3.8 Laboratory Measurements for Warrensburg Site

Three borings were completed at the Warrensburg site as shown in Figure 3.18. Measurements for samples obtained from borings W-B1 and W-B2 are reported in this section. The Warrensburg site is composed of generally soft, silty soils overlying shale, sandstone, or limestone bedrock. In the immediate vicinity of the borings, the depth of the overburden soils is approximately 46 ft. In situ moisture contents and Atterberg limits are generally consistent throughout the upper 46 ft of the profile, except that an increase in the

liquid limit is observed in some samples from 16 to 20 ft below ground (Figure 3.19). The ground water table was located at a depth of approximately 10 feet when the borings were made. The mean specific gravity measured for the overburden soils is 2.71. The mean total unit weight is 117 lb/ft$^3$.

Figure 3.18 Warrensburg site boring locations.

Measurements of preconsolidation stress ( $\sigma_p'$ ), compression index ( $C_c$ ), recompression index ($C_r$) and coefficient of consolidation ($c_v$) are shown in Figure 3.20. The preconsolidation stress profile suggests that the soil is slightly overconsolidated over much of the profile. Results from compression index, recompression index and coefficient of consolidation measurements indicate that these properties are essentially constant over the depth range of sampling and testing. The mean values of compression index and recompression index are 0.238 and 0.032, respectively. The average of coefficient of consolidation was 17.8 ft$^2$/day.

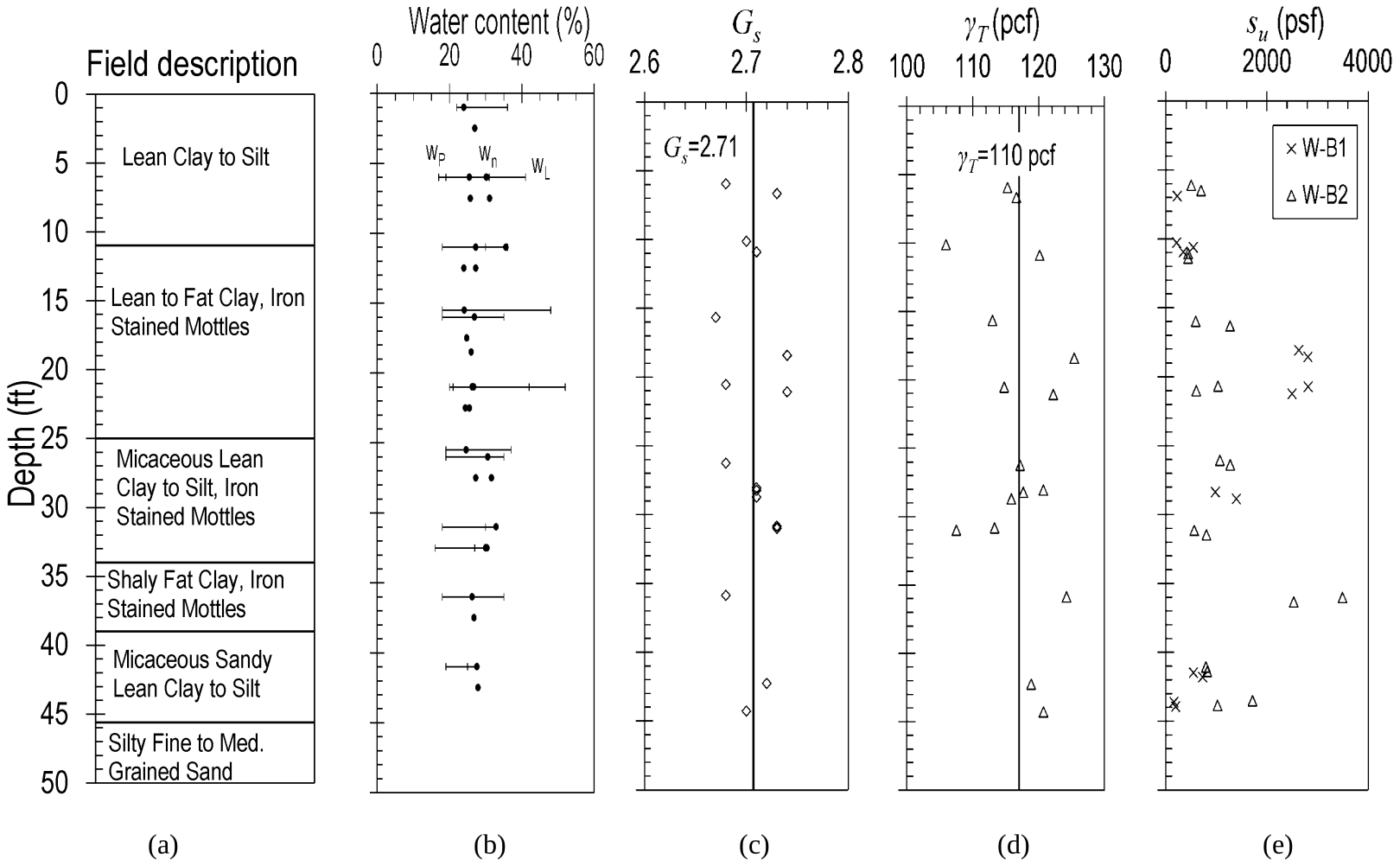


Figure 3.19 Laboratory measurements for the Warrensburg site: (a) field description, (b) water content and Atterberg Limits, (c) specific gravity, (d) total unit weight, and (e) undrained shear strength.

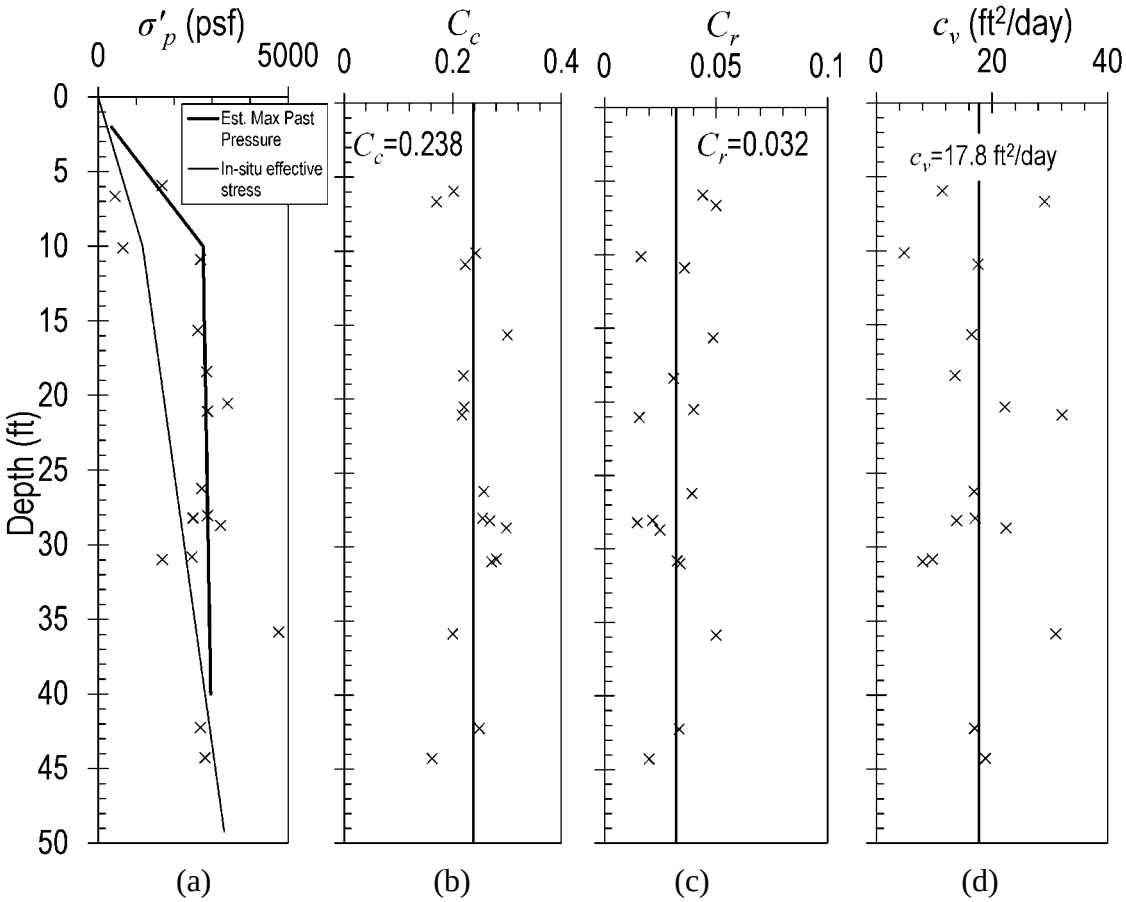


Figure 3.20 Measurements for consolidation parameters from the Warrensburg site: (a) preconsolidation stress, (b) compression index, (c) recompression index, and (d) coefficient of consolidation. (Ding et al., 2014)

Interpretations from $\overline{\text{CU}}$ type triaxial compression tests are shown in Figure 3.21. These results indicate that the angle of internal friction and cohesion intercept in terms of effective stresses are 29 degrees and 1.8 psi, respectively. The normalized undrained shear strength parameters were found to be $S = 0.31$ and $m = 0.85$, respectively.

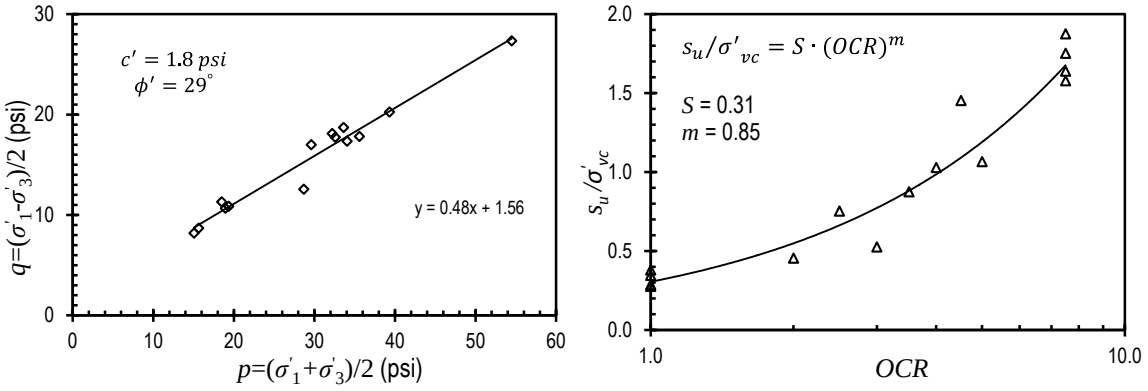


(a) (b)

Figure 3.21 Measurements from $\overline{CU}$ type triaxial compression tests for the Warrensburg site: (a) modified Mohr-Coulomb diagram, and (b) normalized undrained shear strength.

## 3.9 Summary

Laboratory measurements for specimens taken from the Pemiscot site, the St. Charles site, the New Florence site and the Warrensburg site have been presented in this chapter. All reported measurements were obtained using samples acquired using state of the art boring and sampling techniques and from tests performed at the University of Missouri (MU) laboratory. The undrained shear strength measurements for each site were analyzed to evaluate how the number of measurements affects the magnitude of uncertainty in the estimated strength parameters. Additional analyses using these undrained shear strength measurements were subsequently used to evaluate how the number of measurements for undrained shear strength affects the reliability of shallow foundations designed using Load and Resistance Factor Design (LRFD). Probabilistic models of undrained shear strength for each site are presented in Chapter 4.

# Chapter 4 Probabilistic Interpretation of Undrained Shear Strength Measurements

## 4.1 Introduction

The undrained shear strength measured by unconsolidated undrained (UU) type triaxial compression tests using soil samples acquired by state of the art sampling techniques and tested in the University of Missouri (MU) soil research laboratory are used to estimate soil undrained shear strength design parameters for foundation designs. To interpret those values and then apply them in design, two probabilistic models—the linear regression model and the constant regression model— were selected to estimate the mean and uncertainty of undrained shear strength. This chapter will introduce two selected probabilistic models and illustrate calculations of mean and uncertainties of undrained shear strength using these models at the Pemiscot site, the St. Charles site, the New Florence site and the Warrensburg site.

## 4.2 Sources of Uncertainties

As mentioned in Chapter 3, the soil samples were acquired using state of the art sampling techniques, thus, the measured undrained shear strength values at each of these four sites are regarded to be good quality measurements. The measured uncertainty is assumed to represent the "true" soil uncertainty and the shear strength profiles are considered to reflect the "true" soil properties. Generally, the possible sources of uncertainties and bias are:

- Uncertainty from sampling;

- Uncertainty from storage;
- Uncertainty from testing, equipment and operator;
- Uncertainty from transformation models;
- Uncertainty from limited data.

Since samples were acquired using state of the art sampling techniques, it is reasonable to assume the uncertainty from sampling is controlled at an acceptable level and is consistent throughout all samples. Since sampling and testing were completed in 1-2 weeks which is over a relatively short time frame, the shear strength results are assumed to be time invariant (Rethati, 1988). All tests were conducted in the MU soil research laboratory using same equipment, following same procedures and conducted by the same operator, so the uncertainty from testing, equipment and operator was consistent, hence, it is reasonable to assume that any measurements errors or variability resulting from equipment, user and procedural variations are minimal in research program (Orchant et al., 1988). Since undrained shear strength from unconsolidated undrained (UU) type triaxial compression tests provides direct measurements of soil undrained shear strength, no transformation models are needed, thus no transformation model variability or uncertainty is introduced (Phoon and Kulhawy, 1996). In addition, the number of acquired soil undrained shear strength measurements is relatively large at each site. For the Pemiscot site, the St. Charles site and the New Florence site, the number of undrained shear strength measurements was around 55 at each site, which provides 95% confidence that the measurements will reflect 90% of the population (Christian 2000). Thus, the measured undrained shear strength values at each site can be regarded to reflect "true" site conditions.

The total number of undrained shear strength measurements will serve as the total population size of measurements at each site to study the effect of different numbers of measurements on interpretation of design parameters, as well as the effect on the reliability of spread footings designed using LRFD. The mean and uncertainty estimated from the total population size of measurements will be regarded to reflect the "true" soil properties.

Even if the uncertainties from sampling, storage, testing and modeling are not well controlled, the conclusions of this research on the reliability of spread footings designed using LRFD will not be affected. The design methods use resistance factors calibrated as a function of uncertainties in undrained shear strength and then size foundation areas to satisfy the design criteria. Thus, if greater uncertainties are introduced from sampling, storage, testing and modeling, a smaller resistance factor will be selected to size a larger foundation area to satisfy the design criteria. The calibration of resistance factors will be explained in Chapter 5.

## 4.3 Total, Model and Data Uncertainties

When analyzing experimental measurements to estimate true values or to predict new values, statistical models are usually applied. Therefore, three types of uncertainties are incorporated: data uncertainty, model uncertainty and total uncertainty.

Data uncertainty reflects variations between measurements and estimated values from statistical models. Data uncertainty is calculated as the mean square error (*MSE*), which equals to the sum of residuals divided by the degree of freedom.

Model uncertainty represents uncertainty about true values. Statistical models are applied to estimate the true value for a given measurement. Model uncertainty reflects uncertainty in a fitted statistical model.

Total uncertainty is uncertainty in the predicted values using statistical models. When using statistical model to predict a new measurement, the uncertainty in the prediction is the total uncertainty which equals to the sum of model uncertainty and data uncertainty.

With increasing number of measurements, data uncertainty will gradually approach a constant value of true uncertainty in the data, while model uncertainty will gradually be reduced to zero and thus, total uncertainty will gradually approach the value of data uncertainty.

## 4.4 Probabilistic Models for Undrained Shear Strength Measurements

After obtaining undrained shear strength measurements at each site, statistical models are selected and then used to estimate undrained shear strength at a given design depth. The estimated undrained shear strength value will be used as a characteristic value to design a foundation at that given depth and the uncertainty about the undrained shear strength value will be applied in design to estimate the reliability of designed foundations. Therefore, statistical models will be selected herein and the undrained shear strength values and uncertainties from all measurements at each site will be calculated at a given depth.

### 4.4.1 Choice of Models

Two statistical models— linear and constant regression models— are selected to estimate the profile of soil undrained shear strength and to represent the soil properties at each site. Since soil undrained shear strength values are non-negative, also, in order to avoid introducing too many unknown parameters, and causing great model uncertainties by using complicated models, thus, strength measurements are assumed following lognormal distribution. The rationality of selection of lognormal models will be testified

using statistical hypothesis test in Sections 4.5 to 4.8 for undrained shear strength measurements at each site.

The linear regression model assumes logarithm values of undrained shear strength measurements following normal distribution with depth. Hypothesis tests for normality were conducted on residuals of the linear regression model using measurements at each site. The results show that it cannot reject normality at all sites. The constant regression model assumes logarithm value of undrained shear strength measurements following normal distribution regardless of depth. The constant regression model may not be a good model for the measurements and may not reflect the soil properties at the site, however, the reason for selecting the constant regression model in this research lies in the fact that the constant model has been widely adopted both in research and in practice for its simplicity in calculation and application.

4.4.2 Linear Regression Model

If $s_u$ follows a lognormal distribution with depth, we have:

$$s_u|z \sim LN(\hat{\mu}_{\ln(s_u)}, \hat{\sigma}^2_{\ln(s_u)}) \quad \text{(Eq. 4.1)}$$

where, $s_u$ is undrained shear strength at depth $z$, and $\hat{\mu}_{\ln(s_u)}$ and $\hat{\sigma}^2_{\ln(s_u)}$ are the estimated mean and variance of the logarithm value of $s_u$, respectively.

The linear regression model can be written in the general form of:

$$\ln(s_{u_i}) = \hat{\beta}_0 + \hat{\beta}_1 \cdot z_i + \epsilon_i \quad \text{(Eq. 4.2)}$$

where, $\ln(s_{u_i})$ is the logarithm value of $i^{\text{th}}$ undrained shear strength value, $s_{u_i}$, at a depth of $z_i$, and $\hat{\beta}_0$ and $\hat{\beta}_1$ are regression parameters for intercept and slope, respectively, $\epsilon_i$ is the random error term with $E(\epsilon_i) = 0$ and $var(\epsilon_i) = \sigma^2$ and are independent at $i$=1, 2, …, $n$.

The estimated mean and variance for $\ln(s_u)$ are calculated as:

$$\hat{\mu}_{\ln(s_{u_i})} = E\left[\hat{\beta}_0 + \hat{\beta}_1 \cdot z_i\right] = \hat{\beta}_0 + \hat{\beta}_1 \cdot z_i \quad \text{(Eq. 4.3)}$$

$$\sigma^2 = MSE = \frac{\sum_{i=1}^{n}\left[\hat{\mu}_{\ln(s_{u_i})} - \ln(s_{u_i})\right]^2}{(n-2)} \quad \text{(Eq. 4.4)}$$

$$\sigma^2_{\hat{\mu}_{\ln(s_{u_i})}} = MSE \cdot \left(\frac{1}{n} + \frac{(\bar{z}-z)^2}{\sum_{i=1}^{n}(z_i-\bar{z})^2}\right) \quad \text{(Eq. 4.5)}$$

$$\sigma^2_{\ln(s_{u_i})} = \sigma^2 + \sigma^2_{\hat{\mu}_{\ln(s_{u_i})}} = MSE \cdot \left(1 + \frac{1}{n} + \frac{(\bar{z}-z)^2}{\sum_{i=1}^{n}(z_i-\bar{z})^2}\right) \quad \text{(Eq. 4.6)}$$

where, $\hat{\mu}_{\ln(s_{u_i})}$ is the estimated mean of $\ln(s_u)$ at depth of $z_i$, $\sigma^2$ is the variance from the data, $\ln(s_{u_i})$ is the logarithm value of $i^{\text{th}}$ undrained shear strength value, $s_{u_i}$, at depth of $z_i$, $n$ is the number of measurements, $\sigma^2_{\hat{\mu}_{\ln(s_{u_i})}}$ is the variance about the estimated mean which is from the regression model, $\bar{z}$ is the average depth for all measurements, and $\sigma^2_{\ln(s_{u_i})}$ is the total variance which equals the sum of variance from both data and regression model.

Coefficient of variation (*COV*) is used to represent uncertainty in undrained shear strength. Unlike variance and standard deviation, coefficient of variation is a dimensionless indicator of uncertainty which equals to the ratio between standard deviation and mean value. Thus, *COV* is selected in this study to represent uncertainty, instead of using standard deviation and variance. The estimated mean and uncertainties for undrained shear strength ($s_u$) at depth of $z$ are:

$$\hat{\mu}_{(s_u)} = \exp\left[\hat{\mu}_{\ln(s_u)}\right] = \exp[\hat{\beta}_0 + \hat{\beta}_1 \cdot z] \quad \text{(Eq. 4.7)}$$

$$COV_{\hat{\mu}_{s_u}} \cong \sigma_{\hat{\mu}_{\ln(s_u)}} = \sqrt{MSE \cdot \left(\frac{1}{n} + \frac{(\bar{z}-z)^2}{\sum_{i=1}^{n}(z_i-\bar{z})^2}\right)} \quad \text{(Eq. 4.8)}$$

$$COV_{s_u} \cong \sigma_{\ln(s_u)} = \sqrt{MSE \cdot \left(1 + \frac{1}{n} + \frac{(\bar{z}-z)^2}{\sum_{i=1}^{n}(z_i-\bar{z})^2}\right)} \quad \text{(Eq. 4.9)}$$

where, $\hat{\mu}_{(s_u)}$ is the estimated undrained shear strength at depth of $z$, $COV_{\hat{\mu}_{s_u}}$ is the model uncertainty of estimated undrained shear strength and $COV_{s_u}$ is the total uncertainty of undrained shear strength.

4.4.3 Constant Regression Model

If undrained shear strength ($s_u$) follows a lognormal distribution regardless of depth, we will have:

$$s_u \sim LN(\hat{\mu}_{\ln(s_u)}, \hat{\sigma}^2_{\ln(s_u)}) \quad \text{(Eq. 4.10)}$$

where, $s_u$ is the undrained shear strength, and $\hat{\mu}_{\ln(s_u)}$ and $\hat{\sigma}^2_{\ln(s_u)}$ are the estimated mean and variance of the logarithm value of $s_u$, respectively. Since undrained shear strength is constant over the whole depth range, the regression model can be written in the general form of:

$$\ln(s_{u_i}) = \hat{\beta}_0 + \epsilon_i \quad \text{(Eq. 4.11)}$$

where, $\ln(s_{u_i})$ is the logarithm value of $i^{\text{th}}$ undrained shear strength value, $s_{u_i}$, at a depth of $z_i$, and $\hat{\beta}_0$ is regression parameters for intercept, $\epsilon_i$ is the random error term with $E(\epsilon_i) = 0$ and $var(\epsilon_i) = \sigma^2$ and are independent at $i$=1, 2, …, $n$.

Thus, the estimated mean and variance for $\ln(s_u)$ are calculated by:

$$\hat{\mu}_{\ln(s_u)} = \hat{\beta}_0 = \frac{\sum_{i=1}^{n}[\ln(s_{u_i})]}{n} \quad \text{(Eq. 4.12)}$$

$$\sigma^2 = MSE = \frac{\sum_{i=1}^{n}[\hat{\mu}_{\ln(s_u)} - \ln(s_{u_i})]^2}{(n-1)} \quad \text{(Eq. 4.13)}$$

$$\sigma^2_{\hat{\mu}_{\ln(s_u)}} = MSE \cdot \frac{1}{n} \quad \text{(Eq. 4.14)}$$

$$\sigma^2_{\ln(s_u)} = \sigma^2 + \sigma^2_{\hat{\mu}_{\ln(s_u)}} = MSE \cdot \left(1 + \frac{1}{n}\right) \quad \text{(Eq. 4.15)}$$

where, $\hat{\mu}_{\ln(s_u)}$ is the mean of the logarithm value of undrained shear strength measurements, $\sigma^2_{\hat{\mu}_{\ln(s_u)}}$ is the variance in the estimated mean of logarithm value of undrained shear strength, $\hat{\mu}_{\ln(s_u)}$, and $\sigma^2_{\ln(s_u)}$ is the total variance of logarithm value of undrained shear strength, which is equal to the sum of the variance from data and regression model.

Since the constant model is applied, only one regression parameter of intercept will be incorporated, thus, the degree of freedom is one. The mean and uncertainty of undrained shear strength will be constant over the depth for the constant regression model:

$$\hat{\mu}_{(s_u)} = \exp\left[\hat{\mu}_{\ln(s_u)} + \frac{\sigma^2_{\hat{\mu}_{\ln(s_u)}}}{2}\right] \quad \text{(Eq. 4.16)}$$

$$COV_{\hat{\mu}_{s_u}} \cong \sigma_{\hat{\mu}_{\ln(s_u)}} = \sqrt{MSE \cdot \left(\frac{1}{n}\right)} \quad \text{(Eq. 4.17)}$$

$$COV_{s_u} \cong \sigma_{\ln(s_u)} = \sqrt{MSE \cdot \left(1 + \frac{1}{n}\right)} \quad \text{(Eq. 4.18)}$$

where, $\hat{\mu}_{(s_u)}$ is the estimated mean of undrained shear strength, $COV_{\hat{\mu}_{s_u}}$ is the uncertainty in estimated mean shear strength, $COV_{s_u}$ is the total uncertainty in undrained shear strength.

The linear regression model and the constant regression model will fit through all undrained shear strength measurements at each site with figures showing the undrained shear strength profile, the uncertainty in estimated mean shear strength and the total uncertainty of undrained shear strength in Sections 4.5-4.8. The characteristic values at design depth will be summarized in Section 4.9.

## 4.5 Pemiscot Site

The Pemiscot site is the least variable site among all four soil sites. Fifty two undrained shear strength measurements were acquired for the Pemiscot site. The estimated mean, uncertainty in the mean value and total uncertainty of undrained shear strength are

plotted as shown in Figure 4.1. Both the linear and constant models assume that undrained shear strength follow lognormal distribution. The residuals are plotted as shown in Figure 4.2. Normality tests are then performed on residuals and hypothesis testing results are listed in Table 4.1.

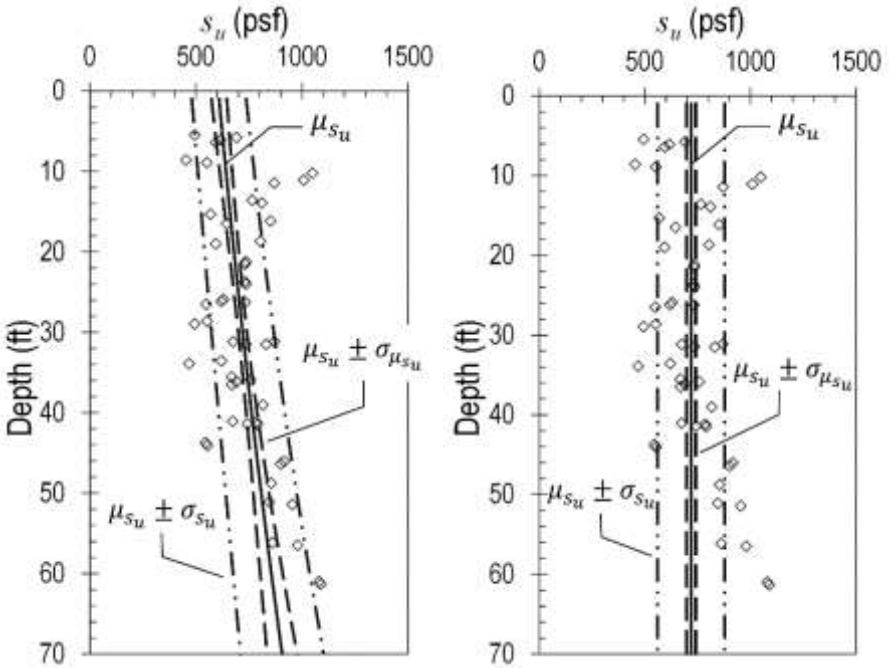


Figure 4.1 Regression models at Pemiscot sites: (a) Linear regression model, and (b) Constant regression model.

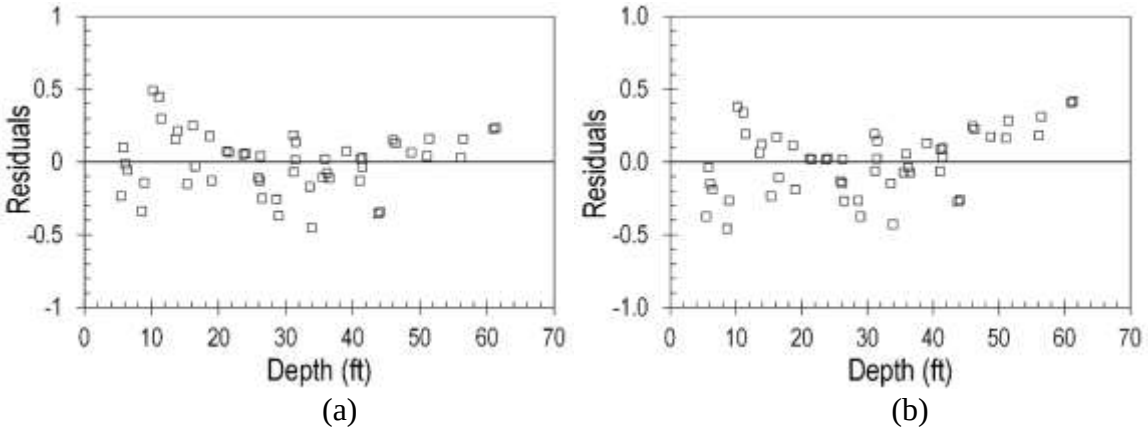


Figure 4.2 Residual plots for: (a) linear regression model, and (b) constant regression model at the Pemiscot site.

Table 4.1 Normality tests on residuals of regression models at Pemiscot site.

| Models | Test | p value | Reject normality (Y/N) |
|---|---|---|---|
| Linear | Shapiro-Wilk | 0.7491 | N |
| | Anderson-Darling | >0.2500 | N |
| | Cramer-Von Mises | >0.2500 | N |
| | Kolmogorov-Smirnov | >0.1500 | N |
| Constant | Shapiro-Wilk | 0.6756 | N |
| | Anderson-Darling | >0.2500 | N |
| | Cramer-Von Mises | >0.2500 | N |
| | Kolmogorov-Smirnov | >0.1500 | N |

As shown in Figure 4.2 and Table 4.1, the assumption of undrained shear strength following lognormal distribution with depth is acceptable. The normality test results in Table 4.1 suggest that it cannot reject normality for both models at a significant level of 0.05 ($\alpha = 0.05$). However, hypothesis test on slope parameter rejects that the slope parameter is zero, which indicates that the lognormal linear regression model is probably a better fit than the lognormal constant regression model.

## 4.6 St. Charles Site

The St. Charles site is the second least variable site among all four sites. Fifty three undrained shear strength measurements were obtained for the St. Charles site. Figure 4.3 shows the linear regression model and constant model fitting through strength measurements with estimated mean shear strength, uncertainty in mean value and total uncertainty of undrained shear strength. Ideally, the residuals should scattered randomly with no obvious patterns. However, as illustrated in Figure 4.4, the residual plot for constant model show an increasing trend with depth. Even though the hypothesis tests (Table 4.2) cannot reject normality for both models, the constant model is regarded as a poor fit. Furthermore, the statistical fit test rejected the hypothesis that the slope parameter is zero.

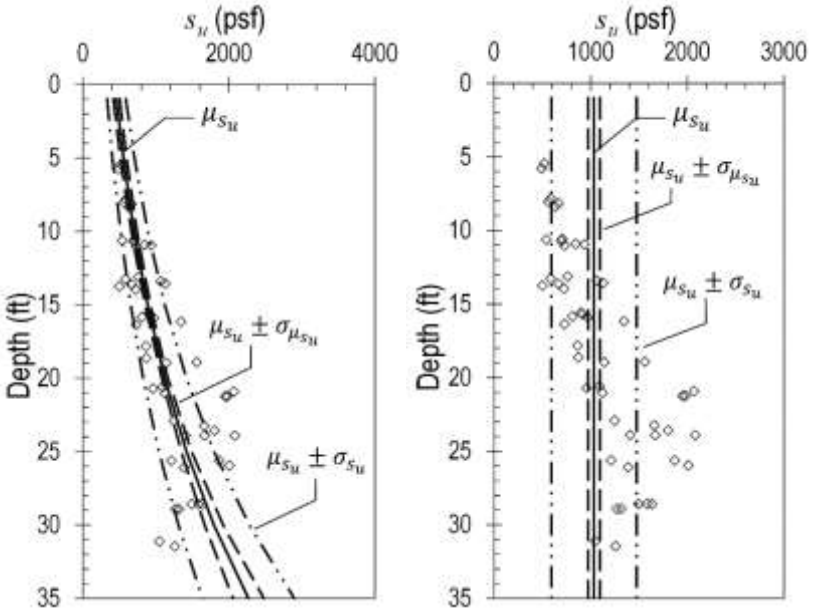


(a) (b)

Figure 4.3 Regression models at St. Charles sites: (a) Linear regression model, and (b) Constant regression model.

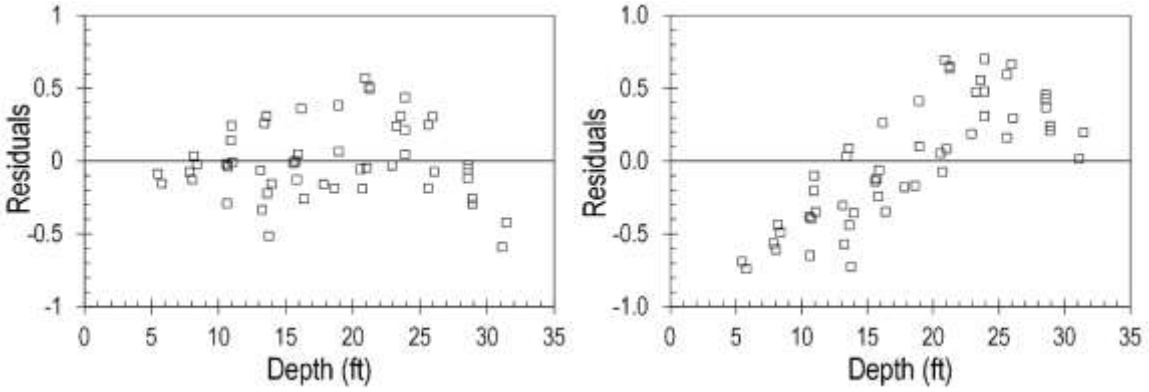


(a) (b)

Figure 4.4 Residual plots for: (a) linear regression model, and (b) constant regression model at the St. Charles site.

Table 4.2 Normality tests on residuals of regression models at St. Charles site.

| Models | Test | p value | Reject normality (Y/N) |
|---|---|---|---|
| Linear | Shapiro-Wilk | 0.2701 | N |
| | Anderson-Darling | 0.0721 | N |
| | Cramer-Von Mises | 0.0331 | Y |
| | Kolmogorov-Smirnov | 0.0190 | Y |
| Constant | Shapiro-Wilk | 0.0901 | N |
| | Anderson-Darling | >0.2500 | N |
| | Cramer-Von Mises | >0.2500 | N |
| | Kolmogorov-Smirnov | >0.1500 | N |

## 4.7 New Florence Site

The New Florence site is much more variable than the previous two sites. Fifty seven undrained shear strength measurements were acquired for New Florence site. The mean value, uncertainty in the mean value and total uncertainty of undrained shear strength are plotted with depth for both models as shown in Figure 4.5. Residual plots are shown in Figure 4.6 with results from normality tests on residuals listed in Table 4.3. The residuals from constant model show an obvious trend with depth (Figure 4.6) and the hypothesis tests reject normality for content model (Table 4.3), which suggest that the constant regression model cannot reflect soil properties at the New Florence site. The statistic fit test also rejects the hypothesis of slope parameter of regression model is zero.

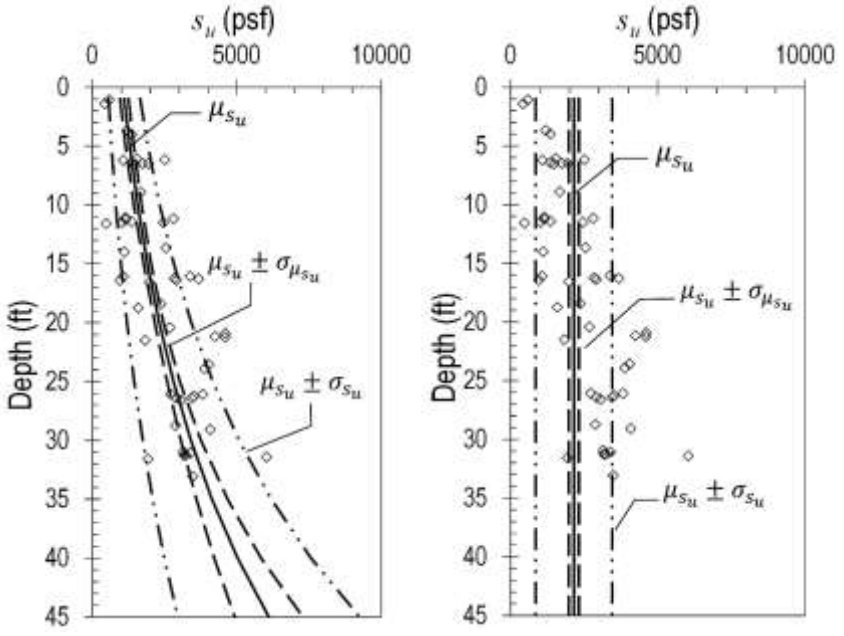


Figure 4.5 Regression models at New Florence sites: (a) Linear regression model, and (b) Constant regression model.

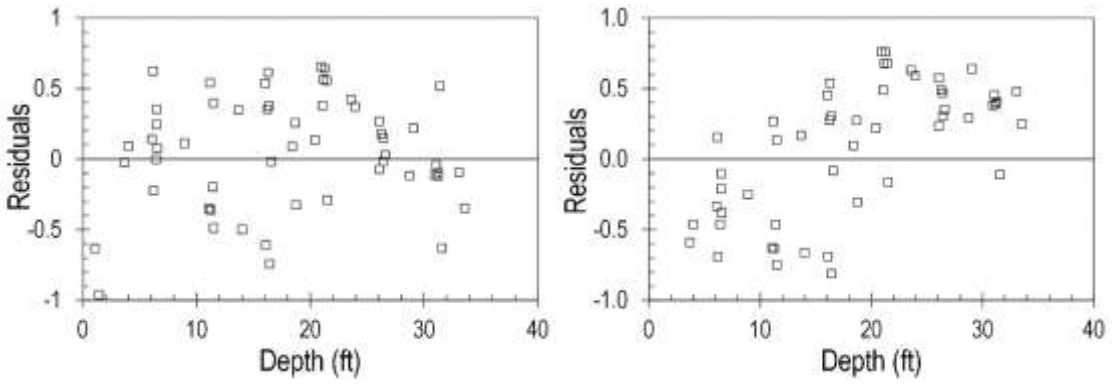


(a) (b)

Figure 4.6 Residual plots for: (a) linear regression model, and (b) constant regression model at the New Florence site.

Table 4.3 Normality tests on residuals of regression models at New Florence site.

| Models | Test | p value | Reject normality (Y/N) |
|---|---|---|---|
| Linear | Shapiro-Wilk | 0.0025 | Y |
| | Anderson-Darling | 0.0293 | Y |
| | Cramer-Von Mises | 0.0644 | N |
| | Kolmogorov-Smirnov | 0.0503 | N |
| Constant | Shapiro-Wilk | 0.0050 | Y |
| | Anderson-Darling | <0.0050 | Y |
| | Cramer-Von Mises | <0.0050 | Y |
| | Kolmogorov-Smirnov | <0.0100 | Y |

## 4.8 Warrensburg Site

The Warrensburg site is the most variable site among all sites. Thirty-two undrained shear strength measurements were obtained at this site. As shown in Figure 4.7, the mean undrained shear strength, uncertainty in mean value and total uncertainty of undrained shear strength are plotted with depth for the linear and constant models. The hypothesis testing results listed in Table 4.4 cannot reject normality for both models. The statistical fit test results also cannot reject the hypothesis of slope parameters of regression model is zero. The residual plot as shown in Figure 4.8 may indicate an increasing trend with depth. The lognormal constant regression model might be a reasonable model to reflect undrained shear strength at the Warrensburg site.

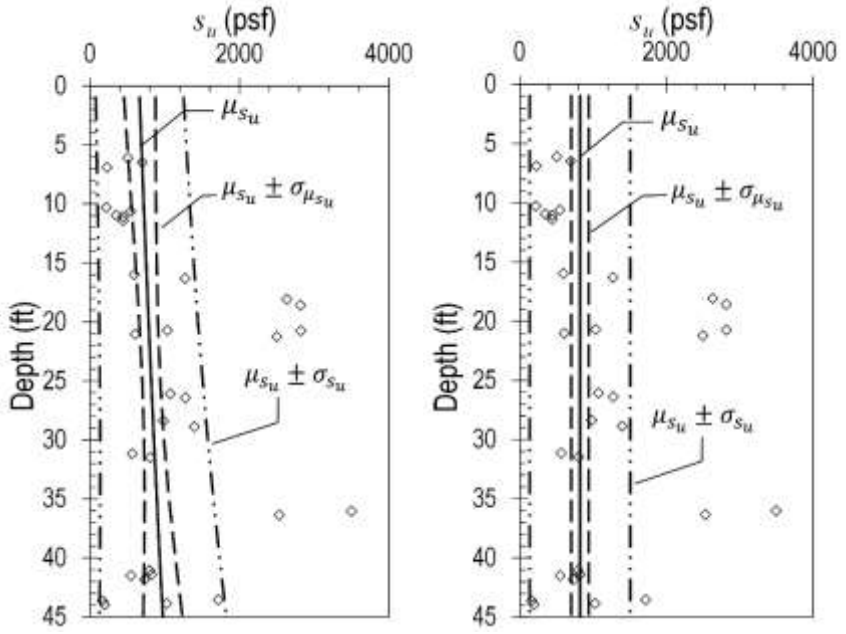


(a) (b)

Figure 4.7 Regression models at Warrensburg sites: (a) Linear regression model, and (b) Constant regression model.

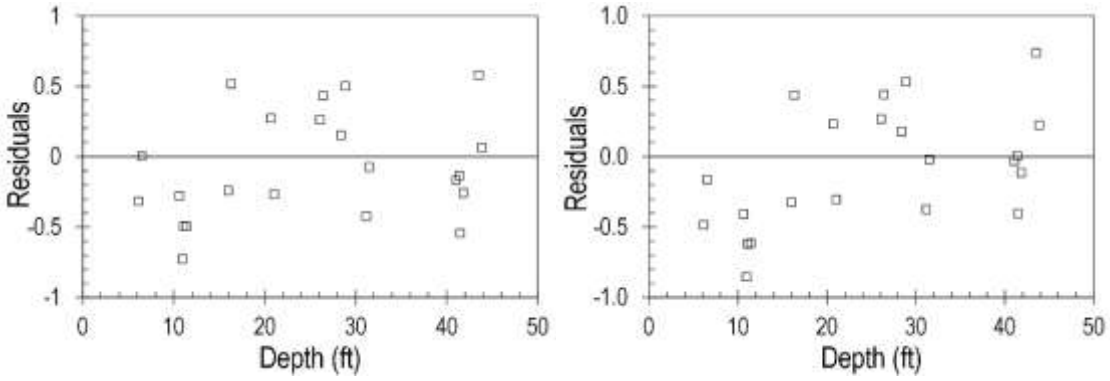


(a) (b)

Figure 4.8 Residual plots for: (a) linear regression model, and (b) constant regression model at the Warrensburg site.

Table 4.4 Normality tests on residuals of regression models at Warrensburg site.

| Models | Test | p value | Reject normality (Y/N) |
|---|---|---|---|
| Linear | Shapiro-Wilk | 0.3120 | N |
| | Anderson-Darling | >0.2500 | N |
| | Cramer-Von Mises | >0.2500 | N |
| | Kolmogorov-Smirnov | >0.1500 | N |
| Constant | Shapiro-Wilk | 0.4207 | N |
| | Anderson-Darling | >0.2500 | N |
| | Cramer-Von Mises | >0.2500 | N |
| | Kolmogorov-Smirnov | >0.1500 | N |

## 4.9 Characterized Values at Design Depths

As described in previous sections of this chapter, two statistical models are adopted for undrained shear strength at each site— the linear and the constant regression models. Based on residual plots and hypothesis tests on residuals for normality and on slope parameters of regression model, the lognormal linear regression model is regarded to be a reasonable model to reflect soil properties at each site. The lognormal constant model is a poor model and is selected as a convenient and conventional model herein.

The mean value, uncertainty in mean value and total uncertainty of undrained shear strength are calculated at given design depth. The mean and uncertainties vary with depth for linear regression model while remain constant for constant model. The characteristic values of undrained shear strength interpreted from each site using lognormal linear model and constant model are shown in Table 4.5 and 4.6, separately.

Table 4.5 Characteristic values of undrained shear strength from linear model.

| Site | Depth (ft) | $\hat{\mu}_{(s_u)}$ (psf) | $COV_{\hat{\mu}_{s_u}}$ | $COV_{s_u}$ |
|---|---|---|---|---|
| Pemiscot | 7 | 630 | 0.050 | 0.208 |
| | 30 | 720 | 0.028 | 0.204 |
| St. Charles | 7 | 609 | 0.068 | 0.270 |
| | 16 | 929 | 0.038 | 0.264 |
| New Florence | 7 | 1392 | 0.099 | 0.489 |
| | 16 | 1975 | 0.065 | 0.483 |
| Warrensburg | 7 | 699 | 0.257 | 0.867 |
| | 16 | 783 | 0.159 | 0.843 |

Table 4.6 Characteristic values of undrained shear strength from constant model.

| Site | Depth (ft) | $\hat{\mu}_{(s_u)}$ (psf) | $COV_{\hat{\mu}_{s_u}}$ | $COV_{s_u}$ |
|---|---|---|---|---|
| Pemiscot | 0-70 | 719 | 0.030 | 0.221 |
| St. Charles | 0-35 | 1033 | 0.059 | 0.427 |
| New Florence | 0-45 | 2155 | 0.079 | 0.604 |
| Warrensburg | 0-50 | 821 | 0.145 | 0.835 |

## 4.10 Summary

Two regression models were introduced in this chapter to interpret the characteristic values of undrained shear strength. Hypothesis tests were performed to test whether the model can reflect the data. Characteristic values of undrained shear strength at design depth using the total population of measurements for each site were summarized. The regression models and the characteristic values presented in this chapter were used throughout the research described in this thesis to study how the number of undrained shear strength measurements affects the design parameters and thus affects the reliability of spread footings design using LRFD.

Other statistical models, such as weighted least square and nonlinear regression models can also be applied to accomplish the same research objectives. Nevertheless, lognormal regression models were selected due to the simplicity in application and the non-negative properties of undrained shear strength.

# Chapter 5 Load and Resistance Factor Design (LRFD) for Shallow Foundations

## 5.1 Introduction

In the present work, the effect of considering different numbers of measurements for load and resistance factor design (LRFD) is evaluated considering the stability of spread footings at the Strength I limit state under undrained loading conditions. In this chapter, the fundamental LRFD criterion for design of spread footings at the Strength I limit state is presented. Analysis performed to establish resistance factors as a function of the uncertainty present for undrained shear strength at certain target probabilities of failure are also described and the resulting resistance factors are presented. The effect of considering different mean values for several design parameters in the calibration analyses is also discussed.

## 5.2 Load and Resistance Factor Design (LRFD) for Shallow Foundations

The basic criterion for design of spread footings under undrained conditions in terms of total stresses ($\phi = 0$) at the Strength I limit state is expressed as:

$$\varphi \cdot R = \gamma_{DL} \cdot Q_{DL} + \gamma_{LL} \cdot Q_{LL} \quad \text{(Eq. 5.1)}$$

where $\varphi$ is a resistance factor intended to account for uncertainty in the bearing resistance, $R$ is the nominal bearing resistance, $Q_{DL}$ is the nominal dead load, $\gamma_{DL}$ is a load factor for dead load, $Q_{LL}$ is the nominal live load, and $\gamma_{LL}$ is a load factor for live load. For soil having undrained shear strength, $s_u$, the nominal bearing resistance can be taken as:

$$R = s_u \cdot N_c \cdot A \quad \text{(Eq. 5.2)}$$

where $N_c$ is a bearing capacity factor, and $A$ is the area of the foundation. Thus, the LRFD criterion can be written in expanded form as:

$$\varphi \cdot s_u \cdot N_c \cdot A \geq \gamma_{DL} \cdot Q_{DL} + \gamma_{LL} \cdot Q_{LL} \quad \text{(Eq. 5.3)}$$

## 5.3 Calibration of Resistance Factors

The resistance factor in Equation 5.3 can be established in any number of ways; resistance factors can be established from probabilistic calibration, from calibration with historical "allowable stress design" practice, or simply established from individual or collective judgment. Current U.S. practice for geotechnical design of transportation infrastructure generally adopts a resistance factor equal to 0.50 for design of spread footings at the Strength I limit state (AASHTO, 2010). This resistance factor was established from combined consideration of historical practice and probabilistic analyses (Allen et al., 2005) and is generally adopted regardless of the uncertainty present for geotechnical design parameters. The target probability of failure associated with the resistance factor of 0.50 is not strictly established. However, Allen et al. (2005) concluded that this resistance factor achieves a reliability index of approximately 3.5, which corresponds to a probability of failure of approximately 1 in 4,300 if the performance function is assumed to be normally distributed (Allen, 2005).

For the present work, resistance factors for design of spread footings were probabilistically calibrated (Loehr et al, 2011b; 2011c) to achieve one of several target probabilities of failure adopted by the Missouri Department of Transportation (Huaco et al., 2012). For these calibrations, the parameters $Q_{DL}$, $Q_{LL}$, $N_c$, and $s_u$ were taken to be probabilistic variables while the footing area, $A$, was considered to be a deterministic

variable. Specific values used for each of these parameters are described in the following sections along with more detailed description of the calibration procedure.

5.3.1 Probabilistic Representation of Design Parameters

For the probabilistic calibrations, the ratio of dead load to live load was taken to be equal to two. Both load effects were assumed to follow a normal distribution, such that:

$$Q_{DL} \sim N(\mu_{DL} = 1000kips, COV_{DL} = 0.12) \quad \text{(Eq. 5.4)}$$

$$Q_{LL} \sim N(\mu_{LL} = 500kips, COV_{LL} = 0.10) \quad \text{(Eq. 5.5)}$$

where $Q_{DL}$ is dead load having mean $\mu_{DL}$ and coefficient of variation $COV_{DL}$, and $Q_{LL}$ is live load having mean $\mu_{LL}$ and coefficient of variation $COV_{LL}$. Values for $COV_{DL}$ and $COV_{LL}$ in Eqs. 5.4 and 5.5 were taken from Kulicki et al. (2007). Values for $\mu_{DL}$ and $\mu_{LL}$ were assumed based on loading for a typical bridge. The load factors for dead load and live load were taken to be 1.25 and 1.75, respectively, based on current design practice (AASHTO, 2010).

The undrained shear strength ($s_u$) was assumed to follow a lognormal distribution with a constant mean value, $\mu_{s_u}$, and coefficients of variation ranging from 0 to 1.0. The bearing capacity factor, $N_c$, was assumed to be normally distributed with a mean value ($\mu_{N_c}$) equal to 6.0 and a coefficient of variation ($COV_{N_c}$) equal to 0.12

$$N_c \sim N(\mu_{N_c} = 6, COV_{N_c} = 0.12) \quad \text{(Eq. 5.6)}$$

to reflect uncertainties in the design model. In general, the bearing capacity factor is affected by the foundation shape and depth, among other factors, and its value is uncertain even for specific values of shape and depth. For undrained ($\phi = 0$) conditions, Terzaghi (Terzaghi, 1996) recommends a bearing capacity factor of 5.7 while Vesic (1974) recommends a bearing capacity factor of 5.14. Shape and depth corrections generally

increase the magnitude of the bearing capacity factor by zero to approximately 40 percent. Thus, $\mu_{N_c}$ was taken to be 6.0 and $COV_{N_c}$ was taken to be 0.12 considering the "six sigma rule" and that $N_c$ might vary between a value as low as 4 and a value as great as 9 (Skempton, 1951) for spread footings.

As described in more detail in Section 5.5, the specific mean values of the bearing capacity factor ($\mu_{N_c}$), undrained shear strength ($\mu_{s_u}$), dead load ($\mu_{DL}$) and live load ($\mu_{LL}$) have a negligible effect on the value of calibrated resistance factors presented subsequently in this chapter. Thus, the values used for calibration apply across a broad range of values for these design parameters.

### 5.3.2 Calibration Procedure

The Monte Carlo simulation method was used to establish resistance factors for use in Equation 5.3. Given the probabilistic values for the design parameters documented in the previous section, 100,000 Monte Carlo simulations were performed to establish the foundation area, $A_c$, that produces a simulated probability of failure just equal to the target probability of failure:

$$p(s_u \cdot N_c \cdot A_c \leq Q_{DL} + Q_{LL}) = p_T \qquad \text{(Eq. 5.7)}$$

where $p(s_u \cdot N_c \cdot A_c \leq Q_{DL} + Q_{LL})$ represents the probability that the foundation resistance (the left hand side of the inequality) is less than or equal to the combined dead and live load (the right hand side of the inequality) and $p_T$ represents the target probability of failure. Area $A_c$ thus represents the foundation area where the probability of the combined nominal load exceeding the nominal resistance is equal to the target probability of failure for the specific $p_T$ and $COV_{s_u}$ considered. Area $A_c$ was then used to calculate the corresponding resistance factor, $\varphi$, according to:

$$\varphi = \frac{\gamma_{DL} \cdot \mu_{DL} + \gamma_{LL} \cdot \mu_{LL}}{\mu_{s_u} \cdot \mu_{N_c} \cdot A_c} \quad \text{(Eq. 5.8)}$$

Simulations were repeated considering $COV_{s_u}$ values varying from 0 to 1.0 and for four different target probabilities of failure ($p_T$) –1/300, 1/1500, 1/5000, and 1/10000 – which represent target values established for minor roads, major roads, major bridges costing less than $100 million, and major bridges costing greater than $100 million, respectively (Huaco et al., 2012).

## 5.4 Calibrated Resistance Factors

The computed values for $\varphi$ are plotted in Figure 5.1 to produce relationships between $\varphi$ and $COV_{s_u}$ for the four different target probabilities of failure. Downward trends in the relationships reflect the fact that lower resistance factors are required to produce the same probability of failure for conditions where there is greater uncertainty in the undrained shear strength. Similarly, lower resistance factors are required for all values of $COV_{s_u}$ to achieve smaller target probabilities of failure.

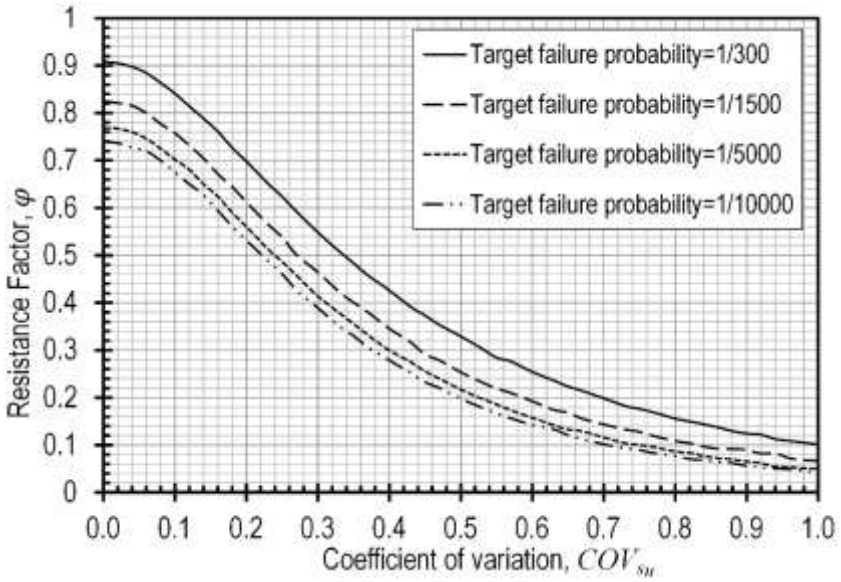


Figure 5.1 Resistance factors for undrained bearing capacity of spread footings at strength limit states for different target probabilities of failure.

If the uncertainty in undrained shear strength is precisely known, the resistance factors in Figure 5.1 will produce designs that achieve the target probability of failure with a high degree of precision as illustrated in an example shown in Figure 5.2. The accuracy with which the target probability of failure is achieved for a specific design is therefore largely dependent on how accurately the undrained shear strength and the uncertainty in the undrained shear strength is known. The accuracy of the undrained shear strength and the uncertainty in the undrained shear strength is, in turn, dependent on the number of undrained shear strength measurements used to interpret the soil design parameters as illustrated in more detail in Chapter 6.

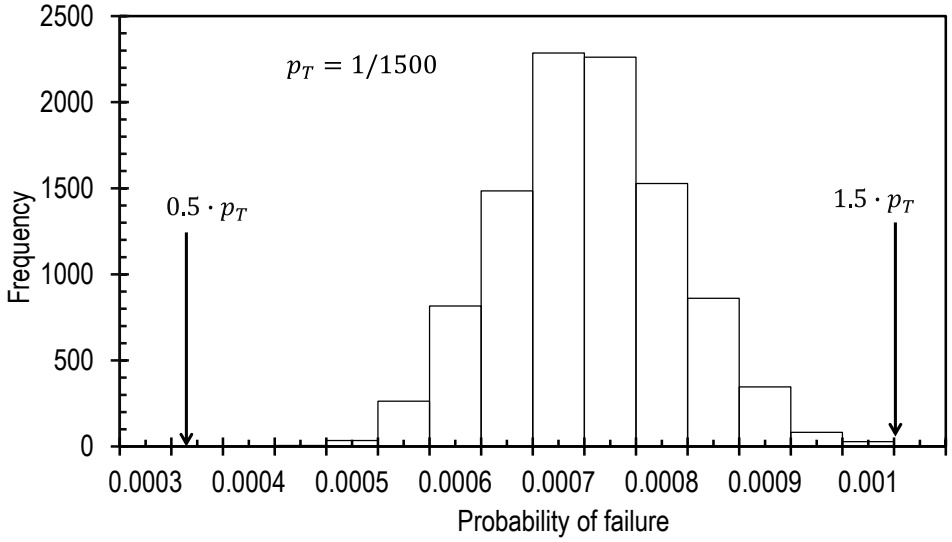


Figure 5.2 Simulated probabilities of failure fall within a range of target probability of failure when undrained shear strength is precisely known.

## 5.5 Effect of Calibration Parameters

While the resistance factors shown in Figure 5.1 were computed using parameters described in Section 5.3, practically identical resistance factors will be computed if alternative values of the bearing capacity factor ($\mu_{N_c}$), undrained shear strength ($\mu_{s_u}$), dead load ($\mu_{DL}$) and live load ($\mu_{LL}$) are considered. To illustrate why the computed resistance

factors are insensitive to the specific values of these parameters used for the calibrations, each of these parameter can be written in general probabilistic form as:

$$Q_{DL} = N(\mu_{DL}, \sigma_{DL}) = \mu_{DL} \cdot N(1, COV_{DL}) \quad \text{(Eq. 5.9)}$$

$$Q_{LL} = N(\mu_{LL}, \sigma_{LL}) = \mu_{LL} \cdot N(1, COV_{LL}) \quad \text{(Eq. 5.10)}$$

$$N_c = N\left(\mu_{N_c}, \sigma_{N_c}\right) = \mu_{N_c} \cdot N(1, COV_{N_c}) \quad \text{(Eq. 5.11)}$$

$$s_u = lN(\mu_{lns_u}, \sigma_{lns_u}) \quad \text{(Eq. 5.12)}$$

From Equation 5.3, and considering that the area is established according to the mean (i.e. nominal) values of these design parameters and fixed values of the load and resistance factors, the area can be written as:

$$A = \frac{\gamma_{DL} \cdot \mu_{DL} + \gamma_{LL} \cdot \mu_{LL}}{\mu_{N_c} \cdot \mu_{s_u} \cdot \varphi} \quad \text{(Eq. 5.13)}$$

Substituting this area into Equation 5.7 produces:

$$p\left[lN(\mu_{lns_u}, \sigma_{lns_u}) \cdot \mu_{N_c} \cdot N(1, COV_{N_c}) \cdot \frac{\gamma_{DL} \cdot \mu_{DL} + \gamma_{LL} \cdot \mu_{LL}}{\mu_{N_c} \cdot \mu_{s_u} \cdot \varphi} \leq \mu_{DL} \cdot N(1, COV_{DL}) + \mu_{LL} \cdot N(1, COV_{LL})\right] = p_T \quad \text{(Eq. 5.14)}$$

which can be rearranged to become:

$$p\left[\frac{lN(\mu_{lns_u}, \sigma_{lns_u}) \cdot \mu_{N_c} \cdot N(1, COV_{N_c})}{\mu_{N_c} \cdot \mu_{s_u} \cdot \varphi} - \frac{\mu_{DL} \cdot N(1, COV_{DL}) + \mu_{LL} \cdot N(1, COV_{LL})}{(\gamma_{DL} \cdot \mu_{DL} + \gamma_{LL} \cdot \mu_{LL})} \leq 0\right] = p_T \quad \text{(Eq. 5.15)}$$

The undrained shear strength in Equation 5.15 follows a lognormal distribution. However, when a large number of undrained shear strength values are used, the distribution can be approximated using a normal distribution. Thus, Eq. 5.15 can be approximated as:

$$p\left[\frac{\mu_{s_u} \cdot N(1, COV_{s_u}) \cdot \mu_{N_c} \cdot N(1, COV_{N_c})}{\mu_{N_c} \cdot \mu_{s_u} \cdot \varphi} - \frac{\mu_{DL} \cdot N(1, COV_{DL}) + \mu_{LL} \cdot N(1, COV_{LL})}{(\gamma_{DL} \cdot \mu_{DL} + \gamma_{LL} \cdot \mu_{LL})} \leq 0\right] = p_T \quad \text{(Eq. 5.16)}$$

The mean values of the bearing capacity factor, $\mu_{N_c}$, and the undrained shear strength, $\mu_{s_u}$, in the first term of Equation 5.16 can be canceled out. Similarly, the second term can be simplified by dividing the numerator and denominator by $\mu_{LL}$ to produce:

$$p\left[\frac{N(1,COV_{s_u})\cdot N(1,COV_{N_c})}{\varphi}-\frac{\frac{\mu_{DL}}{\mu_{LL}}\cdot N(1,COV_{DL})+N(1,COV_{LL})}{\left(\frac{\mu_{DL}}{\mu_{LL}}\cdot\gamma_{DL}+\gamma_{LL}\right)}\leq 0\right]=p_T \qquad \text{(Eq. 5.17)}$$

which demonstrates that the resistance factor to satisfy the probabilistic criterion is independent of the mean values of the undrained shear strength ($\mu_{s_u}$) and the bearing capacity factor ($\mu_{N_c}$). Furthermore, the resistance factor does not depend on the individual magnitudes of the live load ($\mu_{LL}$) and dead load ($\mu_{DL}$) components, but does depend on the dead load to live load ratio ($^{\mu_{DL}}/_{\mu_{LL}}$). The resistance factors shown in Figure 5.1 are thus dependent on the coefficients of variation of each parameter ($COV_{s_u}$, $COV_{N_c}$, $COV_{DL}$ and $COV_{LL}$) and the ratio of dead load to live load ($^{\mu_{DL}}/_{\mu_{LL}}$).

## 5.6 Summary

The LRFD criterion adopted for design of spread footings at the Strength I limit state was described in this chapter. Methods adopted for probabilistically calibrating resistance factors for this limit state were also described and probabilistic representations of relevant design parameters used for calibration of resistance factors were documented. The calibrated resistance factors presented in this chapter were used throughout the research described in this thesis to study how the number of undrained shear strength measurements affects the reliability of spread footings design using LRFD with the established resistance factors.

# Chapter 6 Effect of Number of Measurements on Design Values for Undrained Shear Strength

## 6.1 Introduction

The undrained shear strength at the four test sites described in previous chapters was characterized from a large number of high quality measurements, which results in accurate estimates of undrained shear strength. In most practical design situations, however, far fewer measurements are available. Design parameters derived from small numbers of measurements involve much greater uncertainty, which results in less consistency in selected design parameters less consistency in foundations designed using those parameters.

In general, there are two broad types of uncertainty for soil properties used in design— aleatory uncertainty and epistemic uncertainty. Aleatory uncertainty represents the natural variability of soil properties while epistemic uncertainty represents uncertainty in the value of a soil property due to lack of knowledge. The present research focuses on the magnitude of epistemic uncertainty when using regression models to establish soil design parameters from different numbers of measurements. In this chapter, the relation between the number of measurements and the characterized undrained shear strength is quantitatively evaluated. Analyses conducted by repeatedly selecting random subsamples of undrained shear strength measurements to simulate measurements that could be obtained from different site investigations are described. Estimates of the mean undrained shear strength, the uncertainty in the mean undrained shear strength, and the total variability and uncertainty of the undrained shear strength for each subsample are presented to

characterize the variability of these estimates as a function of the number of measurements considered.

## 6.2 Populations of Undrained Shear Strength Measurements

As introduced in Chapter 3, comprehensive site characterization programs were conducted at four sites: the Pemiscot site, the St. Charles site, the New Florence site and the Warrensburg site. Thirty five undrained shear strength measurements were obtained at the Warrensburg site while greater than fifty undrained shear strength measurements were obtained at the other three sites. The measurements were obtained from unconsolidated-undrained (UU) type triaxial compression tests performed on high quality soil specimens acquired using state of the art boring and sampling techniques. Regression models representing the mean and uncertainty of the undrained shear strength measurements for each site were summarized in Chapter 4; these interpretations are regarded to represent the "true" soil properties at each site.

While the number of measurements obtained at the four sites is quite large relative to common site characterization practice, the "populations" of actual measurements are relatively small in a statistical sense. Use of these populations for the simulations described subsequently in this chapter would introduce some bias because the randomly selected measurements may not be practically independent. Larger populations of simulated undrained shear strength measurements were therefore generated to eliminate potential bias. As shown in Figures 6.1-6.4, the simulated undrained shear strength measurements were generated to have the same mean value and variability and uncertainty as the actual measurements for each site. The simulated measurements are deemed to represent a realistic population from which the actual measurements could have been obtained and to

reflect the true undrained shear strength at each site. The simulated populations of measurements were used as the population of measurements for the random sampling described throughout the remainder of this chapter.

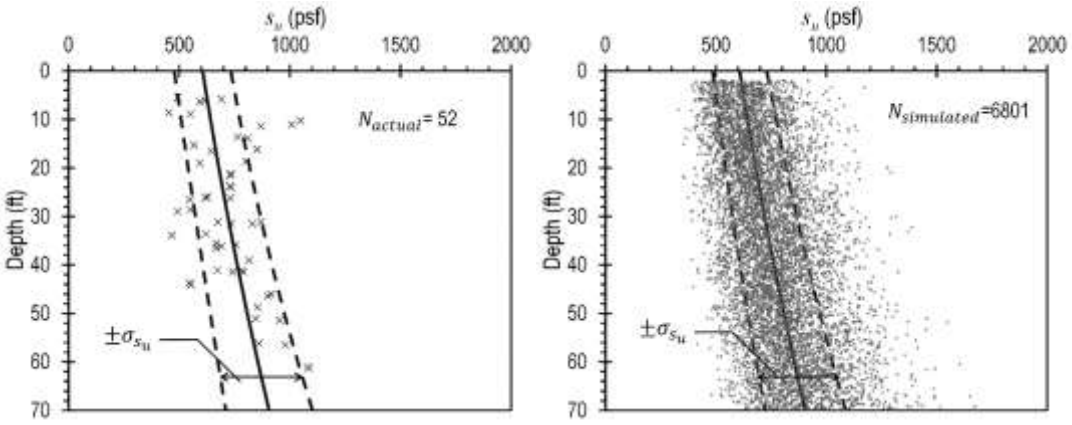


(a) (b)

Figure 6.1 Undrained shear strength from (a) actual measurements, and (b) simulated measurements for the Pemiscot site.

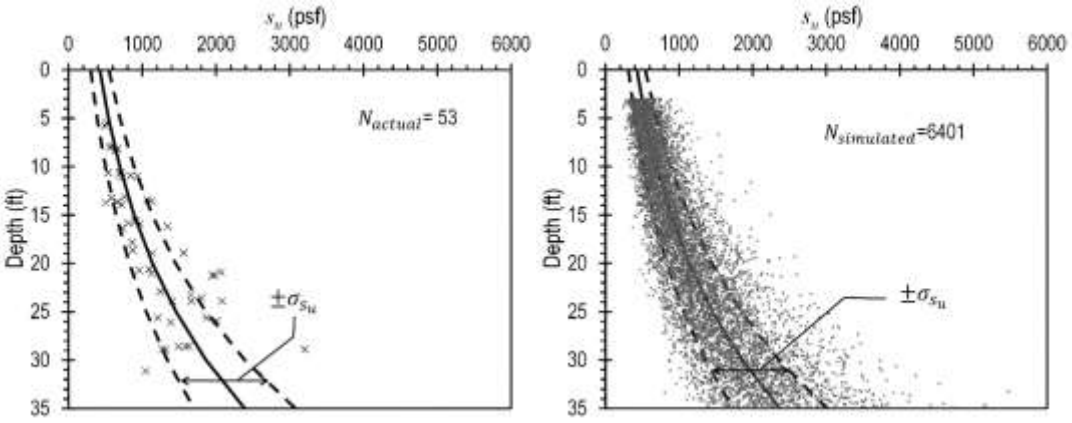


(a) (b)

Figure 6.2 Undrained shear strength from (a) actual measurements, and (b) simulated measurements for the St. Charles site.

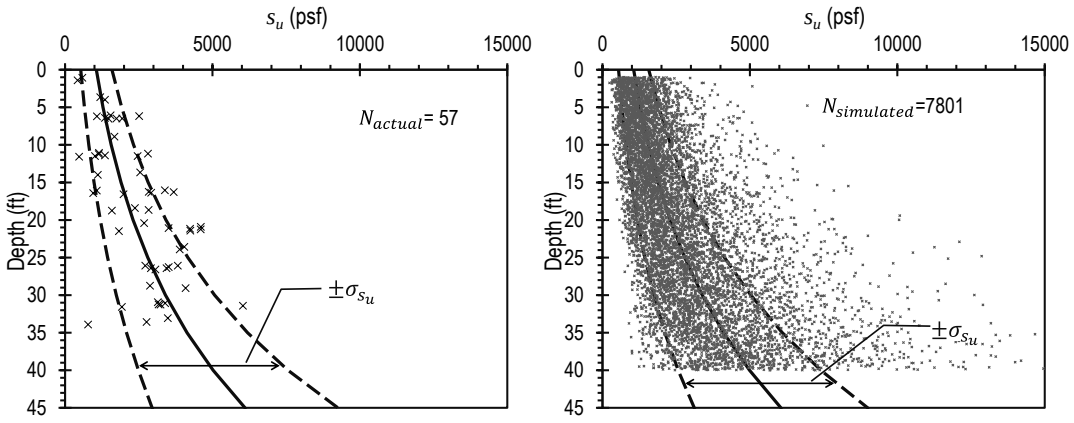


(a) (b)

Figure 6.3 Undrained shear strength from (a) actual measurements, and (b) simulated measurements for the New Florence site.

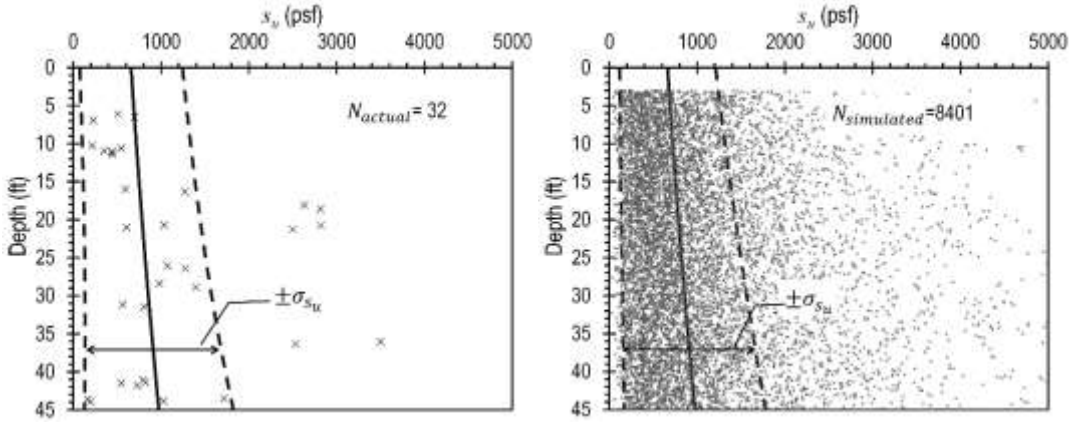


(a) (b)

Figure 6.4 Undrained shear strength from (a) actual measurements, and (b) simulated measurements for the Warrensburg site.

## 6.3 Random Sampling of Undrained Shear Strength Measurements

Random sampling was performed from the population of simulated undrained shear strength measurements for each site to simulate different collections of measurements that could be obtained from different site investigations. For each random "subsample" of measurements, the mean value and the uncertainty of the undrained shear strength were computed to reflect what would be estimated from different subsamples. The procedure used for these calculations included the following steps:

1. Randomly select *n* measurements from the total population of simulated undrained shear strength measurements, *N*.
2. Perform linear regression on the logarithms of the selected measurements to establish an "estimation model" for undrained shear strength based on the selected measurements alone. The regression analyses were identical to those described in Chapter 4 but consider only the measurements included in each subsample.
3. Calculate the mean value ($\mu_{s_u}$), the uncertainty in the mean value ($COV_{\mu_{s_u}}$), and the total variability and uncertainty for the undrained shear strength ($COV_{s_u}$) at a depth of 7 ft from the estimation model using Eqs. 4.7-4.9.
4. Repeat Steps 1 through 3 for 10,000 different random subsamples to simulate results that could be obtained from different site investigations to evaluate how the computed parameters vary with different collections of measurements.

This procedure was repeated for subsamples of different sizes from $n = 3$ to $n = 50$ to evaluate how the estimated parameters vary with different numbers of measurements.

Figure 6.5 shows several interpretations derived using this procedure to qualitatively illustrate interpretations that could be obtained for different subsamples of measurements. The interpretations shown were selected from those obtained considering the simulated population of measurements for the New Florence site and considering subsamples of seven measurements ($n = 7$). Probabilistic measures of the undrained shear strength at a depth of 7 ft from the respective interpretations are summarized in Table 6.1.

As illustrated in Figure 6.5 and Table 6.1, substantially different interpretations of undrained shear strength can be rationally established depending upon the specific measurements considered. Figure 6.5a shows one interpretation that is reasonably

consistent with the interpretation obtained using the entire population of measurements (Fig. 6.3), but that slightly overestimates the mean value for undrained shear strength at a depth of 7 ft. The uncertainty in the mean value of undrained shear strength ($COV_{\mu_{s_u}}$) at a depth of 7 ft is slightly greater than that determined from the population but the estimated total variability and uncertainty ($COV_{s_u}$) is less than observed for the population. As will be illustrated subsequently, this interpretation is representative of many of the interpretations derived from different subsamples.

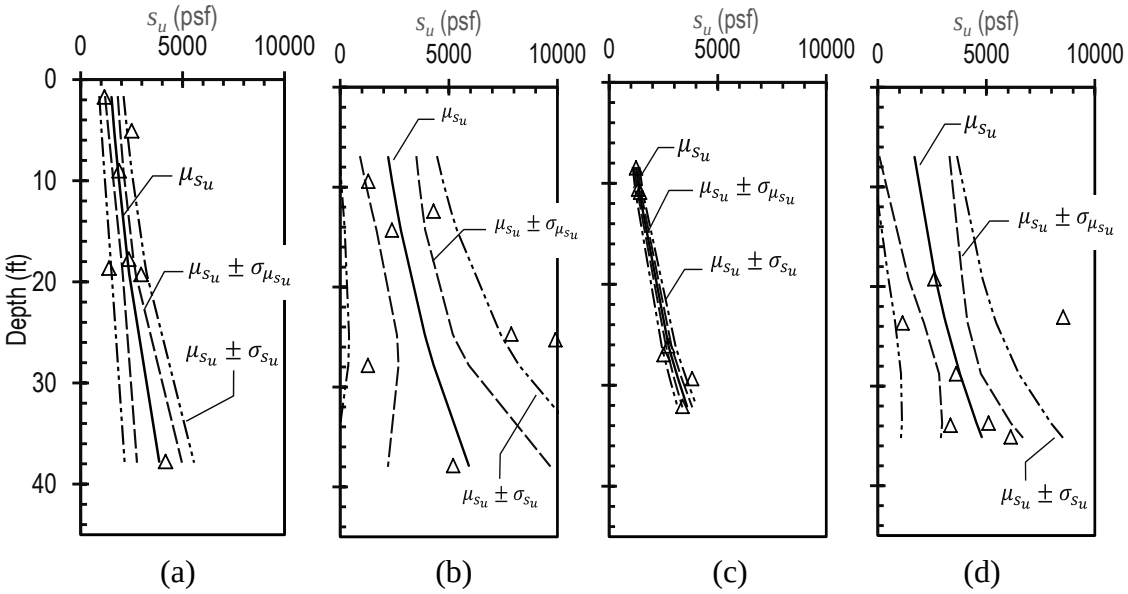


Figure 6.5 Interpretations of undrained shear strength derived from four select subsamples of simulated measurements for the New Florence site for $n = 7$: (a) Subsample A, (b) Subsample B, (c) Subsample C, (d) Subsample D.

Table 6.1 Probabilistic interpretations of undrained shear strength determined at a depth of 7 ft for the select subsamples shown in Figure 6.5.

| Probabilistic Parameter | Subsample A | Subsample B | Subsample C | Subsample D | True soil properties from real measurements |
|---|---|---|---|---|---|
| $\mu_{s_u}$ (psf) | 1731 | 2211 | 1162 | 1689 | 1392 |
| $COV_{\mu_{s_u}}$ | 0.161 | 0.586 | 0.071 | 0.955 | 0.099 |
| $COV_{s_u}$ | 0.3741 | 1.019 | 0.128 | 1.167 | 0.489 |

In contrast, the interpretations shown in Figures 6.5b, 6.5c, and 6.5d represent interpretations that substantially differ from the interpretation established from the entire population of measurements because of the specific measurements that were used for the interpretation. Figure 6.5b reflects a case where the subsample measurements are quite scattered; in this case, estimates for $\mu_{s_u}$, $COV_{\mu_{s_u}}$, and $COV_{s_u}$ at 7 ft exceed the values determined from the entire population. Figure 6.5c illustrates a case with little variability in the subsampled measurements, which produces estimates for $COV_{\mu_{s_u}}$ and $COV_{s_u}$ that are substantially lower than determined for the entire population. Finally, Figure 6.5d illustrates a case where all subsampled measurements are from depths that are substantially greater than 7 ft. In this case, the selected measurements provide less information about the undrained strength at 7 ft than when some measurements are from depths nearer to 7 ft, and this is reflected in the greater variability and uncertainty shown in Table 6.1.

Figures 6.6-6.8 show histograms of $\mu_{s_u}$, $COV_{\mu_{s_u}}$, and $COV_{s_u}$, respectively, computed from the 10,000 different random subsamples for the New Florence site when $n$=7. Figure 6.6 illustrates that, while the most likely value of $\mu_{s_u}$ determined from the different simulations is very close to the value established from the entire population, it is possible to estimate mean undrained strengths that are substantially different from the population. In the specific cases shown, estimates of the mean undrained shear strength determined from subsamples of seven measurements commonly range from approximately 800 psf to 2400 psf and a select few simulations produce estimates that fall outside of these bounds.

Figures 6.7 and 6.8 show that estimates of $COV_{\mu_{s_u}}$ and $COV_{s_u}$ also vary substantially depending on the specific measurements considered. The most likely estimate for $COV_{\mu_{s_u}}$ is substantially greater than determined from the entire population; however, this logically

follows from the fact that $COV_{\mu_{s_u}}$ is a probabilistic measure of confidence in the mean value, which is substantially improved with greater numbers of measurements. The most likely estimate for $COV_{s_u}$ is observed to be only slightly greater than that derived from the entire population, because $COV_{s_u}$ represents both variability and uncertainty in $s_u$.

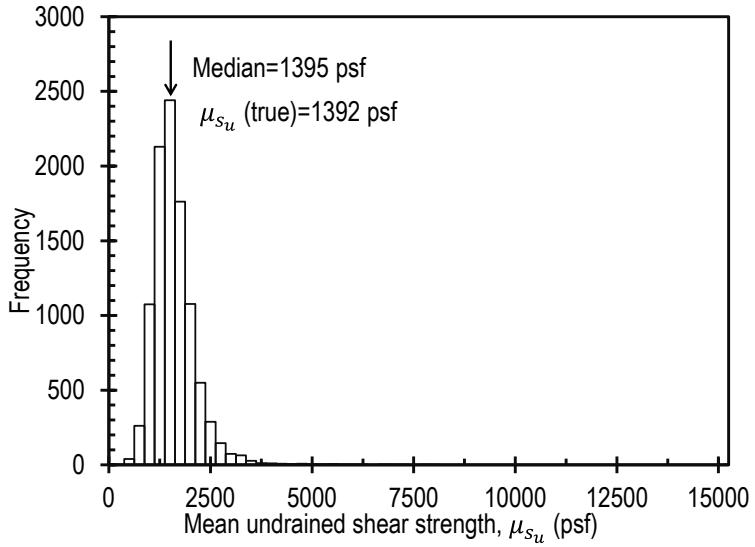


Figure 6.6 Histogram of mean undrained shear strength from 10,000 different random subsamples when $n = 7$.

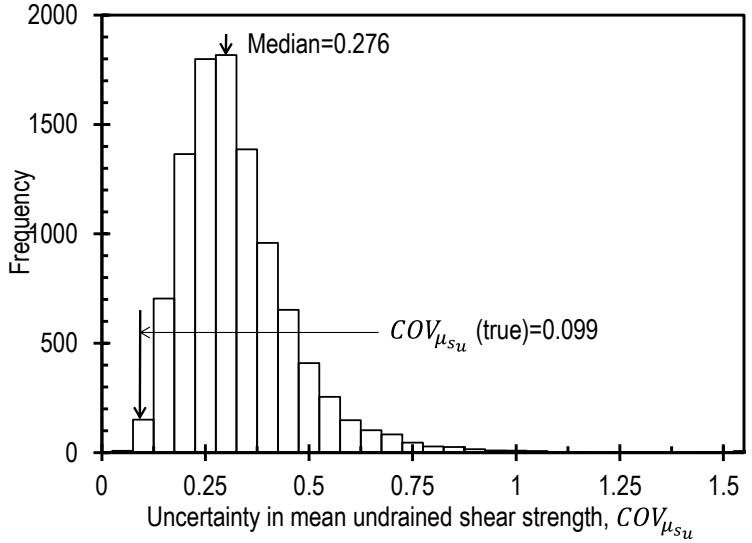


Figure 6.7 Histogram of uncertainty in mean undrained shear strength from 10,000 different random subsamples when $n = 7$.

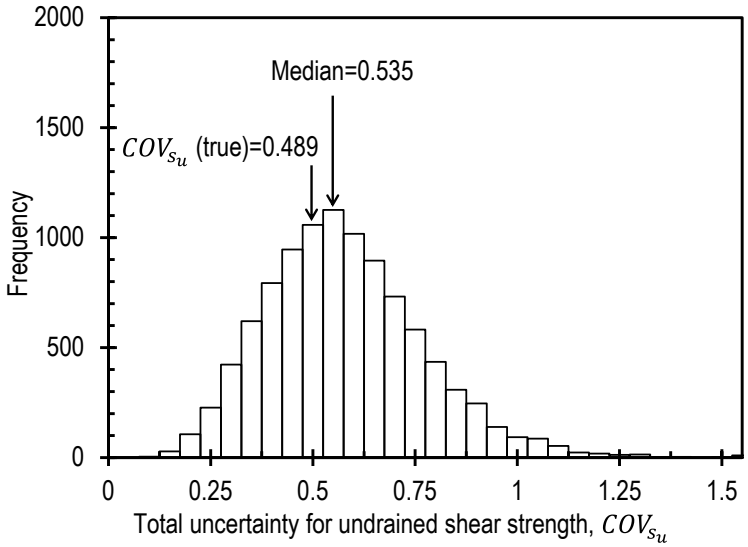


Figure 6.8 Histogram of total variability and uncertainty for undrained shear strength from 10,000 different random subsamples when $n = 7$.

It is worth noting that the purely algorithmic approach adopted for these analyses does not precisely reflect interpretations that would be made with human intervention and engineering judgment. In rare cases, the estimation models derived from the subsampled measurements will produce extreme and irrational results because of the random selection procedure. In actual practice, such interpretations would generally be revised based on engineering judgment to produce interpretations that are likely, but not certain to be more representative of the broader population. The variability of the interpretations established from the regression procedure are therefore likely to be somewhat greater than would actually be experienced in practice. Nevertheless, the interpretations established using the random sampling and regression procedure provide an estimate for the range of different interpretations that could be developed.

In order to evaluate the effect of the number of measurements considered, the procedure described in this section was repeated considering different numbers of measurements to evaluate how the number of measurements used for interpretation of

undrained shear strength affects the mean value, the uncertainty in the mean value, and the total variability and uncertainty in the undrained shear strength. Random samples were taken for $n = 3$ to $n = 50$ to represent the range of measurements that might be available for design of spread footing foundations. Results of these analyses are presented in the following sections.

## 6.4 Mean Undrained Shear Strength

Figures 6.9-6.12 show the median and range of the mean undrained shear strengths estimated from 10,000 different subsamples from the Pemiscot, St. Charles, New Florence, and Warrensburg sites, respectively, plotted as a function of the number of measurements from each subsample. The ranges indicated by the vertical bars in the figures were computed using the $5^{th}$ and $95^{th}$ percentiles of the estimated mean values because the minimum and maximum values are sensitive to the number of different random subsamples considered. Use of the $5^{th}$ and $95^{th}$ percentiles also tends to neglect potentially irrational or unrealistic interpretations that can result from rote application of the random sampling procedure described in the previous section. The ranges shown are thus a better representation of the range of different interpretations that might result from consideration of different measurements. The means and ranges shown all reflect estimates at a depth of 7 ft.

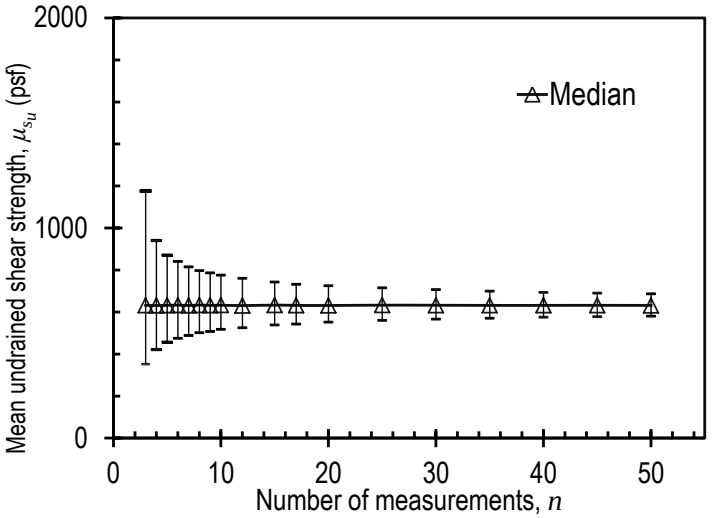

Figure 6.9 Computed mean values of undrained shear strength determined from random subsamples of simulated measurements for the Pemiscot site.

As shown in Figures 6.9-6.12, the median of the estimated mean values of undrained shear strength is practically independent of the number of measurements considered in each subsample. The median of the mean values is also practically identical to the mean value of undrained shear strength established from the entire population of measurements. These observations suggest that estimates for the mean are, on average, accurate when considering large numbers of site investigations.

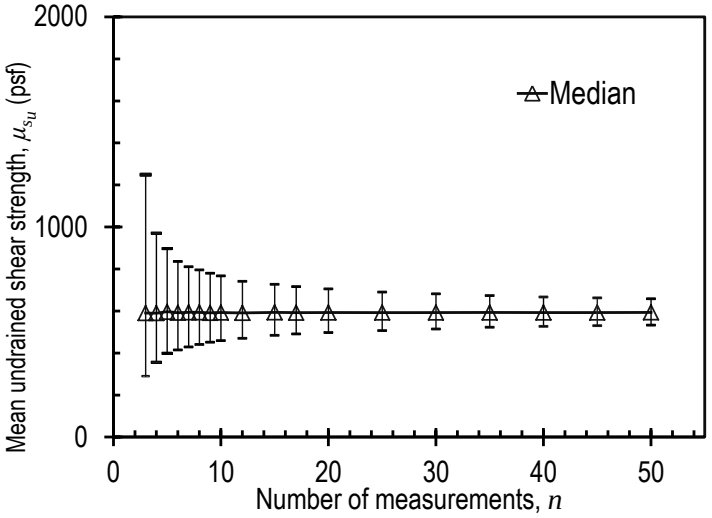

Figure 6.10 Computed mean values of undrained shear strength determined from random subsamples of simulated measurements for the St. Charles site.

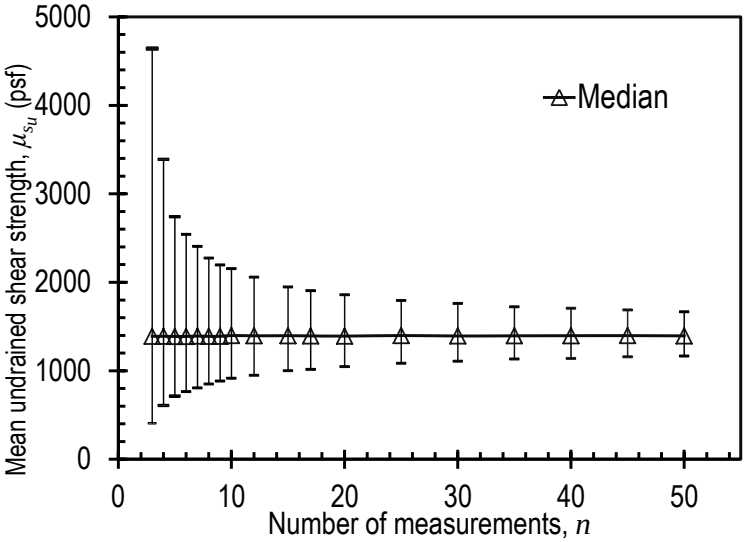


Figure 6.11 Computed mean values of undrained shear strength determined from random subsamples of simulated measurements for the New Florence site.

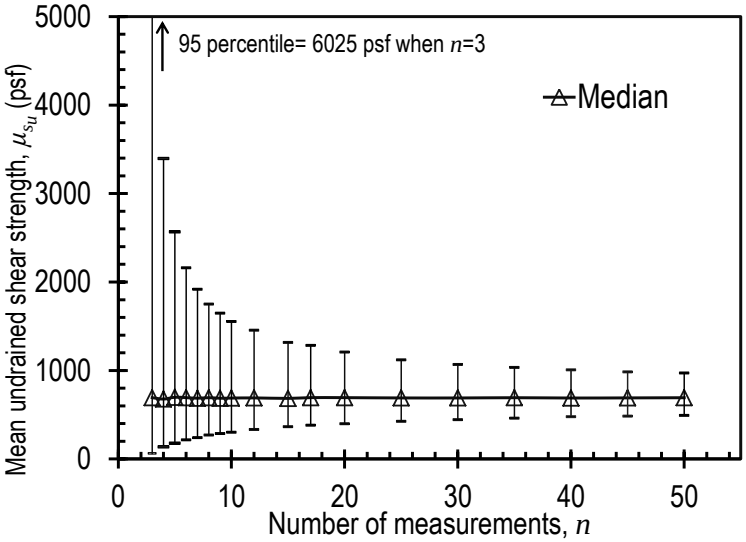


Figure 6.12 Computed mean values of undrained shear strength determined from random subsamples of simulated measurements for the Warrensburg site.

In contrast to the median values, the 5$^{th}$-95$^{th}$ percentile range of the estimated mean values of undrained shear strength decreases dramatically with the number of measurements. For small numbers of measurements, the range may be several times greater than the nominal magnitude of the median of mean value. However, the range of

the estimated mean values decreases rapidly with increasing numbers of measurements until becoming practically constant for $n$ greater than approximately 30. The $5^{th}$-$95^{th}$ percentile ranges do vary from site to site, with the ranges generally being smaller at the less variable sites. Numeric values for the median value and the $5^{th}$-$95^{th}$ percentile ranges from the simulations are provided in Tables 6.2-6.5 for the respective test sites.

Table 6.2 Computed median, $5^{th}$ percentile, $95^{th}$ percentile, and $5^{th}$-$95^{th}$ percentile ranges of the mean undrained shear strength determined from random subsamples of simulated measurements for the Pemiscot site.

| Number of Measurements per Subsample, *n* | Median Mean Value (psf) | $5^{th}$ Percentile Mean Value (psf) | $95^{th}$ Percentile Mean Value (psf) | $5^{th}$-$95^{th}$ Percentile Range (psf) |
|---|---|---|---|---|
| 3 | 631 | 352 | 1176 | 824 |
| 4 | 631 | 421 | 940 | 519 |
| 5 | 632 | 457 | 871 | 414 |
| 6 | 633 | 475 | 841 | 366 |
| 7 | 631 | 488 | 815 | 327 |
| 8 | 633 | 501 | 797 | 296 |
| 9 | 632 | 508 | 786 | 278 |
| 10 | 633 | 517 | 775 | 258 |
| 15 | 633 | 539 | 742 | 203 |
| 20 | 631 | 552 | 725 | 173 |
| 25 | 633 | 560 | 715 | 155 |
| 30 | 632 | 566 | 707 | 141 |
| 40 | 632 | 575 | 694 | 119 |
| 50 | 632 | 580 | 687 | 107 |

Table 6.3 Computed median, 5th percentile, 95th percentile, and 5th-95th percentile ranges of the mean undrained shear strength determined from random subsamples of simulated measurements for the St. Charles site.

| Number of Measurements per Subsample, *n* | Median Mean Value (psf) | 5th Percentile Mean Value (psf) | 95th Percentile Mean Value (psf) | 5th-95th Percentile Range (psf) |
|---|---|---|---|---|
| 3 | 591 | 290 | 1249 | 959 |
| 4 | 590 | 356 | 971 | 615 |
| 5 | 596 | 399 | 897 | 498 |
| 6 | 592 | 415 | 836 | 421 |
| 7 | 594 | 428 | 810 | 382 |
| 8 | 593 | 440 | 796 | 356 |
| 9 | 591 | 451 | 780 | 329 |
| 10 | 593 | 459 | 767 | 308 |
| 15 | 593 | 484 | 727 | 243 |
| 20 | 593 | 498 | 705 | 207 |
| 25 | 592 | 507 | 690 | 183 |
| 30 | 593 | 514 | 681 | 167 |
| 40 | 593 | 526 | 667 | 141 |
| 50 | 593 | 533 | 658 | 125 |

Table 6.4 Computed median, 5th percentile, 95th percentile, and 5th-95th percentile ranges of the mean undrained shear strength determined from random subsamples of simulated measurements for the New Florence site.

| Number of Measurements per Subsample, *n* | Median Mean Value (psf) | 5th Percentile Mean Value (psf) | 95th Percentile Mean Value (psf) | 5th-95th Percentile Range (psf) |
|---|---|---|---|---|
| 3 | 1390 | 405 | 4642 | 4237 |
| 4 | 1389 | 607 | 3388 | 2781 |
| 5 | 1388 | 713 | 2740 | 2027 |
| 6 | 1388 | 764 | 2541 | 1777 |
| 7 | 1392 | 805 | 2404 | 1599 |
| 8 | 1389 | 849 | 2273 | 1424 |
| 9 | 1389 | 882 | 2196 | 1314 |
| 10 | 1398 | 915 | 2154 | 1239 |
| 15 | 1397 | 999 | 1946 | 947 |
| 20 | 1392 | 1046 | 1859 | 813 |
| 25 | 1398 | 1084 | 1794 | 710 |
| 30 | 1393 | 1107 | 1759 | 652 |
| 40 | 1396 | 1139 | 1706 | 567 |
| 50 | 1395 | 1167 | 1667 | 500 |

Table 6.5 Computed median, 5th percentile, 95th percentile, and 5th-95th percentile ranges of the mean undrained shear strength determined from random subsamples of simulated measurements for the Warrensburg site.

| Number of Measurements per Subsample, *n* | Median Mean Value (psf) | 5th Percentile Mean Value (psf) | 95th Percentile Mean Value (psf) | 5th-95th Percentile Range (psf) |
|---|---|---|---|---|
| 3 | 693 | 63 | 6025 | 5962 |
| 4 | 677 | 136 | 3394 | 3258 |
| 5 | 698 | 178 | 2566 | 2388 |
| 6 | 693 | 215 | 2161 | 1946 |
| 7 | 687 | 241 | 1916 | 1675 |
| 8 | 693 | 270 | 1749 | 1479 |
| 9 | 686 | 287 | 1647 | 1360 |
| 10 | 688 | 300 | 1554 | 1254 |
| 15 | 685 | 364 | 1317 | 953 |
| 20 | 693 | 396 | 1207 | 811 |
| 25 | 690 | 426 | 1120 | 694 |
| 30 | 690 | 443 | 1068 | 625 |
| 40 | 689 | 477 | 1006 | 529 |
| 50 | 692 | 493 | 971 | 478 |

## 6.5 Uncertainty in the Mean Undrained Shear Strength

The uncertainty in the estimated mean undrained shear strength is represented by the coefficient of variation of the mean value, $COV_{\mu_{s_u}}$. Figures 6.13-6.16 show the median and 5th-95th percentile ranges for $COV_{\mu_{s_u}}$, plotted versus the number of measurements from each subsample. The figures show that both the median values and the 5th-95th percentile ranges of $COV_{\mu_{s_u}}$ decrease with the number of measurements and approach zero when *n* becomes large ($n \to \infty$) for all sites. However, the magnitude of both the range and median values are substantially greater for the more variable sites and greater numbers of measurements are needed to reduce $COV_{\mu_{s_u}}$ to a given level at the more variable sites. Tables 6.6-6.9 provide the numeric values that are plotted in Figures 6.13-6.16.

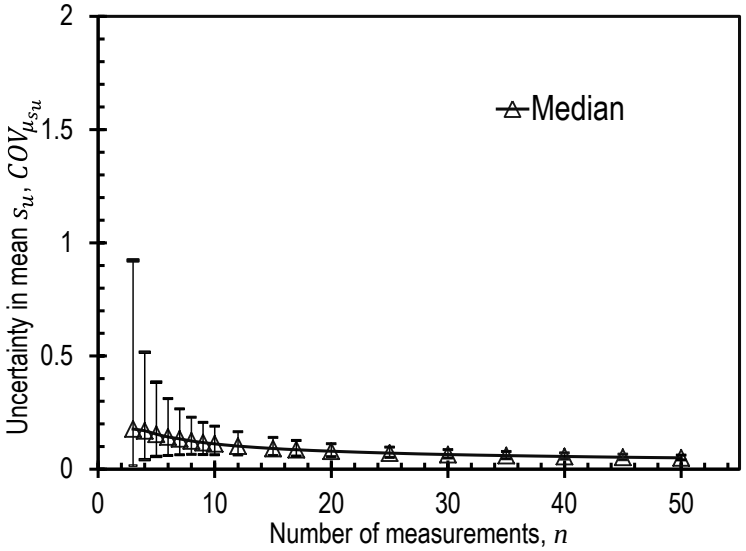


Figure 6.13 Computed *COV* of mean values of undrained shear strength determined from random subsamples of simulated measurements for the Pemiscot site.

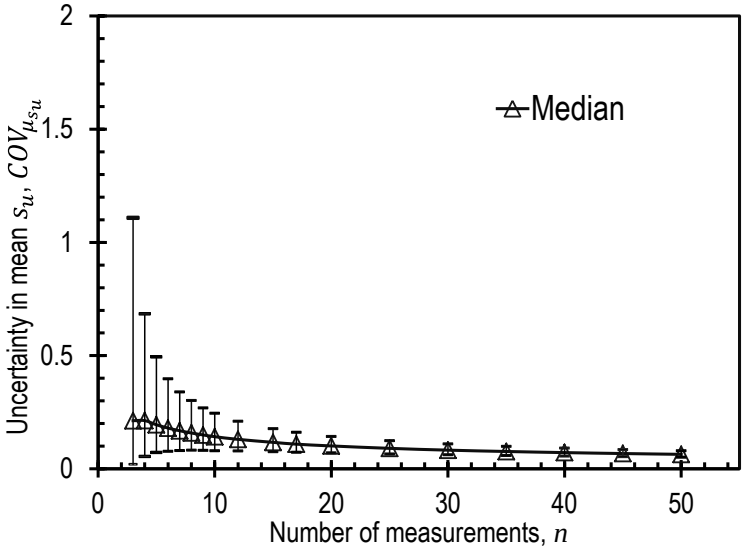


Figure 6.14 Computed *COV* of mean values of undrained shear strength determined from random subsamples of simulated measurements for the St. Charles site.

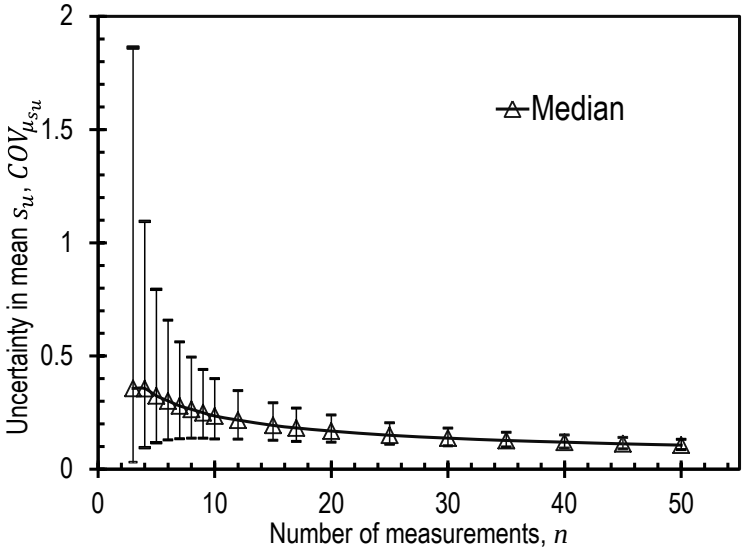


Figure 6.15 Computed *COV* of mean values of undrained shear strength determined from random subsamples of simulated measurements for the New Florence site.

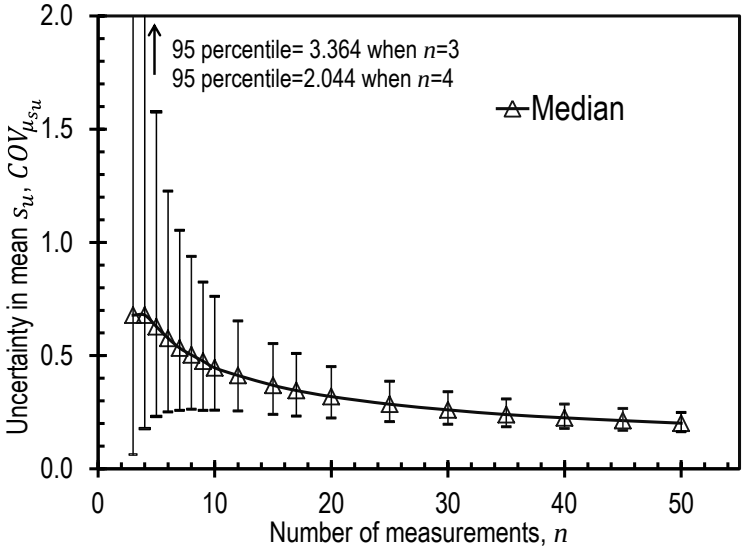


Figure 6.16 Computed *COV* of mean values of undrained shear strength determined from random subsamples of simulated measurements for the Warrensburg site.

The results shown in Figures 6.13-6.16 indicate that the mean undrained shear strength can be characterized with great accuracy when large numbers of measurements are available but that greater number of measurements are required to achieve a specific level of uncertainty for more variable sites (e.g. Warrensburg site). The 5$^{th}$-95$^{th}$ percentile range of $COV_{\mu_{s_u}}$ is quite large when few measurements are considered but decreases with

increasing numbers of measurements. These observations suggest that there is significant likelihood that the uncertainty in the mean undrained shear strength will be dramatically underestimated or overestimated when small numbers of measurements are considered, in addition to the similar likelihood that the mean value itself could be under- or over-estimated. The results also suggest that our confidence in the mean value should generally increase steadily with increasing numbers of measurements.

Table 6.6 Computed median, 5th percentile, 95th percentile, and 5th-95th percentile ranges of $COV_{\mu_{s_u}}$ determined from random subsamples of simulated measurements for the Pemiscot site.

| Number of Measurements per Subsample, *n* | Median Mean Value (psf) | 5th Percentile Mean Value (psf) | 95th Percentile Mean Value (psf) | 5th-95th Percentile Range (psf) |
|---|---|---|---|---|
| 3 | 0.178 | 0.016 | 0.922 | 0.906 |
| 4 | 0.170 | 0.042 | 0.517 | 0.475 |
| 5 | 0.155 | 0.056 | 0.385 | 0.329 |
| 6 | 0.143 | 0.060 | 0.312 | 0.252 |
| 7 | 0.134 | 0.064 | 0.266 | 0.202 |
| 8 | 0.125 | 0.066 | 0.230 | 0.164 |
| 9 | 0.118 | 0.065 | 0.206 | 0.141 |
| 10 | 0.112 | 0.064 | 0.190 | 0.126 |
| 15 | 0.092 | 0.060 | 0.140 | 0.080 |
| 20 | 0.080 | 0.055 | 0.112 | 0.057 |
| 25 | 0.071 | 0.052 | 0.097 | 0.045 |
| 30 | 0.065 | 0.049 | 0.087 | 0.038 |
| 40 | 0.056 | 0.044 | 0.072 | 0.028 |
| 50 | 0.051 | 0.041 | 0.062 | 0.021 |

Table 6.7 Computed median, 5th percentile, 95th percentile, and 5th-95th percentile ranges of $COV_{\mu_{s_u}}$ determined from random subsamples of simulated measurements for St. Charles site.

| Number of Measurements per Subsample, *n* | Median Mean Value (psf) | 5th Percentile Mean Value (psf) | 95th Percentile Mean Value (psf) | 5th-95th Percentile Range (psf) |
|---|---|---|---|---|
| 3 | 0.213 | 0.020 | 1.108 | 1.088 |
| 4 | 0.213 | 0.054 | 0.684 | 0.630 |
| 5 | 0.195 | 0.072 | 0.494 | 0.422 |
| 6 | 0.180 | 0.078 | 0.397 | 0.319 |
| 7 | 0.168 | 0.081 | 0.339 | 0.258 |
| 8 | 0.158 | 0.082 | 0.301 | 0.219 |
| 9 | 0.150 | 0.081 | 0.269 | 0.188 |
| 10 | 0.142 | 0.079 | 0.245 | 0.166 |
| 15 | 0.117 | 0.076 | 0.178 | 0.102 |
| 20 | 0.101 | 0.070 | 0.143 | 0.073 |
| 25 | 0.091 | 0.066 | 0.124 | 0.058 |
| 30 | 0.083 | 0.062 | 0.110 | 0.048 |
| 40 | 0.072 | 0.056 | 0.092 | 0.036 |
| 50 | 0.064 | 0.051 | 0.080 | 0.029 |

Table 6.8 Computed median, 5th percentile, 95th percentile, and 5th-95th percentile ranges of $COV_{\mu_{s_u}}$ determined from random subsamples of simulated measurements for New Florence site.

| Number of Measurements per Subsample, *n* | Median Mean Value (psf) | 5th Percentile Mean Value (psf) | 95th Percentile Mean Value (psf) | 5th-95th Percentile Range (psf) |
|---|---|---|---|---|
| 3 | 0.357 | 0.031 | 1.862 | 1.831 |
| 4 | 0.356 | 0.095 | 1.094 | 0.999 |
| 5 | 0.324 | 0.116 | 0.794 | 0.678 |
| 6 | 0.302 | 0.130 | 0.658 | 0.528 |
| 7 | 0.280 | 0.135 | 0.562 | 0.427 |
| 8 | 0.265 | 0.137 | 0.495 | 0.358 |
| 9 | 0.250 | 0.137 | 0.440 | 0.303 |
| 10 | 0.235 | 0.134 | 0.400 | 0.266 |
| 15 | 0.194 | 0.128 | 0.293 | 0.165 |
| 20 | 0.169 | 0.119 | 0.239 | 0.120 |
| 25 | 0.150 | 0.110 | 0.205 | 0.095 |
| 30 | 0.137 | 0.103 | 0.182 | 0.079 |
| 40 | 0.120 | 0.093 | 0.151 | 0.058 |
| 50 | 0.107 | 0.086 | 0.131 | 0.045 |

Table 6.9 Computed median, 5th percentile, 95th percentile, and 5th-95th percentile ranges of $COV_{\mu_{s_u}}$ determined from random subsamples of simulated measurements for the Warrensburg site.

| Number of Measurements per Subsample, *n* | Median Mean Value (psf) | 5th Percentile Mean Value (psf) | 95th Percentile Mean Value (psf) | 5th-95th Percentile Range (psf) |
|---|---|---|---|---|
| 3 | 0.679 | 0.063 | 3.364 | 3.301 |
| 4 | 0.679 | 0.177 | 2.044 | 1.867 |
| 5 | 0.628 | 0.231 | 1.576 | 1.345 |
| 6 | 0.577 | 0.251 | 1.226 | 0.975 |
| 7 | 0.533 | 0.258 | 1.053 | 0.795 |
| 8 | 0.503 | 0.263 | 0.938 | 0.675 |
| 9 | 0.475 | 0.258 | 0.824 | 0.566 |
| 10 | 0.446 | 0.258 | 0.761 | 0.503 |
| 15 | 0.369 | 0.240 | 0.553 | 0.313 |
| 20 | 0.319 | 0.225 | 0.451 | 0.226 |
| 25 | 0.285 | 0.208 | 0.386 | 0.178 |
| 30 | 0.260 | 0.196 | 0.340 | 0.144 |
| 40 | 0.225 | 0.178 | 0.286 | 0.108 |
| 50 | 0.202 | 0.164 | 0.249 | 0.085 |

## 6.6 Total Variability and Uncertainty for Undrained Shear Strength

The total variability and uncertainty for the undrained shear strength is a combined measure that includes the uncertainty in the mean undrained shear strength (i.e. the "model") and the variability of the measurements. The total variability and uncertainty is generally used to reflect the level of uncertainty for new predictions (e.g. the uncertainty for a new measurement of undrained shear strength) whereas the model uncertainty described in Section 6.5 is used to reflect the accuracy of the model given the available measurements.

Figures 6.17-6.20 show the median value and the 5th-95th percentile range of $COV_{s_u}$ for the four sites, respectively, as a function of the number of measurements from each subsample. The figures show that the median value of $COV_{s_u}$ tends to be less than $COV_{s_u}$ established from the entire population for small $n$, but to relatively consistent for $n \geq 5$.

The magnitude of $COV_{s_u}$ decreases with the number of measurements and approaches the value of $COV_{s_u}$ for the entire population when larger numbers of measurements are considered. The 5th-95th percentile range varies with the complexity of the site, with greater ranges being observed for the more variable sites, i.e., the Warrensburg site as shown in Figure 6.20 and the New Florence site as shown in Figure 6.19. The range of $COV_{s_u}$ decreases with the number of measurements for all sites. Tables 6.10-6.13 summarize the median, 5th percentile and 95th percentile values of $COV_{s_u}$ for different numbers of measurements at the Pemiscot site, the St. Charles site, the New Florence site and the Warrensburg site, respectively.

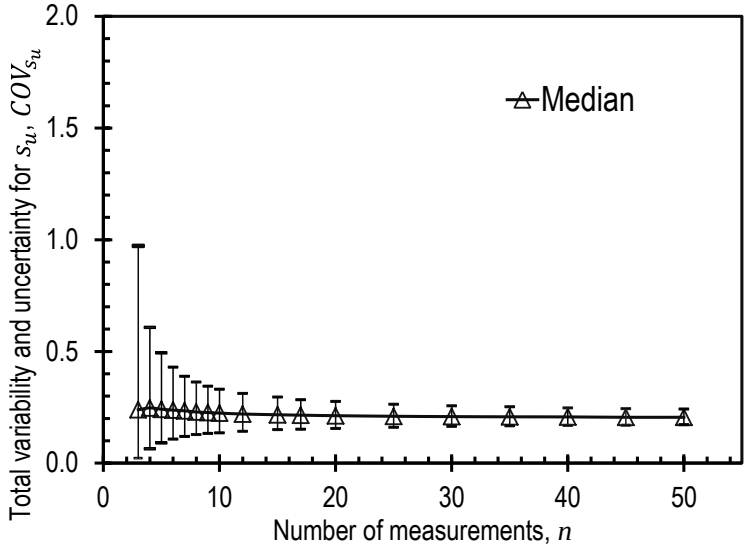


Figure 6.17 Computed $COV$ of undrained shear strength determined from random subsamples of simulated measurements for the Pemiscot site.

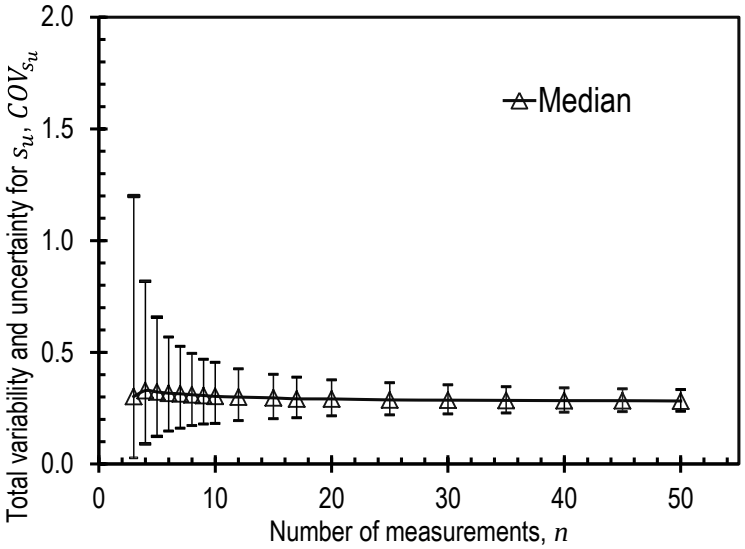


Figure 6.18 Computed $COV$ of undrained shear strength determined from random subsamples of simulated measurements for the St. Charles site.

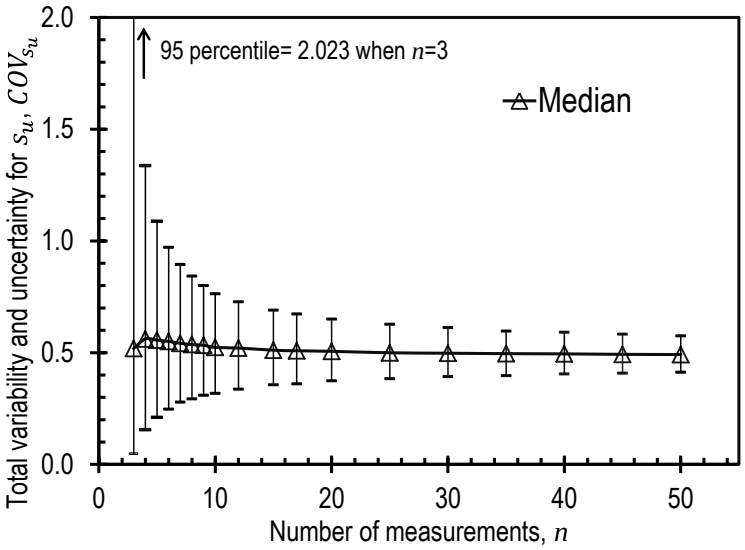


Figure 6.19 Computed $COV$ of undrained shear strength determined from random subsamples of simulated measurements for the New Florence site.

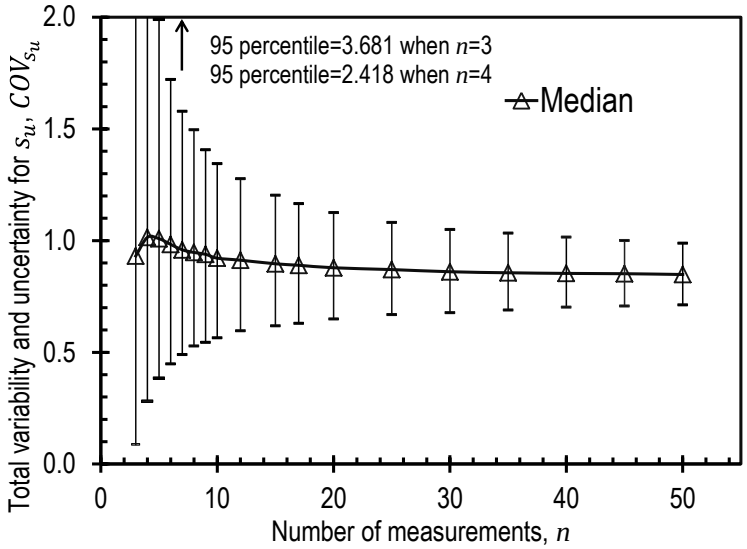


Figure 6.20 Computed $COV$ of undrained shear strength determined from random subsamples of simulated measurements for the Warrensburg site.

Table 6.10 Computed median, 5th percentile, 95th percentile, and 5th-95th percentile ranges of $COV_{s_u}$ determined from random subsamples of simulated measurements for the Pemiscot site.

| Number of Measurements per Subsample, *n* | Median Mean Value (psf) | 5th Percentile Mean Value (psf) | 95th Percentile Mean Value (psf) | 5th-95th Percentile Range (psf) |
|---|---|---|---|---|
| 3 | 0.239 | 0.022 | 0.972 | 0.950 |
| 4 | 0.247 | 0.064 | 0.608 | 0.544 |
| 5 | 0.241 | 0.090 | 0.493 | 0.403 |
| 6 | 0.237 | 0.107 | 0.429 | 0.322 |
| 7 | 0.234 | 0.119 | 0.388 | 0.269 |
| 8 | 0.229 | 0.127 | 0.363 | 0.236 |
| 9 | 0.226 | 0.133 | 0.344 | 0.211 |
| 10 | 0.224 | 0.135 | 0.330 | 0.195 |
| 15 | 0.217 | 0.150 | 0.295 | 0.145 |
| 20 | 0.212 | 0.155 | 0.276 | 0.121 |
| 25 | 0.210 | 0.160 | 0.263 | 0.103 |
| 30 | 0.208 | 0.164 | 0.257 | 0.093 |
| 40 | 0.207 | 0.169 | 0.247 | 0.078 |
| 50 | 0.205 | 0.172 | 0.241 | 0.069 |

Table 6.11 Computed median, 5th percentile, 95th percentile, and 5th-95th percentile ranges of $COV_{s_u}$ determined from random subsamples of simulated measurements for the St. Charles site.

| Number of Measurements per Subsample, *n* | Median Mean Value (psf) | 5th Percentile Mean Value (psf) | 95th Percentile Mean Value (psf) | 5th-95th Percentile Range (psf) |
|---|---|---|---|---|
| 3 | 0.302 | 0.027 | 1.200 | 1.173 |
| 4 | 0.329 | 0.089 | 0.818 | 0.729 |
| 5 | 0.323 | 0.124 | 0.657 | 0.533 |
| 6 | 0.317 | 0.148 | 0.568 | 0.420 |
| 7 | 0.314 | 0.160 | 0.527 | 0.367 |
| 8 | 0.310 | 0.172 | 0.495 | 0.323 |
| 9 | 0.307 | 0.179 | 0.469 | 0.290 |
| 10 | 0.303 | 0.181 | 0.455 | 0.274 |
| 15 | 0.296 | 0.203 | 0.402 | 0.199 |
| 20 | 0.291 | 0.215 | 0.377 | 0.162 |
| 25 | 0.287 | 0.219 | 0.364 | 0.145 |
| 30 | 0.286 | 0.224 | 0.354 | 0.130 |
| 40 | 0.284 | 0.232 | 0.340 | 0.108 |
| 50 | 0.282 | 0.236 | 0.333 | 0.097 |

Table 6.12 Computed median, 5th percentile, 95th percentile, and 5th-95th percentile ranges of $COV_{s_u}$ determined from random subsamples of simulated measurements for the New Florence site.

| Number of Measurements per Subsample, *n* | Median Mean Value (psf) | 5th Percentile Mean Value (psf) | 95th Percentile Mean Value (psf) | 5th-95th Percentile Range (psf) |
|---|---|---|---|---|
| 3 | 0.519 | 0.048 | 2.023 | 1.975 |
| 4 | 0.562 | 0.155 | 1.337 | 1.182 |
| 5 | 0.556 | 0.211 | 1.088 | 0.877 |
| 6 | 0.550 | 0.247 | 0.971 | 0.724 |
| 7 | 0.542 | 0.278 | 0.895 | 0.617 |
| 8 | 0.536 | 0.293 | 0.842 | 0.549 |
| 9 | 0.533 | 0.309 | 0.800 | 0.491 |
| 10 | 0.524 | 0.317 | 0.763 | 0.446 |
| 15 | 0.511 | 0.356 | 0.690 | 0.334 |
| 20 | 0.506 | 0.374 | 0.650 | 0.276 |
| 25 | 0.499 | 0.383 | 0.627 | 0.244 |
| 30 | 0.498 | 0.393 | 0.612 | 0.219 |
| 40 | 0.495 | 0.405 | 0.591 | 0.186 |
| 50 | 0.492 | 0.412 | 0.575 | 0.163 |

Table 6.13 Computed median, 5th percentile, 95th percentile, and 5th-95th percentile ranges of $COV_{s_u}$ determined from random subsamples of simulated measurements for the Warrensburg site.

| Number of Measurements per Subsample, *n* | Median Mean Value (psf) | 5th Percentile Mean Value (psf) | 95th Percentile Mean Value (psf) | 5th-95th Percentile Range (psf) |
|---|---|---|---|---|
| 3 | 0.931 | 0.088 | 3.681 | 3.593 |
| 4 | 1.015 | 1.015 | 2.418 | 1.403 |
| 5 | 1.009 | 1.009 | 1.990 | 0.981 |
| 6 | 0.983 | 0.983 | 1.721 | 0.738 |
| 7 | 0.959 | 0.959 | 1.579 | 0.620 |
| 8 | 0.947 | 0.947 | 1.496 | 0.549 |
| 9 | 0.939 | 0.939 | 1.407 | 0.468 |
| 10 | 0.922 | 0.922 | 1.345 | 0.423 |
| 15 | 0.896 | 0.896 | 1.203 | 0.307 |
| 20 | 0.878 | 0.878 | 1.125 | 0.247 |
| 25 | 0.870 | 0.870 | 1.081 | 0.211 |
| 30 | 0.861 | 0.861 | 1.050 | 0.189 |
| 40 | 0.853 | 0.853 | 1.015 | 0.162 |
| 50 | 0.848 | 0.848 | 0.989 | 0.141 |

## 6.7 Practical Implications

The results shown in this chapter illustrate how estimates for the undrained shear strength can be affected by considering different numbers of measurements. The large ranges of $\mu_{s_u}$, $COV_{\mu_{s_u}}$, and $COV_{s_u}$ when few measurements are considered indicates that design parameters interpreted from a small number of measurements may be dramatically under- or over-estimated depending on the specific measurements considered. On average, the median values of these parameters are similar to those for the entire population, but specific estimates may be substantially in error. Fortunately, the potential magnitude of such errors decreases substantially with greater numbers of measurements and the magnitude of the potential errors appears to become practically constant when the number of measurements exceeds about 30 for the four sites considered. The results shown also

indicate that the number of measurements required to achieve a given level of precision depends on the general variability of a given site, with fewer measurements being required for less variable sites and greater numbers of measurements being required for more variable sites.

## 6.8 Summary

The research described in this chapter shows that the accuracy and precision of estimates for design parameters is heavily dependent on the number of measurements used to derive the estimates. The likelihood of underestimating or overestimating the mean undrained shear strength, the uncertainty in mean undrained shear strength, and the total variably and uncertainty in undrained shear strength is extremely high when few measurements are considered. The likelihood of overestimating or underestimating these parameters decreases substantially when considering greater numbers of measurements. Since the reliability of shallow foundations is highly dependent on the reliability of the design parameters, it follows that the reliability of shallow foundations is also largely dependent on the number of measurements used for design. Analyses to evaluate how the reliability of spread footings designed using the LRFD methods described in Chapter 5 is affected by the number of measurements of undrained shear strength are presented in subsequent chapters.

# Chapter 7 Reliability of Spread Footings Designed using LRFD with Different Numbers of Measurements

## 7.1 Introduction

The principal objective of design using load and resistance factor design (LRFD) is to consistently achieve a selected target probability of failure. Failure to achieve the target probability of failure within some practical tolerance leads to undesirable consequences. In cases where the probability of failure is substantially greater than the target value, undesirable consequences include inferior performance and excessive risk. In cases where the probability of failure is substantially less than the target value, consequences include unnecessary costs for construction of foundations in excess of what is required.

The reliability of shallow foundations designed using LRFD is heavily dependent on the uncertainty in the undrained shear strength, which in turn is heavily influenced by the number of available measurements as shown in Chapter 6. To evaluate how the number of measurements affects the reliability of shallow foundations, spread footings were designed using the LRFD methods as described in Chapter 5 with randomly sampled subsets of the undrained shear strength measurements presented in Chapter 4. The probabilities of failure for these footings were then computed based on the "true" undrained shear strength and compared with the target probability of failure to draw conclusions regarding the reliability of designs developed using different numbers of measurements. This chapter describes the analyses performed and the results obtained from these analyses.

## 7.2 Evaluation Procedure

The undrained shear strength, $s_u$, at the four test sites described in previous chapters is characterized by a relatively large number of measurements . However, in most practical applications, design must be accomplished based on far fewer measurements. Use of fewer measurements introduces greater uncertainty into the design parameters, and greater potential for variability in estimates of both the mean value and the uncertainty in the mean value for design parameters. Therefore, use of fewer measurements may lead to designs that do not achieve the target probability of failure to some practical precision.

To evaluate how the number of measurements affects the precision with which the target probability of failure is achieved, simulated designs were performed considering different numbers of $s_u$ measurements. For each simulated design, a spread footing was sized considering a randomly selected "subsample" of $n$ undrained shear strength measurements from the entire population of $N$ measurements. The probability of failure for the resulting spread footing was then calculated based on the "true" undrained shear strength as characterized in Tables 4.5 and 4.6. The computed probabilities of failure reflect the probability of failure that would be achieved if the only measurements available were those from the subsample.

The subsampling and simulation procedure included the following steps:

1. Randomly select $n$ measurements from the total population of $N$ undrained shear strength measurements.
2. Fit a linear or constant regression model through the selected $n$ measurements to establish an "estimation model" for undrained shear strength based on the selected

measurements alone. These regression analyses were identical to those described in Chapter 4 but consider only the measurements included in each subsample.

3. Calculate the mean value ($\mu_{s_u}$) and the uncertainty in the mean value ($COV_{\mu_{s_u}}$) at a selected footing depth from the estimation model using Eqs. 4.7 and 4.8 for linear regression models and Eqs. 4.16 and 4.17 for constant regression models.
4. Determine the appropriate resistance factor, $\varphi_{s_u}$, from Figure 5.1 based on the $COV_{\mu_{s_u}}$ estimated in Step 3 and for the selected target probability of failure.
5. Use the resistance factor, $\varphi_{s_u}$, and the mean value of undrained shear strength, $\mu_{s_u}$, at the selected footing depth to size the foundation area, $A$, according to the LRFD design criterion:

$$A = \frac{\gamma_{DL} \cdot \mu_{DL} + \gamma_{LL} \cdot \mu_{LL}}{\mu_{N_c} \cdot \mu_{s_u} \cdot \varphi} \quad \text{(Eq.7.1)}$$

6. Compute the probability of failure for the footing area calculated in Step 5 using the "true" undrained shear strength established from the entire population of measurements. Probabilities of failure were computed using the Monte Carlo simulation method with 100,000 simulations considering appropriate variability and uncertainty for all design parameters as described in Chapter 5.
7. Repeat Steps 1 through 6 for 10,000 different random subsamples of measurements to simulate designs that would be produced from different site investigations to evaluate how the foundation reliability varies with different collections of measurements.

The entire procedure was repeated considering the measurements from each of the four sites and considering different numbers of measurements ($n = 3$ to $n = 50$) in each subsample.

To characterize how well the simulated designs achieve the target probability of failure for different numbers of measurements, the computed probability of failure for each design was assigned to one of three ranges. Designs producing probabilities of failure within 50 percent of the respective target value ($0.5 \cdot p_T \leq p_f \leq 1.5 \cdot p_T$) were considered to be "satisfactory". Designs producing probabilities of failure that were more than 50 percent greater than the target ($p_f > 1.5 \cdot p_T$) were deemed to be "under reliable", and designs producing probabilities of failure less than 50 percent of the target ($p_f < 0.5 \cdot p_T$) were deemed to be "over reliable". The percentage of all computed cases falling within each range was quantified to reflect the effectiveness of designs established using different numbers of measurements. It is important to note that the term "under reliable" does not imply that the foundation resistance is less than the applied load (i.e. that failure will occur), but rather that the probability of the foundation resistance being less than the applied load is substantially greater than the target probability of failure.

## 7.3 Reliability of Designs for Different Numbers of Measurements

Figures 7.1-7.4 show the percentage of satisfactory, under reliable, and over reliable cases determined from simulations for each of the four sites plotted as a function of the number of measurements in the subsample. The results shown in these figures were obtained for a target probability of failure of 1/1500 when the undrained shear strength is interpreted using a linear regression model and the foundation is located at a depth of 7 feet. Figs 7.1-7.4 show that the percentage of satisfactory cases increases steadily with the number of subsample measurements (*n*) from near zero when few measurements are used for design to a maximum value when *n* approaches the population size (*N*). The percentage of satisfactory cases varies for each site, especially for large *n*, with the percentage

approaching 100 percent for the Pemiscot site (the least variable site) and approaching only 50 percent for the Warrensburg site (the most variable site). This suggests that greater numbers of measurements are required to achieve similar percentages of satisfactory cases as site variability increases.

The percentage of under reliable cases is largely independent of the number of measurements, particularly in the range of $7 < n < 40$, which suggests that design using resistance factors established to be a function of uncertainty in the undrained shear strength effectively controls the percentage of under reliable cases. The nominal percentage of under reliable cases for both the Pemiscot and New Florence sites is approximately 16 percent. The percentage of under reliable cases for the St. Charles and Warrensburg sites is smaller, varying from 8 percent to 12 percent.

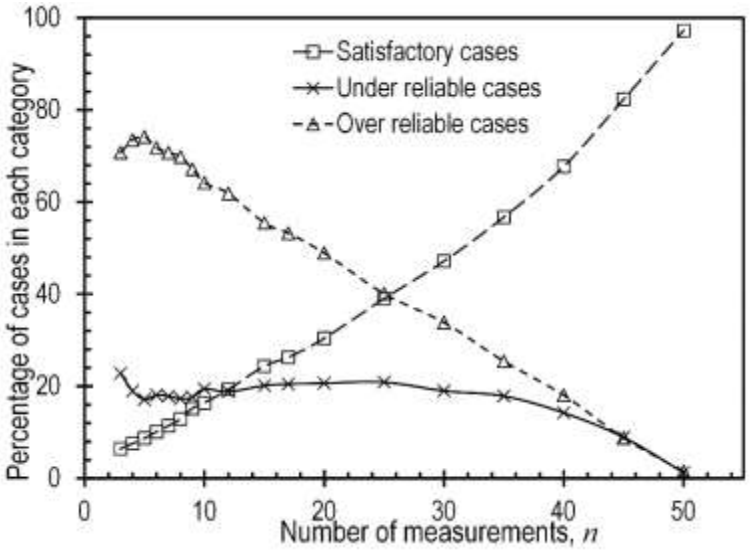


Figure 7.1 Percentage of satisfactory, under reliable and over reliable cases for the Pemiscot site using linear regression models and $p_T = 1/1500$.

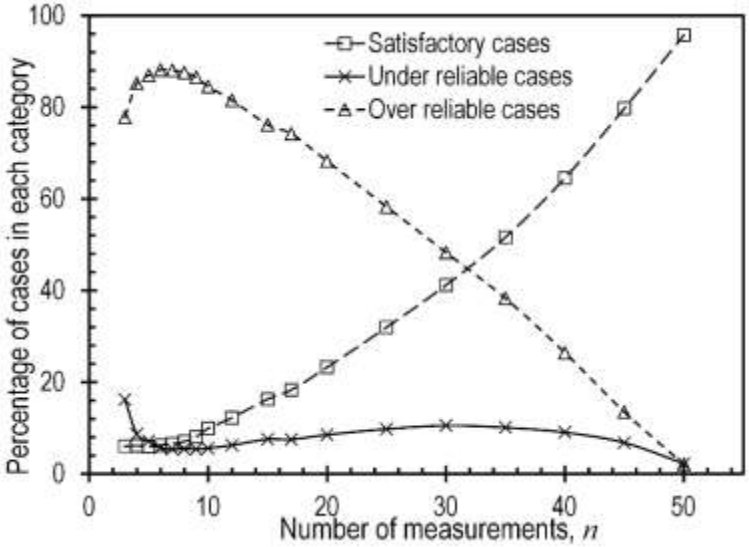


Figure 7.2 Percentage of satisfactory, under reliable and over reliable cases for the St. Charles site using linear regression models and $p_T = 1/1500$.

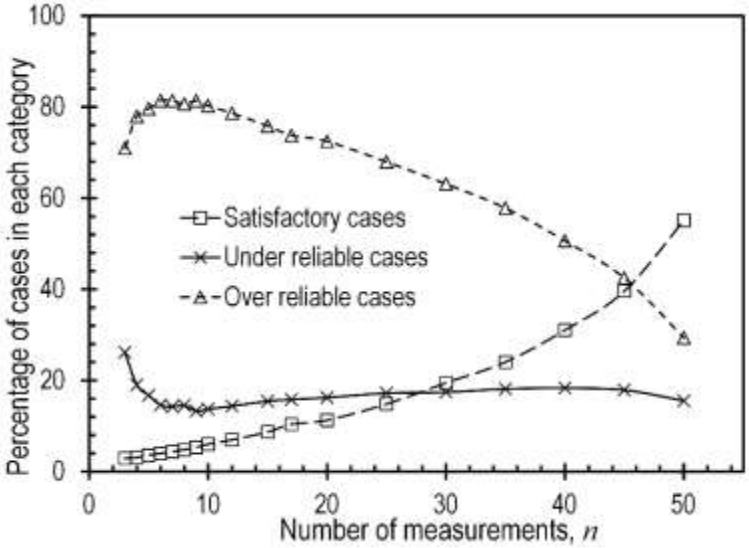


Figure 7.3 Percentage of satisfactory, under reliable and over reliable cases for the New Florence site using linear regression models and $p_T = 1/1500$.

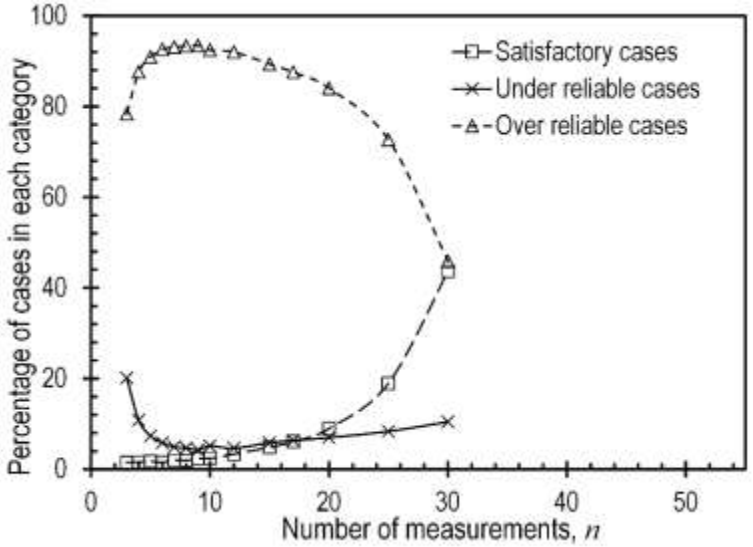


Figure 7.4 Percentage of satisfactory, under reliable and over reliable cases for the Warrensburg site using linear regression models and $p_T = 1/1500$.

As discussed in Chapter 6, there is great uncertainty in estimated values of undrained shear strength when small numbers of measurements are considered. As a result of this uncertainty, estimates of undrained shear strength from individual collections of measurements can dramatically overestimate or underestimate the true undrained shear strength of the formation. Figures 7.1-7.4 show that such poor estimates affect the percentage of under reliable and over reliable cases for $n \leq 7$, with substantially greater percentages of under reliable cases and smaller percentages of over reliable cases occurring in this range. Two alternative methods to account for the greater percentage of under reliable cases for small $n$ are described and evaluated in Chapters 8 and 9.

The percentage of under reliable cases is also observed to decrease as the subsample size $(n)$ approaches the population size $(N)$. This observed decrease for large $n$ is presumably a result of different subsamples being correlated as the subsample size approaches the population size, rather than being a true reflection of a decreasing

percentage of under reliable cases. This effect of population size is discussed in more detail later in this chapter.

The percentage of over reliable cases is observed to decrease steadily with increasing subsample size for $n > 7$. The percentage of over reliable cases varies from approximately 70 to 90 percent for small $n$ to between zero and 40 percent as $n$ approaches $N$. This result suggests that the most likely outcome of design using small numbers of measurements is therefore to produce a design with a probability of failure that is substantially less than the target value. Such an outcome is obviously preferable to produce an under reliable design, but will usually result in costs for construction that exceed what is truly desired.

Figures 7.5-7.8 similarly show results determined from simulations for each of the four sites but for analyses where the undrained shear strength is interpreted using constant regression models. Similar to the results obtained when using linear regression models, the percentage of satisfactory cases increases steadily with the number of subsample measurements ($n$) from near zero when few measurements are used for design to a maximum value when $n$ approaches the population size ($N$). The percentage of satisfactory cases varies for each site, especially for large $n$, with the percentage approaching 100 percent for the Pemiscot site (the least variable site) and approaching only 60 percent for the Warrensburg site (the most variable site). This again suggests that greater numbers of measurements are required to achieve similar percentages of satisfactory cases for more variable sites.

The percentage of under reliable cases is practically consistent over the range $5 < n < 40$ for all sites, which again suggests that the resistance factors established in Chapter 5 effectively control the percentage of under reliable cases. The nominal

percentage of under reliable cases for all sites is approximate 16 percent. The percentage of under reliable cases is generally greater for $n \leq 6$, as was observed for analyses performed using linear regression models. The percentage of under reliable cases is also observed to decrease as the subsample size ($n$) approaches the population size ($N$), presumably because of constraint from the population size.

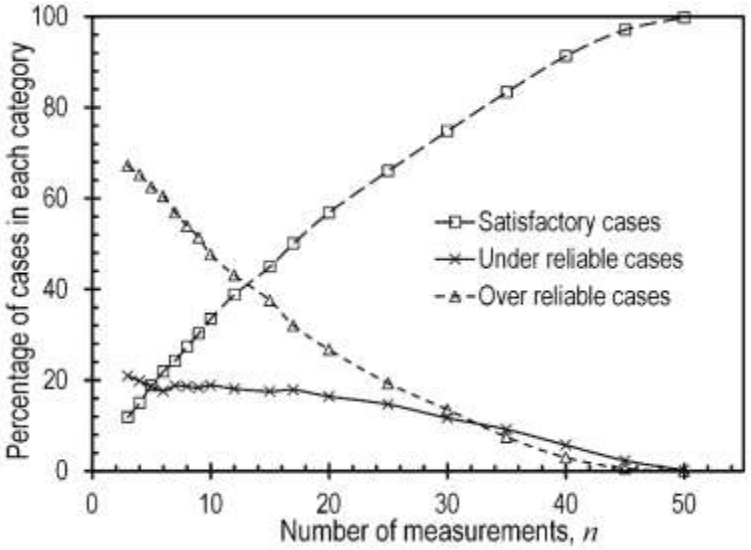


Figure 7.5 Percentage of satisfactory, under reliable and over reliable cases for the Pemiscot site using constant regression models and $p_T = 1/1500$.

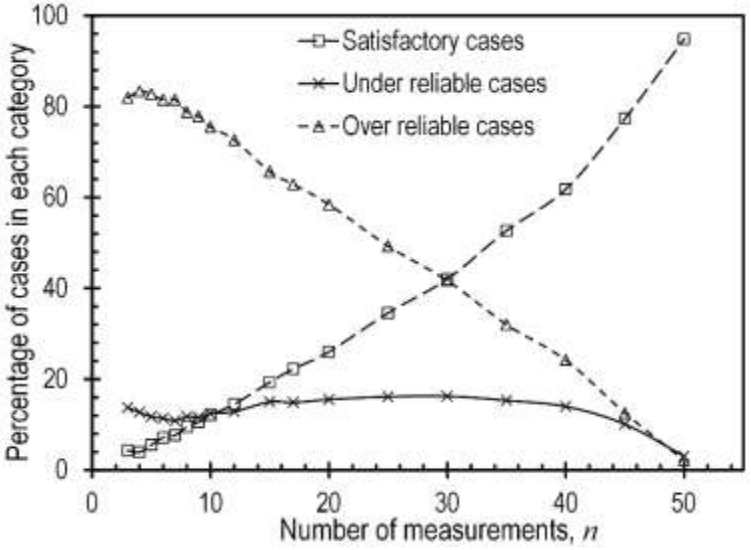


Figure 7.6 Percentage of satisfactory, under reliable and over reliable cases for the St. Charles site using constant regression models and $p_T = 1/1500$.

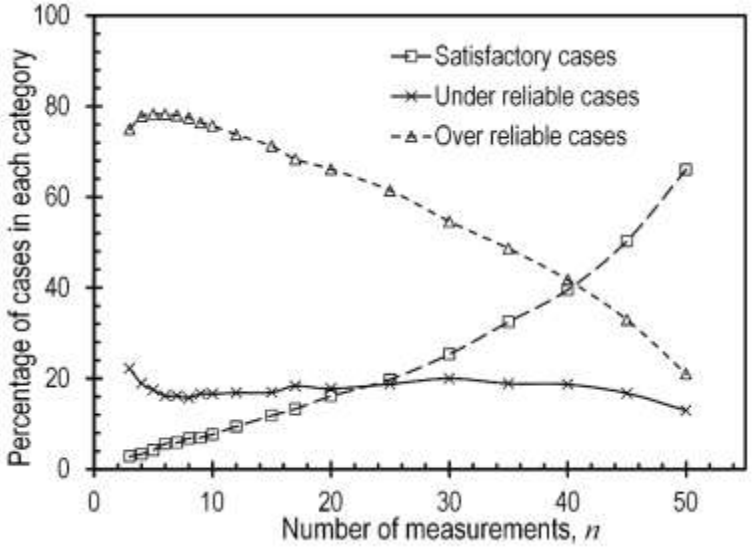


Figure 7.7 Percentage of satisfactory, under reliable and over reliable cases for the New Florence site using constant regression models and $p_T = 1/1500$.

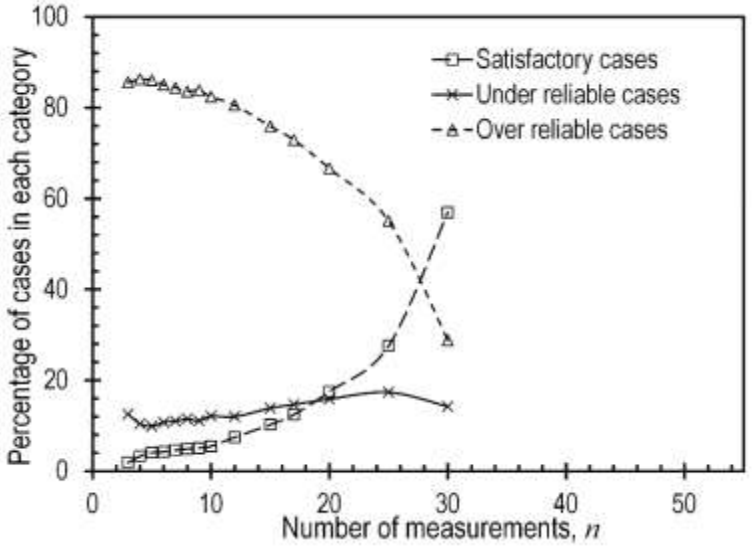


Figure 7.8 Percentage of satisfactory, under reliable and over reliable cases for the Warrensburg site using constant regression models and $p_T = 1/1500$.

The percentage of over reliable cases decreases steadily with increasing subsample size for $n > 6$. The percentage of over reliable cases varies from approximately 70 to 90 percent for small $n$ to between zero and 30 percent as $n$ approaches $N$. The percentage of over reliable cases is greater at the more variable sites than at less variable sites. Approximately 90 percent of cases were over reliable for the Warrensburg site when $n =$

3 while only 70 percent of cases at the Pemiscot site were over reliable. When $n = 50$, approximate 30 percent of the cases at the Warrensburg site were over reliable while practically no cases were over reliable (0 percent) for the Pemiscot site. This result suggests that the most likely outcome of design using small numbers of measurements is therefore to produce a design with a probability of failure that is substantially less than the target value, especially at more variable sites.

## 7.4 Effect of Target Probabilities of Failure

Results presented in Section 7.3 reflect spread footings designed for target probabilities of failure equal to 1/1500. Similar analyses were performed using resistance factors calibrated for target probabilities of failure equal to 1/300, 1/5,000 and 1/10,000 to evaluate whether the target probability of failure affects the percentage of satisfactory, under reliable, or over reliable cases or the influence of the number of measurements. Figures 7.9-7.12 show percentages of under reliable and over reliable cases and Figures 7.13-7.16 show percentages of satisfactory cases for the four different target probabilities of failure calculated using measurements interpreted from linear regression models for the four test sites. Figures 7.17-7.7.24 show similar results obtained using undrained shear strengths estimated using constant regression models. These figures collectively show that the target probability of failure has a small but practical inconsequential effect on the percentage of satisfactory, under reliable and over reliable cases, with nominal differences of approximately 4 percent or less and maximum differences of less than 10 percent.

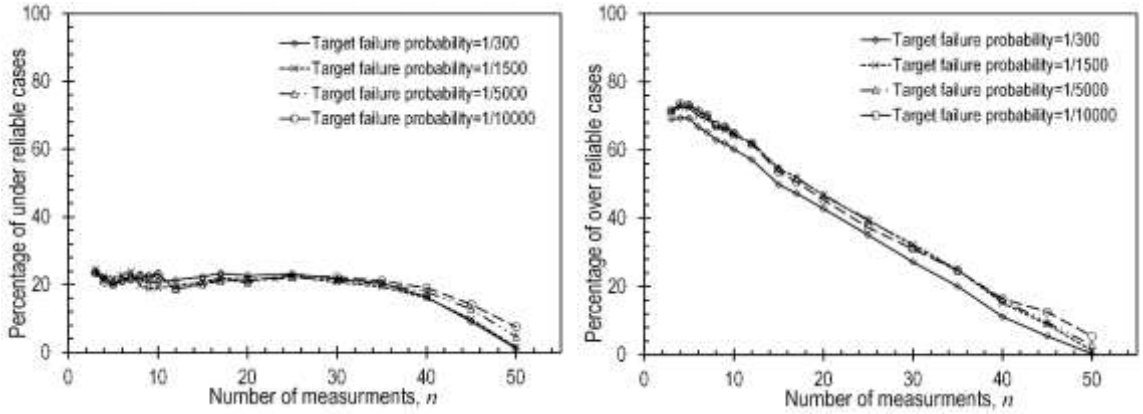


(a) (b)

Figure 7.9 Percentage of: (a) under reliable and (b) over reliable cases for the Pemiscot site using linear regression models at different target probabilities of failure.

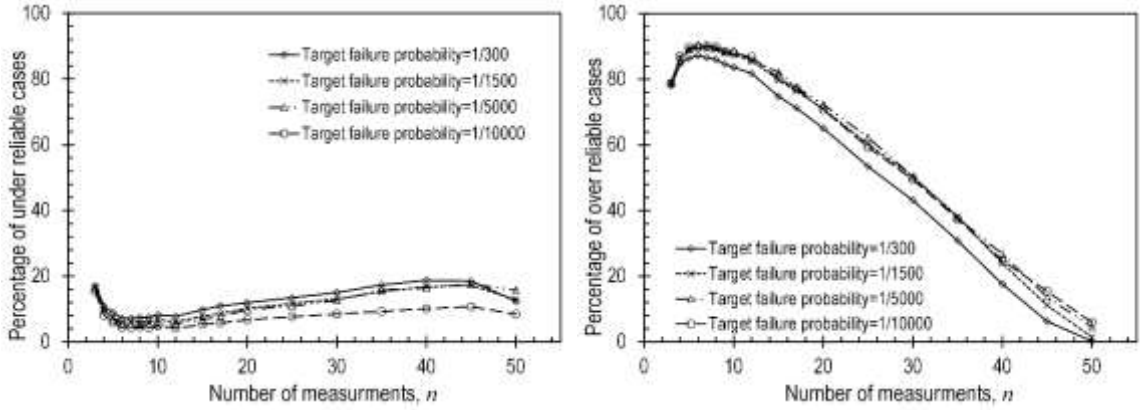


(a) (b)

Figure 7. 10 Percentage of: (a) under reliable and (b) over reliable cases for the St. Charles site using linear regression models at different target probabilities of failure.

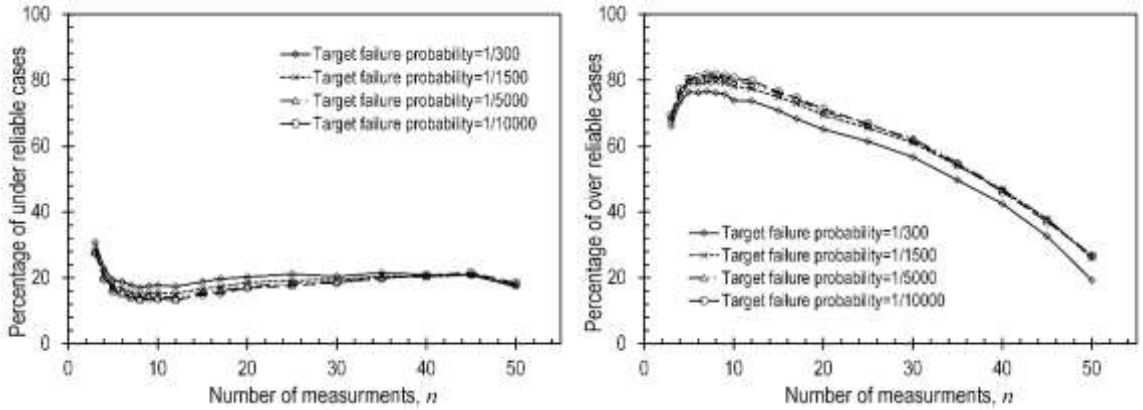


(a) (b)

Figure 7.11 Percentage of: (a) under reliable and (b) over reliable cases for the New Florence site using linear regression models at different target probabilities of failure.

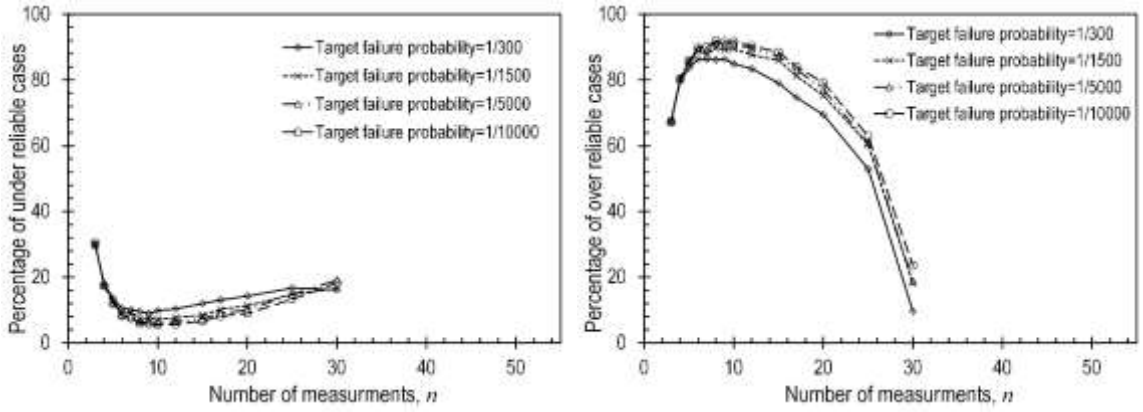


(a) (b)

Figure 7.12 Percentage of: (a) under reliable and (b) over reliable cases for the Warrensburg site using linear regression models at different target probabilities of failure.

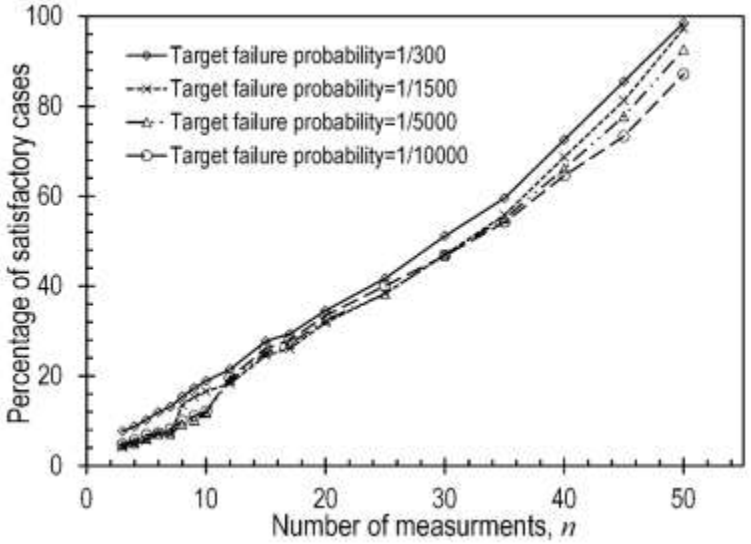


Figure 7.13 Percentage of satisfactory cases for the Pemiscot site using linear regression models at different target probabilities of failure.

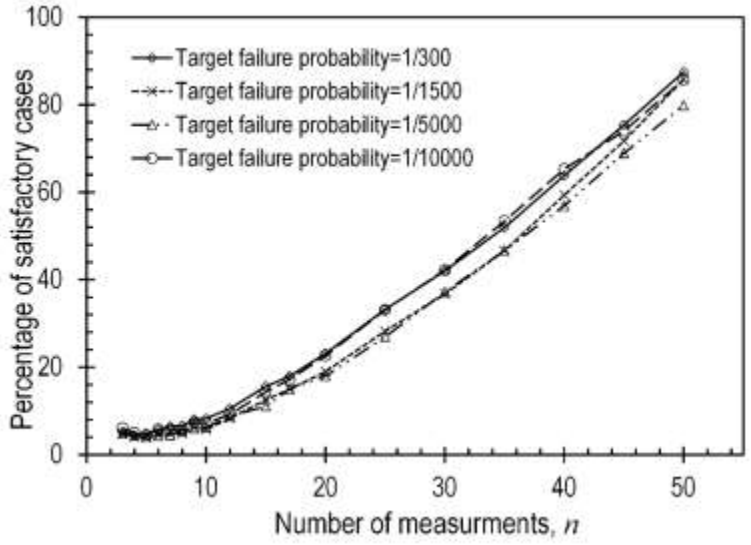


Figure 7.14 Percentage of satisfactory cases for the St. Charles site using linear regression models at different target probabilities of failure.

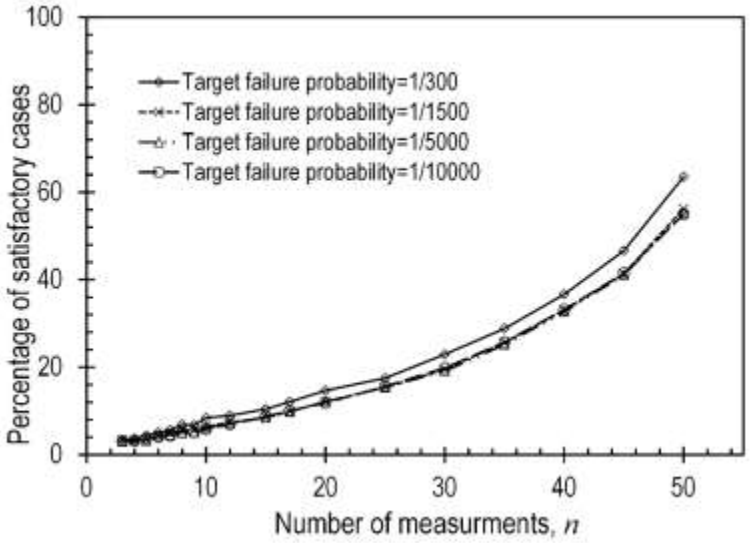


Figure 7.15 Percentage of satisfactory cases for the New Florence site using linear regression models at different target probabilities of failure.

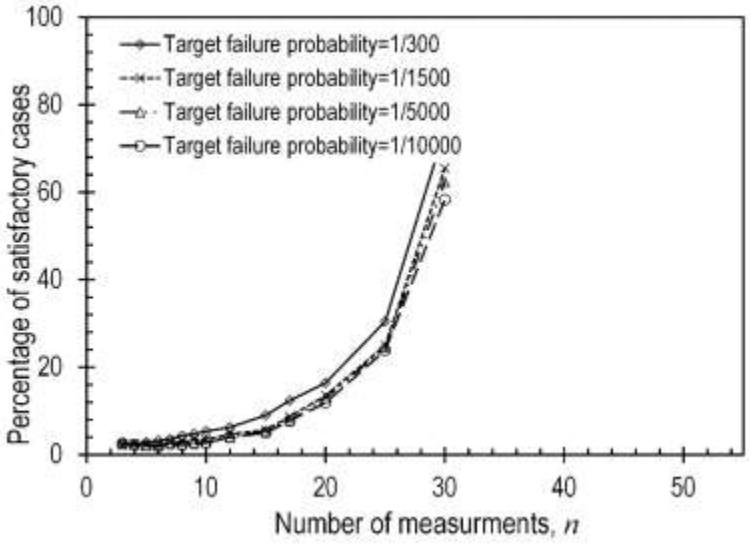


Figure 7.16 Percentage of satisfactory cases for the Warrensburg site using linear regression models at different target probabilities of failure.

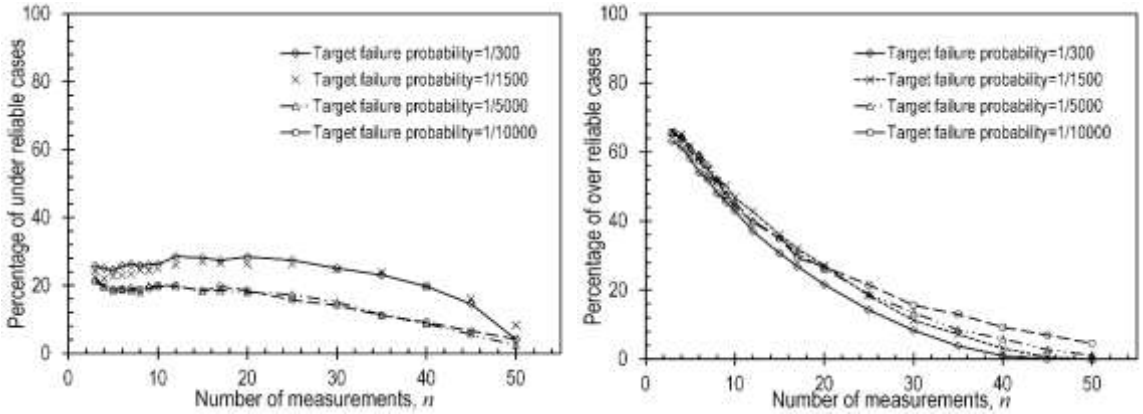


(a) (b)

Figure 7.17 Percentage of: (a) under reliable and (b) over reliable cases for the Pemiscot site using constant regression models at different target probabilities of failure.

The collective results presented in Figures 7.9-7.24 consistently show that the target probability of failure has little influence on how well the target probability of failure is achieved when design is performed using the resistance factors presented in Chapter 5. Furthermore, the figures show that the influence of the target probability of failure is substantially less than the influence of the number of measurements considered. Results

determined for a target probability of failure of 1/1500 are therefore representative of results that would be obtained for other target values.

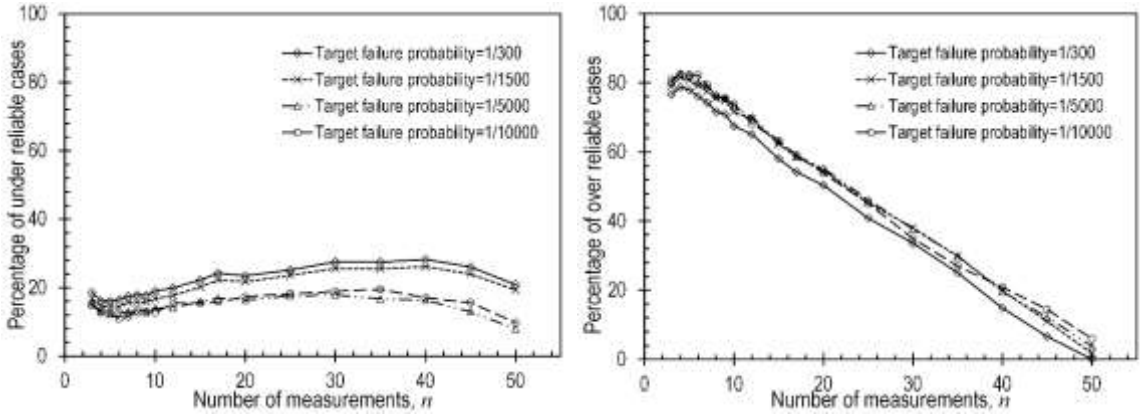


(a) (b)

Figure 7.18 Percentage of: (a) under reliable and (b) over reliable cases for the St. Charles site using constant regression models at different target probabilities of failure.

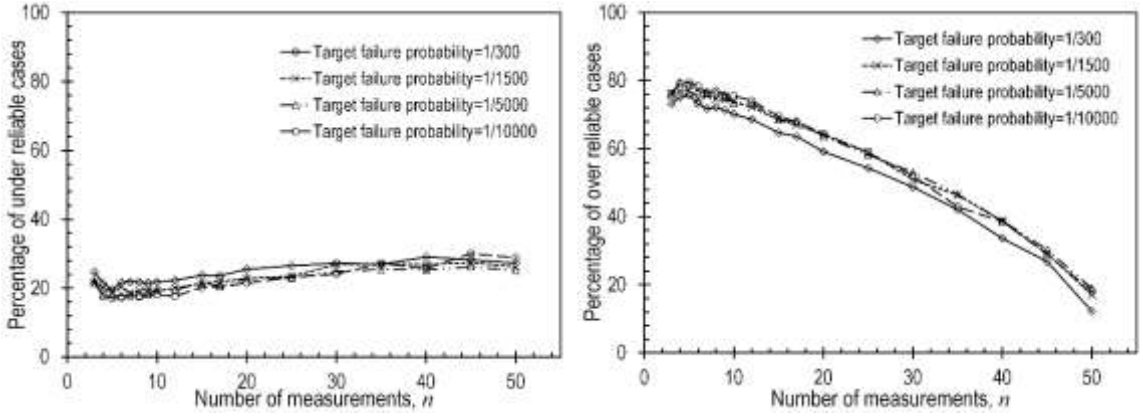


(a) (b)

Figure 7.19 Percentage of: (a) under reliable and (b) over reliable cases for the New Florence site using constant regression models at different target probabilities of failure.

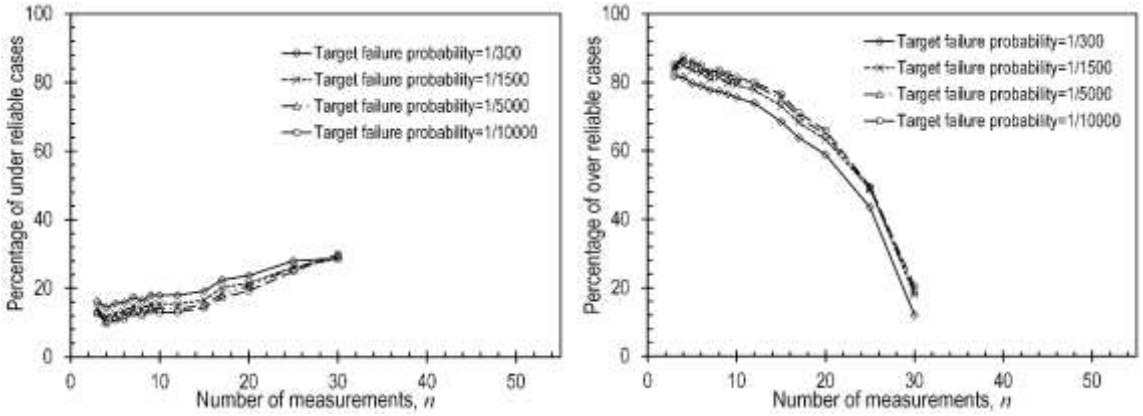


(a) (b)

Figure 7.20 Percentage of: (a) under reliable and (b) over reliable cases for the Warrensburg site using constant regression models at different target probabilities of failure.

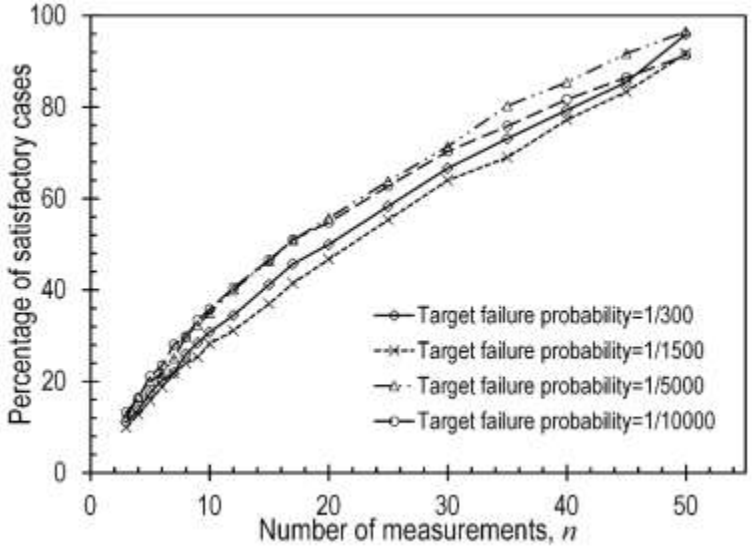


Figure 7.21 Percentage of satisfactory cases for the Pemiscot site using constant regression models at different target probabilities of failure.

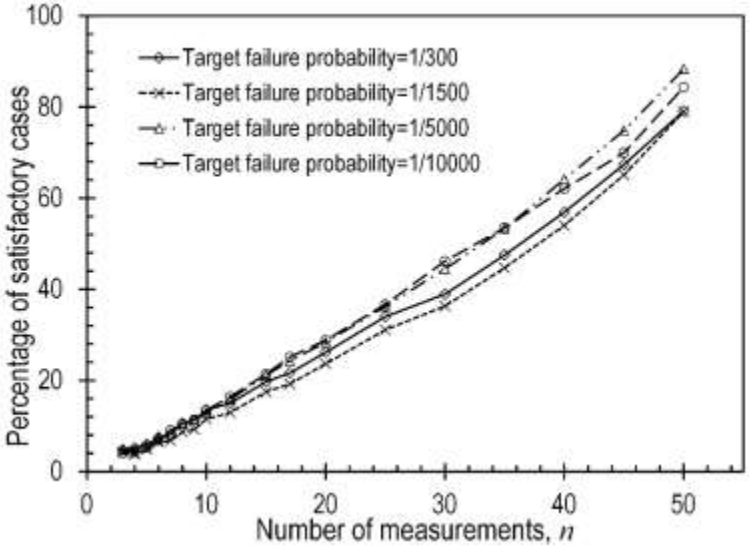


Figure 7.22 Percentage of satisfactory cases for the St. Charles site using constant regression models at different target probabilities of failure.

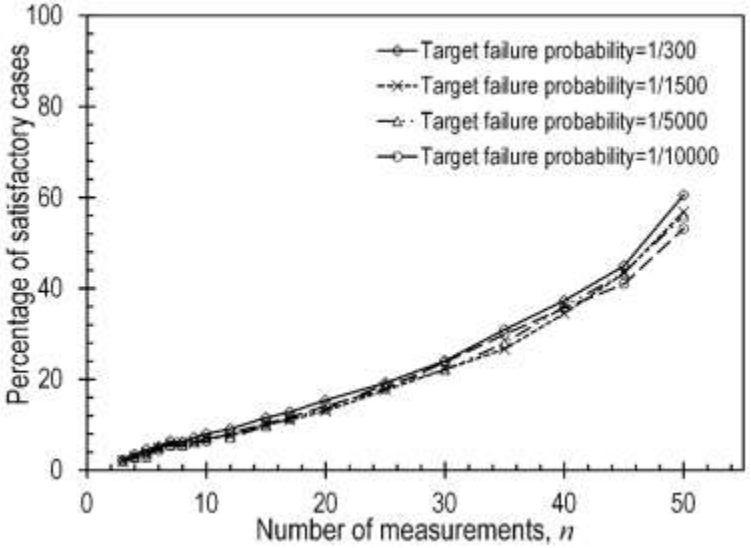


Figure 7.23 Percentage of satisfactory cases for the New Florence site using constant regression models at different target probabilities of failure.

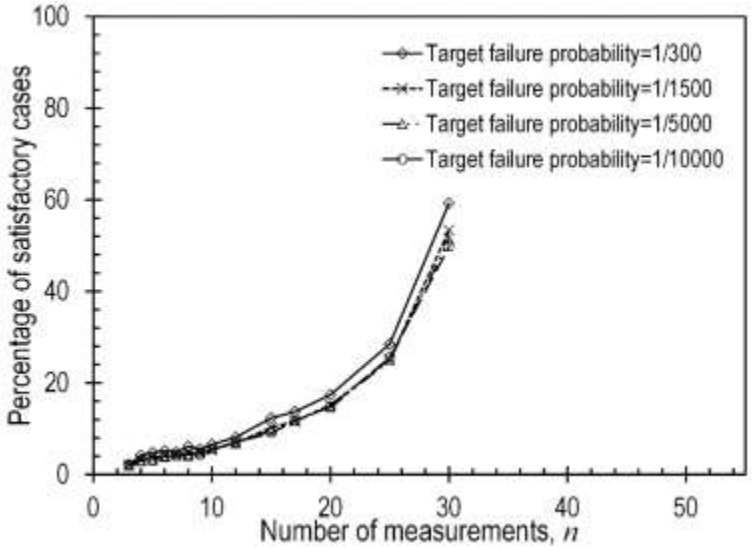

Figure 7.24 Percentage of satisfactory cases for the Warrensburg site using constant regression models at different target probabilities of failure.

## 7.5 Effect of Design Depth

Results presented in Section 7.3 were obtained considering a footing depth of 7 feet. When using constant regression models, the estimated mean and uncertainty of the undrained shear strength is independent of the footing depth; thus, consideration of different footing depths will have no influence on footing sizes or the percentages of satisfactory, under reliable, and over reliable cases. However, both the estimated mean value of undrained shear strength and the uncertainty in the mean undrained shear strength vary with depth when using linear regression models for interpreting the undrained shear strength. The mean value tends to increase with depth for most of the linear regression models (depending on the specific measurements selected) while the uncertainty in the mean value tends to be least near the middle depth of the undrained shear strength measurements and greatest near the upper and lower extreme depths of the measurements. These variations will affect the computed size of the footings and have the potential to affect the reliability of the footings.

To evaluate the potential influence of footing depth, the analyses were repeated for a deeper footing depth representative of the mid-depth of the undrained strength measurements. Figures 7.25-7.28 show comparisons of percentages of satisfactory, under reliable and over reliable cases for two footing depths at each of the four sites, respectively. The "shallow" footing depth was selected to be 7 feet for all four sites. The deeper footing depth was located near the mid-depth of the available population of measurements for each site; 30 feet for Pemiscot site and 16 feet for the other three sites.

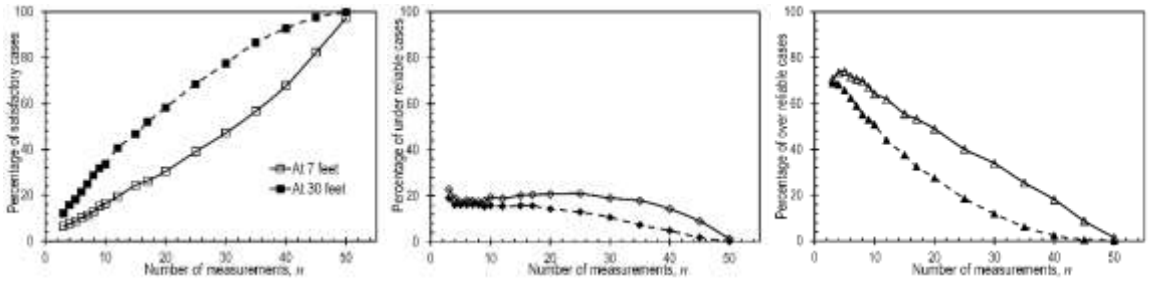


(a) (b) (c)

Figure 7.25 Comparison of percentages of: (a) satisfactory, (b) under reliable and (c) over reliable cases for different footing depths at the Pemiscot site.

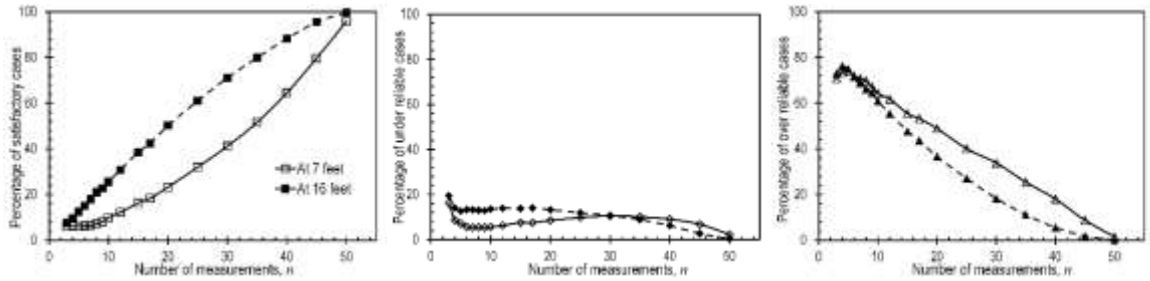


(a) (b) (c)

Figure 7.26 Comparison of percentages of: (a) satisfactory, (b) under reliable and (c) over reliable cases for different footing depths at the St. Charles site.

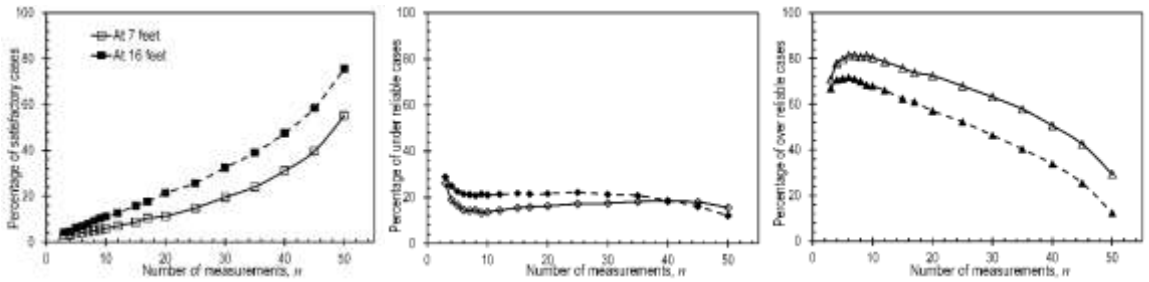


(a) (b) (c)

Figure 7.27 Comparison of percentages of: (a) satisfactory, (b) under reliable and (c) over reliable cases for different footing depths at the New Florence site.

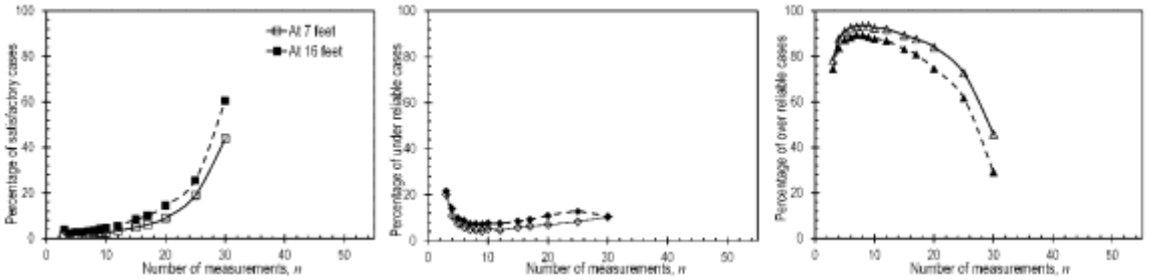


(a) (b) (c)

Figure 7.28 Comparison of percentages of: (a) satisfactory, (b) under reliable and (c) over reliable cases for different footing depths at the Warrensburg site.

The figures show that footing depth has a noticeable influence on the reliability of the footings. The deeper footings generally produced more satisfactory cases and fewer over reliable cases without substantially changing the percentage of under reliable cases. The differences are more apparent for the Pemiscot and St. Charles sites, which are the less variable sites. The observed differences are attributed to the fact that the uncertainty in the mean undrained shear strength is lower at the deeper depth, which generally corresponds to the middle depth of the population of measurements, than at the shallow depth when linear regression models are used to interpret the undrained shear strength measurements.

## 7.6 Effect of Spatial Averaging

When designing spread footings at the strength limit state, the average undrained shear strength within the depth range of one footing width beneath the footing is generally

considered to be most appropriate for analysis. The analyses presented previously in this chapter for interpretations based on a constant regression model generally satisfy this requirement since the estimated undrained shear strength is the average undrained shear strength for such models. However, the analyses presented previously for linear regression models utilize the mean value and uncertainty established at the footing depth; these analyses therefore do not account for spatial averaging.

Consideration of spatial averaging may lead to nominal changes in estimates of the mean undrained shear strength because the mean undrained strength changes with depth when a linear regression model is used. However, such changes in the mean undrained shear strength have little practical influence on whether the target reliability is achieved because changes in the mean undrained shear strength lead to corresponding changes in the required footing area. More importantly, spatial averaging leads to reduced uncertainty because the uncertainty in a spatially averaged value will always be less than the uncertainty in the value at a given point. Additional analyses, similar to those described previously, were therefore performed using spatially averaged values of the undrained shear strength to evaluate how spatial averaging affects achievement of the target reliability.

Spatially averaged values of undrained shear strength were computed over depths between the footing and a distance of one footing width below the footing. Since these calculations require knowledge of the footing size, an iterative approach was used where the footing size and spatially averaged value of undrained shear strength were repeatedly calculated until the change of footing size was minimal compared to the previous iteration. When this approach produced footing dimensions that exceeded the depth range of available measurements at each site, the depth for averaging undrained shear strength was

taken to be equal to the depth range with available measurements. Figures 7.29-7.31 show results of these analyses compared to results presented previously that do not consider spatial averaging for the Pemiscot site, the St. Charles site and the New Florence site.

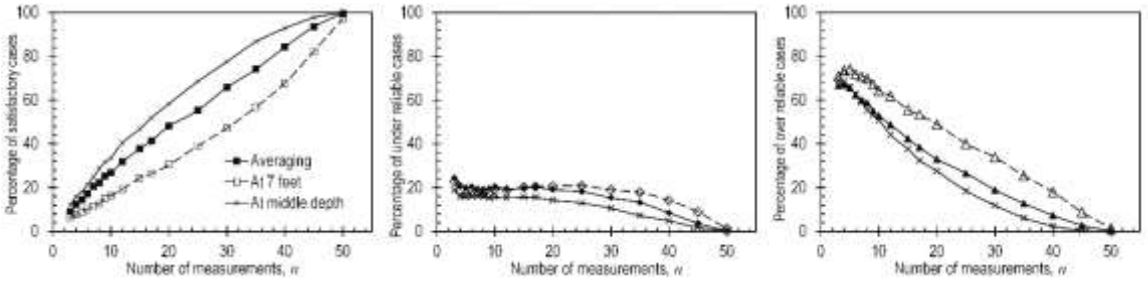


(a) (b) (c)

Figure 7.29 Comparison of percentages of: (a) satisfactory cases, (b) under reliable cases, and (c) over reliable cases with and without spatial averaging at 7 feet and without spatial averaging at the "middle" depth for the Pemiscot site.

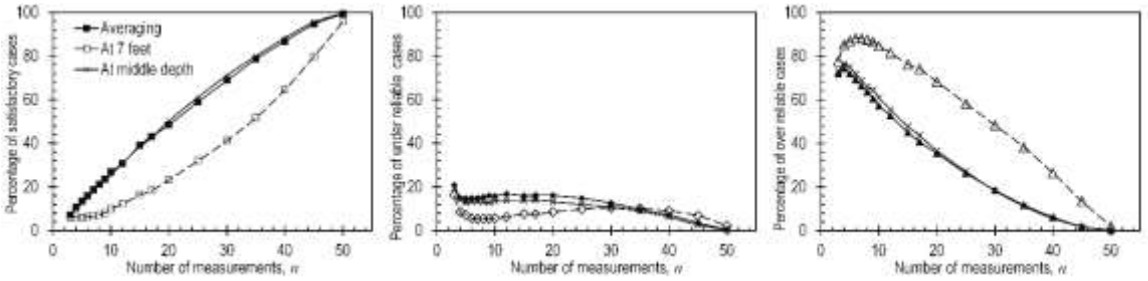


(a) (b) (c)

Figure 7.30 Comparison of percentages of: (a) satisfactory cases, (b) under reliable cases, and (c) over reliable cases with and without spatial averaging at 7 feet and without spatial averaging at the "middle" depth for the St. Charles site.

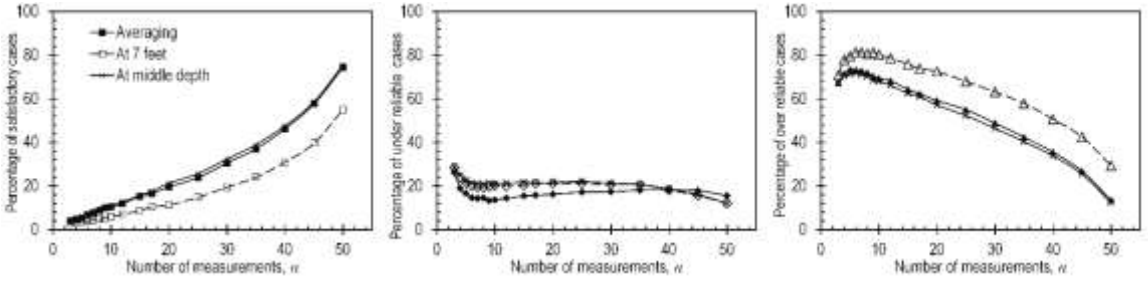


(a) (b) (c)

Figure 7.31 Comparison of percentages of: (a) satisfactory cases, (b) under reliable cases, and (c) over reliable cases with and without spatial averaging at 7 feet and without spatial averaging at the "middle" depth for the New Florence site.

The results shown in the figures indicate that spatial averaging does slightly affect achievement of the target reliability, but that the effect of spatial averaging is similar to that observed when considering different footing depths. Consideration of spatial averaging generally leads to an increase in the percentage of satisfactory cases with a complementary decrease in the percentage of over reliable cases without substantial changes to the percentage of under reliable cases. This observation is not surprising given that consideration of spatial averaging and consideration of different depths, both effects reduce uncertainty in the mean undrained shear strength. While spatial average does have a slight effect on achievement of the target reliability, this effect is substantially less significant than the effect observed due to the number of measurements considered.

## 7.7 Effect of Total Population Size

As mentioned in Section 7.3, the percentage of under reliable cases is relatively constant when the number of measurements falls in the range of $5<n<40$. However, results presented previously in this chapter suggest that there is a notable drop in the percentage of under reliable cases as the number of measurements approaches the total population size. It was postulated that the drop in the percentage of under reliable cases can be attributed to the fact that different subsamples will be less and less independent as the subsample size approaches the population size (in the limit when the subsample size is equal to the population size, all subsamples are the same). To evaluate this postulate, the analyses were repeated using substantially larger populations of simulated undrained shear strength measurements. The simulated populations of undrained shear strength measurements were developed to closely mimic the actual undrained shear strength measurements, as described in Chapter 6, and to represent a larger population of measurements from which the

population of actual measurements could have been obtained. The simulated populations of measurements are shown in Figures 7.32-7.35 for four sites, respectively.

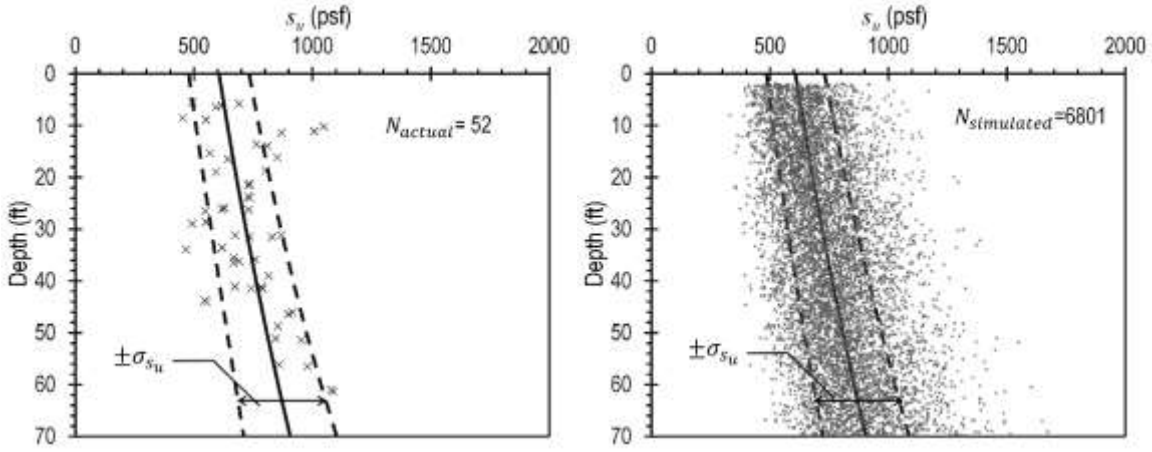


(a) (b)

Figure 7.32 Undrained shear strength measurements for the Pemiscot site: (a) real measurements with *N*=52, and (b) simulated measurements with *N*=6801.

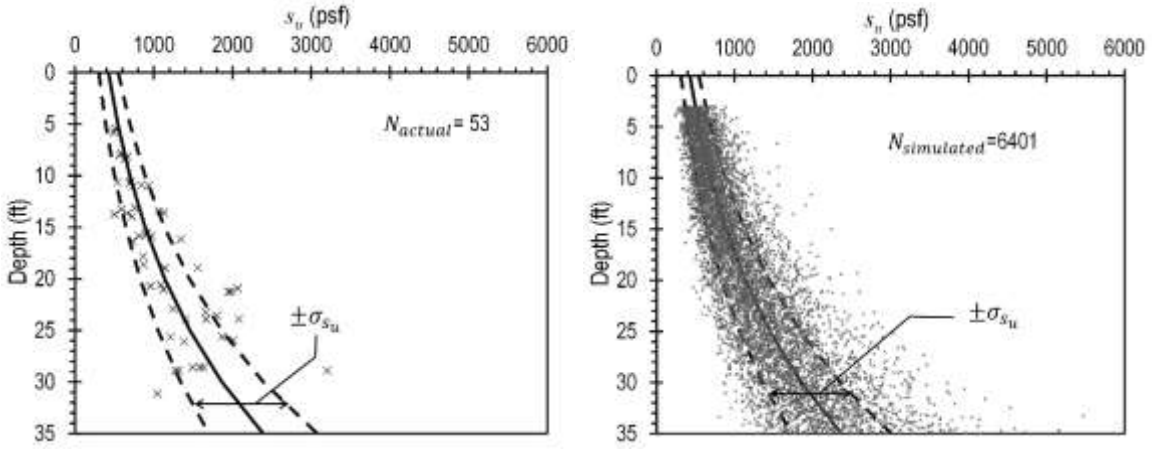


(a) (b)

Figure 7.33 Undrained shear strength measurements for the St. Charles site: (a) real measurements with *N*=53, and (b) simulated measurements with *N*=6401.

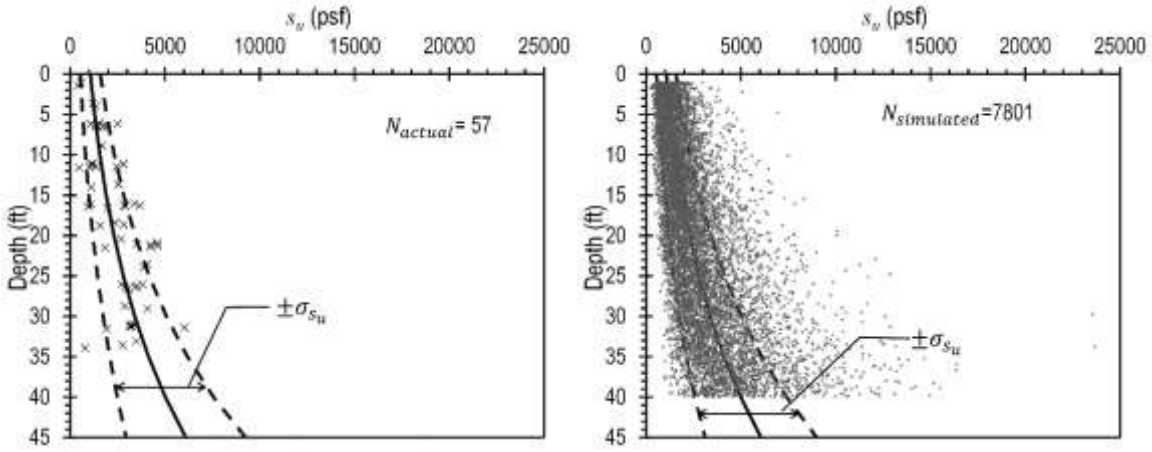


(a) (b)

Figure 7.34 Undrained shear strength measurements for the New Florence site: (a) real measurements with *N*=57, and (b) simulated measurements with *N*=7801.

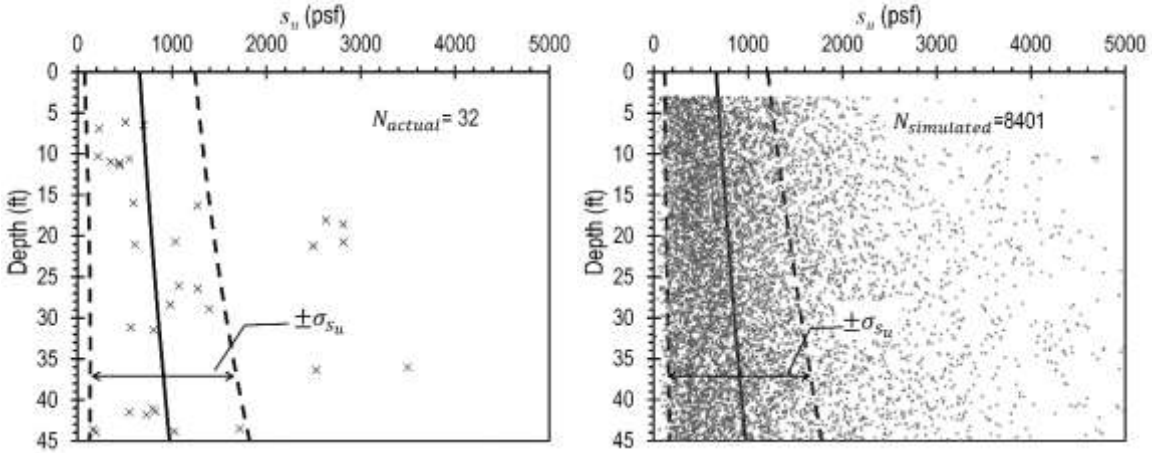


(a) (b)

Figure 7.35 Undrained shear strength measurements at the Warrensburg site: (a) real measurements with *N*=32, and (b) simulated measurements with *N*=8401.

The same subsampling and simulation procedures described in Section 7.2 were used to randomly select $n$ measurements from simulated total population of $N$ measurements. Computed percentages of satisfactory, under reliable and over reliable cases determined using the populations of actual and simulated measurements are compared in Figures 7.36-7.39.

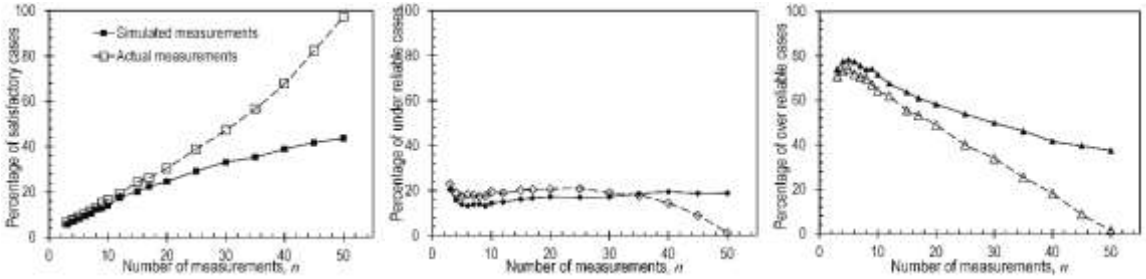


(a) (b) (c)

Figure 7.36 Percentages of: (a) satisfactory cases, (b) under reliable cases, and (c) over reliable cases when using actual and simulated measurements for the Pemiscot site.

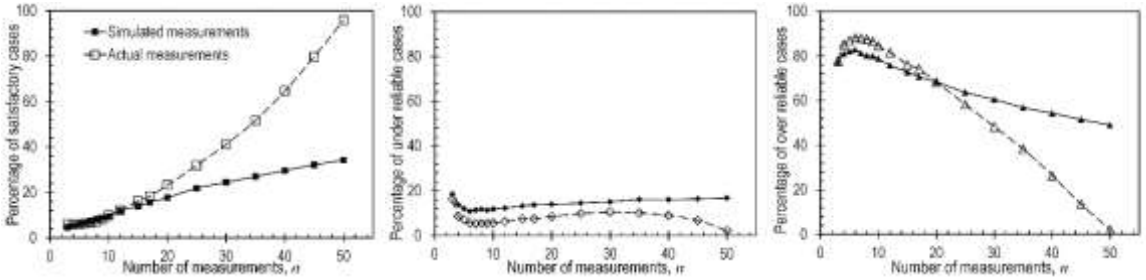


(a) (b) (c)

Figure 7.37 Percentages of: (a) satisfactory cases, (b) under reliable cases, and (c) over reliable cases when using actual and simulated measurements for the St. Charles site.

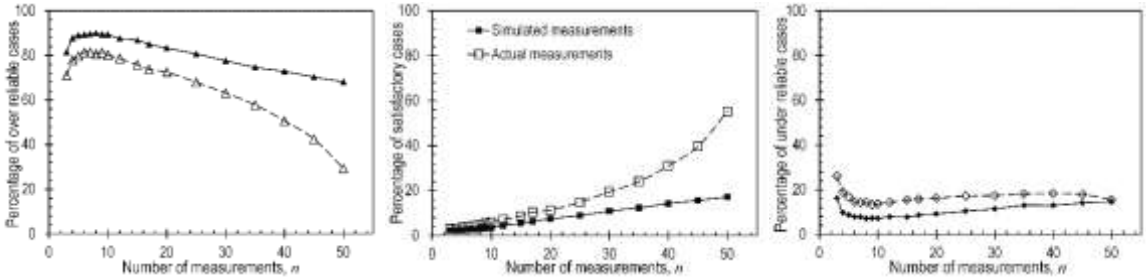


(a) (b) (c)

Figure 7.38 Percentages of: (a) satisfactory cases, (b) under reliable cases, and (c) over reliable cases when using actual and simulated measurements for the New Florence site.

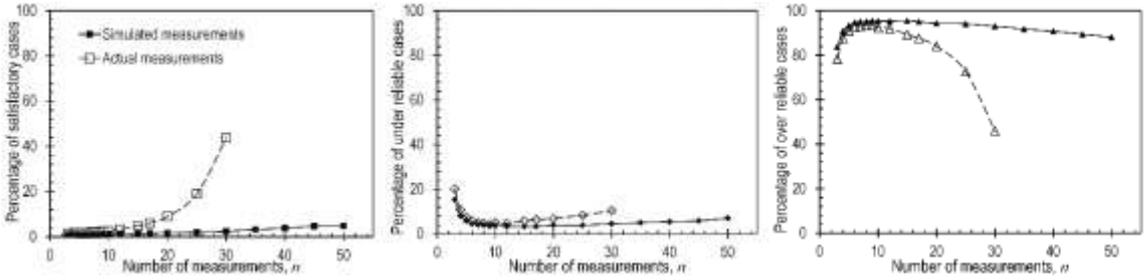


(a) (b) (c)

Figure 7.39 Percentages of: (a) satisfactory cases, (b) under reliable cases, and (c) over reliable cases when using actual and simulated measurements for the Warrensburg site.

Results shown in Figures 7.36 and 7.37 support the postulate that the decrease in the percentage of under reliable cases observed for $n > 30$ is a result of the limited population size. The results obtained using the larger simulations populations further show that the percentage of under reliable cases is practically independent of the number of measurements when $n$>7.

For small $n$, Figures 7.36-7.39 show that population size has little effect on the percentages of satisfactory, under reliable and over reliable cases. For larger $n$, however, use of the larger populations has the effect of reducing the percentage of satisfactory cases and increasing the percentage of over reliable cases compared to the percentages determined using much smaller populations. The general influence of the number of measurements (i.e. increasing or decreasing trends in the different percentages) is consistent, but these results suggest that larger populations of measurements should be used to quantify achievement of target reliability when relative large numbers of measurements (i.e. large $n$) are being considered.

## 7.8 Effect of Different Regression Models

Two different regression models were applied in this research to interpret undrained shear strength measurements—linear regression models and constant regression models. Results obtained using these alternative regression models are compared in Figures 7.40-7.43 for footings located at the respective "middle" depths.

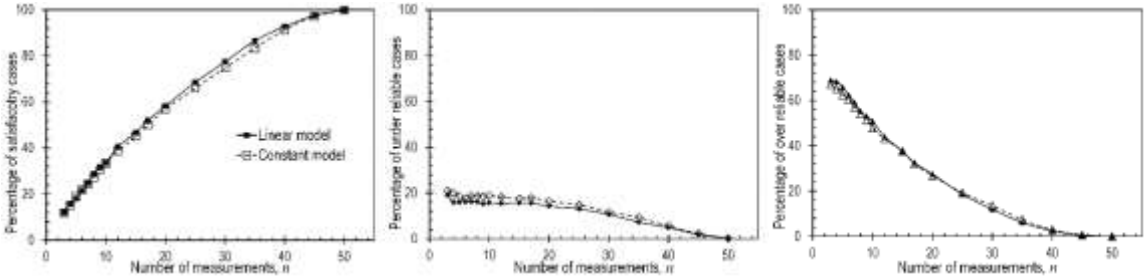


(a) (b) (c)

Figure 7.40 Comparison of: (a) satisfactory cases, (b) under reliable cases, and (c) over reliable cases for the Pemiscot site from constant and linear regression models for footing depth of 30 feet.

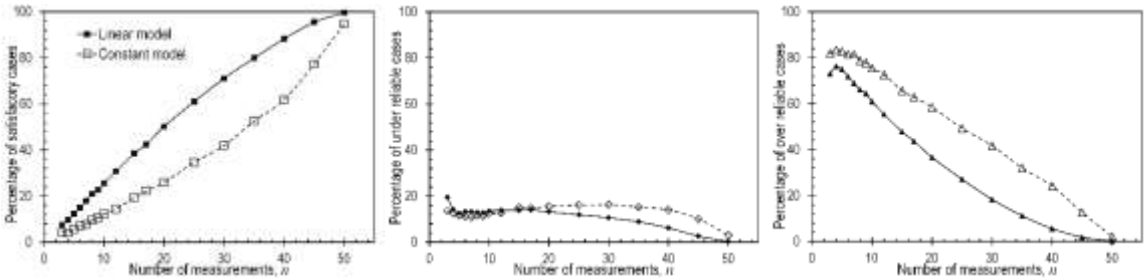


(a) (b) (c)

Figure 7.41 Comparison of: (a) satisfactory cases, (b) under reliable cases, and (c) over reliable cases for the St. Charles site from constant and linear regression models for footing depth of 16 feet.

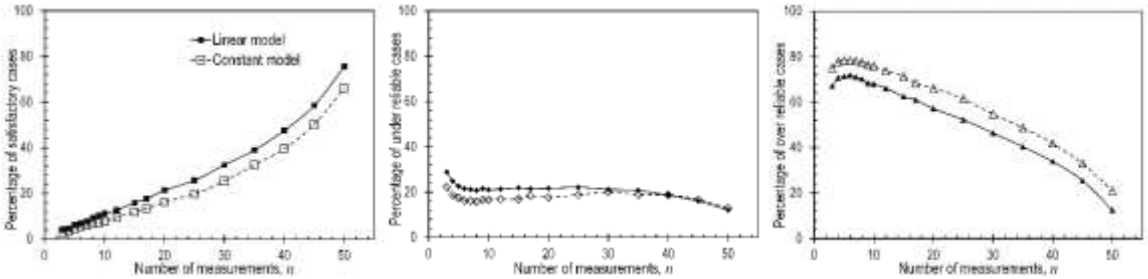


(a) (b) (c)

Figure 7.42 Comparison of: (a) satisfactory cases, (b) under reliable cases, and (c) over reliable cases for the New Florence site from constant and linear regression models for footing depth of 16 feet.

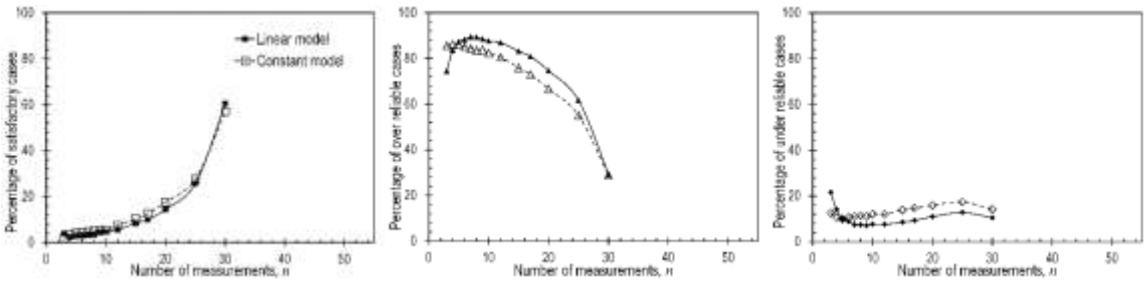


(a) (b) (c)

Figure 7.43 Comparison of: (a) satisfactory cases, (b) under reliable cases, and (c) over reliable cases for the Warrensburg site from constant and linear regression models for footing depth of 16 feet.

The results show that the percentage of satisfactory cases is similar for both models for the Pemiscot and Warrensburg sites. For the St. Charles and New Florence sites, the percentage of satisfactory cases is greater for the linear regression models than for the constant models while the percentage of over reliable cases are similarly less, without substantial changes in the percentage of under reliable cases. The hypothesis tests and residual plots presented in Chapter 4 indicate that constant regression models poorly represent the actual measurements from the St. Charles and New Florence sites. These comparisons thus suggest that use of a more appropriate regression model will generally produce more satisfactory cases.

## 7.9 Effect of Site Variability

The percentage of satisfactory cases is significantly affected by site variability regardless of the selected form of regression models or what footing depths are considered. As shown in Figures 7.44-7.46, the percentage of satisfactory cases at the Pemiscot site (least variable site) is greatest among all sites, followed sequentially by the St. Charles site, the New Florence site and the Warrensburg site. The results shown also suggest that the percentage of satisfactory cases increases more dramatically at the less variable sites (the

Pemiscot and St. Charles sites) than at the more variable sites (the New Florence and Warrensburg sites).

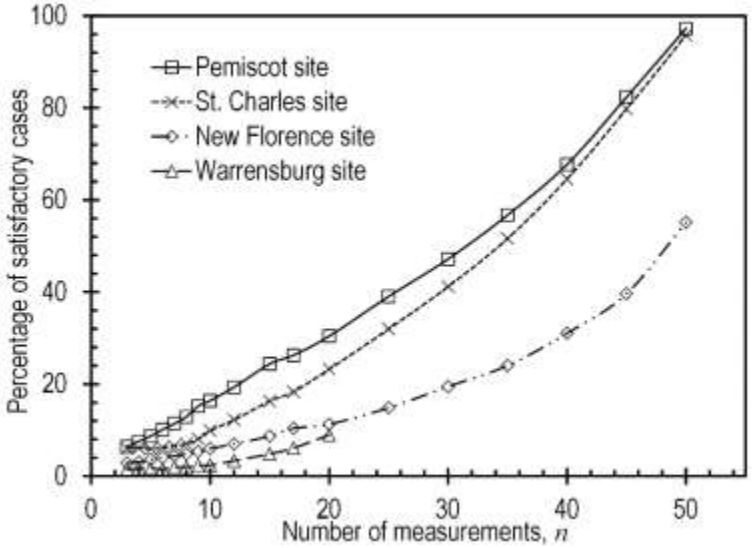


Figure 7.44 Percentages of satisfactory cases from four sites using linear regression models with shallow footing depth.

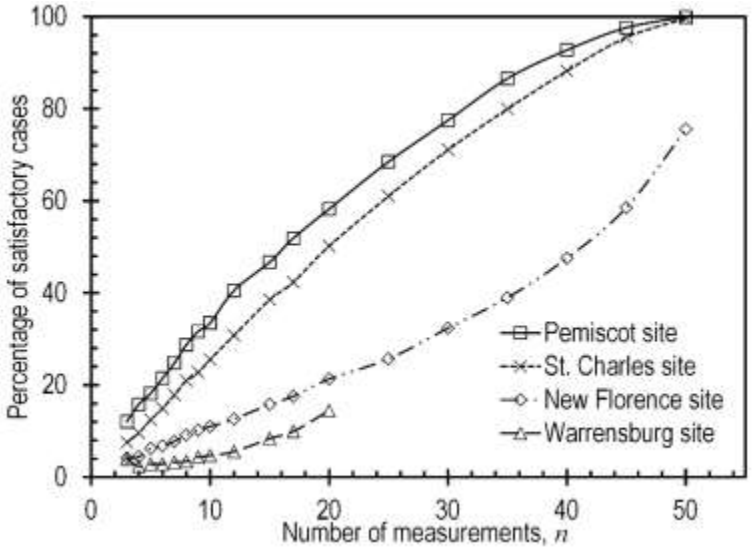


Figure 7.45 Percentages of satisfactory cases from four sites using linear regression models with deeper footing depths.

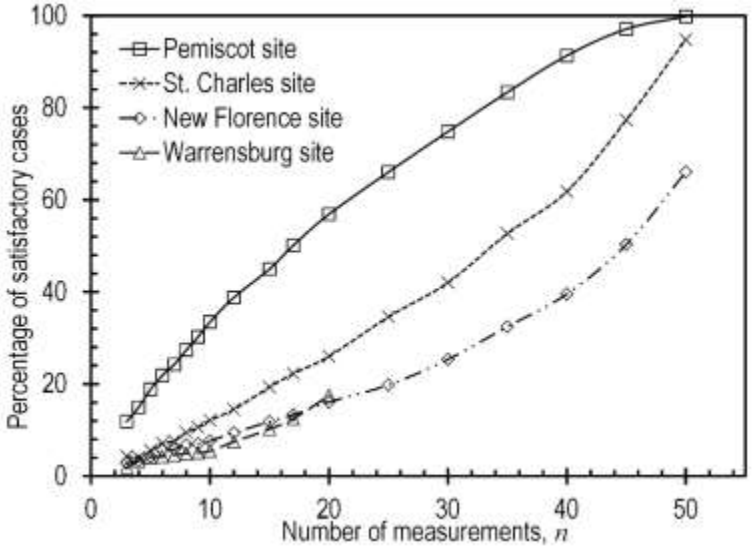

Figure 7.46 Percentages of satisfactory cases from four sites using constant regression models.

## 7.10 Summary

In this chapter, the effect of the number of undrained shear strength measurements on the reliability of spread footings designed using LRFD was evaluated based on simulated designs using the LRFD methods described in Chapter 5 and the measured undrained shear strength measurements presented in Chapter 4. The influence of considering different target probabilities of failure, footing depths, spatial averaging, total population size, and different regression models and considering sites with different variability were also discussed. The results presented show that the percentage of cases that practically achieve the target reliability increases with the number of measurements considered while the percentage of cases with reliabilities that substantially exceed the target value (over reliable cases) decreases in a largely complementary manner. The percentage of cases with reliabilities that are substantially less than the target value (under reliable cases) was found to practically independent of the number of measurements when greater than seven measurements are considered. However, the percentage of cases with

reliabilities that are substantially less than the target value (under reliable cases) was observed to increase dramatically when less than seven measurements were used for design. Two alternative methods developed to address the latter issue will be introduced and evaluated in Chapters 8 and 9.

# Chapter 8 Reliability of Spread Footings Designed Using LRFD with a Penalty Function for Small Numbers of Measurements

## 8.1 Introduction

The analyses presented in Chapter 7 show that the percentage of spread footings that practically achieve the target probability of failure is strongly affected by the number of undrained shear strength measurements when design using the load and resistance factor design (LRFD) methods as described in Chapter 5. The percentage of designs with reliabilities that are substantially less than the target reliability was found to be practically independent of the number of measurements considered when greater than about seven measurements are used for design. However, this percentage of "under reliable" designs increases dramatically when designing with fewer than seven measurements. Two different approaches for reducing the percentage of under reliable designs when small numbers of measurements are used were evaluated as part of this research. In this chapter, an empirical "penalty function" method to reduce the percentage of under reliable designs for small numbers of measurements is described and evaluated using analyses similar to those presented in Chapter 7. An alternative method involving use of upper confidence bounds of the uncertainty in the mean undrained shear strength is subsequently described and evaluated in Chapter 9.

## 8.2 Penalty Function Method

A "penalty function" method was proposed by Loehr et al. (2011a) to account for the potential to dramatically underestimate the uncertainty in mean values of design parameters when small numbers of measurements are available. The method was developed for application with LRFD provisions of the Missouri Department of Transportation (MoDOT, 2011), which are generally consistent with the methods described in Chapter 5 for design of shallow foundations. The penalty function incorporates a multiplicative uncertainty modifier, $\zeta$, that is applied to the coefficient of variation of the mean undrained shear strength ($COV_{\mu_{s_u}}$) prior to selecting resistance factors from charts similar to Figure 5.1. The empirically established uncertainty modifier is taken to be a function of the number of measurements, $n$ used to compute $COV_{\mu_{s_u}}$:

$$\zeta = \frac{(n+2.5)}{(n-1)} \qquad \text{(Eq. 8.1)}$$

As shown in Figure 8.1, the uncertainty modifier takes a value of 2.75 when three measurements are used to establish $COV_{\mu_{s_u}}$, decreases with increasing numbers of measurements ($n$), and gradually approaches 1.0 as $n$ approaches infinity.

The general effect of the uncertainty modifier is to empirically increase the uncertainty considered for design when design parameters are estimated from small numbers of measurements. The greater uncertainty considered for design results in use of samller resistance factors (e.g. from Figure 5.1), which in turn results in selecting larger foundation sizes to compensate for the potential to produce foundations that may not achieve the established target reliability.

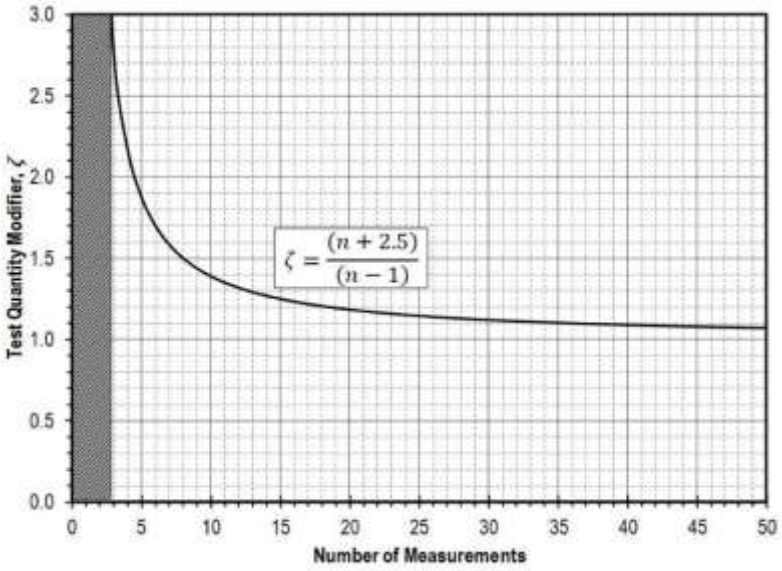


Figure 8.1 Empirical uncertainty modifier used to modify computed $COV$ of the mean value of a design parameter. (Loehr et al., 2011a)

Equation 8.1 and Figure 8.1 were developed from limited analyses performed using empirical measurements of undrained shear strength using the following procedure:

1. Randomly subsample a small number of measurements, *n*, and calculate the standard deviation of the mean value of the measurements;
2. Repeat Step 1 ten to twelve times and calculate the average and standard deviation of the computed values of standard deviation;
3. Compute the value of the average standard deviation plus *s* times the standard deviation of standard deviation and divide that value by the average standard deviation, where *s*=1.0, 2.0 and 3.0;
4. Repeat Steps 1 to 3 for different numbers of measurements $(n)$ and plot the calculated values from Step 3 versus $n$ as shown in Figure 8.2;
5. Fit rational curves through the points computed for $s = 1.0$ to obtain Eq. 8.1.

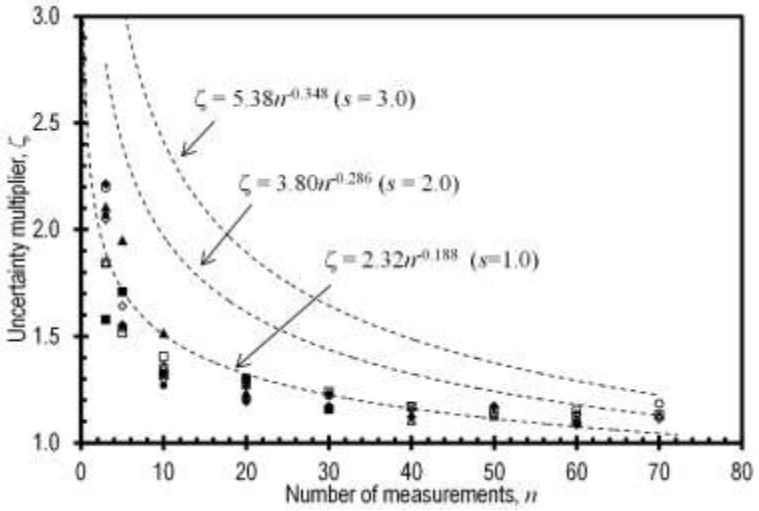


Figure 8.2 Illustration of analyses used to develop uncertainty modifier, $\zeta$. (Likos and Loehr, personal communication, 2010).

## 8.3 Evaluation Procedure

To evaluate the reliability of foundations designed using the penalty function with different numbers of measurements, design simulations were performed following the procedure described in Chapter 7 except that the penalty function was applied to the computed value of $COV_{\mu_{s_u}}$. The steps include:

1. Randomly subsample $n$ measurements from the total population of $N$ measurements.
2. Calculate the mean value ($\mu_{s_u}$) and the uncertainty in the mean value ($COV_{\mu_{s_u}}$) of undrained shear strength from the $n$ subsampled measurements.
3. Apply the empirical uncertainty modifier, $\zeta$, to the computed $COV_{\mu_{s_u}}$:

$$\zeta \cdot COV_{\mu_{s_u}}$$

4. Determine the appropriate resistance factor ($\varphi_{s_u}$) from Figure 5.1 based on the modified $COV$ with the value of ($\zeta \cdot COV_{\mu_{s_u}}$).

5. Use the resistance factor ($\varphi_{s_u}$) and the calculated mean undrained shear strength ($\mu_{s_u}$) to size the spread footing.
6. Finally, compute the reliability of the spread footing using Monte Carlo simulations with 100,000 simulations and considering the true soil properties established using the entire population of measurements.

The procedure was repeated for 10,000 different subsamples for each $n$ ranging from 3 to 50 to reflect cases where design is performed using very limited information and cases where design is performed using plentiful information.

The computed probabilities of failure were again compared with the target probability of failure, $p_T$, and classified as satisfactory ($0.5 \cdot p_T < p_f < 1.5 \cdot p_T$), "under reliable" ($p_f > 1.5 \cdot p_T$), and "over reliable" ($p_f < 0.5 \cdot p_T$) as introduced in Chapter 7. The percentage of cases within each category was quantified to reflect the accuracy of designs established using the penalty function method with different numbers of measurements. Since results presented in Chapter 7 demonstrate that the target probability of failure had negligible effect on how closely designs achieve the target reliability, all analyses were performed for a target probability of failure of 1/1500.

## 8.4 Results Using Linear Regression Models for Undrained Shear Strength

To be consistent with the analysis in Chapter 7, the spread footing foundations are designed at the same depths as shown in Table 4.5. The total number of measurements at each site is taken to serve as the total population of measurements, $N$. The percentages of satisfactory cases ($0.5 \cdot p_T < p_f < 1.5 \cdot p_T$), under reliable cases ($p_f > 1.5 \cdot p_T$) and over reliable cases ($p_f < 0.5 \cdot p_T$) are plotted as a function of the number of measurements considered in Figures 8.3-8.6.

At the Pemiscot site (Figure 8.3), the percentage of under reliable cases is no longer practically constant as was observed in Chapter 7. Application of the penalty function produces the result that the percentage of under reliable cases is relatively low for small $n$, increases with increasing $n$ to a maximum value at approximately 30 measurements, and finally decreases with additional measurements (which is a result of the finite population considered as described in Chapter 7). While the percentage of under reliable cases is no longer constant, the substantial increase in the percentage of under reliable cases observed for very small numbers of measurements in Chapter 7 is not present, which suggests that the penalty function has effectively controlled the potential for having excessive numbers of under reliable cases with small numbers of measurements. Similar results are observed in Figures 8.4-8.6 for the other sites. Although results for some sites indicate a slight increase in the percentage of under reliable cases for $n = 3$, the absolute percentage is less than is observed when the penalty function is not applied, and less than the percentage observed for greater numbers of measurements. More detailed comparisons of analysis results from Chapters 7, 8, and 9 will be presented in Chapter 10.

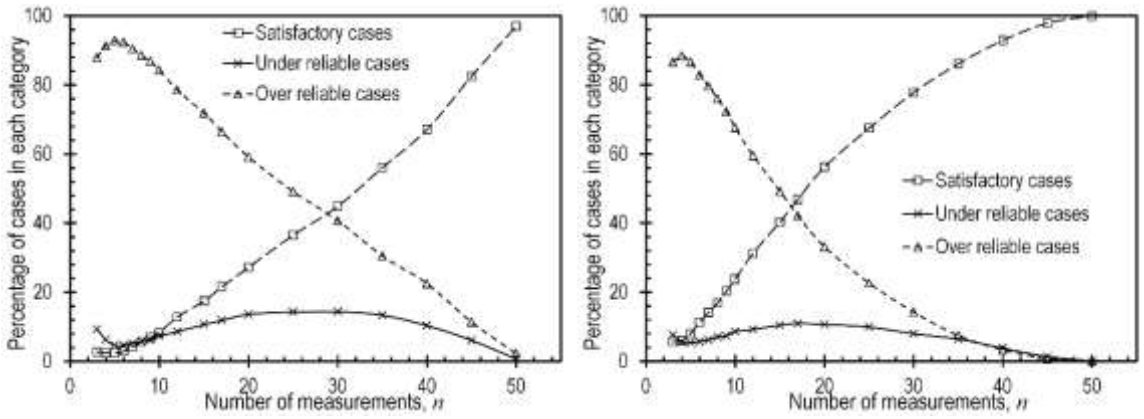


Figure 8.3 Percentage of satisfactory, under reliable and over reliable cases for Pemiscot site using linear regression models: (a) depth of 7 ft, and (b) depth of 30 ft.

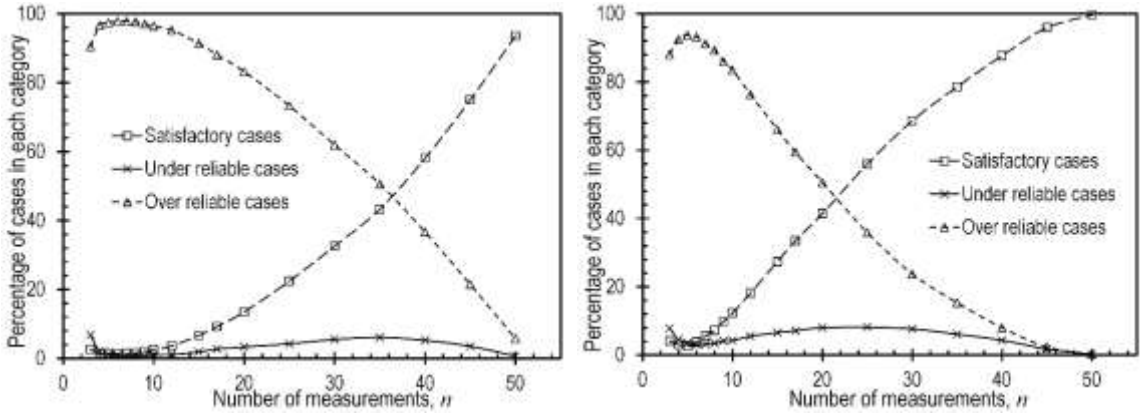


Figure 8.4 Percentage of satisfactory, under reliable and over reliable cases for St. Charles site using linear regression models: (a) depth of 7 ft, and (b) depth of 16 ft.

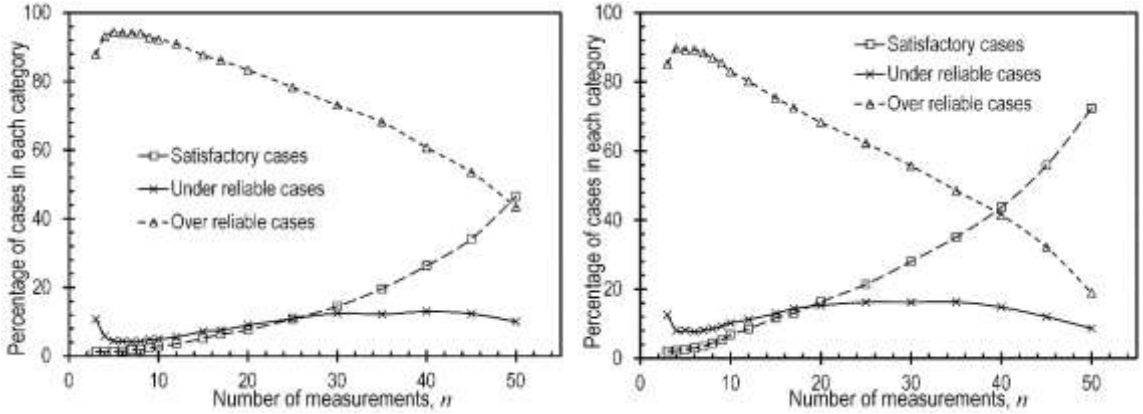


Figure 8.5 Percentage of satisfactory, under reliable and over reliable cases for New Florence site using linear regression models: (a) depth of 7 ft, and (b) depth of 16 ft.

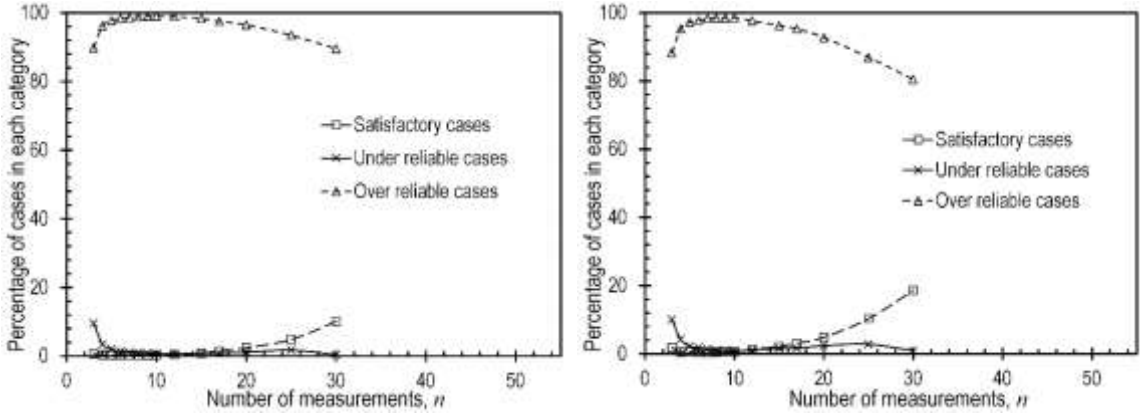


Figure 8.6 Percentage of satisfactory, under reliable and over reliable cases for Warrensburg site using linear regression models: (a) depth of 7 ft, and (b) depth of 16 ft.

## 8.5 Results Using Constant Regression Models for Undrained Shear Strength

Results of analyses performed using constant regression models for interpretation of the selected measurements are shown in Figures 8.7-8.10. These results again show that application of the penalty function effectively reduces the percentage of under reliable cases when small numbers of measurements are considered. Use of the penalty function does result in having inconsistent percentages of under reliable cases. Furthermore, use of the penalty function produces fewer under reliable cases when smaller numbers of measurements are used than when greater numbers of measurements are used for design, which seems counter-intuitive. However, the reduction in the percentage of under reliable cases for small $n$ satisfies the purpose of reducing the potential for performance problems when designing with small numbers of measurements.

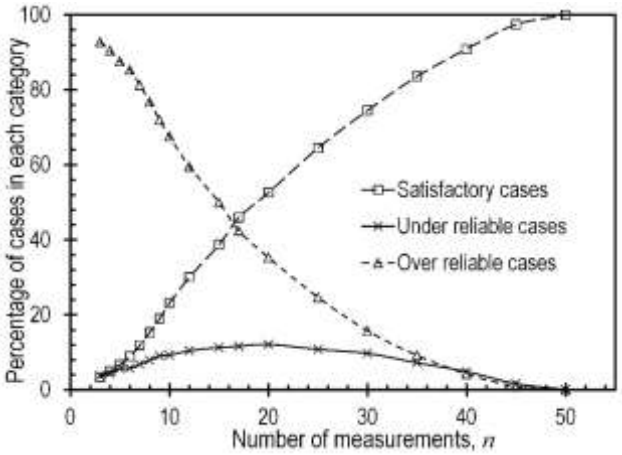


Figure 8.7 Percentage of satisfactory, under reliable and over reliable cases for the Pemiscot site using constant regression model.

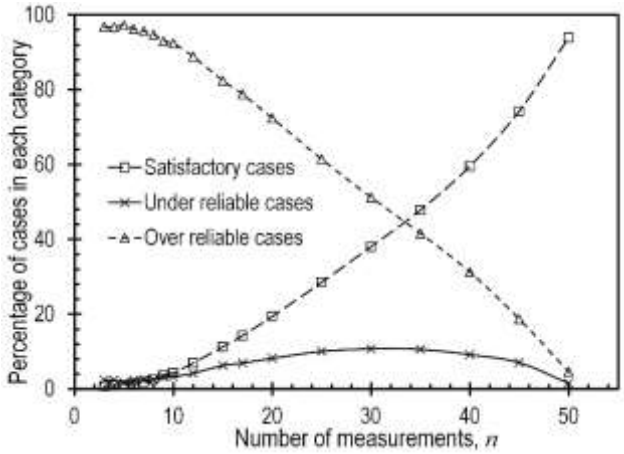

Figure 8.8 Percentage of satisfactory, under reliable and over reliable cases for the St. Charles site using constant regression model.

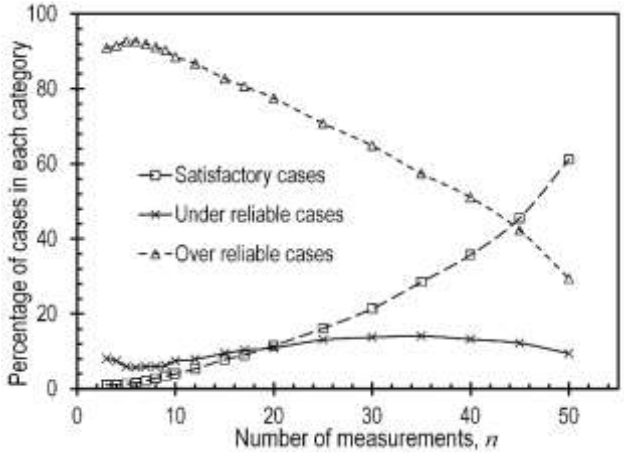

Figure 8.9 Percentage of satisfactory, under reliable and over reliable cases for the New Florence site using constant regression model.

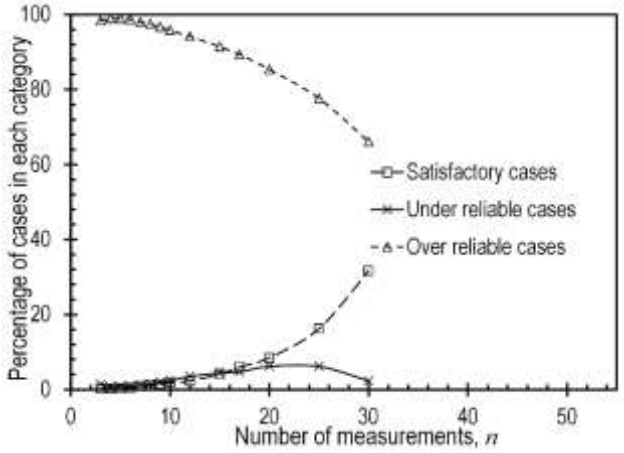

Figure 8.10 Percentage of satisfactory, under reliable and over reliable cases for the Warrensburg site using constant regression model.

## 8.6 Summary

A "penalty function" method that incorporates an empirical uncertainty modifier has been described in this chapter. The purpose of the method is to compensate for the potential to dramatically underestimate uncertainties in soil design parameters and to reduce the potential for foundation performance problems when small numbers of measurements are used for design. Results of analyses presented in this chapter indicate that the method does effectively control the substantial increases in the percentage of "under reliable" cases that are observed when small numbers of measurements are used for design without the uncertainty modifier. In doing so, the percentage of under reliable cases is no longer practically independent of the number of measurements considered for design. A more rigorous and rational alternative method to control the substantial increases in the percentage of under reliable cases for small numbers of measurements will be introduced in Chapter 9.

# Chapter 9 Reliability of Spread Footings Designed Using LRFD and Upper Confidence Bounds for the Coefficient of Variation

## 9.1 Introduction

As illustrated in previous chapters, the reliability of foundations designed using load and resistance factor design (LRFD) methods is dependent on the uncertainty in the estimated undrained shear strength. The uncertainty in the undrained shear strength is, in turn, strongly dependent on the number of measurements that are available for design. Analyses presented in Chapter 7 show that use of LRFD methods described in Chapter 5 produces footings with a practically constant likelihood of being "under reliable" when greater than seven undrained shear strength measurements are used for design. However, these same analyses reveal that the likelihood of footings being under reliable increases substantially when fewer measurements are used for design. An empirical "penalty function" approach to control the percentage of under reliable footings when designing with small numbers of measurements was described and evaluated in Chapter 8. In this chapter, an alternative method for controlling the percentage of under reliable footings when designing with small numbers of measurements is described and evaluated based on analyses similar to those presented in the preceding chapter.

## 9.2 Upper Confidence Bound of Uncertainty Method

The proposed method is similar to the penalty function method described in Chapter 8 in that it utilizes a modified coefficient of variation ($COV$) for selection of resistance

factors. However, rather than modify the computed $COV$ determined from available measurements using an empirically established multiplier, an upper confidence bound of the $COV$ is used. Use of the upper confidence bound produces the same general effect as the penalty function: it produces a larger $COV$, which in turn produces a lesser resistance factor and a larger footing to limit the percentage of under reliable cases. However, the upper confidence bound approach represents a more formal and rigorous approach that takes advantage of the available measurements at a given site rather than relying on completely empirical results from select sites.

## 9.3 Calculation of Upper Confidence Bound for Coefficient of Variation

In the book *Statistics and Data Analysis*, Tamhane and Dunlop (2000) defined confined intervals for an unknown parameter as "a random interval computed from sample data that will contain the true parameter with probability of $1 - \alpha$", where $\alpha$ defines the particular confidence level for the interval. The confidence interval is commonly used in inferential statistics and says that there is a probability of $1 - \alpha$ that the true value will fall within the range of the upper and lower bounds. For the present work, only the upper confidence bound of $COV$ will be considered. Stated probabilistically, the upper confidence bound can be defined as:

$$p(COV < UCB) = 1 - \alpha \qquad \text{(Eq. 9.1)}$$

where $UCB$ is the upper confidence bound of $COV$ and $1 - \alpha$ is called the confidence level. As an example, a one-sided 95% upper confidence bound for the $COV$ means the probability that true *COV* value is less than the upper confidence bound is 95% if the 95% confidence level is used.

Computing the upper confidence bound for $COV$ is more complicated than computing upper confidence bounds for the mean and standard deviation of a parameter. Based on work from McKay (1932) and Johnson and Welch (1940) regarding the distribution of the $COV$, Vangel (1996) proposed equations for the confidence interval for a normally distributed coefficient of variation. Verrill (2003) and Verrill and Johnson (2007) further developed confidence bounds for normally and lognormally distributed $COV$. For the present work, the upper confidence bound of the $COV$ established for linear regression models are further developed; the upper confidence bound of the *COV* for constant regression models are adapted from Verrill (2003). Approximate methods are applied to find the upper confidence bound of $COV$ for linear regression models and constant regression models with lognormally distributed parameters. Since normally distributed parameters are often used in engineering practice, the upper confidence bound of $COV$ for linear and constant regression models with normally distributed parameters will be introduced later in this chapter.

### 9.3.1 Upper Confidence Bound for Linear Regression Models with Lognormally Distributed Parameters

As described in Chapter 4, linear regression models have mean values and $COV$ that vary with depth. The undrained shear strength, $s_u$, follows a lognormal distribution with depth:

$$s_u|z \sim LN(\hat{\mu}_{\ln(s_u)}, \hat{\sigma}^2_{\ln(s_u)}) \qquad \text{(Eq. 9.2)}$$

where $s_u$ is soil undrained shear strength at depth $z$, and $\hat{\mu}_{\ln(s_u)}$ and $\hat{\sigma}^2_{\ln(s_u)}$ are the estimated mean and variance of the logarithm of $s_u$ at depth $z$, respectively. The estimated mean undrained shear strength, $\hat{\mu}_{(s_u)}$, at depth $z$ can be calculated using:

$$\hat{\mu}_{(s_u)} = \mathrm{e}^{\hat{\mu}_{\ln(s_u)}} = \mathrm{e}^{(\hat{\beta}_0 + \hat{\beta}_1 \cdot z)} \quad \text{(Eq. 9.3)}$$

where $\hat{\beta}_0$ and $\hat{\beta}_1$ are the estimated intercept and slope of the linear regression model, respectively.

The difference between the estimated mean, $\hat{\mu}_{(s_u)}$, and actual mean, $\mu_{(s_u)}$, values of undrained shear strength is:

$$\hat{\mu}_{(s_u)} - \mu_{(s_u)} = \mathrm{e}^{\hat{\mu}_{\ln(s_u)}} - e^{\mu_{\ln(s_u)}} \quad \text{(Eq. 9.4)}$$

Taking the first derivative of $\mu_{ln(s_u)}$ on the right hand side of Eq. 9.4 leads to:

$$\hat{\mu}_{(s_u)} - \mu_{(s_u)} \cong e^{\mu_{\ln(s_u)}} \cdot (\hat{\mu}_{ln(s_u)} - \mu_{ln(s_u)}) \quad \text{(Eq. 9.5)}$$

From Eq. 9.5, the variance and standard deviation of undrained shear strength can respectively be approximated using the Delta method (Oehlert, 1992) as:

$$var(\hat{\mu}_{(s_u)} - \mu_{(s_u)}) \cong (e^{\mu_{\ln(s_u)}})^2 \cdot var(\hat{\mu}_{ln(s_u)} - \mu_{ln(s_u)}) \quad \text{(Eq. 9.6)}$$

$$\sigma_{(s_u)} \cong e^{\mu_{\ln(s_u)}} \cdot \sigma_{ln(s_u)} \cong \mu_{(s_u)} \cdot \sigma_{ln(s_u)} \quad \text{(Eq. 9.7)}$$

where $var(\hat{\mu}_{(s_u)} - \mu_{(s_u)})$ is the variance of undrained shear strength and $var(\hat{\mu}_{ln(s_u)} - \mu_{ln(s_u)})$ is the variance of the logarithm of undrained shear strength, both of which are calculated at depth *z*. $\sigma_{(s_u)}$ and $\sigma_{ln(s_u)}$ are standard deviations of undrained shear strength and the logarithm of undrained shear strength at depth *z*, respectively. Substituting Eq. 9.7 into the equation for $COV$:

$$COV = \frac{\sigma_{(s_u)}}{\hat{\mu}_{(s_u)}} \cong \frac{\mu_{(s_u)} \cdot \sigma_{ln(s_u)}}{\hat{\mu}_{(s_u)}} \cong \sigma_{ln(s_u)} \quad \text{(Eq. 9.8)}$$

leads to the observation that the COV can be approximated from the standard deviation of the logarithm of the undrained shear strength. Thus, the one-sided upper confidence bound for $COV$ can be approximated by calculating the one-sided upper confidence bound of the standard deviation of the logarithm of undrained shear strength, $\sigma_{ln(s_u)}$.

Since $\sigma_{ln(s_u)}$ follows a chi-square distribution, the $1-\alpha$ upper confidence bound of *COV* can be calculated as:

$$UCB(1-\alpha) = \sqrt{\frac{(n-2)\cdot\sigma^2_{\ln(s_u)}}{\chi^2_{\alpha;n-2}}} \qquad \text{(Eq. 9.9)}$$

where $\alpha$ is called the significance level, $UCB(1-\alpha)$ is the one-side $1-\alpha$ upper confidence bound of $COV$, and $\chi^2_{\alpha;n-2}$ is the chi-square value with $(n-2)$ degrees of freedom at the $\alpha$ significance level. Substituting $\sigma^2_{\widehat{\mu}_{\ln(s_{ui})}}$ for $\sigma^2_{\ln(s_u)}$, the one-sided $1-\alpha$ upper confidence bound of $COV_{\widehat{\mu}_{s_u}}$ can be computed as:

$$UCB(1-\alpha) = \sqrt{\frac{(n-2)\cdot\sigma^2_{\widehat{\mu}_{\ln(s_{ui})}}}{\chi^2_{\alpha;n-2}}} \cong COV\cdot\sqrt{\frac{(n-2)}{\chi^2_{\alpha;n-2}}} \qquad \text{(Eq. 9.10)}$$

where $\sigma^2_{\widehat{\mu}_{\ln(s_{ui})}}$ is the variance about the estimated mean. $\sigma^2_{\widehat{\mu}_{\ln(s_{ui})}}$ is taken from the regression model and calculated as:

$$\sigma^2_{\widehat{\mu}_{\ln(s_{ui})}} = \left(\frac{\sum_{i=1}^{n}[\ln(s_{u_i})-\ln(\hat{s}_{u_i})]^2}{n-2}\right)\cdot\left(\frac{1}{n}+\frac{(\bar{z}-z)^2}{\sum_{i=1}^{n}(z_i-\bar{z})^2}\right) \qquad \text{(Eq. 9.11)}$$

where $\sigma^2_{\widehat{\mu}_{\ln(s_{ui})}}$ is the variance about the estimated mean at depth *z*, $\ln(s_{u_i})$ is the logarithm of the $i^{\text{th}}$ undrained shear strength value, $\ln(\hat{s}_{u_i})$ is the estimated undrained shear strength at depth $z_i$, $n$ is the number of measurements, and $\bar{z}$ is the average depth of all measurements.

Equation 9.10 shows that the upper confidence bound depends on the $COV$, the significance level, $\alpha$, and the number of measurements, *n*. Figure 9.1 shows computed values of the upper confidence bound of COV for different numbers of measuremetns and three different confidence levels assuming the variance about the estimated mean value of the logarithm of undrained shear strength, $\sigma^2_{\widehat{\mu}_{\ln(s_{ui})}} = 0.09$ and assuming $COV = 0.3$.

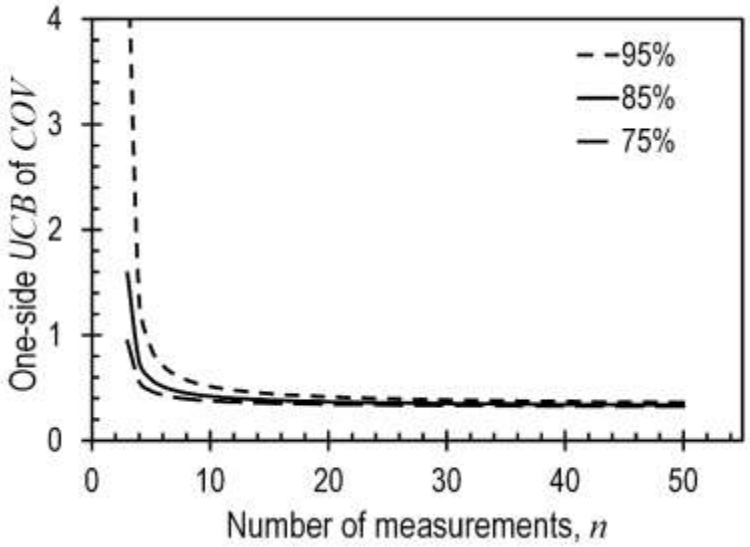

Figure 9.1 One-sided upper confidence bound (*UCB*) values of coefficient of variation for 95%, 85% and 75% confidence levels and $COV = 0.3$.

As shown in Figure 9.1, the upper confidence bound values decrease with increasing numbers of measurements and decreasing confidence level. The upper confidence bound values drop dramatically with increasing numbers of measurements from $n = 3$ to $n = 5$ and then gradually approach the $COV$ in the limit as $n$ approaches infinity.

Dividing both sides of Eq. 9.10 by $COV$, the equation can be rewritten as:

$$\frac{UCB(1-\alpha)}{COV} = \sqrt{\frac{(n-2)}{\chi^2_{\alpha;n-2}}} \qquad \text{(Eq. 9.12)}$$

which shows that the ratio between $UCB$ and $COV$ is a function of the number of measurements and the confidence level. This ratio is functionally similar to the uncertainty modifier, $\zeta$, that is used with the penalty function method described in Chapter 8. Figure 9.2 shows this ratio plotted as a function of the number of measurements for different several different confidence levels. Similar to what was determined for $\zeta$ in Chapter 8, the $UCB$ to $COV$ ratio is relatively large for very small $n$, and decreases rapidly with increasing $n$ until approaching a value of 1.0 as $n$ approaches infinity.

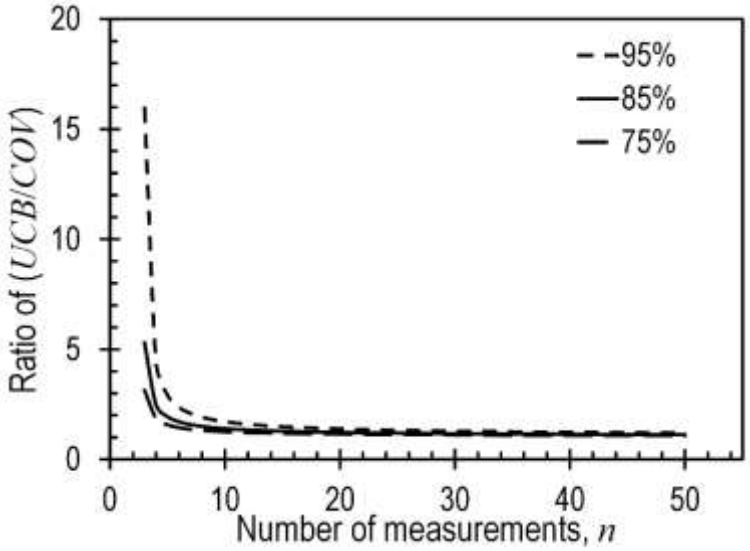

Figure 9.2 Ratio of one-sided upper confidence bound ($UCB$) to the coefficient of variation ($COV$) for confidence levels of 95%, 85% and 75%.

9.3.2 Upper Confidence Bounds for Constant Regression Models with Lognormally Distributed Parameters

As described in Chapter 4, the constant model for a lognormally distributed parameter can be written in the general form of:

$$\ln(s_{u_i}) = \hat{\beta}_0 + \epsilon_i \qquad \text{(Eq. 9.12)}$$

where $\ln(s_{u_i})$ is the logarithm of the $i^{\text{th}}$ undrained shear strength value at depth $z_i$, $\hat{\beta}_0$ is a regression parameter, and $\epsilon_i$ is the random error term with $E(\epsilon_i) = 0$ and $var(\epsilon_i) = \sigma^2$. The estimated mean value and variance of undrained shear strength for this form of model can respectively be calculated as:

$$\hat{\mu}_{s_u} = e^{\left(\hat{\mu}_{\ln(s_u)} + \frac{\sigma^2_{\ln(s_u)}}{2}\right)} \qquad \text{(Eq. 9.13)}$$

$$\sigma^2_{\hat{\mu}_{s_u}} = e^{\left(2\cdot\hat{\mu}_{\ln(s_u)} + \sigma^2_{\ln(s_u)}\right)} \cdot \left(e^{\sigma^2_{\ln(s_u)}} - 1\right) \qquad \text{(Eq. 9.14)}$$

Thus, the $COV$ of undrained shear strength ($COV_{s_u}$) can be written as:

$$COV_{s_u} = \frac{\sqrt{\sigma^2_{\hat{\mu}_{s_u}}}}{\hat{\mu}_{s_u}} = \frac{\sqrt{e^{\left(2\cdot\hat{\mu}_{\ln(s_u)}+\sigma^2_{\ln(s_u)}\right)}.\left(e^{\sigma^2_{\ln(s_u)}}-1\right)}}{e^{\left(\hat{\mu}_{\ln(s_u)}+\sigma^2_{\ln(s_u)}\right)}} = \sqrt{\left(e^{\sigma^2_{\ln(s_u)}}-1\right)} \quad \text{(Eq. 9.15)}$$

where $\hat{\mu}_{\ln(s_u)}$ and $\sigma^2_{\ln(s_u)}$ are the estimated mean and variance values for the logarithm of undrained shear strength that are calculated as:

$$\hat{\mu}_{\ln(s_u)} = \hat{\beta}_0 = \frac{\sum_{i=1}^{n}[\ln(s_{u_i})]}{n} \quad \text{(Eq. 9.16)}$$

$$\sigma^2_{\hat{\mu}_{\ln(s_u)}} = \frac{1}{n}\cdot\frac{\sum_{i=1}^{n}\left[\hat{\mu}_{\ln(s_u)}-\ln(s_{u_i})\right]^2}{(n-1)} \quad \text{(Eq. 9.17)}$$

respectively. In Eqs. 9.16 and 9.17, $\ln(s_{u_i})$ is the logarithm of the $i^{th}$ undrained shear strength measurement and $n$ is the number of measurements.

The one-sided $1-\alpha$ upper confidence bound ($UCB$) value of $COV$ can be established based on the one-sided $1-\alpha$ upper confidence bound value of the variance of the logarithm of undrained shear strength (Johnson et al., 1970):

$$UCB(1-\alpha) = \sqrt{e^{a_u}-1} \quad \text{(Eq.9.18)}$$

$$a_u = \frac{(n-1)\cdot\sigma^2_{\hat{\mu}_{\ln(s_u)}}}{\chi^2_{\alpha;n-1}} \quad \text{(Eq. 9.19)}$$

$$UCB(1-\alpha) = \sqrt{exp\left[\frac{(n-1)\cdot\sigma^2_{\hat{\mu}_{\ln(s_u)}}}{\chi^2_{\alpha;n-1}}\right]-1} \quad \text{(Eq. 9.20)}$$

where $a_u$ is the one-sided $1-\alpha$ upper confidence bound value of variance $\sigma^2_{\hat{\mu}_{\ln(s_u)}}$ and $\chi^2_{\alpha;n-1}$ is the chi-square value with $(n-1)$ degrees of freedom at $\alpha$ significance level. $\sigma^2_{\hat{\mu}_{\ln(s_u)}}$ can be calculated from:

$$\sigma^2_{\hat{\mu}_{\ln(s_u)}} = \frac{\sum_{i=1}^{n}\left[\hat{\mu}_{\ln(s_u)}-\ln(s_{u_i})\right]^2}{(n-1)}\cdot\frac{1}{n} \quad \text{(Eq. 9.21)}$$

The upper confidence bound values from Eq. 9.20 are affected by the $COV$, the number of measurements and the confidence level. Figure 9.3 shows the upper confidence bound values for $COV = 0.3$ and $COV = 0.5$ for 95%, 85% and 75% confidence levels.

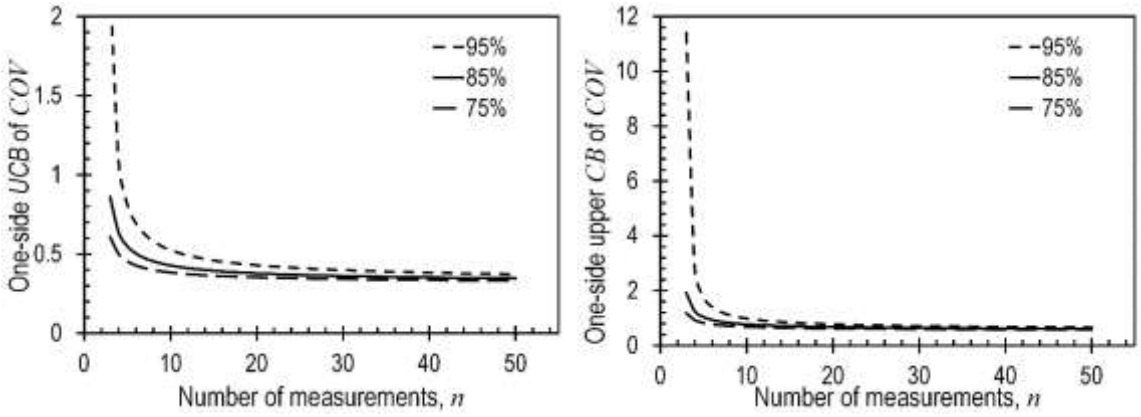


(a) (b)

Figure 9.3 One sided upper confidence bound values for: (a) $COV = 0.3$, and (b) $COV = 0.5$ for 95%, 85% and 75% confidence levels.

Figure 9.3 shows that values of the upper confidence bound of $COV$ depend on values of $COV$ for constant regression models with lognormally distributed parameters and that the upper confidence bound values increase with $COV$. Upper confidence bound values are substantially affected by the number of measurements, especially when the number of measurements is small ($n = 3{\sim}10$). Furthermore, the figure shows that greater values of the upper confidence bound will be obtained for higher confidence levels.

## 9.4 Evaluation Procedure

The reliability of spread footings designed considering the upper confidence bound of the $COV$ was evaluated in a manner similar to that described in Chapters 7 and 8. The design simulations were performed as follows:

1. Randomly subsample $n$ measurements from the total population of $N$ measurements.

2. Calculate the mean value ($\mu_{s_u}$) and the uncertainty in the mean value ($COV_{\mu_{s_u}}$) of undrained shear strength from the $n$ subsampled measurements.
3. Calculate the upper confidence bound ($UCB_{\mu_{s_u}}$) of $COV_{\mu_{s_u}}$ using Eq. 9.10 for linear regression models or Eq. 9.20 for constant regression models.
4. Determine the appropriate resistance factor ($\varphi_{s_u}$) from Figure 5.1 based on $UCB_{\mu_{s_u}}$.
5. Use the resistance factor ($\varphi_{s_u}$) and the calculated mean undrained shear strength ($\mu_{s_u}$) to size the spread footing.
6. Finally, compute the reliability of the spread footing using Monte Carlo simulations with 100,000 simulations and considering the true soil properties established using the entire population of measurements.

This procedure is similar to those use for analyses described in Chapter 7 and 8, except that the upper confidence bound of $COV_{\mu_{s_u}}$ is used to establish the resistance factor, as compared to using $COV_{\mu_{s_u}}$ (Chapter 7) or $\zeta \cdot COV_{\mu_{s_u}}$ (Chapter 8). As was done for previous analyses, the procedure was repeated for 10,000 different subsamples for each $n$ ranging from 3 to 50 to reflect cases where design is performed using very limited information and cases where design is performed using plentiful information.

The computed probabilities of failure were again compared with the target probability of failure, $p_T$, and classified as satisfactory ($0.5 \cdot p_T < p_f < 1.5 \cdot p_T$), "under reliable" ($p_f > 1.5 \cdot p_T$), and "over reliable" ($p_f < 0.5 \cdot p_T$) as introduced in Chapter 7. The percentage of cases within each category was quantified to reflect the accuracy of designs established using the upper confidence bound of the $COV$ with different numbers of measurements. Since results presented in Chapter 7 demonstrate that the target

probability of failure had negligible effect on how closely designs achieve the target reliability, all analyses were performed for a target probability of failure of 1/1500. To be consistent with analyses presents in Chapters 7 and 8 and to compare results from different methods—using *COV*, applying empirical modifier ($\zeta$) and adopting upper confidence bound of *COV*— in next chapter, spread footings were designed for the same depths considered for previous analyses. All results presented subsequently in this chapter were performed using the 95% upper confidence bound, which corresponds to $\alpha = 0.05$. The significance level of $\alpha = 0.05$ was selected following Fisher (1929).

## 9.5 Results of Evaluations Using Upper Confidence Bound for $COV$

Figures 9.4 through 9.7 show the computed percentages of satisfactory, "under reliable", and "over reliable" cases determined as a function of the number of measurements ($n$) for the four different test sites, respectively. These figures show that using the one-side 95% upper confidence bound of $COV$ effectively reduces the percentage of under reliable cases, especially for designs using a small number of measurements ($3 \leq n \leq 10$). The reduction in the percentage of under reliable cases is accompanied by a corresponding increase in the percentage of over reliable cases for small $n$. Collectively, these results support the observation that use of the upper confidence bound of the $COV$ effectively controls the percentage of under reliable cases when small numbers of measurements are used for design.

Results for the St. Charles and Warrensburg sites (Figures 9.5 and 97) indicate that the percentage of under reliable cases is less than 5% for all $n$ when using the one-side 95% upper confidence bound of *COV*. However, results for these sites differ substantially in terms of the percentages of satisfactory and over reliable cases. For the Warrensburg site,

the percentage of satisfactory cases is very small and the percentage of over reliable cases is very large for all values of $n$. In contrast, the percentage of satisfactory cases for the St. Charles site increases substantially with increasing $n$ while the percentage of unsatisfactory cases decreases in a complementary manner. These results again demonstrate the likelihood of designing an over reliable foundation when designing for more variable sites when using the calibrated resistance factors from Chapter 5.

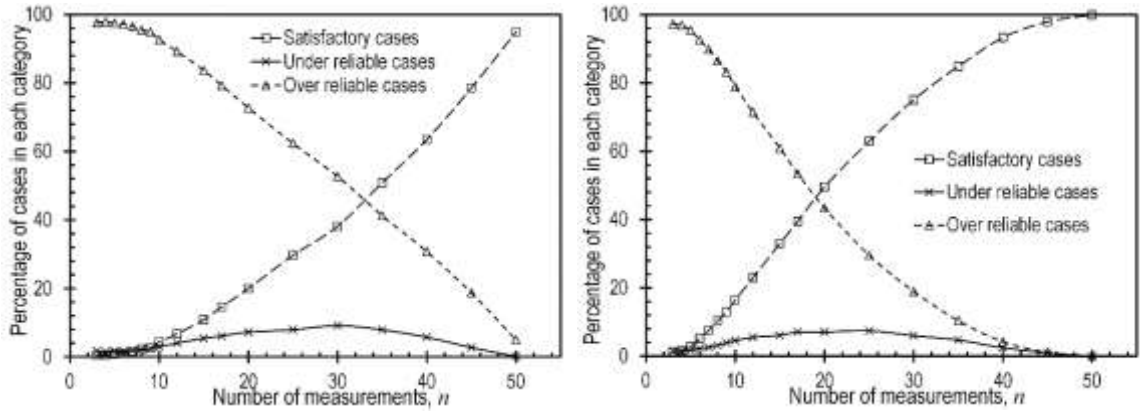


Figure 9.4 Percentage of satisfactory, under reliable and over reliable cases for the Pemiscot site using linear regression models: (a) depth of 7 feet, and (b) depth of 30 feet.

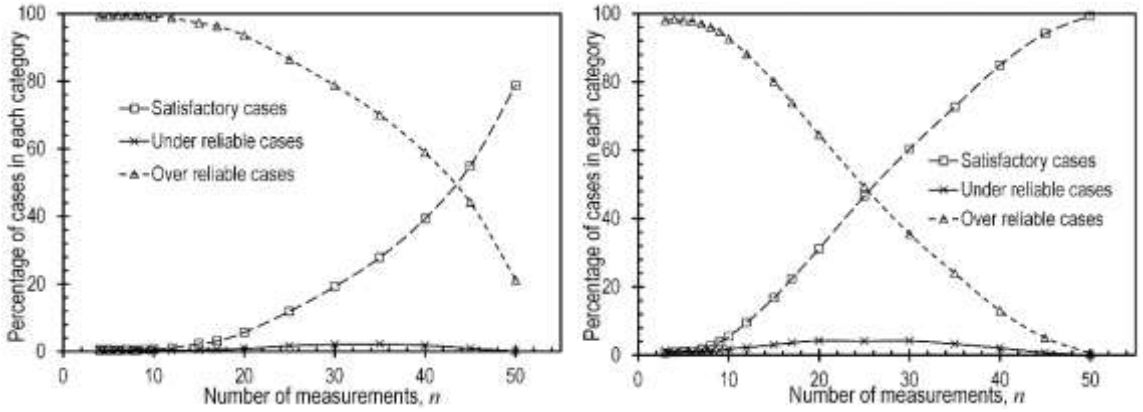


Figure 9.5 Percentage of satisfactory, under reliable and over reliable cases for the St. Charles site using linear regression models: (a) depth of 7 feet, and (b) depth of 16 feet.

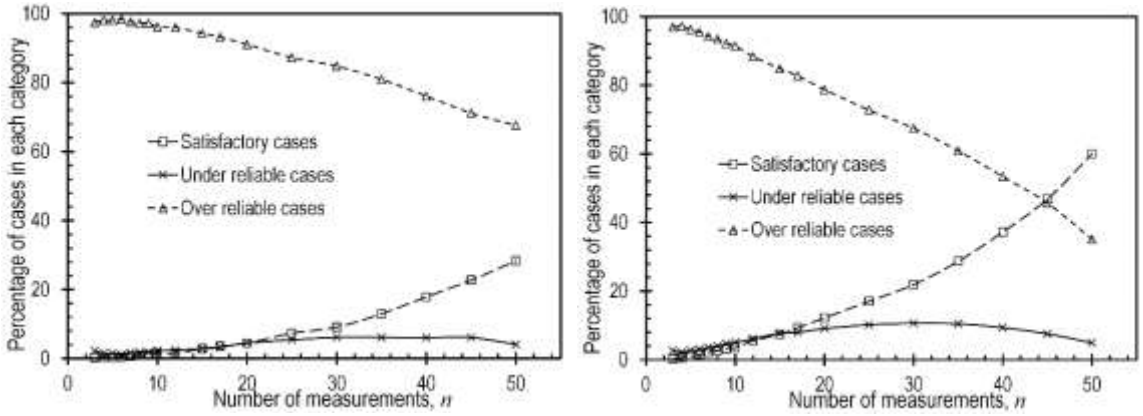


(a) (b)

Figure 9.6 Percentage of satisfactory, under reliable and over reliable cases for the New Florence site using linear regression models: (a) depth of 7 feet, and (b) depth of 16 feet.

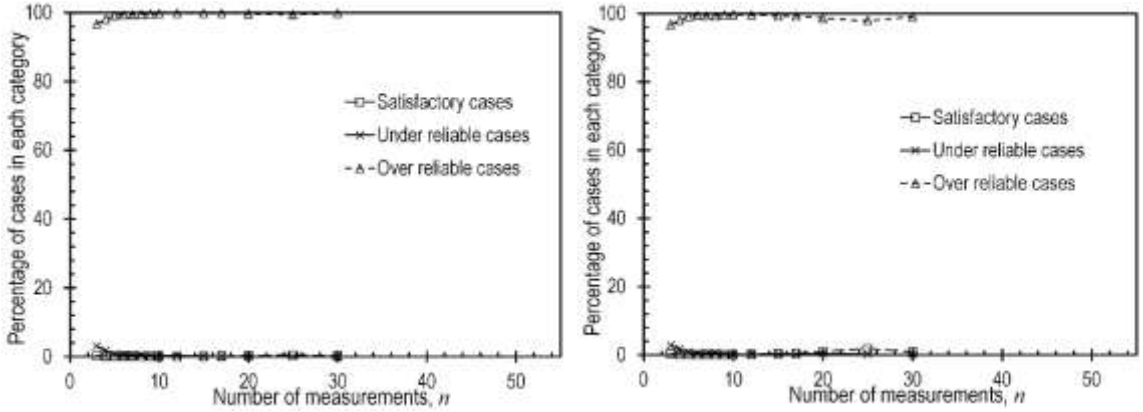


(a) (b)

Figure 9.7 Percentage of satisfactory, under reliable and over reliable cases for the Warrensburg site using linear regression models: (a) depth of 7 feet, and (b) depth of 16 feet.

Figures 9.8-9.11 show results obtained when using constant regression models with the upper confidence bound of the $COV$ for establishing resistance factors for the four sites, respectively. The results shown in the figures are comparable to results shown when using linear regression models and support the observation that use of the upper confidence bound of the $COV$ effectively controls the percentage of under reliable cases when small numbers of measurements are used for design.

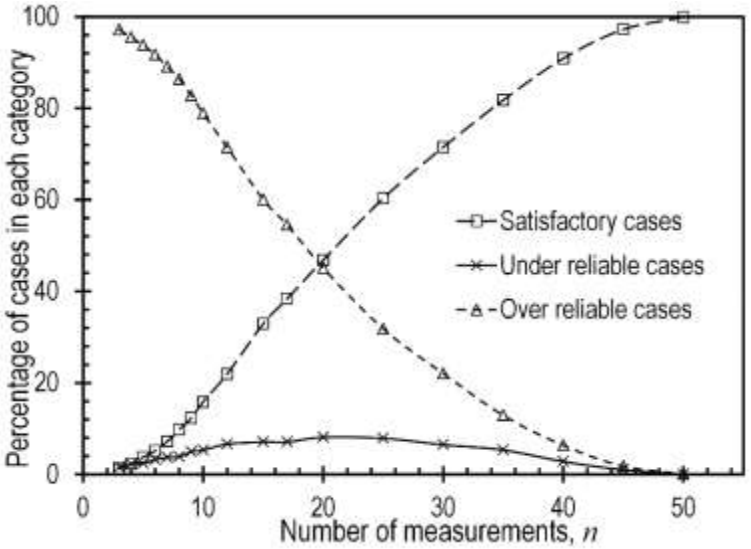


Figure 9.8 Percentage of satisfactory, under reliable and over reliable cases for the Pemiscot site using constant regression models.

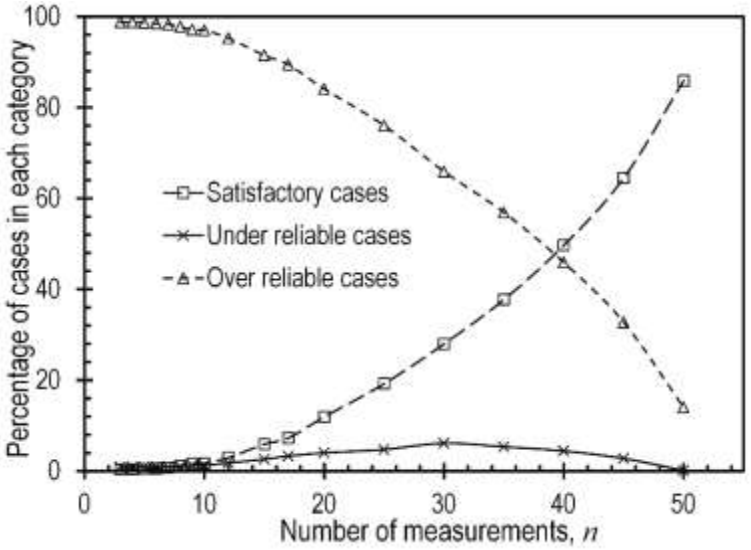


Figure 9.9 Percentage of satisfactory, under reliable and over reliable cases for the St. Charles site using constant regression models.

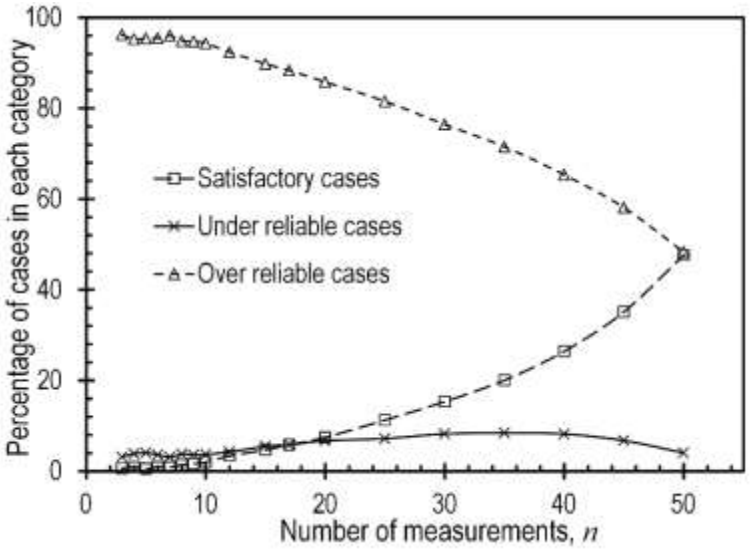

Figure 9.10 Percentage of satisfactory, under reliable and over reliable cases for the New Florence site using constant regression models.

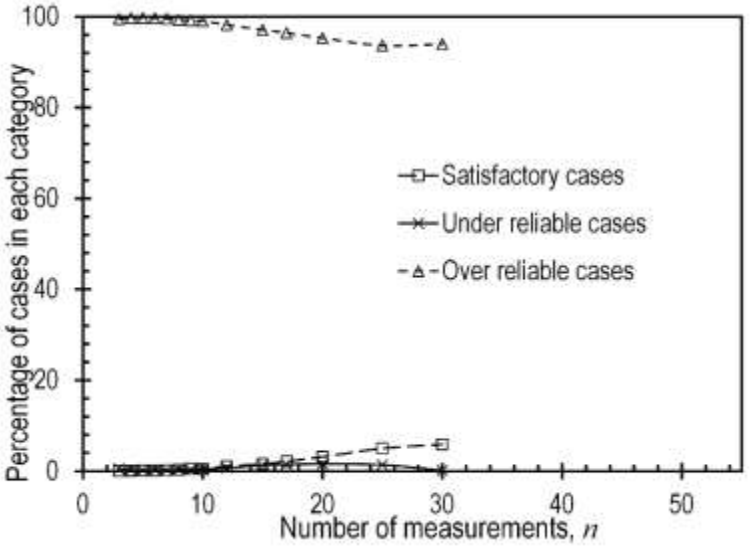

Figure 9.11 Percentage of satisfactory, under reliable and over reliable cases for the Warrensburg site using constant regression models.

## 9.7 Upper Confidence Bounds for Normally Distributed Parameters

In the research described in this thesis, two regression models have been used to estimate the undrained shear strength for different collections of measurements—linear regression models and constant regression models. All regression analyses have also been performed assuming that the residuals are lognormally distributed. However, undrained

shear strength is often assumed to be normally distributed. Furthermore, soil parameters like friction angle, plastic limit, liquid limit, submerged unit weight, and void ratio are also sometimes assumed to be normally distributed. Thus, equations for calculating one-sided upper confidence bounds for the coefficient of variation (*COV*) for linear and constant regression models with normally distributed parameters is presented here.

Assuming that the measurements considered follow a normal distribution with mean ($\bar{X}$) and variance ($s^2$), the ratio of the square root of the number of measurements divided by *COV* follows a noncentral *T* distribution (McKay, 1932; Vangel, 1996):

$$\frac{\sqrt{n}}{COV} = \frac{\bar{X}}{s/\sqrt{n}} \sim F_{NCT}(n-1, \frac{\sqrt{n}}{COV}) \quad \text{(Eq. 9.22)}$$

where $F_{NCT}(n-1, \sqrt{n}/COV)$ denotes a noncentral T distribution with $n-1$ degrees of freedom and noncentrality parameter $\sqrt{n}/COV$. Lehmann (1986) presented the exact calculation of $COV$ confidence intervals for this condition as:

$$F_{NCT}(n-1, \frac{\sqrt{n}}{COV})^{-1} \cdot (\frac{\alpha}{2}) \leq \bar{X}/(s/\sqrt{n}) \leq F_{NCT}\left(n-1, \frac{\sqrt{n}}{COV}\right)^{-1} \cdot (1-\frac{\alpha}{2}) \quad \text{(Eq. 9.23)}$$

Since only the one-sided upper confidence bound is considered, the estimated $COV$ will fall below the upper confidence bound computed as:

$$\bar{X}/(s/\sqrt{n}) \leq F_{NCT}\left(n-1, \frac{\sqrt{n}}{COV}\right)^{-1} \cdot (1-\alpha) \quad \text{(Eq. 9.24)}$$

where $COV$ and $\bar{X}$ are positive for soil properties. Multiplying Eq. 9.24 by the noncentral T-distribution of $F_{NCT}\left(n-1, \frac{\sqrt{n}}{COV}\right)$ results in the following inequality:

$$\bar{X}/(s/\sqrt{n}) \cdot F_{NCT}\left(n-1, \frac{\sqrt{n}}{COV}\right) \leq (1-\alpha) \quad \text{(Eq. 9.25)}$$

Therefore, the value of the one-sided upper confidence bound (*UCB*) of *COV* will be the value which satisfies (Eq. 9.25) in the form of:

$$\frac{\bar{X}}{s/\sqrt{n}} \cdot F_{NCT}\left(n-1, \frac{\sqrt{n}}{UCB}\right) = (1-\alpha) \quad \text{(Eq. 9.26)}$$

Unfortunately, the exact value of the upper confidence bound is very to calculate cumbersome (Johnson and Welch, 1940) so iterative computer methods are generally required. However, from McKay's approximation to the distribution of *COV* (McKay, 1932), Vangel (1996) proposed an approximate method to obtain the upper confidence interval on *COV* that can be written as:

$$UCB = \frac{COV}{\sqrt{\left[\left(\frac{u}{n}-1\right)\cdot COV^2 + \frac{u}{n-1}\right]}} \quad \text{(Eq. 9.27)}$$

$$UCB = \frac{COV}{\sqrt{\left[\left(\frac{u+2}{n}-1\right)\cdot COV^2 + \frac{u}{n-1}\right]}} \quad \text{(Eq. 9.28)}$$

where $u = \chi^2_{\alpha;n-1}$ denotes a chi-square value with $n-1$ degrees of freedom at the $1-\alpha$ confidence level. Equation 9.27 is called McKay's Approximation and Equation 9.28 is called Vangel's approximation.

Usually, Vangel's approximation is more accurate than McKay's approximation except when $\alpha$ and $COV$ are both large. However, neither approach is appropriate when $COV$ is large because it violates the assumption that the probability of $COV$ being negative is negligible. McKay's approximation should only be used when $COV < 0.33$ (McKay, 1932), and Vangel suggested both approximations only concern small $n$ and small $COV$. Fortunately, the small $n$ and small $COV$ condition is often met for cases of interest (when designing foundations using a small number of measurements and the estimated uncertainty of undrained shear strength is smaller than actual uncertainty of soil undrained shear strength).

For a constant regression model for normally distributed parameters, the undrained shear strength is given by:

$$\hat{s}_u = \hat{\beta}_0 \quad \text{(Eq. 9.29)}$$

where $\hat{s}_u$ is the estimated undrained shear strength, which is equal to $\frac{\sum_{i=1}^{n} s_{u_i}}{n}$, and $\hat{\beta}_0$ is the estimated value from the regression model. If the condition of small $n$ and small $COV$ is satisfied, the one-side upper confidence bound of $COV$ can be calculated from Equation 9.28 as:

$$COV = \frac{\sqrt{\frac{\sum_{i=1}^{n}(s_{u_i} - \hat{s}_u)^2}{n-1}}}{\hat{s}_u} \quad \text{(Eq. 9.30)}$$

For a linear regression model for normally distributed parameters, the undrained shear strength is given by:

$$\hat{s}_u = \hat{\beta}_0 + \hat{\beta}_1 \cdot z \quad \text{(Eq. 9.31)}$$

where $\hat{\beta}_0$ and $\hat{\beta}_1$ are the estimated intercept and slope parameters of the linear regression model, respectively, and $z$ is depth. For this form of model, the upper confidence bound of $COV$ is determined from Equation 9.18 and can be approximately calculated as:

$$UCB \cong \frac{K}{\sqrt{t(\theta K^2+1)-K^2}} \cdot \sqrt{\frac{1}{n} + \frac{(z-\bar{z})^2}{\sum_{i=1}^{n}(z_i-\bar{z})^2}} \quad \text{(Eq. 9.32)}$$

where

$$K = \sqrt{MSE}/\mu_{s_u} \quad \text{(Eq. 9.33)}$$

$$t = \chi^2_{\alpha;n-2}/(n-2) \quad \text{(Eq. 9.34)}$$

$$\theta = \frac{n-2}{n-1} \cdot \left[\frac{2}{\chi^2_{\alpha;n-2}} + 1\right] \quad \text{(Eq. 9.35)}$$

$UCB$ is the upper confidence bound of $COV$, $n$ is the number of measurements, $z_i$ is the depth of the measurements, $z$ is the depth where undrained shear strength is being

estimated, $\bar{z}$ is the average depth for the $n$ measurements, $\mu_{s_u}$ is the estimated undrained shear strength at depth $z$, and $MSE$ is the mean square error calculated as:

$$MSE = \frac{\sum_{i=1}^{n}\left(s_{u_i} - \hat{s}_{u_i}\right)^2}{n-2} \quad \text{(Eq. 9.36)}$$

## 9.8 Summary

In this chapter, a rigorous and fundamentally sound method to control the potential for producing substantially under reliable designs when using small numbers of measurements was described and evaluated. The method is conceptually similar to those described in previous chapters, but uses the one-sided upper confidence bound of the $COV$ for undrained shear strength to establish resistance factors. Use of the upper confidence bound for COV has the effect of reducing resistance factors, which in turn produces larger footing areas when small numbers of measurements are considered. Results of analyses presented in this chapter demonstrate that the approach effectively reduces the percentage of under reliable cases when designing with small numbers of measurements. Results obtained for design using the upper confidence bound values of COV will be compared to alternative methods described in previous chapters in Chapter 10.

# Chapter 10 Comparison of Reliability of Foundations Designed Using Alternative Methods

## 10.1 Introduction

Results from analyses presented in previous chapters show that the percentage of designs with probabilities of failure that dramatically exceed the target value is practically consistent when greater than seven undrained shear strength measurements are used for design. However, the percentage of cases with probabilities of failure that dramatically exceed the target value increases substantially when designing with fewer measurements. The percentage of designs with probabilities of failure that are dramatically less than the target probability of failure was found to decrease with increasing numbers of measurements. Thus, the percentage of designs that practically meet the target probability of failure increases with increasing numbers of measurements. Two methods for reducing the percentage of under reliable cases when designing with small numbers of measurements have been introduced in Chapters 8 and 9; one is referred to as the "penalty function" method and the other is referred to as the "upper confidence bound" method. In this chapter, the reliability of foundations designed using resistance factors selected from uncertainties determined by these three methods are compared for both linear and constant regression models for undrained shear strength measurements at four sites. In order to make "fair" comparisons among the different methods, the upper confidence bound of $COV$ is calculated at the 75% confidence level.

## 10.2 Comparison of Reliability of Foundations for Alternative Methods

The reliability of foundations designed using three alternative approaches has been evaluated as discussed in Chapter 7, Chapter 8 and Chapter 9. The same three categories are adopted to compare how well the different methods achieve the target probability of failure for different numbers of measurements. Designs producing probabilities of failure within 50 percent of the respective target value ($0.5 \cdot p_T \leq p_f \leq 1.5 \cdot p_T$) were considered to be "satisfactory". Designs producing probabilities of failure that were more than 50 percent greater than the target ($p_f \geq 1.5 \cdot p_T$) were deemed to be excessively "under reliable", and designs producing probabilities of failure less than 50 percent of the target ($p_f \leq 0.5 \cdot p_T$) were deemed to be excessively "over reliable". The percentage of cases falling within each range is quantified to reflect the effectiveness of designs developed using the alternative methods for different numbers of measurements.

Percentages of "satisfactory", "under reliable", and "over reliable" cases are compared for designs using resistance factors established from the calculated *COV*, and from modified *COV* values determined using the penalty function and a one- side 75% upper confidence bound of *COV*. The 75% confidence level was selected because it produces a modified *COV* that is similar to the modified *COV* determined using the penalty function method. Both the penalty function and upper confidence bound methods tend to reduce the percentage of under reliable cases by considering a coefficient of variation (*COV*) for undrained shear strength that is greater than the value calculated from measurements alone, as shown in Figure 10.1. In doing so, both methods produce smaller resistance factors than would be used considering calculated values of the *COV*, which leads to larger footing areas that have greater reliability.

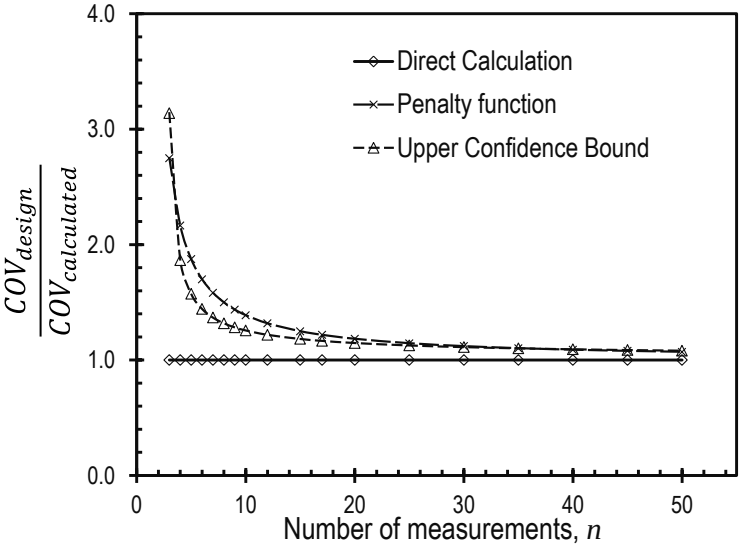


Figure 10.1 Comparison of normalized coefficients of variation used for the alternative design methods as a function of number of measurements considered.

10.2.1 Comparison for Linear Regression Models

In this section, the comparisons among alternative methods are provided based on the lognormal linear regression models for undrained shear strength that were presented in Chapter 4. To be consistent with work described in previous chapters, a foundation depth of 7 feet was used as an arbitrary "shallow" depth for all sites, a depth of 30 feet was used as an arbitrary "middle" depth for the Pemiscot site and a depth of 16 feet was used as an arbitrary "middle" depth for the St. Charles, New Florence, and Warrensburg sites.

Figures 10.2 and 10.3 show comparisons of results among the three methods at both the top and middle depths for the Pemiscot site, respectively. The percentage of satisfactory cases using the directly calculated values of *COV* is slightly greater than the percentage of satisfactory cases determined using either the penalty function or upper confidence bound methods. The percentage of under reliable cases for both the penalty function and upper confidence bound methods is generally similar, and noticeably less than observed for the "direct method", particularly when the number of measurements is small

($n < 10$). The percentage of under reliable cases has been reduced from 17% to 7% for designs at 7 feet and from 16% to 7% for designs at 30 feet when $n = 5$. The percentage of over reliable cases for the penalty function method is slightly greater than is observed for the upper confidence bound method, and both of these methods produce approximately 20% more over reliable cases than the direct method when *n* is relatively small ($n < 10$) and 5% more over reliable cases when *n* is relatively large ($n > 30$). Thus, the net result of these comparisons is that both the penalty function and upper confidence bound methods produce fewer under reliable cases, more over reliable cases, and slightly fewer satisfactory cases compared to the direct calculation method. The differences among the methods are generally greater for small numbers of measurements and decrease when considering greater numbers of measurements.

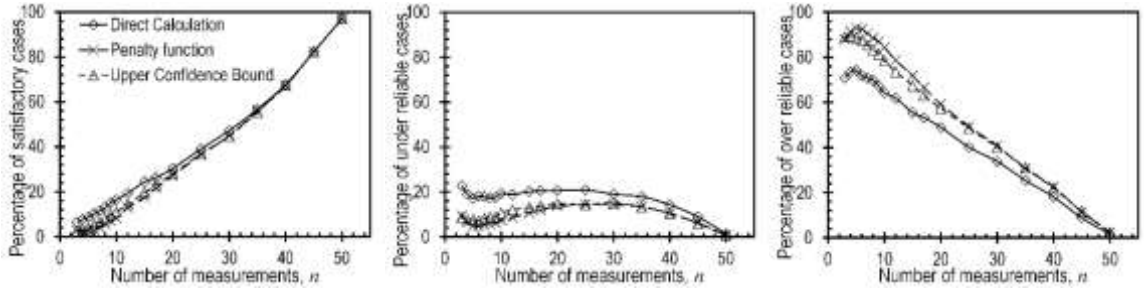


(a) (b) (c)

Figure 10.2 Comparison of percentages of (a) satisfactory, (b) under reliable, and (c) over reliable cases using alternative methods for design using linear regression models from the Pemiscot site at a depth of 7 feet.

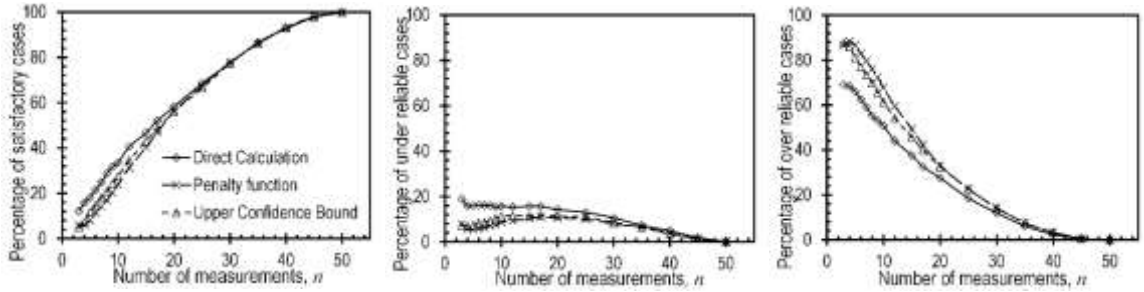


(a) (b) (c)

Figure 10.3 Comparison of percentages of (a) satisfactory, (b) under reliable, and (c) over reliable cases using alternative methods for design using linear regression models from the Pemiscot site at a depth of 30 feet.

Comparisons for measurements from the St. Charles site are shown in Figs 10.4 and 10.5. These figures lead to similar conclusions regarding the relative percentages for the alternative methods. Results for the penalty function and upper confidence bound methods are quite similar for all values of $n$. The direct calculation method tends to produce greater numbers of satisfactory and under reliable cases, and fewer over reliable cases, than either the penalty function or upper confidence bound methods, with the magnitude of the differences range from approximately 5% to 20%. The one distinction among the comparisons observed for the St. Charles site is that the differences are relatively consistent for all values of $n$, especially for the comparisons shown for the shallower foundation depth (Figure. 10.4).

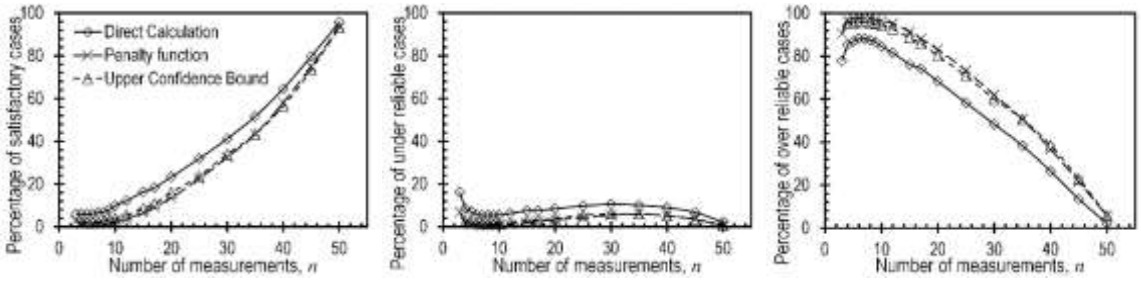


(a) (b) (c)

Figure 10.4 Comparison of percentages of (a) satisfactory, (b) under reliable, and (c) over reliable cases using alternative methods for design using linear regression models from the St. Charles site at a depth of 7 feet.

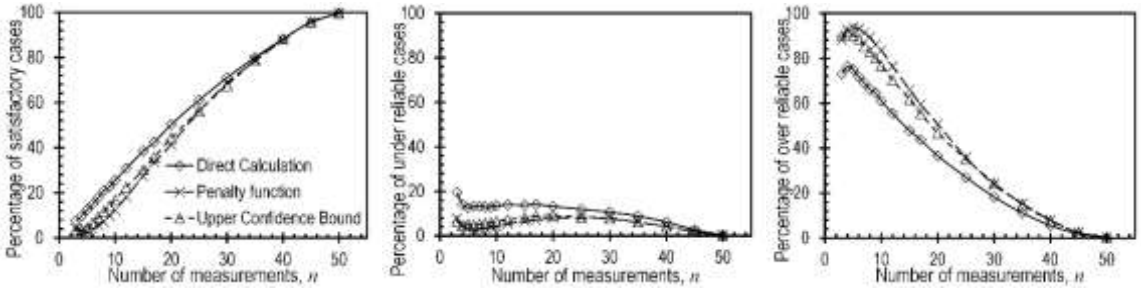


(a) (b) (c)

Figure 10.5 Comparison of percentages of (a) satisfactory, (b) under reliable, and (c) over reliable cases using alternative methods for design using linear regression models from the St. Charles site at a depth of 16 feet.

Comparisons for the New Florence site (Figs 10.6-10.7) also lead to similar observations about the comparisons among the different methods. The penalty function and upper confidence bound methods produce similar percentages of satisfactory, under reliable, and over reliable cases for all value of $n$, and these methods generally produce fewer satisfactory and under reliable cases and more over reliable cases than is observed for the direct method. The differences among the different methods again range from between 5 to 20 percent and the differences are practically consistent for all values of $n$.

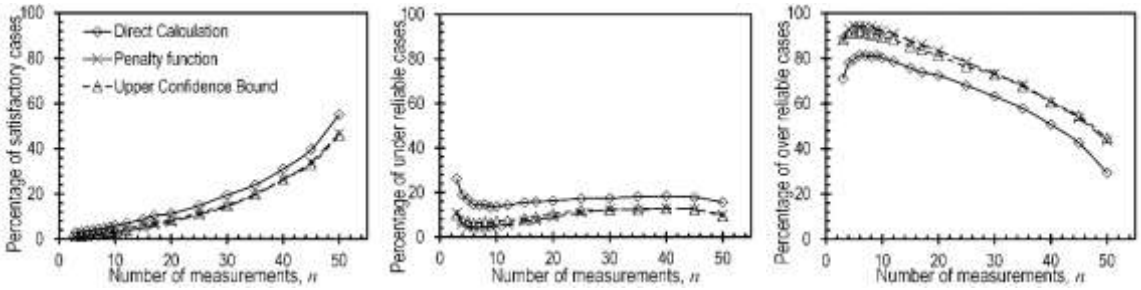


(a) (b) (c)

Figure 10.6 Comparison of percentages of (a) satisfactory, (b) under reliable, and (c) over reliable cases using alternative methods for design using linear regression models from the New Florence site at a depth of 7 feet.

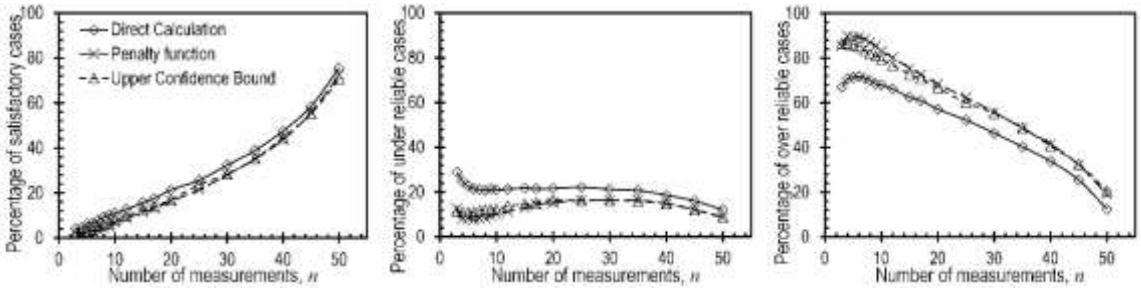


(a) (b) (c)

Figure 10.7 Comparison of percentages of (a) satisfactory, (b) under reliable, and (c) over reliable cases using alternative methods for design using linear regression models from the New Florence site at a depth of 16 feet.

Results determined from measurements at the Warrensburg site are shown in Figs 10.8 and 10.9, which again show that the penalty function and upper confidence bound methods produce similar percentages of satisfactory, under reliable, and over reliable cases

for all values of $n$. The figures also show that these methods tend to produce fewer satisfactory and under reliable cases, and more over reliable cases, than is produced using the direct calculation method. However, the magnitude of the differences between the direct calculation method and the penalty function and upper confidence bound methods is substantially greater than was observed for analyses at the other sites. The differences are particularly large when *n* approaches the total population size of measurements ($N = 34$). One possible explanation for this observation is due to the relatively limited total population size as compared to the other sites.

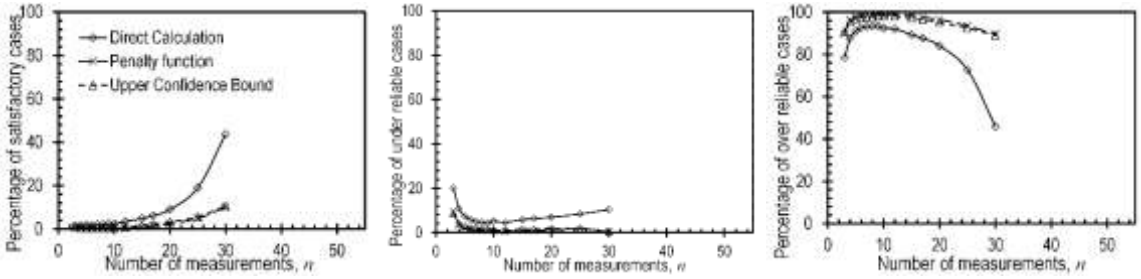


(a) (b) (c)

Figure 10.8 Comparison of percentages of (a) satisfactory, (b) under reliable, and (c) over reliable cases using alternative methods for design using linear regression models from the Warrensburg site at a depth of 7 feet.

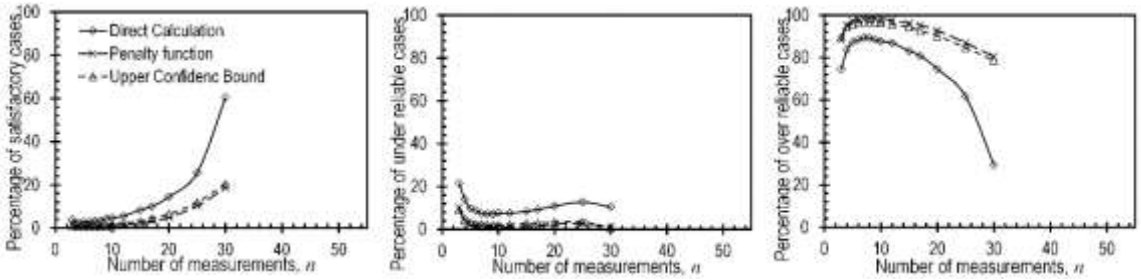


(a) (b) (c)

Figure 10.9 Comparison of percentages of (a) satisfactory, (b) under reliable, and (c) over reliable cases using alternative methods for design using linear regression models from the Warrensburg site at a depth of 16 feet.

10.2.2 Comparison for Constant Regression Models

Comparisons of results determined using the lognormal constant regression models presented for each site in Chapter 4 are shown in Figures 10.10 through 10.13. Because both the mean value of undrained shear strength and the coefficient of variation of the mean value of undrained shear strength are independent of depth for the constant regression models, the results presented are identical for all potential foundation depths.

The comparisons shown in Figures. 10.10 through 10.13 lead to observations that are quite similar to those described in the previous section based on results for the linear regression models. The direct calculation method generally produces greater percentages of satisfactory and under reliable cases, and fewer over reliable cases than either the penalty function method or the upper confidence bound method for all sites. The one slight distinction among the comparisons for the constant regression models is that differences between the penalty function and upper confidence bound methods tend to be slightly larger when the constant regression models are considered. While the differences are practically small, the penalty function method does tend to produce slightly fewer satisfactory cases, slightly fewer under reliable cases, and slightly more over reliable cases than are produced using the upper confidence bound method.

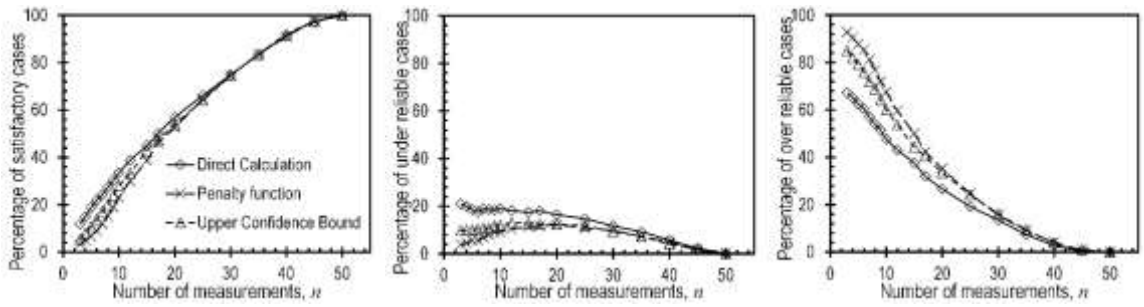


(a) (b) (c)

Figure 10.10 Comparison of percentages of (a) satisfactory, (b) under reliable, and (c) over reliable cases using alternative methods for design using constant regression models from the Pemiscot site.

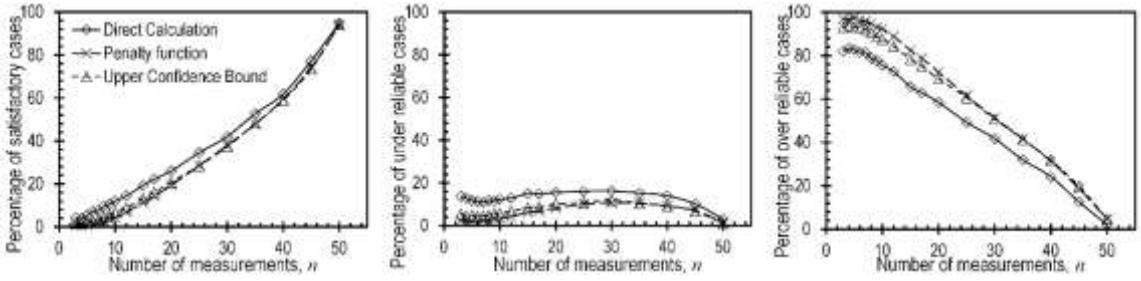


(a) (b) (c)

Figure 10.11 Comparison of percentages of (a) satisfactory, (b) under reliable, and (c) over reliable cases using alternative methods for design using constant regression models from the St. Charles site.

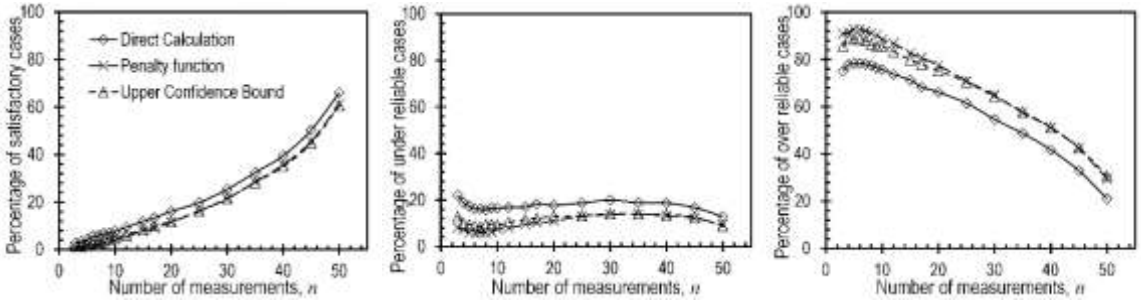


(a) (b) (c)

Figure 10.12 Comparison of percentages of (a) satisfactory, (b) under reliable, and (c) over reliable cases using alternative methods for design using constant regression models from the New Florence site.

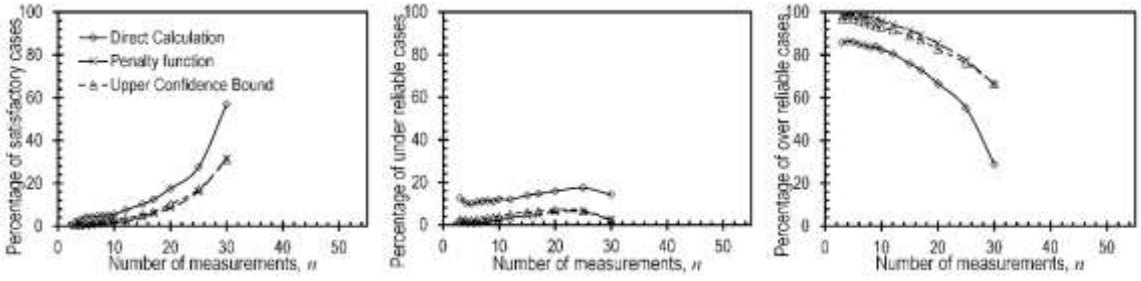


(a) (b) (c)

Figure 10.13 Comparison of percentages of (a) satisfactory, (b) under reliable, and (c) over reliable cases using alternative methods for design using constant regression models from the Warrensburg site.

## 10.3 Practical Advantages and Disadvantages of the Alternative Methods

As described in the previous section, the three alternative methods considered for design of spread footings using the LRFD method described in Chapter 5 have advantages

and disadvantages in terms of technical precision and accuracy. Each of the methods also have practical advantages and disadvantages as described in the following paragraphs.

In the "direct calculation method, resistance factors are selected based on values of $COV$ that are calculated directly from available measurements. The "direct calculation" method has the advantage of being relatively straightforward to execute while still producing a relatively consistent percentage of under reliable cases. However, the method suffers from the fact that it tends to produce a slightly greater percentage of under reliable cases than the alternative methods, especially when small numbers of measurements are used for design. The direct method does tend to produce a greater percentage of designs that practically achieve the target reliability than the other methods, however.

In the penalty function method, resistance factors are selected based on modified *COV*s of undrained shear strength, which generally produces larger spread footings compared to those produced using the direct calculation method. While the penalty function method does involve the additional step of selecting and applying the empirical uncertainty modified, the method is still relatively straightforward and easy to execute. The penalty function method produces fewer under reliable cases than the direct calculation method, especially when small numbers of measurements are considered. However, the penalty function method also produces fewer satisfactory cases and more over reliable cases than the direct calculation method. The penalty function method also produces less consistent percentages of under reliable cases, and tends to produce fewer under reliable cases for small $n$ than for larger $n$, which is somewhat counterintuitive.

When applying the "upper confidence bound" method, resistance factors are selected based on the upper confidence bound of $COV$ rather than based on the $COV$ determined

directly from available measurements. The method is more fundamentally sound than the penalty function method, and is more easily adapted to address different confidence levels. Like the penalty function method, the upper confidence bound method tends to produce greater footing areas than produced using the direct calculation method. Also like the penalty function method, the upper confidence bound method tends to produce fewer under reliable cases, fewer satisfactory cases, and more over reliable cases than the direct calculation method. The percentages of satisfactory, under reliable and over reliable cases for the upper confidence bound method are generally similar to percentages for the penalty function method when the 75% upper confidence bound is used. Perhaps the biggest drawback of the upper confidence bound method is its apparent complexity, although some generality is gained through the added complexity.

## 10.4 Summary

The reliability of foundations designed using resistance factors selected based on three alternative methods for accounting for uncertainty in the undrained shear strength are compared in this chapter. The first method, termed the "direct calculation" method uses the *COV* that is calculated directly from available measurements to determine appropriate resistance factors. The other two methods, referred to as the "penalty function" and "upper confidence bound" methods use modified *COV* values that are greater than the value calculated from available measurements in an effort to reduce the likelihood of producing designs that do not achieve the target probability of failure.

The comparisons presented in this chapter generally show that the penalty function and upper confidence bound methods generally produce similar numbers of satisfactory, under reliable, and over reliable cases when the 75% upper confidence bound is used for

the upper confidence bound method. However, the penalty function and upper confidence bound methods tend to produce fewer satisfactory cases, fewer under reliable cases, and greater numbers of over reliable cases than the direct calculation method. Differences in the percentages of satisfactory, under reliable, and over reliable cases are generally less than 20 percent, and often, but not always, diminish as the number of measurements considered increases. Both the penalty function and upper confidence bound methods tend to produce slightly larger footings that are produced using the direct calculation method.

The penalty function and the upper confidence bound method can be used to reduce the percentage of under reliable cases when the number of measurements is small. Generally, the penalty function is easier to calculate and use in practice. The upper confidence bound method is more complex; however, the upper confidence bound explicitly dictates a level of confidence that the true *COV* is smaller than the modified greater *COV* used in design.

# Chapter 11 Summary, Conclusions and Recommendations

## 11.1 Introduction

In the research described in this thesis, soil strength measurements obtained from a comprehensive site characterization project at four different sites were used to study how the number of available measurements for soil design parameters affects the reliability of designs that utilize those measurements. This chapter includes a summary of the work described in this thesis, description of the major findings drawn from the work, and a description of some limitations of the work. Recommendations for future study are also provided.

## 11.2 Summary

Sources of uncertainty in geotechnical engineering design include natural soil variability, uncertainty from boring, sampling and testing techniques, uncertainty from applying mathematical, statistical or simulation methods to interpret soil design parameters and uncertainty associated with design models. To understand the true soil properties and site conditions, a comprehensive site characterization project needs to be performed. However, there are many cases where conducting such site characterization is impossible. In such cases, the uncertainty in soil design parameters may be overestimated or underestimated, which can lead to designs being more costly or risky than desired.

A comprehensive site characterization project was conducted at four different sites using state of the art sampling and testing techniques. A great number of engineering property measurements were made for each site. The undrained shear strength

measurements from this project were selected to serve as the total population of measurements for the present study. The collective laboratory measurements from these sites suggest that it is reasonable to assume that all of the measurements are derived from a single stratum at each site.

Linear and constant regression models were used to interpret the strength measurements acquired using state of the art sampling and testing techniques at each site. Both models assume that residuals are lognormally distributed. The validity of both models for interpreting the undrained strength measurements was verified using statistical hypothesis testing and residual plots. These hypothesis tests show that the lognormal linear regression model is a reasonable model to represent measurements at each of the sites. The hypothesis tests show that the lognormal constant regression model is not a good model for measurements at some of the sites; however, constant regression models were nevertheless used due to their simplicity and wide application in geotechnical engineering design practice.

The analyses presented consider design of spread footings on cohesive soil at the Strength I Limit State under total stress conditions using load and resistance factor design (LRFD) with resistance factors calibrated to be a function of uncertainty in the undrained shear strength. Design parameters include the bearing capacity factor, load components and load factors were selected from existing research or design manuals. Resistance factors were calibrated according to the uncertainty in the mean undrained shear strength using Monte Carlo Simulations for different target probabilities of failure. Lower resistance factors are required to produce the same probability of failure for conditions where there is

greater uncertainty in the undrained shear strength. Similarly, lower resistance factors are required to achieve smaller target probabilities of failure.

Random subsets of the undrained shear strength measurements were repeatedly selected to simulate measurements that could have been obtained from different site investigations. The estimated values of the mean undrained shear strength, and the uncertainty in the mean undrained shear strength, derived from the individual subsamples are greatly affected by the number of measurements considered. The range of estimated mean values and uncertainty in the mean value from the random subsamples is extremely large when small numbers of measurements are considered, which suggests that uncertainty in design parameters may be dramatically underestimated or overestimated when small numbers of measurements are available. Ranges of estimated mean values and the uncertainty in the mean values decrease as more measurements are considered, gradually approaching the "true" soil properties when large numbers of measurements are available. The number of measurements considered has a greater effect on the uncertainty of the mean design parameters than on estimated mean values and more measurements are needed to reduce the range of the estimated uncertainty of relevant design parameters. The likelihood of over- or under-estimating these parameters depends upon the variability of a given site, but decreases substantially with increasing numbers of measurements for all sites.

The degree to which shallow foundations designed using LRFD with resistance factors that are calibrated to be a function of uncertainty in the undrained shear strength achieve the target reliability is greatly affected by uncertainty in the undrained shear strength, which in turn is greatly affected by the number of measurements. Designs

developed using randomly sampled subsets of the undrained shear strength measurements were categorized into "Satisfactory", "Under reliable" and "Over reliable" cases by comparing simulated probabilities of failure with target values. The "satisfactory" cases reflect designs having probabilities of failure within a reasonable range of target probability of failure. The "under reliable" cases reflect designs having probabilities of failure that dramatically exceed the target value. The "over reliable" cases reflect designs having probabilities of failure that are dramatically less than the target value. The analyses presented show that the percentage of satisfactory cases increases as the number of measurements increases while the percentage of over reliable cases steadily decreases with increasing numbers of measurements. The analyses also show that the designs tend to produce a consistent percentage of under reliable cases when resistance factors calibrated considering the uncertainty in soil parameters are used.

The magnitude of target probabilities of failure were found to have a negligible effect on the degree to which the target reliability is achieved since the resistance factors are calibrated to achieve the respective target probability of failure. The percentages of satisfactory cases, under reliable cases and over reliable cases were found to be affected by the total population size of measurements when the number of subsampled measurements approaches the population size; however, the total population size was observed to have little effect designing with small numbers of measurements. At more variable sites, more measurements are required to achieve similar levels of reliability than at less variable site.

Three different methods for establishing the uncertainty in the undrained shear strength were considered. The first of these methods, termed the "direct calculation" method, simply considers the coefficient of variation (*COV*) that is directly computed from

the subsampled measurements. An alternative "penalty function" method was also considered to account for the potential to dramatically underestimate uncertainty when small numbers of measurements are considered. In this method, the *COV* computed from the subsampled measurements is modified by a penalty function that is dependent on the number of measurements considered to produce a *COV* that is greater than what is calculated directly from the subsampled measurements. The third alternative, referred to as the "upper confidence bound" method, also uses a *COV* that is greater than is directly calculated from the subsampled measurements, but derives the specific *COV* used from the 75 percent upper confidence bound. Since the *COV* is greater than that directly calculated from the measurements considered, both the penalty function and upper confidence bound methods utilize more conservative (smaller) resistance factors than are used for the direct calculation method and, thus, tend to produce slightly larger foundation areas.

Comparisons presented for the three alternative methods in Chapter 10 show that all three methods tend to produce a relatively consistent percentage of under reliable designs, regardless of the number of measurements considered. The penalty function and upper confidence bound methods tend to produce fewer under reliable cases than the direct calculation method, particularly when the number of available measurements is relatively small, with the percentages varying between 3 and 20 percent.

All three methods tend to produce increasing percentages of satisfactory designs as the number of measurements considered increases, ranging from near 0 percent when very few measurements are considered and approach 100 percent when many measurements are considered. Both the penalty function and upper confidence bound methods tend to

produce slightly fewer cases where the target probability of failure is practically achieved compared to the direct calculation method.

All three methods also tend to produce decreasing percentages of over reliable designs as the number of measurements considered increases. The percentage of over reliable design is generally greater than 70 percent when very few measurements are considered, but decreases substantially and may approach zero as greater numbers of measurements are considered. The penalty function and upper confidence bound methods tend to produce somewhat greater percentages of over reliable cases than the direct calculation method.

The direct method is the easiest to apply if *COV* has been determined from available measurements, followed by penalty function. The upper confidence bound of *COV* requires more understanding and is generally more theoretical than practical in application.

## 11.3 Conclusions

The research described in this thesis quantitatively evaluated the reliability of spread footings designed using LRFD considering different numbers of undrained shear strength measurements. Significant observations and conclusions drawn from this work include:

- The potential for dramatically overestimating or underestimating the mean value, and the uncertainty in the mean value, of soil design parameters is extremely high when small numbers of measurements are available.
- The percentage of designs with probabilities of failure that fall within a reasonable range of the target probability of failure (i.e. “satisfactory” cases) is very small when small numbers of measurements are available, but increases substantially as greater numbers of measurements are considered.

- The percentage of designs with probabilities of failure that dramatically exceed the target value probability of failure (i.e. “under reliable” cases) is largely independent of the number of available measurements when design is performed using LRFD resistance factors that are calibrated as a function of uncertainty in the undrained shear strength.
- The percentage of designs where probabilities of failure are dramatically less than the target value (i.e. “over reliable” cases) is quite large when small numbers of measurements are considered but steadily decreases with increasing numbers of measurements.
- For very small numbers of measurements ($n \leq 5$), the potential for producing substantially under reliable or over reliable designs is extremely high.
- The reliability of designs is slightly affected by the depth of the footing relative to the depth of available measurements, the regression models used to interpret soil design parameters, and natural site variability. However, these effects are secondary compared to the effect of the number of available measurements.
- The magnitude of the target probability of failure and spatial averaging of undrained shear strength beneath the footing have little effect on the reliability of designs.
- Use of the penalty function and one-sided upper confidence bound methods produces more conservative resistance factors and, thus, larger foundation areas compared to the direct calculation method. The more conservative resistance factors act to compensate for the greater likelihood for underestimating the uncertainty in design parameters when the number of measurements is small.

- The penalty function method produces similar foundation reliabilities to the upper confidence bound method when the 75% upper confidence bound of the coefficient of variation is used with similar percentages of satisfactory, under reliable, and over reliable cases. Both methods effectively reduce the percentage of under reliable cases while also increasing the percentage of over reliable cases compared to the direct calculation method. Both methods also produce slightly fewer satisfactory cases than the direct calculation method.

## 11.4 Recommendation for Research

The research in this thesis mainly focuses on the reliability of spread footings using load and resistance factor design considering different numbers of measurements. The effect of different numbers of measurements on reliability of foundation is evaluated and a method is proposed for conditions where foundations have to design based on a small number of measurements. Based on work of the research, future studies can be carried out in areas as following.

### 11.4.1 Consider more complex soil conditions

A single stratum of soil layer is assumed for analysis. More complex soil conditions can be considered to evaluate the effect of the number of measurements on estimated soil design parameters. Moreover, how the reliability of foundations designed in complex soil conditions will be affected by the number of measurements.

### 11.4.2 Use other failure modes

Strength I limit state is considered for spread footing designs. In future studies, service limit state should also be considered to evaluate the reliability of foundations using load and resistance factor design with different numbers of measurements. Meanwhile, the

load components used in design model are dead and live loads. Spread footings can be designed subjected to vibratory loading.

11.4.3 Apply to other foundation types

Spread footings are designed using soil strength measurements in the research of this thesis. More foundation types can be considered, such as pile, drilled shaft, etc. to study the effect of the number of measurements on reliability of foundation designs.

11.4.4 Combine multiple sources of measurements

The strength measurements used in analyses are acquired by undrained triaxial compression tests using soil specimens obtained from state of the art sampling techniques. More often, field tests are performed at the same time with boring and sampling in site characterization projects. Thus, combining multiple sources of measurements to interpret soil design parameters is an efficient way to reduce uncertainty of soil parameters. However, measurements from different testing methods cannot be lumped together arbitrarily. Thus, future work involves evaluating uncertainty of soil parameter for different testing methods, effectively and accurately estimating the true soil properties using multiple sources of measurements, evaluating reliability of designs with different numbers of measurements obtained from different testing methods.

11.4.5 Use of other regression models

A lognormal linear and a constant regression model are applied to estimate soil. Different models have been used to analyze soil design parameters (e.g., normal linear regression model, normal constant regression model, weighted least square regression model, nonlinear regression model, etc.). For different design parameters, the selected

statistical model should be tested with hypothesis testing to check whether the model is good enough to reflect the data.

### 11.4.6 Conduct risk analysis

Reliability of foundations is evaluated with different numbers of measurements. Future research can be carried out in risk analysis of foundations with different numbers of measurements. The cost of site characterization, design, construction and the cost of failure can be assigned and then the cost of foundations can be calculated when using different numbers of measurements.

## 11.5 Recommendations for Practice

Based on results from research of this thesis, recommendations for practice are provided in site characterization, data interpretation and designs.

### 11.5.1 Use of state of the art boring, sampling and testing techniques

Site characterization using state of the art boring, sampling and testing techniques should be apply to obtain high quality soil specimens. Thus, the uncertainty introduce by boring, sampling and testing procedures may be reduced and controlled at a consistent level.

### 11.5.2 Obtain more measurements

Always obtain more measurements or more site information before perform analysis and designs. Measurements from multiple types of testing should be combined using correlations.

### 11.5.3 Use an appropriate statistical model to interpret soil design parameters

A representative regression model should be selected for analysis of measurements. If the model does not reflect the data, the uncertainty estimated using the model will be great than expected, or may be seriously in error.

11.5.4 Resistance factors calibrated to be dependent on the uncertainty of soil design parameters should be adopted

Resistance factors should be calibrated by uncertainty in soil design parameters for specific design models with selected design parameters. The calibrated resistance factors will provide a consistent percentage of designs where the probabilities of failure excessively exceed the target value.

11.5.4 Avoid using small numbers of measurements

Understand that the uncertainty in estimated soil parameters is extremely high when use a small number of measurements is used for interpretation and design. A minimum of six ($n \geq 6$) undrained shear strength measurements should be use for design of spread footings for most sites. For notably variable sites, even greater numbers of measurements should be used.

11.5.5 Use penalty function or upper confidence bound method to design conservatively for small numbers of measurements or insufficient site information

For cases where designs have to be performed based on a small number of measurements, the penalty function or upper confidence bound of coefficient of variation method can be used with engineering judgment to serve the purpose of ensuring design safety. However, it is important to recognize that such design comes at the cost of producing larger foundations than may be truly necessary.

11.6 Limitations in Research

Design model adopted in the research of this thesis is a spread footing designed on cohesive soil at the Strength I limit state under total stress conditions. Resistance factors

calibrated in this research (Figure 5.1) can only apply for this specific design model with same bearing capacity factor, load components and load factors.

Uncertainty in estimated soil design parameters is used to reflect the accuracy of interpreted soil design parameters. The research of this thesis focuses on uncertainty brought into design when applying statistical models using limited numbers of measurements. Uncertainty from boring, sampling and testing procedures is assumed to be controlled at a consistent level. Uncertainty from design model is taken into consideration by incorporating design model uncertainty into bearing capacity factors.

The number of measurements acquired at each site is regarded as the total number of measurements. The number of measurements is assumed to be large enough to accurately reflect true soil properties, which might not be valid for a variable site. Thus, the Warrensburg site is more affected by the total population size of measurements.

A single stratum of soil layer is used to characterize soil design parameters by assuming soil specimens are acquired from same layer and have same engineering properties, which may not be a common case in practice.

The upper confidence bound of coefficient of variation method is developed for cases where foundations have to be designed conservatively to compensate for uncertainties when use small numbers of measurements. The calculations of upper confidence bound of coefficient of variation depend on the type of regression model. For a complicated regression model, it might be difficult to derive equations to calculate the upper confidence bound of coefficient of variation.

# Reference


AASHTO (2010). *AASHTO LRFD Bridge Design Specifications*, American Association of State Highway and Transportation Officials, Washington, DC.

Allen, T.M. (2005). *Development of Geotechnical Resistance Factors and Downdrag Load Factors for LRFD Foundation Strength Limit State Design*, National Highway Institute, Federal Highway Administration, FHWA-NHI-05-052.

Allen, T.M., A.S. Nowak, and R.J. Bathurst (2005). *Calibration to Determine Load and Resistance Factors for Geotechnical and Structural Design*. Transportation Research E-Circular E-C079, 83 pp.

Ang, A.H. and W.H. Tang (1975). *Probability Concepts in Engineering Planning and Design, Vol. 1: Basic Principles*. J. Wiley, New York, 409pp.

Ang, A.H. and W.H. Tang (1984). *Probability Concepts in Engineering Planning and Design, Vol. 2: Decision, Risk and Reliability*. J. Wiley, New York, 562 pp.

Ang, A.H. and W.H. Tang (2007). *Probability Concepts in Engineering: Emphasis on Applications to Civil and Environmental Engineering*. J. Wiley, New York, 405 pp.

ASTM D2850-03a (2007). "Standard Test Method for Unconsolidated-Undrained Triaxial Compression Test on Cohesive soils," *ASTM International*, West Conshohocken, PA, DOI: 10.1520/D2850-03AR07, www.astm.org.

ASTM D4186 (2012). "Standard Test Method for One-Dimensional Consolidation Properties of Saturated Cohesive Soils Using Controlled-Strain Loading," *ASTM International*, West Conshohocken, PA, DOI: 10.1520/D4186_D4186M-12E01, www.astm.org.

ASTM D4767-11 (2011). "Standard Test Method for Consolidated Undrained Triaxial Compression Test for Cohesive Soils," *ASTM International*, West Conshohocken, PA, DOI: 10.1520/D4767-11, www.astm.org.

ASTM D6528-07 (2007). "Standard Test Method for Consolidated Undrained Direct Simple Shear Testing of Cohesive Soils," *ASTM International*, West Conshohocken, PA, DOI: 10.1520/D6528-07, www.astm.org.

Baecher, G.B. (1972). *Site Exploration: A Probabilistic Approach*, Massachusetts Institute of Technology, Thesis work in completion of PhD, 515 pp.

Baecher, G.B. (1982). "Statistical methods in site characterization," *Proceedings of the Engineering Foundation Conference on Updating Subsurface Exploration and Testing for Engineering Purposes*, Santa Barbara, pp. 463-492.

Baecher, G.B. (1983). "Simplified geotechnical data analysis," In *Reliability Theory and Its Application in Structural and Soil Mechanics*, Springer, pp. 257-277.

Baecher, G.B. (1984). "Just a few more tests and we'll be sure," Paper read at *Probabilistic Characterization of Soil Properties: Bridge between Theory and Practice*, Atlanta, GA.

Baecher, G.B. (1987). *Error Analysis for Geotechnical Engineering*, Report to US Army Corps of Engineers, GL-87-3, 126 pp.

Baecher, G.B., and J.T. Christian (2000). "Natural Variation, Limited Knowledge, and the Nature of Uncertainty in Risk Analysis," *Paper read at Risk Based Decision-Making in Water Resources IX*, Santa Barbara, pp.1-16.

Baecher, G.B., and J.T. Christian (2003). *Reliability and Statistics in Geotechnical Engineering*, J. Wiley, New York, 605 pp.

Baecher, G.B., J.T. Christian, D. Fratta, A.J. Puppata, and B. Munhunthan (2010). "Risk modeling issues and appropriate technology," *Proceedings of GeoFlorida 2010: Advances in Analysis, Modeling and Design*, West Palm Beach, FL, pp. 1944-1951.

Baker, Jr C.N. (2010). "Uncertain Geotechnical Truth and Cost Effective High-Rise Foundation Design," *Proceedings of GeoFlorida 2010: Art of Foundation Engineering Practice*, West Palm Beach, FL, pp. 1-43.

Bea, R. (2006). "Reliability and Human Factors in Geotechnical Engineering," *Journal of Geotechnical and Geoenvironmental Engineering*, ASCE, Vol. 132, No. 5, pp. 631-643.

Becker, D.E. (1997). "Eighteen Canadian Geotechnical Colloquium: Limit States Design for Foundations. Part I: An Overview of the Foundation Design Process," *Canadian Geotechnical Journal*, Vol. 33, No. 3, pp. 956-983.

Casagrande, A. (1965). "Role of the 'Calculated Risk' in Earthwork and Foundation Engineering," *Journal of the Soil Mechanics and Foundations Division*, Vol. 91, No. 4, pp. 1-40.

CEN (2004). *Eurocode 7: Geotechnical Design— Part I: General Rules*. EN 1997-1: 2004, European Committee for Standardization, 168 pp.

Ching, J., K.K. Phoon, and Y.C. Chen (2010). "Reducing Shear Strength Uncertainties in Clays by Multivariate Correlations," *Canadian Geotechnical Journal*, Vol. 47, No. 1, pp. 16-33.

Ching, J., K.K. Phoon, J. Chen, and J.H. Park (2012). "Robustness of Constant Load and Resistance Factor Designs for Drilled Shafts in Multiple Strata," *Journal of Geotechnical and Geoenvironmental Engineering*, Vol. 139, No. 7, pp. 1104-1114.

Christian, J.T., C.C. Ladd and G.B. Baecher (1994). "Reliability Applied to Slope Stability Analysis," *Journal of Geotechnical Engineering*, Vol. 120, No. 12, pp. 2180-2207.

Christian, J.T. (2000). "Statistical Implications of Limited Field Data," *Proceedings of Performance Confirmation of Constructed Geotechnical Facilities*, ASCE, pp. 298-306.

Christian, J.T. (2004). "Geotechnical Engineering Reliability: How Well Do We Know What We Are Doing?" *Journal of Geotechnical and Geoenvironmental Engineering*, ASCE, Vol. 130, No. 10, pp. 985-1003.

Christian, J.T., and G.B. Baecher (2006). "The Meaning(s) of Statistical Inference in Geotechnical Practice." *GeoCongress 2006: Geostatistics: Applications and Visualizations*, pp. 1-6.

Christian, J.T., and A. Urzua (2009). "Reliability Related to Factor of Safety and Uncertainty," *Proceedings of International Foundation Congress and Equipment Expo: Contemporary Topics in In Situ Testing, Analysis, and Reliability of Foundations*, pp. 372-378.

Christian, J.T. and G.B. Baecher (2011). "Unresolved Problems in Geotechnical Risk and Reliability," *Geo-Risk: Risk Assessment and Management*, GSP 224, ASCE, pp. 50-63.

DeGroot, D.J., S.E. Poirier, and M.M. Landon (2005). "Sample Disturbance — Soft Clays," *Studia Geotechnica et Mechanica*, Vol. XXVII, No. 3-4, pp. 107-120.

Ding, D., W.J. Likos, and J.E. Loehr (2014). "Variability and Uncertainty in Consolidation and Settlement Parameters from Different Sampling and Testing Methods," *From Soil Behavior Fundamentals to Innovations in Geotechnical Engineering*, Proceedings of a Special Symposium Honoring Roy. E. Olson, ASCE, GSP 233, pp 338-351.

Duncan, J.M. (2000). "Factors of Safety and Reliability in Geotechnical Engineering," *Journal of Geotechnical and Geoenvironmental Engineering*, Vol. 126, No. 4, pp. 307-316.

Einstein, H.H., and G.B. Baecher (1983). "Probabilistic and Statistical Methods in Engineering Geology," *Rock Mechanics and Rock Engineering*, Vol. 16, No. 1, pp. 39-72.

Fenton, G.A. and E.H. Vanmarcke (1990). "Simulation of Random Field via Local Average Subdivision," *Journal of Engineering Mechanics*, Vol. 116, No. 8, pp. 1733-1749.

Fenton, G.A. (1999a). "Estimation for Stochastic Soil Models," *Journal of Geotechnical and Geoenvironmental Engineering*, ASCE, Vol. 125, No. 6, pp. 470-485.

Fenton, G.A. (1999b). "Random Field Modeling of CPT Data," *Journal of Geotechnical and Geoenvironmental Engineering*, ASCE, Vol. 125, No. 6, pp. 486-498.

Fenton, G.A., and E.H. Vanmarcke (2003). "Random Field Characterization of NGES Data," *Proceedings of the Workshop on Probabilistic Site Characterization at NGES*, pp. 61-78.

Fenton, G.A., and D.V. Griffiths (2003). "Bearing Capacity Prediction of Spatially Random $c - \phi$ soils," *Canadian Geotechnical Journal*, Vol. 40, pp.54-65.

Fenton, G.A., and D.V. Griffiths (2005). "Three-Dimensional Probabilistic Foundation Settlement," *Journal of Geotechnical and Geoenvironmental Engineering*, ASCE, Vol. 131, No. 2, pp. 232-239.

Fenton, G.A., D.V. Griffiths, and M.B. Williams (2005). "Reliability of Traditional Retaining Wall Design," *Geotechnique*, Vol. 55, No. 1, pp. 55-62.

Fenton, G.A., and D.V. Griffiths (2007). "Reliability-Based Deep Foundation Design," *Probabilistic Applications in Geotechnical Engineering*, ASCE, Vol. 170, pp. 1-12.

Fenton, G.A., D.V. Griffiths, and X. Zhang (2008). "Load and Resistance Factor Design of Shallow Foundations against Bearing Failure," *Canadian Geotechnical Journal*, Vol. 45, No. 11, pp. 1556-1571.

Fenton, G.A., X. Zhang, and D.V. Griffiths (2008). "Load and Resistance Factor Design of Spread Footings," *GeoCongress: Geosustainability and Geohazard Mitigation*, ASCE, pp. 106-113.

Fenton, G.A., and M. Naghibi (2011). "Geotechnical Resistance Factors for Ultimate Limit State Design of Deep Foundations in Frictional Soils," *Canadian Geotechnical Journal*, Vol. 48, No. 11, pp. 1742-1756.

Fisher, R.A. (1929). "The Statistical Method in Psychical Research," *Paper read at Proceedings of the Society for Psychical Research*.

Foye, K.C., R. Salgado, and B. Scott (2006a). "Assessment of Variables Uncertainties for Reliability-Based Design of Foundations," *Journal of Geotechnical and Geoenvironmental Engineering*, Vol. 132, No. 9, pp. 1197-1207.

Foye, K.C., R. Salgado, and B. Scott (2006b). "Resistance Factors for Use in Shallow Foundation LRFD," *Journal of Geotechnical and Geoenvironmental Engineering*, Vol. 132, No. 9, pp. 1208-1218.

Gilbert, R., S. Gambino, and R. Dupin (1999). "Reliability-Based Approach for Foundation Design without Site-Specific Soil Borings," *Paper read at Offshore Technology Conference*, Houston, TX.

Gilbert, R., M.C. McBrayer, and W.H. Tang (2000). "Statistical Considerations in Calibrating Performance Models with Field Data," *Proceedings of Specialty Conference on Performance Confirmation of Constructed Geotechnical Facilities: Statistical Analyses*, Amherst, MA, pp. 307-321.

Goh, A.T.C., and F.H. Kulhawy (2003). "Neural Network Approach to Model the Limit State Surface for Reliability Analysis," *Canadian Geotechnical Journal*, Vol. 40, No. 6, pp. 1235-1244.

Goldsworthy, J.S., M.B. Jaksa, G.A. Fenton, W. Kaggwa, D.V. Griffiths, H.G. Poulos, and Y.L. Kuo (2004). "Influence of Site Investigation on the Design of Pad Footings," *proceedings of the 9th Australia New Zealand conference on Geomechanics*, Auckland, NZ, pp. 282-288.

Goldsworthy, J.S., M.B. Jaksa, W. Kaggwa, G.A. Fenton, D.V. Griffiths, and H.G. Poulos (2004). "Cost of Foundation Failures due to Limited Site Investigation," *The International Conference on Structural and Foundation Failures*, pp. 2-4.

Goldsworthy, J.S., M.B. Jaksa, W. Kaggwa, G.A. Fenton, D.V. Griffiths, and H.G. Poulos (2005). "Reliability of Site Investigations using Different Reduction Techniques for Foundation Design," *In 9th International Conference on Structural Safety and Reliability*, pp. 901-908.

Goldsworthy, J.S. (2006). *Quantifying the Risk of Geotechnical Site Investigation*, Department of Civil and Environmental Engineering, University of Adelaide, Australia, Thesis in completion of work for PhD, 475 pp.

Goldsworthy, J.S., M.B. Jaksa, G.A. Fenton, D.V. Griffiths, W.S. Kaggwa, and H.G. Poulos (2007). "Measuring the Risk of Geotechnical Site Investigation," *Proceedings of In Probabilistic Applications in Geotechnical Engineering*, ASCE, pp. 1-12.

Goldsworthy, J.S., M.B. Jaksa, G.A. Fenton, W.S. Kaggwa, D.V. Griffiths, and H.G. Poulos (2007). "Effect of Sample Location on the Reliability Based Design of Pad Foundations," *GeoRisk: Assessment and Management of Risk for Engineered Systems and Geohazards*, ASCE, Vol. 1, No. 3, pp. 155-166.

Griffiths, D.V., and G.A. Fenton (2000). "Influence of Soil Strength Spatial Variability on the Stability of an Undrained Clay Slope by Finite Elements," *GeoDenver: Slope Stability*, ASCE, pp. 184-193.

Griffiths, D.V., and G.A. Fenton (2001). "Bearing Capacity of Spatially Random Soil: The Undrained Clay Prandtl Problem Revisited," *Geotechnique*, Vol. 51, No. 4, pp. 351-359.

Griffiths, D.V., G.A. Fenton, and C.B. Lemons (2002). "Probabilistic Analysis of Underground Pillar Stability," *International Journal for Numerical and Analytical Methods in Geomechanics*, Vol. 26, No. 8, pp. 775-791.

Griffiths, D.V., G.A. Fenton, and N. Manoharan (2002). "Bearing Capacity of Rough Rigid Strip Footing on Cohesive Soil: Probabilistic Study," *Journal of Geotechnical and Geoenvironmental Engineering*, Vol. 128, No. 9, pp. 743-755.

Griffiths, D.V., G.A. Fenton, and H.R. Ziemann (2006). "Seeking Out Failure: The Random Finite Element Method RFEM in Probabilistic Geotechnical Analysis," *GeoCongress: Geotechnical Engineering in the Information Technology Age, Proceedings of Mini-Symposium on Numerical Modeling and Analysis*, pp. 1-6.

Griffiths, D.V., G.A. Fenton, and N. Manoharan (2006). "Undrained Bearing Capacity of Two-Strip Footings on Spatially Random Soil," *International Journal of Geomechanics*, Vol. 6, No. 6, pp. 421-427.

Hacking, I. (1975). *The Emergence of Probability*, Cambridge University Press, 246 pp.

Hight, D.W. (2003). "Sampling Effects in Soft Clay: An Update on Ladd and Lambe (1963)," *Soil Behavior and Soft Ground Construction*, ASCE GSP 119, MTI, pp. 86-122.

Huaco, D.R., J.J. Bowders, and J.E. Loehr (2012). "Method to Develop Target Levels of Reliability for Design Using LRFD," *Compendium of Papers for Transportation Research Board 91st Annual Meeting*, Transportation Research Board, Washington, D.C. (CD-ROM).

Jaksa, M.B., P. Brooker, and W.S. Kagwa (1997). "Inaccuracies Associated with Estimating Random Measurement Errors," *Journal of Geotechnical and Geoenvironmental Engineering*, Vol. 123, No. 5, pp. 393-401.

Jaksa, M.B., W.S. Kaggwa, G.A. Fenton, and H.G. Poulos (2003). "A Framework for Quantifying the Reliability of Geotechnical Investigation," *In the 9th Conference on the Application of Statistics and Probability in Civil Engineering*, pp. 1285-1291.

Jakasa, M.B., J.S. Goldsworthy, G.A. Fenton, W.S. Kaggwa, D.V. Griffiths, Y.L. Kuo, and H.G. Poulos (2005). "Towards Reliable and Effective Site Investigation," *Geotechnique*, Vol. 55, No. 2, pp. 109-121.

Johnson, N.L., and B.L. Welch (1940). "Applications of the Non-Central *t* Distribution," *Biometrika*, pp. 362-389.

Johnson, N.L., S. Kotz, and N. Balakrishnan (1970). *Distribution is Statistics: Continuous Univariate Distributions*, Vol. 2, Houghton Mifflin, New York.

Kulhway, F.H. (1993). "On the Evaluation of Static Soil Properties," *Proceedings of Stability and Performance of Slopes and Embankments II*, pp. 95-115.

Kulicki, J.M., Z. Prucz, C.M. Clancy, D.R. Mertz, and A.S. Nowak (2007). "Updating the Calibration Report for AASHTO LRFD Code," *Final Report for National Cooperative Highway Research Program (NCHRP)*, pp. 20-27.

Lacasse, S., and F. Nadim (1994). "Reliability Issues and Future Challenges in Geotechnical Engineering for Offshore Structures," *Proceedings of 7th International Conference on Behavior of Offshore Structures*, Massachusetts Institute of Technology, Cambridge, Mass.

Lacasse, S., and F. Nadim (1996). "Uncertainties in Characterizing Soil Properties," *Proceedings of ASCE GED Special Conference on Uncertainty in the Geologic Environment: From Theory to Practice*, Madison, Wisconsin, pp. 49-75.

Lacasse, S., and F. Nadim (1996). "Model Uncertainty in Pile Axial Capacity Calculations," *Proceedings of Offshore Technology Conference*, Houston, TX, pp. 369-380.

Lacasse, S., and F. Nadim (1998). "Risk and Reliability in Geotechnical Engineering," *Proceedings of 4th International Conference on Case Histories in Geotechnical Engineering*, St. Louis, Missouri, pp. 1172-1192.

Lacasse, S., F. Nadim, K. Hoeg, and O. Gregersen (2004). "Risk Assessment in Geotechnical Engineering: the Importance of Engineering Judgment," *Proceedings of Advances in Geotechnical Engineering: Skempton Conference*, Thomas Telford, London, pp. 856-867.

Lacasse, S., F. Nadim, and M. Uzielli (2007). "Hazard and Risk Assessment of Landslides," *Proceedings of Computer Application in Geotechnical Engineering: Geotechnical Hazards Analysis and Mitigation*, pp. 1-10.

Ladd, C.C., and D.J. DeGroot (2003). "Recommended Practice for Soft Ground Site Characterization: The Authur Casagrande Lecture," *Proceedings of the 12th Panamerican Conference on Soil Mechanics and Geotechnical Engineering*, ASCE, Vol. 1, pp. 3-57.

Ladd, C.C., and T.W. Lambe (1963). "The Strength of Undisturbed Clay Determined from Undrained Tests," *Laboratory Shear Testing of Soils, ASTM STP 361*, pp.342-371.

Lehmann, E.L. (1986). *Testing Statistical Hypothesis (2nd Edition)*, John Wiley, New York, 600 pp.

Littlejohn, G.S., K. Cole, and T.W. Mellors (1994). "Without Site Investigation Ground is Hazard," *Proceedings of ICE- Civil Engineering*, Vol. 102, No. 2, pp. 72-78.

Loehr, J. E., J.J. Bowders, L. Ge, W.J. Likos, R. Luna, N. Maerz, and R.W. Stephenson (2011a). *Engineering Policy Guidelines for Estimation of Geotechnical Parameter Values and Coefficients of Variation*, unpublished report to Missouri Department of Transportation, 13 pp.

Loehr, J. E., J.J. Bowders, L. Ge, W.J. Likos, R. Luna, N. Maerz, and R.W. Stephenson (2011b). *Engineering Policy Guidelines for Design of Spread Footings*, Missouri Department of Transportation, Report cmr12005, 36 pp.

Loehr, J. E., J.J. Bowders, L. Ge, W.J. Likos, R. Luna, N. Maerz, and R.W. Stephenson (2011c). *Engineering Policy Guidelines for Design of Drilled Shafts*, Missouri Department of Transportation, Report cmr12003, 69 pp.

McKay, A.T. (1932). "Distribution of the Coefficient of Variation and the Extended "t" Distribution," *Journal of the Royal Statistical Society*, pp. 695-698.

Meyerhof, G.G. (1976). "Concepts of Safety in Foundation Engineering Ashore and Offshore," *Proceedings of the 1st International Conference on the Behavior of Offshore Structures, Trondheim*, Norway, Vol. 1, 1976, pp. 501-515.

Mitchell, J.K. (2009). "Geotechnical Surprises— Or Are They? 1: The 2004 H. Bolton Seed Lecture." *Journal of Geotechnical and Geoenvironmental Engineering*, Vol. 135, No. 8, pp. 998-1010.

MoDOT (2011). *MoDOT Engineering Policy Guide*, Missouri Department of Transportation, http://epg.modot.org, accessed July 25, 2014.

Nadim, F., S. Lacasse and T.R. Guttormsen (1994). "Probabilistic Foundation Stability Analysis: Mobilized Friction Angle vs. Available Shear Strength Approach,"

*Proceedings of Structural Safety and Reliability*, Balkema, Rotterdam, NL, pp. 2001-2008.

Naghibi, M., and G.A. Fenton (2011). "Geotechnical Resistance Factors for Ultimate Limit State Design of Deep Foundations in Cohesive Soils," *Canadian Geotechnical Journal*, Vol. 48, No. 11, pp. 1729-1741.

Najjar, S.S., and R.B. Gilbert (2009). "Importance of Lower-Bound Capacities in the Design of Deep Foundations," *Journal of Geotechnical and Geoenvironmental Engineering*, Vol. 135, No. 7, pp. 890-900.

Oehlert, G. W. (1992). "A Note on the Delta Method," The American Statistician, Vol. 46, No. 1, p. 27-29.

Orchant, C.J., F.H. Kulhawy, and C.H. Trautmann (1988). *Reliability-Based Foundation Design for Transmission Line Structures: Critical Evaluation of In-Situ Test Method*, Electric Power Research Institute, Palo Alto, Calif., Report EL-5507(2).

Peck, R.B. (1969). "Advantages and Limitations of the Observational Method in Applied Soil Mechanics," *Geotechnique*, Vol. 19, No. 2, pp. 171-187.

Peck, R.B. (1977). "Pitfalls of Overconservatism in Geotechnical Engineering," *Civil Engineering*, ASCE, Vol. 47, No. 2, pp. 62-66.

Phoon, K.K., F.H. Kulhawy, and M.D. Grigoriu (1995). *Reliability-Based Design of Foundations for Transmission Line Structures*, Electric Power Research Institute, EPRI TR-105000, 384 pp.

Phoon, K.K., and F.H. Kulhawy (1996). "On Quantifying Inherent Soil Variability," *Uncertainty in the Geologic Environment: from Theory to Practice, Proceedings of Uncertainty*, Vol. 58, pp. 326-340.

Phoon, K.K., and F.H. Kulhawy (1999a). "Evaluation of Geotechnical Property Variability," *Canadian Geotechnical Journal*, Vol. 36, No. 4, pp. 625-639.

Phoon, K.K., and F.H. Kulhawy (1999b). "Characterization of Geotechnical Variability," *Canadian Geotechnical Journal*, Vol. 36, No. 4, pp. 612-624.

Phoon, K.K., S.T. Quek, and P. An (2003). "Identification of Statistically Homogenous Soil Layers using Modified Bartlett Statistics," *Journal of Geotechnical and Geoenvironmental Engineering*, Vol. 129, No. 7, pp. 649-659.

Phoon, K.K., F.H. Kulhawy, and M.D, Grigoriu (2003a). "Development of a Reliability-Based Design Framework for Transmission Line Structure Foundations," *Journal of Geotechnical and Geoenvironmental Engineering*, Vol. 129, No. 9, pp.798-806.

Phoon, K.K., F.H.Kulhawy, and M.D. Grigoriu (2003b). "Multiple Resistance Factor Design for Shallow Transmission Line Structure Foundations," *Journal of Geotechnical and Geoenvironmental Engineering*, Vol. 129, No. 9, pp. 807-819.

Phoon, K.K. (2006). "Modeling and Simulation of Stochastic Data," *GeoCongress: Geotechnical Engineering in the Information Technology Age*, pp. 1-17.

Rethati (1988). *Probabilistic Solutions in Geotechnics*, Elsevier, New York, 451 pp.

Santagata, M.C., and J.T. Germaine (2002). "Sampling Disturbance Effects in Normally Consolidated Clays," *Journal of Geotechnical and Geoenvironmental Engineering*, Vol. 128, No. 12, pp. 997-1006.

Schmertmann, J.H. (1978). *Guidelines for Cone Penetration Test: Performance and Design*, Report No: FHWA- TS-78-209, US Dept of Transportation, Federal Highway Administration, Washington, USA, 145 pp.

Shirato, M., M. Suzuki, K. Matsui, and J. Fukui (2003). "Modification Factor for Pile Resistance Considering Both Number and Variability," *Proceedings of the International Workshop on Limit State Design in Geotechnical Engineering Practice*, Massachusetts Institute of Technology, pp. 29-30.

Skempton, A.W. (1951). "The Bearing Capacity of Clay," *Proceedings of Building Research Congress*, Vol. 1, pp. 180-189.

Skempton, A. W. (1954). "The Pore-Pressure Coefficients A and B," *Geotechnique*, Vol. 4, No. 4, pp. 143-147.

Tamhane, A.C., and D.D. Dunlop (2000). *Statistics and Data Analysis: from elementary to intermediate*, Prentice Hall, 722 pp.

Tang, W.H. (1984). "Principles of Probabilistic Characterization of Soil Properties," *Probabilistic characterization of soil properties: bridge between theory and practice*, pp. 74-89.

Temple, M.W.B., and G. Stukhart (1987). "Cost Effectiveness of Geotechnical Investigation," *Journal of Management in Engineering*, Vol. 3, No. 1, pp. 8-19.

Terzaghi, K., L. Bjerrum, A. Casagrande, R.B. Peck and A.W. Skempton (1960). *From Theory to Practice in Soil Mechanics; Selection from the Writings of Karl Terzaghi*, Wiley, 425 pp.

Terzaghi, K., R.B. Peck, and G. Mesri (1996). *Soil Mechanics in Engineering Practice*, Wiley, 529 pp.

Tversky, A., and D. Kahneman (1971). "Belief in the Law of Small Numbers," *Psychological Bulletin*, Vol. 76, No. 2, pp. 105-110.

Vangel, M.G. (1996). "Confidence Intervals for a Normal Coefficient of Variation," *The American Statistician*, Vol. 50, No. 1, pp. 21-26.

Vanmarcke, E. (2010). *Random Fields: Analysis and Synthesis*, World Scientific, 347 pp.

Verrill, S.P. (2003). *Confidence Bounds for Normal and Lognormal Distribution Coefficients of Variation*, Research paper FPL-RP-609, Madison, WI, United States Department of Agriculture, Forest Service, 13 pp.

Verrill, S.P., and R.A. Johnson (2007). "Confidence Bounds and Hypothesis Tests for Normal Distribution Coefficients of Variation," *Communications in Statistics — Theory and Methods*, Vol. 36, No. 12, pp. 2187-2206.

Vesic, A.S. (1974). "Analysis of Ultimate Loads of Shallow Foundations: Closure of Discussion of Original Paper in Journal of Soil Mechanics and Foundation Division, 1973. Vol. 100, GT8, pp. 949–951," *Paper read at International Journal of Rock Mechanics and Mining Sciences & Geomechanics Abstracts*.

Whitman, R.V. (1984). "Evaluating Calculated Risk in Geotechnical Engineering," *Journal of Geotechnical Engineering*, Vol. 110, No. 2, pp. 143-188.

Whitman, R.V. (2000). "Organizing and Evaluating Uncertainty in Geotechnical Engineering," *Journal of Geotechnical and Geoenvironmental Engineering*, Vol. 126, No. 7, pp. 583-593.

Wu, T.H., and L.M. Kraft (1967). "The Probability of Foundation Safety," *Journal of Soil Mechanics and Foundation Division*, Vol. 92, No. 2, pp. 609-630.

Wu, T.H. (1974). "Uncertainty, Safety, and Decision in Soil Engineering," *Journal of the Geotechnical Engineering Division*, ASCE, Vol. 100, No. GT3, pp. 329-348.

Wu, T.H., and K. Wong (1981). "Probabilistic Soil Exploration: Case History," *Journal of the Geotechnical Engineering Division*, Vol. 107, No. 12, pp. 1693-1711.

Wu, T.H., I.M. Lee, J.C. Potter, and O. Kjekstad (1987). "Uncertainties in Evaluation of Strength of Marine Sand," *Journal of Geotechnical and Geoenvironmental Engineering*, Vol. 113, No. 7, pp. 719-738.

Wu, T.H., W.H. Tang, D.A. Sangrey, and G.B. Baecher (1989). "Reliability of Offshore Foundations-State of the Art," *Journal of Geotechnical Engineering*, Vol. 115, No. 2, pp. 157-178.

Wu, T.H. (2001). "2008 Peck Lecture: The Observational Method: Case History and Models," *Journal of Geotechnical and Geoenvironmental Engineering*, Vol. 137, No. 10, pp. 862-873.

Wu, T.H. (2013). "Geotechnical Uncertainties and Reliability-Based Design," *Foundation Engineering in the Face of Uncertainty*, pp. 271-282.

Yong, R.N. (1984). "Probabilistic Nature of Soil Properties," *Probabilistic characterization of soil properties: bridge between theory and practice*, pp. 19-73.

Zhang, L., W.H. Tang, L. Zhang, and J. Zheng (2004). "Reducing Uncertainty of Prediction from Empirical Correlations," *Journal of Geotechnical and Geoenvironmental Engineering*, Vol. 130, No. 5, pp. 526-534.

Zhang, J, L. Zhang, and W.H. Tang (2009). "Bayesian Framework for Characterizing Geotechnical Model Uncertainty," *Journal of Geotechnical and Geoenvironmental Engineering*, Vol. 135, No. 7, pp. 932-940.

# Vita

Dan Ding obtained her Bachelor of Science in Civil Engineering at the Chongqing University and Master of Science in Geotechnical Engineering at the Chengdu University of Technology in China. Dan Ding started her doctoral study in the Geotechnical Engineering program at the University of Missouri in 2008 and completed her PhD in 2014 with a PhD minor in Statistics.